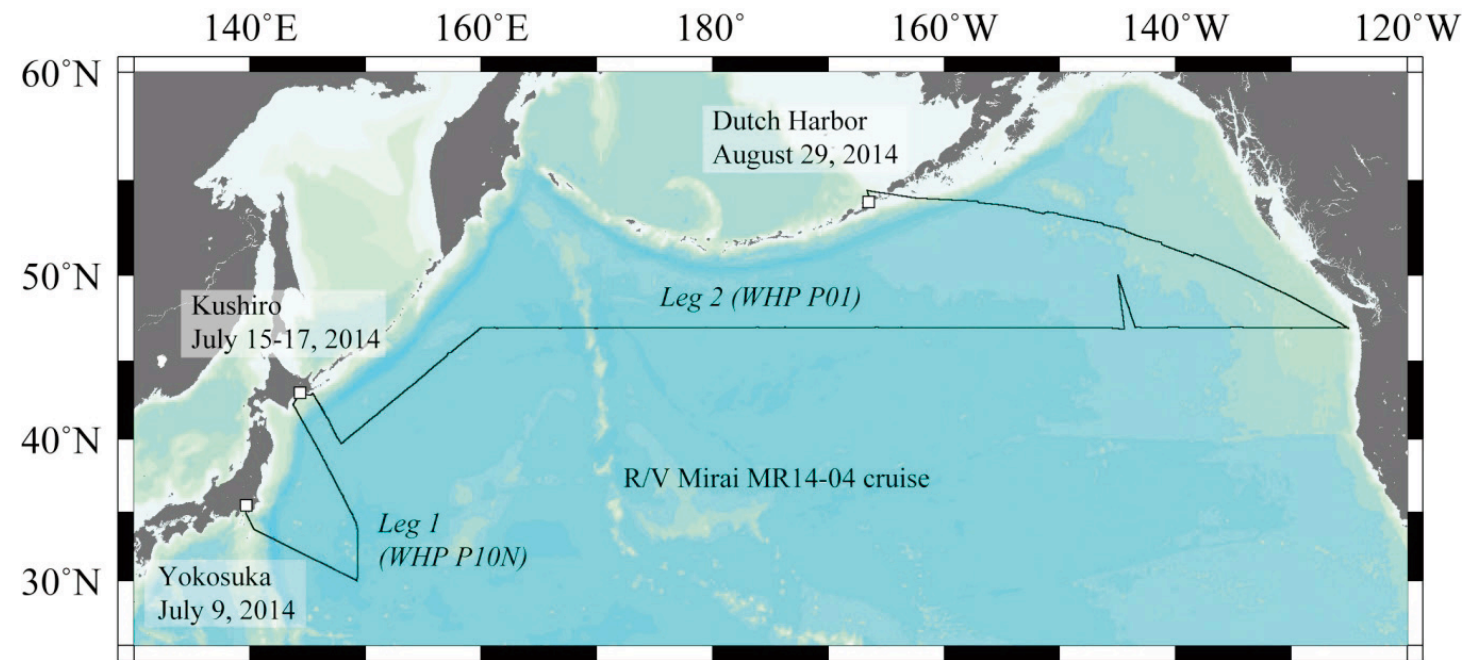


CRUISE REPORT: P01/P10

(Updated MAY 2017)



Contact Information:

Hiroshi Uchida

Research and Development Center for Global Change (RCGC)

Japan Agency for Marine-Earth Science and Technology (JAMSTEC)

2-15 Natsushima • Yokosuka, Kanagawa • Japan • 237-0061

Tel: +81-46-867-9474 • Fax: +81-46-867-9835 • email: huchida@jamstec.go.jp

Links to Select Topics

Shaded sections are not relevant to this cruise or were not available when this report was compiled.

Highlights

Cruise Summary Information

	Leg 1	Leg 2
Section Designation	P10	P01
Expedition designation (ExpoCodes)	49NZ20140709	49NZ20140717
Chief Scientists	Hiroshi Uchida / JAMSTEC	
Dates	2014 JUL 09 – 2014 JUL 15	2014 JUL 17 – 2014 AUG 29
Ship	R/V Mirai	
Ports of call	Yokosuka, Japan – Kushiro, Japan	Kushiro, Japan – Dutch Harbor, USA
Geographic Boundaries	50°N 143°E 125°W 30°N	
Stations	121 stations for CTD/Carousel Water Sampler (Leg 1: 5, Leg 2: 116) 30 stations for XCTD 19 stations for radiosonde and 4 stations for HYVIS 2 stations for ORI net and 10 stations for NORPAC net	
Floats and drifters deployed	6 Argo floats (2 S2A floats with RINKO oxygen sensor and 4 NAVIS floats)	
Moorings deployed or recovered	0	

Cruise Summary Information	Hydrographic Measurements
Description of Scientific Program	CTD Data:
Geographic Boundaries	Acquisition
Cruise Track (Figure): PI CCHDO	Processing
Description of Stations	Calibration
Description of Parameters Sampled	Temperature Pressure
Bottle Depth Distributions (Figure)	Salinities Oxygens
Floats and Drifters Deployed	Bottle Data
Moorings Deployed or Recovered	Salinity
Principal Investigators	Oxygen
Cruise Participants	Nutrients
	Carbon System Parameters
	CFCs
Problems and Goals Not Achieved	Helium / Tritium
Other Incidents of Note	Radiocarbon
Underway Data Information	Lowered Acoustic Doppler Current Profiler
Navigation Bathymetry	References
Acoustic Doppler Current Profiler (ADCP)	Cruise Summary
Thermosalinograph	XCTD
XBT and/or XCTD	Hydrographic Measurements
Meteorological Observations	Salinity
Atmospheric Chemistry Data	Density
	Oxygen
	Nutrients
	Carbon Items
	CDOM
CCHDO Data Processing Notes	Acknowledgments

WHP P01 REVISIT IN 2014 DATA BOOK

*Edited by
Hiroshi Uchida (JAMSTEC),
Toshimasa Doi (JAMSTEC)*



WHP P01 REVISIT IN 2014 DATA BOOK

March 24, 2017 Published

Edited by Hiroshi Uchida (JAMSTEC) and Toshimasa Doi (JAMSTEC)

Published by © JAMSTEC, Yokosuka, Kanagawa, 2017

Japan Agency for Marine-Earth Science and Technology

2-15 Natsushima, Yokosuka, Kanagawa. 237-0061, Japan

Phone +81-46-867-9474, Fax +81-46-867-9835

ISBN 978-4-901833-22-6

Printed by Aiwa Enterprise, Ltd.

3-22-4 Takanawa, Minato-ku, Tokyo 108-0074, Japan

Contents

Contents	i	3.7 Chlorophyll <i>a</i>	88
			<i>K. Sasaoka (JAMSTEC) et al.</i>		
Preface	iii	3.8 Absorption Coefficients of Particulate Matter and		
<i>H. Uchida (JAMSTEC)</i>			Colored Dissolved Organic Matter (CDOM)	90
			<i>K. Sasaoka (JAMSTEC)</i>		
Documents and station summary files			3.9 Calcium	93
1 Cruise Narrative	1	<i>Y. Shinoda (JAMSTEC)</i>		
<i>H. Uchida (JAMSTEC)</i>			3.10 Dissolved Organic Carbon	94
2 Underway Measurements			<i>T. Yoshimura (CRIEPI), D. A. Hansell and A. Margolin (Univ. of Miami)</i>		
2.1 Navigation	10	3.11 Lowered Acoustic Doppler Current Profiler (LADCP)	96
<i>H. Uchida (JAMSTEC), R. Oyama (GODI) et al.</i>			<i>S. Kouketsu and H. Uchida (JAMSTEC)</i>		
2.2 Swath Bathymetry	12			
<i>T. Matsumoto (Univ. Ryukyus), R. Oyama (GODI) et al.</i>			Station Summary		
2.3 Surface Meteorological Observations	14	49NZ20140709 .sum file	97
<i>M. Katsumata (JAMSTEC), R. Oyama (GODI) et al.</i>			49NZ20140717 .sum file	99
2.4 Thermo-Salinograph and Related Measurements	20			
<i>H. Uchida (JAMSTEC) et al.</i>			Figures		
2.5 Underway $p\text{CO}_2$	25	Figure captions	112
<i>A. Murata (JAMSTEC) et al.</i>			Station locations	115
2.6 Shipboard ADCP	27	Bathymetry	117
<i>S. Kouketsu (JAMSTEC) et al.</i>			Surface wind	121
2.7 XCTD	31	Sea surface temperature,	122
<i>H. Uchida (JAMSTEC) et al.</i>			salinity,	123
			oxygen,	124
			chlorophyll <i>a</i>	125
			$\Delta p\text{CO}_2$	126
			Surface current	127
			Cross-sections		
3 Hydrographic Measurement Techniques and Calibrations			Potential temperature	128
3.1 CTDO ₂ Measurements	35	CTD salinity	129
<i>H. Uchida (JAMSTEC) et al.</i>			Absolute salinity	130
3.2 Bottle Salinity	56	Density (σ_θ and σ_s) (EOS-80)	131
<i>H. Uchida (JAMSTEC) et al.</i>			Density (σ_θ and σ_s) (TEOS-10)	132
3.3 Density	59	Neutral Density (γ^n)	133
<i>H. Uchida (JAMSTEC)</i>			CTD oxygen	134
3.4 Oxygen	62	CTD chlorophyll <i>a</i>	135
<i>Y. Kumamoto (JAMSTEC) et al.</i>			CTD beam attenuation coefficient	136
3.5 Nutrients	67			
<i>M. Aoyama (Fukushima Univ./JAMSTEC) et al.</i>					
3.6 Carbon Items (C_T , A_T and pH)	83			
<i>A. Murata (JAMSTEC) et al.</i>					

<i>Bottle sampled dissolved oxygen</i>	137
<i>Silicate</i>	138
<i>Nitrate</i>	139
<i>Nitrite</i>	140
<i>Phosphate</i>	141
<i>Dissolved inorganic carbon (C_T)</i>	142
<i>Total alkalinity (A_T)</i>	143
<i>pH</i>	144
<i>Dissolved organic carbon</i>	145
<i>Current velocity</i>	146
<i>Difference between previous occupations and the revisit</i>		
<i>Potential temperature (2014-2007)</i>	147
<i>CTD Salinity (2014-2007)</i>	148
<i>CTD oxygen (2014-2007)</i>	149

.sum, .sea, .wct and other data files

<https://cchdo.ucsd.edu/cruise/49NZ20140717>

Preface

In the 18 years since Japan Agency for Marine-Earth Science and Technology (JAMSTEC) conducted a repeat hydrography observation along the World Ocean Circulation Experiment (WOCE) Hydrographic Program (WHP) line P01 in 1999, JAMSTEC revisited 17 WHP lines (P01 in 1999, P17N in 2001, P06, A10, I04 in 2003, I03 in 2004, P10, P03 in 2005, P01, P14 in 2007, P21 in 2009, P10 in 2011, P14S in 2012, S04I in 2013, P01 in 2014, I10 in 2015, and P17E in 2017) in the Pacific Ocean, Atlantic Ocean, Indian Ocean, and Southern Ocean.

The trans-Pacific section along 47°N reported in this data book is forth section for WHP P01 in recent 30 years from the original section conducted by the United States of America in 1985. From the results in 1985 and 1999, large-scale bottom water warming was revealed (*Fukasawa et al.*, 2004, doi:10.1038/nature02337). From the results in 2007, it was found that such large-scale bottom water warming continued after 1999 (*Kawano et al.*, 2010, doi:10.1016/j.dsr2.2009.12.003). After these discoveries, bottom water warming was clarified around the world ocean and reported in the fifth assessment report of the Intergovernmental Panel on Climate Change (IPCC) (*Rhein et al.*, 2013).

In recent repeat hydrography observations, measurement uncertainty is greatly reduced. For example, for temperature measurement, it was found that the in-situ reference thermometers have no pressure dependency and the overall expanded uncertainty of the deep ocean temperature measurement is estimated to be 0.7 mK (*Uchida et al.*, 2015, doi:10.1175/JTECH-D-15-0013.1). Also, for nutrients measurement, Reference Materials for Nutrients in Seawater (RMNS) has developed and used globally to improve the comparability of nutrients data (*Aoyama et al.*, Analytical Sciences, 28 (9), 911, 2012). These highly quality controlled data enable us to evaluate long-term changes in not only temperature but also dissolved materials in the ocean.

In the deep North Pacific, however, long-term change in salinity associated with the bottom water warming might be too small (an order of 0.0001 g/kg) to detect by the current measurement technology (a resolution of AUTOSAL salinometer is 0.0002 g/kg and uncertainty of the certified value of the IAPSO Standard Seawater might be ± 0.001 g/kg [*Kawano et al.*, 2006, doi:10.1007/s10872-006-0097-8; Table A1 of this data book]). Also, some parameters (such as dissolved oxygen and pH) require standard materials to improve the comparability. In the repeat hydrography observation, we should try to keep highest level of measurement technology, as well as

to develop more accurate measuring devices and standards.

You may find the contents of this data book, and links to other WHP revisit data books, on the website <http://www.jamstec.go.jp/iorgc/ocorp/data/post-woce.html>. Updates and corrections will be found online.

I would like to acknowledge the dedication and passion that Drs. Takeshi Kawano and Masao Fukasawa have shown in leading Japanese repeat hydrography, and congratulate them for producing such a significant contribution to GO-SHIP activities. I am sure that JAMSTEC's repeat hydrography data will be used as reference data in a world ocean database.

At Screaming Sixties in the Middle of WHP P17E Revisit (February 2017)

Hiroshi Uchida

Global Chemical and Physical Oceanography Group, JAMSTEC

1 Cruise Narrative

September 28, 2014

Hiroshi Uchida (JAMSTEC)

1.1 Highlights

WOCE Section Designation: P10N, P01

Cruise code: MR14-04

Expedition Designation: Leg 1: 49NZ20140709

Leg 2: 49NZ20140717

Chief Scientist and Affiliation:

Hiroshi Uchida

huchida@jamstec.go.jp

Research and Development Center for Global Change (RCGC)

Japan Agency for Marine-Earth Science and Technology (JAMSTEC)

2-15 Natsushima, Yokosuka, Kanagawa, Japan 237-0061

Tel: +81-46-867-9474, Fax: +81-46-867-9835

Ship: R/V Mirai

Ports of call: Leg 1: Yokosuka, Japan – Kushi, Japan

Leg 2: Kushi, Japan – Dutch Harbor, USA

Cruise Dates: Leg 1: July 9, 2014 – July 15, 2014

Leg 2: July 17, 2014 – August 29, 2014

Number of Stations: 121 stations for CTD/Carousel Water Sampler (Leg 1: 5, Leg 2: 116)

30 stations for XCTD

19 stations for radiosonde and 4 stations for HYVIS

2 stations for ORI net and 10 stations for NORPAC net

Geographic Boundaries (for hydrographic stations):

30°N – 50°N

143°E – 125°W

Floats and Drifters Deployed:

6 Argo floats

(2 S2A floats with RINKO oxygen sensor and 4 NAVIS floats)

Mooring Deployed or Recovered Mooring:

None

1.2 Cruise Summary

It is well known that the oceans play a central role in determining global climate. However heat and material transports in the ocean and their temporal changes have not yet been sufficiently quantified. Therefore, global climate change is not understood satisfactorily. The main purposes of this research are to evaluate heat and material transports such as anthropogenic CO₂, nutrients, etc. in the Pacific Ocean and to detect their long-term changes and basin-scale biogeochemical changes since the 1990s.

This cruise is a reoccupation of the hydrographic sections called WHP-P10N along 149°E and WHP-P01 along 47°N of the North Pacific (Fig. 1.1.1). The WHP-P10N section was previously observed by the Japan Agency for Marine-Earth Science and Technology (JAMSTEC) in 2005 (Kawano and Uchida, 2007), in 2011 (Uchida et al., 2014), and in 2014 by the Japan Meteorological Agency. The WHP-P01 section was previously observed in 1985 by the Scripps Institution of Oceanography (USA), in 1999 by the Japan Fisheries Agency / the JAMSTEC / the Institute of Ocean Sciences (Canada) (Uchida et al., 2002), and in 2007 by the JAMSTEC (Kawano et al., 2009). This study was conducted under the Global Ocean Ship-based Hydrographic Investigations Program (abbreviated as GO-SHIP, <http://www.go-ship.org/>). Data obtained from those cruises are available from the CLIVAR & Carbon Hydrographic Data Office (CCHDO) web site (<http://cchdo.ucsd.edu>).

In leg 1 of this cruise, we conducted CTD and discrete water sampling at selected 5 stations and zooplankton sampling by using ORI net at two stations along the WHP-P10N section mainly for estimation of dispersion of radioactive substances released into the sea by the Fukushima Dai-ichi nuclear power plant accident in March 2011. To understand the oceanographic condition along the WHP-P10N section in detail,

we deployed XCTDs between the CTD stations. In addition, we launched radiosondes and HYdrometer Video Sondes (HYVIS) to understand the atmospheric condition along the cruise track. Especially in the section across the Kuroshio Extension, we densely launched radiosondes simultaneously with the XCTDs (Fig. 1.1.2). At station 1, an ARGO float was deployed to take a photograph and recovered after that.

In leg 2 of this cruise, we conducted full-depth CTD, lowered acoustic Doppler current profiler (LADCP), Micro-Rider measurements, and discrete water sampling for physical, chemical and biogeochemical properties of seawater from a maximum of 36 layers along the WHP-P01 section and at the ocean station PAPA (Figs. 1.1.3 and 1.1.4). We deployed two ARGO floats with RINKO oxygen sensor in an anticyclonic eddy off Hokkaido and four ARGO floats in the area where the number of ARGO floats is small to maintain the global array. Furthermore, we sampled marine plankton by using NORPAC net to examine changes in calcification responses of planktonic organisms and pH in the subarctic North Pacific.

Also, we sampled seawater to examine horizontal and vertical distribution of microbial population (picoeukaryotes, bacteria, archaea, and viruses) in gene level to explain relationship between the microbial population and ocean circulations (seawater properties). In addition, we observed physical, chemical, and biogeochemical properties of seawater and atmosphere, and geophysical parameters (sea bottom topography, gravity acceleration, etc.) continuously along the cruise track in order to accumulate basic scientific data in global scale, especially for unobserved regions.

References

- Kawano, T., and H. Uchida (Eds.) (2007): WHP P10 Revisit Data Book, JAMSTEC, 139 pp.
- Kawano, T., H. Uchida, and T. Doi (Eds.) (2009): WHP P01, P14 Revisit Data Book, JAMSTEC, 212 pp.
- Uchida, H., A. Murata, and T. Doi (Eds.) (2014): WHP P10 Revisit in 2011 Data Book, JAMSTEC, 179 pp.
- Uchida, H., M. Fukasawa, and H. J. Freeland (Eds.) (2002): WHP P01 Revisit Data Book, JAMSTEC, 73 pp.

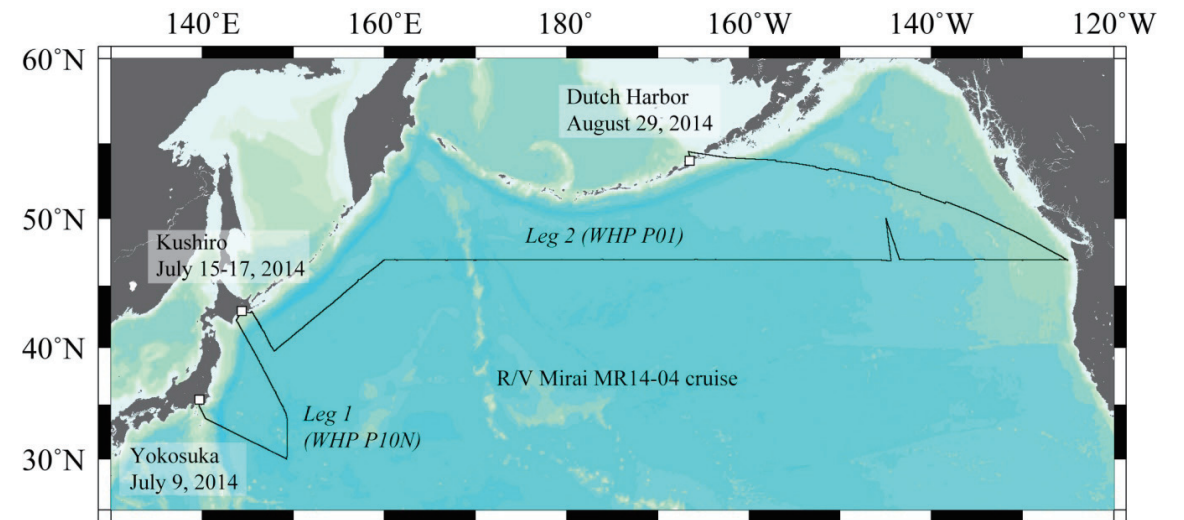


Fig. 1.1.1. Cruise track of the R/V Mirai cruise MR14-04.

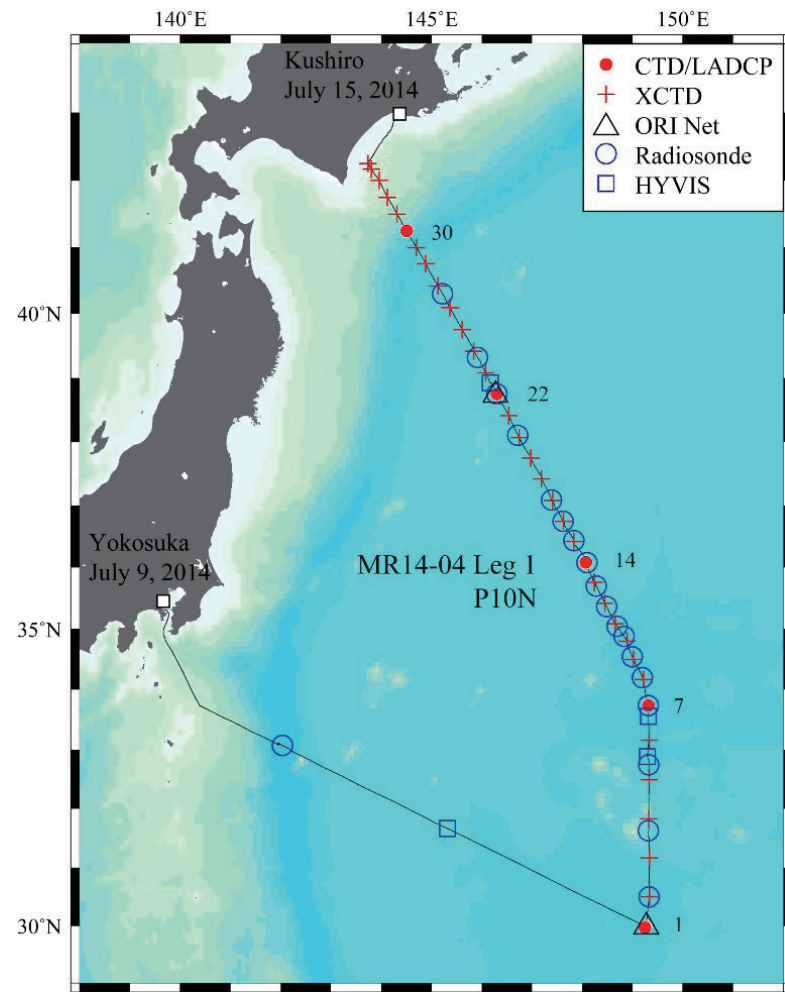


Fig. 1.1.2. Station locations for MR14-04 leg 1.

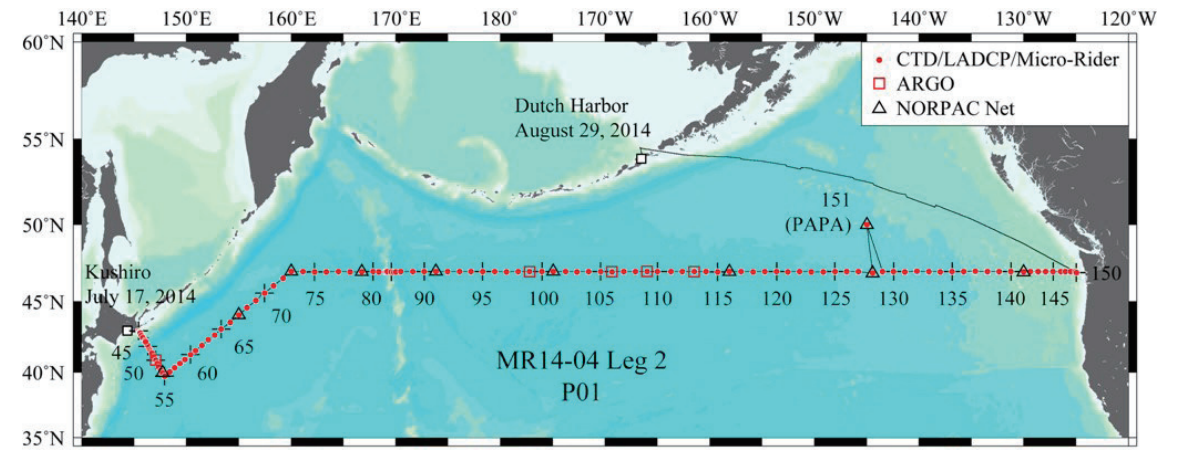


Figure 1.1.3. Station locations for MR14-04 leg 2.

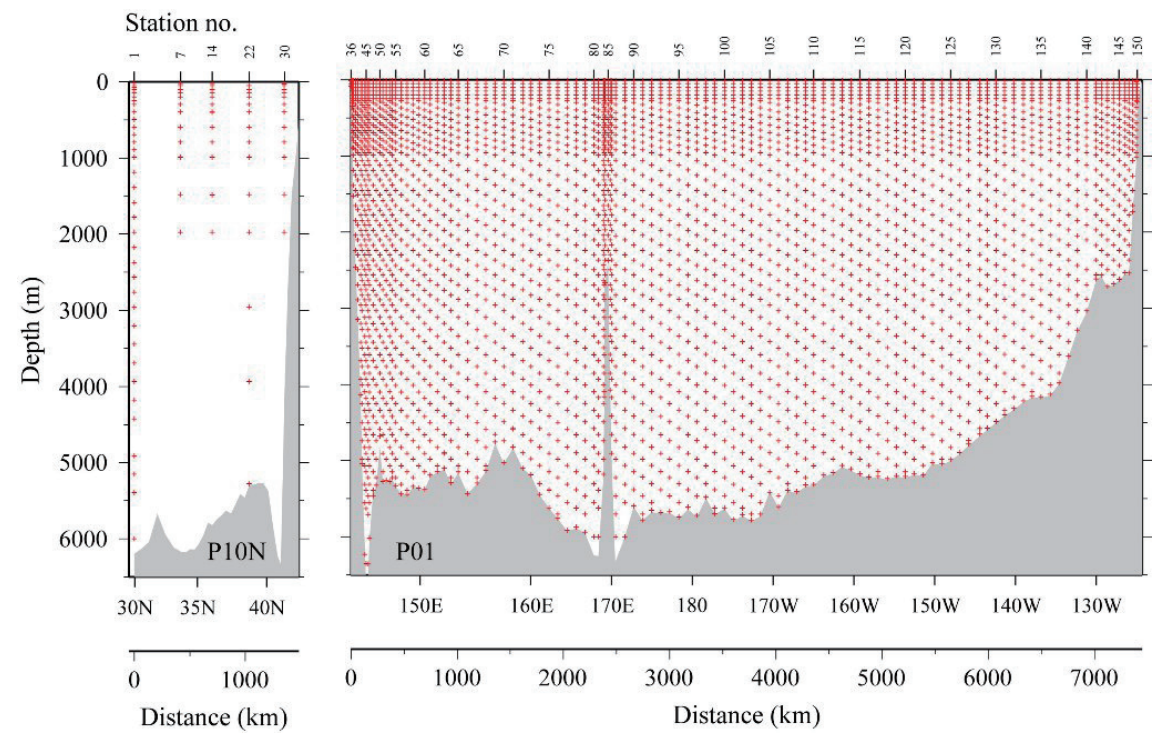


Fig. 1.1.4. Bottle depth diagram.

1.3 List of Principal Investigator and Person in Charge on the Ship

The principal investigator (PI) and the person in charge responsible for major parameters measured on the cruise are listed in Table 1.3.1.

Table 1.3.1. List of principal investigator and person in charge on the ship.

Item	Principal Investigator	Person in charge onboard
Underway		
Navigation	Hiroshi Uchida (JAMSTEC) <i>huchida@jamstec.go.jp</i>	Ryo Oyama (GODI) (leg 1) Wataru Tokunaga (GODI) (leg 2)
Bathymetry	Takeshi Matsumoto (Univ. of Ryukyus) <i>tak@sci.u-ryukyu.ac.jp</i>	Ryo Oyama (GODI) (leg 1) Wataru Tokunaga (GODI) (leg 2)
Meteorology	Masaki Katsumata (JAMSTEC) <i>katsu@jamstec.go.jp</i>	Ryo Oyama (GODI) (leg 1) Wataru Tokunaga (GODI) (leg 2)
TSG	Hiroshi Uchida (JAMSTEC) <i>huchida@jamstec.go.jp</i>	Keitaro Matsumoto (MWJ)
pCO ₂	Akihiko Murata (JAMSTEC) <i>murataa@jamstec.go.jp</i>	Atsushi Ono (MWJ)
ADCP	Shinya Kouketsu (JAMSTEC) <i>skouketsu@jamstec.go.jp</i>	Ryo Oyama (GODI) (leg 1) Wataru Tokunaga (GODI) (leg 2)
XCTD	Hiroshi Uchida (JAMSTEC) <i>huchida@jamstec.go.jp</i>	Ryo Oyama (GODI) (leg 1) Wataru Tokunaga (GODI) (leg 2)
FlowCAM	Hiroshi Uchida (JAMSTEC) <i>huchida@jamstec.go.jp</i>	Hiroshi Uchida (JAMSTEC)
Ceilometer	Masaki Katsumata (JAMSTEC)	Ryo Oyama (GODI) (leg 1)

	<i>katsu@jamstec.go.jp</i>	Wataru Tokunaga (GODI) (leg 2)
Raindrop	Masaki Katsumata (JAMSTEC) <i>katsu@jamstec.go.jp</i>	Masaki Katsumata (JAMSTEC)
Doppler Radar	Masaki Katsumata (JAMSTEC) <i>katsu@jamstec.go.jp</i>	Ryo Oyama (GODI) (leg 1) Wataru Tokunaga (GODI) (leg 2)
Radiosonde	Masaki Katsumata (JAMSTEC) <i>katsu@jamstec.go.jp</i>	Ryo Oyama (GODI)
HYVIS	Masaki Katsumata (JAMSTEC) <i>katsu@jamstec.go.jp</i>	Ryo Oyama (GODI)
Gravity	Takeshi Matsumoto (Univ. of Ryukyus) <i>tak@sci.u-ryukyu.ac.jp</i>	Ryo Oyama (GODI) (leg 1) Wataru Tokunaga (GODI) (leg 2)
Magnetic Field	Takeshi Matsumoto (Univ. of Ryukyus) <i>tak@sci.u-ryukyu.ac.jp</i>	Ryo Oyama (GODI) (leg 1) Wataru Tokunaga (GODI) (leg 2)
Satellite Image	Masaki Katsumata (JAMSTEC) <i>katsu@jamstec.go.jp</i>	Ryo Oyama (GODI) (leg 1) Wataru Tokunaga (GODI) (leg 2)
Sky Radiometer	Kazuma Aoki (Univ. of Toyama) <i>kazuma@sci.u-toyama.ac.jp</i>	none
MAX-DOAS	Hisahiro Takashima (JAMSTEC) <i>hisahiro@jamstec.go.jp</i>	none
Ozone and CO	Yugo Kanaya (JAMSTEC) <i>yugo@jamstec.go.jp</i>	none
Black Carbon	Takuma Miyakawa (JAMSTEC) <i>miyakawat@jamstec.go.jp</i>	none
Fluorescent Aerosol	Fumikazu Taketani (JAMSTEC) <i>taketani@jamstec.go.jp</i>	none

Aerosol Particle Size	Fumikazu Taketani (JAMSTEC) <i>taketani@jamstec.go.jp</i>	none		<i>sasaoka@jamstec.go.jp</i>	
			CDOM/Absorption Coefficients	Kosei Sasaoka (JAMSTEC) <i>sasaoka@jamstec.go.jp</i>	Kosei Sasaoka (JAMSTEC)
Hydrography					
CTD/O ₂	Hiroshi Uchida (JAMSTEC) <i>huchida@jamstec.go.jp</i>	Shinsuke Toyoda (MWJ)	Calcium	Yoshihiro Shinoda (JAMSTEC) <i>Yshinoda@jamstec.go.jp</i>	Yoshihiro Shinoda (JAMSTEC)
Salinity	Hiroshi Uchida (JAMSTEC) <i>huchida@jamstec.go.jp</i>	Tatsuya Tanaka (MWJ)	DOC	Dennis A. Hansell (RSMAS) <i>dhansell@rsmas.miami.edu</i>	Yuichiro Kumamoto (JAMSTEC)
Density	Hiroshi Uchida (JAMSTEC) <i>huchida@jamstec.go.jp</i>	Hiroshi Uchida (JAMSTEC)		Takeshi Yoshimura (CRIEPI) <i>ytakeshi@criepi.denken.or.jp</i>	
Oxygen	Yuichiro Kumamoto (JAMSTEC) <i>kumamoto@jamstec.go.jp</i>	Keitaro Matsumoto (MWJ)	DOC duplicate at station 73 (K2)	Masahide Wakita (JAMSTEC) <i>mwakita@jamstec.go.jp</i>	Hiroshi Uchida (JAMSTEC)
Nutrients	Michio Aoyama (Fukushima Univ.) <i>r706@ipc.fukushima-u.ac.jp</i>	Yasuhiro Arie (MWJ)	$\Delta^{14}\text{C}/\delta^{13}\text{C}$	Yuichiro Kumamoto (JAMSTEC) <i>kumamoto@jamstec.go.jp</i>	Yuichiro Kumamoto (JAMSTEC)
CFCs/SF ₆	Ken'ichi Sasaki (JAMSTEC) <i>ksasaki@jamstec.go.jp</i>	Ken'ichi Sasaki (JAMSTEC) (leg 1) Hironori Sato (MWJ) (leg 2)	$^{134}\text{Cs}/^{137}\text{Cs}$	Yuichiro Kumamoto (JAMSTEC) <i>kumamoto@jamstec.go.jp</i>	Yuichiro Kumamoto (JAMSTEC)
DIC	Akihiko Murata (JAMSTEC) <i>murataa@jamstec.go.jp</i>	Atsushi Ono (MWJ)	Iodine-129	Yuichiro Kumamoto (JAMSTEC) <i>kumamoto@jamstec.go.jp</i>	Yuichiro Kumamoto (JAMSTEC)
Alkalinity	Akihiko Murata (JAMSTEC) <i>murataa@jamstec.go.jp</i>	Tomonori Watai (MWJ)	$\delta^{18}\text{O}/\delta\text{D}$	Hiroshi Uchida (JAMSTEC) <i>huchida@jamstec.go.jp</i>	Hiroshi Uchida (JAMSTEC)
Alkalinity duplicate by potentiometry					
	Yoshihiro Shinoda (JAMSTEC) <i>yshinoda@jamstec.go.jp</i>	Yoshihiro Shinoda (JAMSTEC)	PFASs	Nobuyoshi Yamashita (AIST) <i>nob.yamashita@aist.go.jp</i>	Nobuyoshi Yamashita (AIST) (leg 1) Sachi Taniyasu (AIST) (leg 2)
pH	Akihiko Murata (JAMSTEC) <i>murataa@jamstec.go.jp</i>	Tomonori Watai (MWJ)	N ₂ O/CH ₄	Osamu Yoshida (RGU) <i>yoshida@rakuno.ac.jp</i>	Osamu Yoshida (RGU) (leg 1) Takuya Takahashi (RGU) (leg 2)
Chlorophyll <i>a</i>	Kosei Sasaoka (JAMSTEC)	Keitaro Matsumoto (MWJ)	Cell abundance	Takuro Nunoura (JAMSTEC)	Taichi Yokokawa (Ehime Univ.) (leg 1)

	<i>takuron@jamstec.go.jp</i>	Takuro Nunoura (JAMSTEC) (leg 2)		<i>skouketsu@jamstec.go.jp</i>	Shinya Kouketsu (JAMSTEC) (leg 2)
Microbial diversity	Takuro Nunoura (JAMSTEC) <i>takuron@jamstec.go.jp</i>	Takuro Nunoura (JAMSTEC)	Micro-Rider	Ichiro Yasuda (AORI) <i>ichiro@aori.u-tokyo.ac.jp</i>	Shinya Kouketsu (JAMSTEC)
Microbial carbon uptake			<i>Biology</i>		
	Takuro Nunoura (JAMSTEC) <i>takuron@jamstec.go.jp</i>	Taichi Yokokawa (Ehime Univ.) (leg 1) Takuro Nunoura (JAMSTEC) (leg 2)	ORI net	Minoru Kitamura (JAMSTEC) <i>kitamura@jamstec.go.jp</i>	Minoru Kitamura (JAMSTEC)
Nitrification	Akiko Makabe (TUAT) <i>a-makabe@cc.tuat.ac.jp</i>	Akiko Makabe (TUAT)	NORPAC net	Katsunori Kimoto (JAMSTEC) <i>kimopy@jamstec.go.jp</i>	Shinya Iwasaki (AORI)
Nitrogen fixation	Masanori Kaneko (JAMSTEC) <i>m_kaneko@jamstec.go.jp</i>	Masanori Kaneko (JAMSTEC) (leg 1) Shuichiro Matsushima (TITECH) (leg 2)	Phytoplankton Incubation	Koji Sugie (JAMSTEC) <i>sugie@jamstec.go.jp</i>	Koji Sugie (JAMSTEC)
Methanogen biomarker			<i>Floats</i>		
	Masanori Kaneko (JAMSTEC) <i>m_kaneko@jamstec.go.jp</i>	Masanori Kaneko (JAMSTEC) (leg 1) Takuya Takahashi (RGU) (leg 2)	ARGO float	Toshio Suga (JAMSTEC) <i>sbaba@jamstec.go.jp</i>	Hiroshi Matsunaga (MWJ)
$\delta^{13}\text{C}/\text{CH}_4$	Masanori Kaneko (JAMSTEC) <i>m_kaneko@jamstec.go.jp</i>	Masanori Kaneko (JAMSTEC) (leg 1) Takuya Takahashi (RGU) (leg 2)		JAMSTEC	Japan Agency for Marine-Earth Science and Technology
$\delta^{15}\text{N} \delta^{18}\text{O}/\text{NO}_3^-$	Chisato Yoshikawa (JAMSTEC) <i>yoshikawac@jamstec.go.jp</i>	Chisato Yoshikawa (JAMSTEC) (leg 1) Akiko Makabe (TUAT) (leg 2)		GODI	Global Ocean Development Inc.
$\delta^{15}\text{N}/\text{chlorophyll}$	Chisato Yoshikawa (JAMSTEC) <i>yoshikawac@jamstec.go.jp</i>	Chisato Yoshikawa (JAMSTEC) (leg 1) Takuya Takahashi (TUAT) (leg 2)		MWJ	Marine Works Japan, Ltd.
$\delta^{15}\text{N} \delta^{18}\text{O}/\text{N}_2\text{O}, \text{NO}_2$	Sakae Toyoda (TITECH) <i>toyoda.s.aa@m.titech.ac.jp</i>	Shuichiro Matsushima (TITECH) (leg 2)		RSMAS	Rosenstiel School of Marine and Atmospheric Science, University of Miami
$\delta^{15}\text{N}/\text{NH}_4^+, \text{DON}, \text{urea}$	Akiko Makabe (TUAT) <i>a-makabe@cc.tuat.ac.jp</i>	Akiko Makabe (TUAT)		CRIEPI	Central Research Institute of Electric Power Industry
LADCP	Shinya Kouketsu (JAMSTEC)	Hiroshi Uchida (JAMSTEC) (leg 1)		AIST	National Institute of Advanced Industrial Science and Technology
				RGU	Rakuno Gakuen University
				TUAT	Tokyo University of Agriculture and Technology
				TITECH	Tokyo Institute of Technology
				AORI	Atmosphere and Ocean Research Institute, The Univ. of Tokyo

1.4 List of Cruise Participants

Table 1.4.1. List of cruise participants for leg 1.

Name	Responsibility	Affiliation			
Hiroshi Uchida	Density/FlowCAM/LADCP/ $\delta^{18}\text{O}$	RCGC/JAMSTEC	Fumihiko Saito	TV camera	JBC
Yuichiro Kumamoto	DO/Radionuclides/Water sampling	RCGC/JAMSTEC	Ryo Oyama	Chief technologist /meteorology/ geophysics/ADCP/XCTD	GODI
Yoshihiro Shinoda	Water sampling	RCGC/JAMSTEC	Souichiro Sueyoshi	Meteorology/geophysics/ADCP/XCTD	GODI
Minoru Kitamura	ORI net	RCGC/JAMSTEC	Katsuhisa Maeno	Meteorology/geophysics/ADCP/XCTD	GODI
Masaki Katsumata	HYVIS/Radiosonde/Doppler rader/Raindrop	RCGC/JAMSTEC	Koichi Inagaki	Meteorology/geophysics/ADCP/XCTD	GODI
Biao Geng	HYVIS/Radiosonde/Doppler rader	RCGC/JAMSTEC	Yutaro Murakami	Meteorology/geophysics/ADCP/XCTD	GODI
Shuichi Mori	HYVIS/Radiosonde/Doppler rader	DCOP/JAMSTEC	Shinsuke Toyoda	Chief technologist/CTD/water sampling	MWJ
Ryuichi Shirooka	HYVIS/Radiosonde/Doppler rader	DCOP/JAMSTEC	Hiroshi Matsunaga	CTD/ARGO	MWJ
Ken'ichi Sasaki	CFCs/SF ₆	MIO/JAMSTEC	Kenichi Katayama	CTD	MWJ
Takuro Nunoura	Microbiology	RCMB/JAMSTEC	Rei Ito	CTD	MWJ
Miho Hirai	Microbiology	RCMB/JAMSTEC	Akira Watanabe	CTD	MWJ
Chisato Yoshikawa	Chlorophyll/NO ₃ isotope geochemistry	BGC/JAMSTEC	Tatsuya Tanaka	Salinity	MWJ
Masanori Kaneko	CH ₄ geochemistry/Nitrogen fixation	BGC/JAMSTEC	Sonoka Wakatsuki	Salinity	MWJ
Akiko Makabe	Nitrification/Nitrogen geochemistry	TUAT	Keitaro Matsumoto	DO/Chlorophyll-a/TSG	MWJ
Taichi Yokokawa	Microbiology	Ehime Univ.	Misato Kuwahara	DO/Chlorophyll-a/TSG	MWJ
Nobuyoshi Yamashita	PFASs	AIST	Haruka Tamada	DO/Chlorophyll-a/TSG	MWJ
Osamu Yoshida	N ₂ O/CH ₄	RGU	Yasuhiro Arie	Nutrients	MWJ
Kanta Chida	N ₂ O/CH ₄	RGU	Minoru Kamata	Nutrients	MWJ
Takuya Takahashi	N ₂ O/CH ₄	RGU	Tomomi Sone	Nutrients	MWJ
Tomoyuki Shirakawa	TV camera	JBC	Katsunori Sagishima	CFCs/SF ₆	MWJ
			Hironori Sato	CFCs/SF ₆	MWJ
			Hideki Yamamoto	CFCs/SF ₆	MWJ
			Atsushi Ono	DIC	MWJ
			Yoshiko Ishikawa	DIC	MWJ
			Tomonori Watai	pH/Alkalinity	MWJ

Emi Deguchi	pH/Alkalinity	MWJ
JAMSTEC	Japan Agency for Marine-Earth Science and Technology	
RCGC	Research and Development Center for Global Change	
DCOP	Department of Coupled Ocean-Atmosphere-Land Processes Research	
MIO	Mutsu Institute of Oceanography	
RCMB	Research and Development Center for Marine Biosciences	
BGC	Department of Biogeochemistry	
TUAT	Tokyo University of Agriculture and Technology	
AIST	National Institute of Advanced Industrial Science and Technology	
RGU	Rakuno Gakuen University	
JBC	Japan Broadcasting Corporation	
GODI	Global Ocean Development Inc.	
MWJ	Marine Works Japan, Ltd.	

Table 1.4.2. List of cruise participants for leg 2.

Name	Responsibility	Affiliation
Hiroshi Uchida	Density/FlowCAM/LADCP/Micro-Rider/ $\delta^{18}\text{O}$	RCGC/JAMSTEC
Yuichiro Kumamoto	DO/Radionuclides/Water sampling	RCGC/JAMSTEC
Yoshihiro Shinoda	Calcium/Water sampling	RCGC/JAMSTEC
Shinya Koketsu	LADCP/Micro-Rider/ $\delta^{18}\text{O}$	RCGC/JAMSTEC
Kosei Sasaoka	CDOM/Absorption coefficient	RCGC/JAMSTEC
Koji Sugie	Phytoplankton incubation/NORPAC net	RCGC/JAMSTEC
Shinya Iwasaki	NORPAC net/Phytoplankton incubation	AORI/Univ. of Tokyo
Takuro Nunoura	Microbiology	RCMB/JAMSTEC
Akiko Makabe	Nitrification/Nitrogen geochemistry	TUAT
Shuichiro Matsushima	Nitrogen fixation/Nitrogen geochemistry/ CH_4	TITECH
Seiya Takahashi	Microbiology	Tsukuba Univ.
Sachi Taniyasu	PFASs	AIST
Kanta Chida	$\text{N}_2\text{O}/\text{CH}_4$	RGU
Takuya Takahashi	$\text{N}_2\text{O}/\text{CH}_4$	RGU
Wataru Tokunaga	Chief technologist /meteorology/ geophysics/ADCP/XCTD	GODI
Kazuho Yoshida	Meteorology/geophysics/ADCP/XCTD	GODI
Yutaro Murakami	Meteorology/geophysics/ADCP/XCTD	GODI
Tetsuya Kai	Meteorology/geophysics/ADCP/XCTD	GODI
Shinsuke Toyoda	Chief technologist/CTD/water sampling	MWJ
Hiroshi Matsunaga	CTD/ARGO	MWJ
Tomoyuki Takamori	CTD	MWJ

Rei Ito	CTD	MWJ	JAMSTEC	Japan Agency for Marine-Earth Science and Technology
Akira Watanabe	CTD	MWJ	RCGC	Research and Development Center for Global Change
Tatsuya Tanaka	Salinity	MWJ	AORI	Atmosphere and Ocean Research Institute, The Univ. of Tokyo
Sonoka Wakatsuki	Salinity	MWJ	RCMB	Research and Development Center for Marine Biosciences
Keitaro Matsumoto	DO/Chlorophyll-a/TSG	MWJ	TUAT	Tokyo University of Agriculture and Technology
Katsunori Sagishima	DO/Chlorophyll-a/TSG	MWJ	TITECH	Tokyo Institute of Technology
Haruka Tamada	DO/Chlorophyll-a/TSG	MWJ	AIST	National Institute of Advanced Industrial Science and Technology
Yasuhiro Arie	Nutrients	MWJ	RGU	Rakuno Gakuen University
Kenichiro Sato	Nutrients	MWJ	GODI	Global Ocean Development Inc.
Elena Hayashi	Nutrients	MWJ	MWJ	Marine Works Japan, Ltd.
Hironori Sato	CFCs/SF ₆	MWJ		
Hideki Yamamoto	CFCs/SF ₆	MWJ		
Shoko Tatamisashi	CFCs/SF ₆	MWJ		
Kanako Yoshida	CFCs/SF ₆	MWJ		
Atsushi Ono	DIC	MWJ		
Yoshiko Ishikawa	DIC	MWJ		
Tomonori Watai	pH/Alkalinity	MWJ		
Emi Deguchi	pH/Alkalinity	MWJ		
Rina Tajima	Water sampling	MWJ		
Toshiki Nosho	Water sampling	MWJ		
Miho Arai	Water sampling	MWJ		
Kohei Kumagai	Water sampling	MWJ		
Yuki Kawabuchi	Water sampling	MWJ		
Yuki Komuro	Water sampling	MWJ		

2 Underway Measurements

2.1 Navigation

September 17, 2014

(1) Personnel

Hiroshi Uchida	JAMSTEC: Principal investigator	
Ryo Oyama	Global Ocean Development Inc., (GODI)	- leg 1 -
Souichiro Sueyoshi	GODI	- leg 1 -
Katsuhisa Maeno	GODI	- leg 1 -
Koichi Inagaki	GODI	- leg 1 -
Wataru Tokunaga	GODI	- leg 2 -
Kazuho Yoshida	GODI	- leg 2 -
Tetsuya Kai	GODI	- leg 2 -
Yutaro Murakami	GODI	- leg 1, leg 2 -
Masanori Murakami	MIRAI crew	- leg 1, leg 2 -

(2) System description

Ship's position and velocity were provided by Navigation System on R/V MIRAI. This system integrates GPS position, Doppler sonar log speed, Gyro compass heading and other basic data for navigation, and calculated speed and course over ground on workstation. This system also distributed ship's standard time synchronized to GPS time server via Network Time Protocol. These data were logged on the network server as "SOJ" data every 5 seconds.

Sensors for navigation data are listed below;

i) GPS system:

R/V MIRAI has four GPS systems, all GPS positions were offset to radar-mast position, datum point.

Anytime changeable manually switched as to GPS receiving state.

- a) MultiFix6 (software version 1.01), Differential GPS system.

Receiver: Trimble SPS751, with GPS antenna located on navigation deck, starboard.

Decoder: FUGURO STARFIX 4100LRS

- b) MultiFix6 (software version 1.01), Differential GPS system.

Receiver: Trimble SPS751, with two GPS antenna located on compass deck, port side.

Decoder: FUGURO STARFIX 4100LRS

- c) Standalone GPS system.

Receiver: Trimble 4000DS, GPS antenna located on navigation deck, port side.

- d) Standalone GPS system.

Receiver: FURUNO GP-36, GPS antenna located on navigation deck, starboard.

- ii) Doppler sonar log:

FURUNO DS-30, which use three acoustic beam for current measurement under the hull.

- iii) Gyro compass:

TOKYO KEIKI TG-6000, sperry type mechanical gyrocompass.

- iv) GPS time server:

SEIKO TS-2540 Time Server, synchronizing to GPS satellites every 1 second.

(3) Data period (Times in UTC)

Leg 1: 22:10, 08 Jul. 2014 to 04:00, 15 Jul. 2014

Leg 2: 02:00, 17 Jul. 2014 to 18:00, 29 Aug. 2014

(4) Remarks (Times in UTC)

- i) The following periods, navigation data (position, speed and course over ground) was often invalid due to position fix error for loss of GPS satellites.

Leg 1: 14 Jul. to 15 Jul., 2014

Leg 2: 17 Jul. to 16 Aug., 2014

- ii) The following periods, navigation data was invalid due to the system error.

Leg 2: 12:37 to 12:45 23 Aug., 2014

iii) Some data records were lacked due to the system error or GPS trouble. See data "readme.txt" which contains the time of data lost.

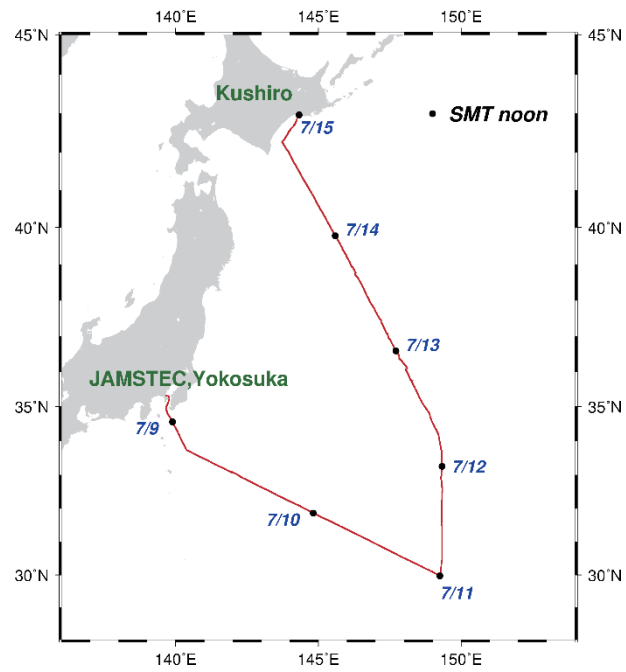


Fig.2.1.1. Cruise track of MR14-04 Leg 1.

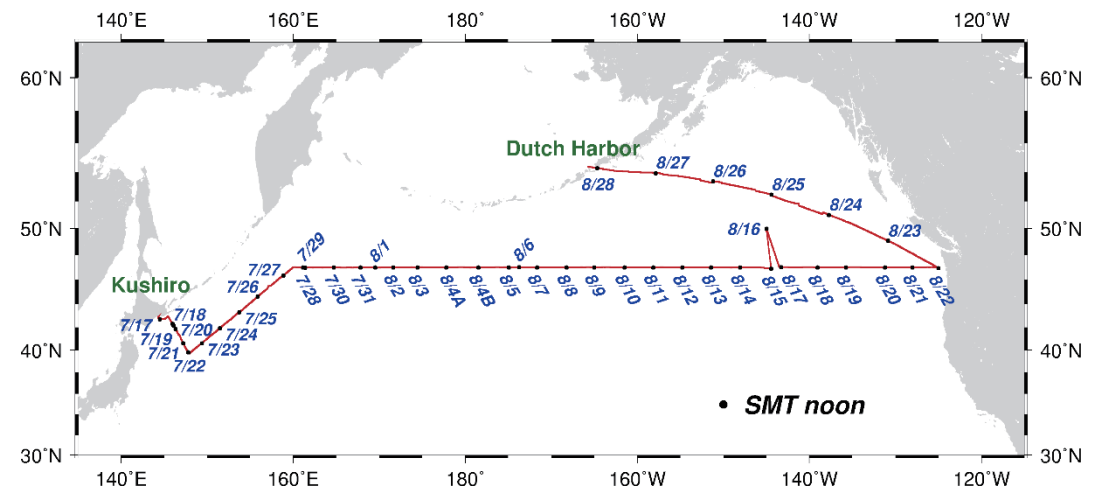


Fig.2.1.2. Cruise track of MR14-04 Leg 2.

2.2 Swath Bathymetry

September 17, 2014

(1) Personnel

Takeshi Matsumoto	Univ. of Ryukyus: Principal investigator	(Not-onboard)
Ryo Oyama	Global Ocean Development Inc., (GODI)	- leg 1 -
Souichiro Sueyoshi	GODI	- leg 1 -
Katsuhisa Maeno	GODI	- leg 1 -
Koichi Inagaki	GODI	- leg 1 -
Wataru Tokunaga	GODI	- leg 2 -
Kazuho Yoshida	GODI	- leg 2 -
Tetsuya Kai	GODI	- leg 2 -
Yutaro Murakami	GODI	- leg 1, leg 2 -
Masanori Murakami	MIRAI crew	- leg 1, leg 2 -

(2) Introduction

R/V MIRAI is equipped with a Multi narrow Beam Echo Sounding system (MBES), SEABEAM 3012 (L3 Communications, ELAC Nautik). The objective of MBES is collecting continuous bathymetric data along ship's track to make a contribution to geological and geophysical investigations and global datasets.

(3) Data Acquisition

The "SEABEAM 3012" on R/V MIRAI was used for bathymetry mapping during the MR14-04 cruise.

To get accurate sound velocity of water column for ray-path correction of acoustic multibeam, we used Surface Sound Velocimeter (SSV) data to get the sea surface sound velocity (at 6.62m), and the deeper depth sound velocity profiles were calculated by temperature and salinity profiles from CTD and XCTD data by the equation in Del Grosso (1974) during this cruise.

Table 2.2.1 shows system configuration and performance of SEABEAM 3012.

Table 2.2.1. SEABEMA 3012 system configuration and performance.

Frequency:	12 kHz
Transmit beam width:	2.0 degree
Transmit power:	4 kW
Transmit pulse length:	2 to 20 msec.
Receive beam width:	1.6 degree
Depth range:	50 to 11,000 m
Number of beams:	301 beams (Spacing mode: Equi-angle)
Beam spacing:	1.5 % of water depth (Spacing mode: Equi-distance)
Swath width:	60 to 150 degrees
Depth accuracy:	< 1 % of water depth (average across the swath)

(4) Data processing

i) Sound velocity correction

Each bathymetry data were corrected with sound velocity profiles calculated from the nearest CTD or XCTD data in the distance. The equation of Del Grosso (1974) was used for calculating sound velocity. The data correction were carried out using the HIPS software version 8.1.7 (CARIS, Canada)

ii) Editing and Gridding

Editing for the bathymetry data were carried out using the HIPS. Firstly, the bathymetry data during ship's turning was basically deleted, and spike noise of each swath data was removed. Then the bathymetry data were checked by "BASE surface (resolution: 100 m averaged grid)".

Finally, all accepted data were exported as XYZ ASCII data (longitude [degree], latitude [degree],

depth [m]), and converted to 150 m grid data using “nearneighbor” utility of GMT (Generic Mapping Tool) software.

Table 2.2.2. Parameters for gridding on “nearneighbor” in GMT

Gridding mesh size:	150 m
Search radius size (-S):	150 m
Number of sectors (-N):	1

(5) Data Archives

Bathymetric data obtained during this cruise will be submitted to the Data Management Group (DMG) of JAMSTEC, and will be archived there.

(6) Remarks (Times in UTC)

i) The following periods, the observations were carried out.

Leg 1: 02:52 09 Jul. to 23:22 14 Jul., 2014

Leg 2: 06:19 17 Jul. to 12:29 28 Aug., 2014

ii) The following periods, navigation data (position, speed and course over ground) was often invalid due to position fix error for loss of GPS satellites. If bathymetric data were included error position and heading information, we interpolated from the just before and behind correct data using the HIPS.

Leg 1: 14 Jul. to 15 Jul., 2014

Leg 2: 17 Jul. to 16 Aug., 2014

iii) The following periods, navigation data was invalid due to the server error.

Leg 2: 12:37 to 12:45 23 Aug., 2014

iv) The following periods, data acquisition was suspended due to the system error and maintenance.

01:55 30 Jul. to 01:59 30 Jul., 2014

06:43 30 Jul. to 07:40 30 Jul., 2014

2.3 Surface Meteorological Observations

September 17, 2014

(1) Personnel

Masaki Katsumata	(JAMSTEC): Principal Investigator	
Ryo Oyama	(Global Ocean Development Inc., GODI)	-leg1-
Souichiro Sueyoshi	(GODI)	-leg1-
Katsuhisa Maeno	(GODI)	-leg1-
Koichi Inagaki	(GODI)	-leg1-
Wataru Tokunaga	(GODI)	-leg2-
Kazuho Yoshida	(GODI)	-leg2-
Tetsuya Kai	(GODI)	-leg2-
Yutaro Murakami	(GODI)	-leg1, leg2-
Masanori Murakami	(MIRAI Crew)	-leg1, leg2-

(2) Objectives

Surface meteorological parameters are observed as a basic dataset of the meteorology. These parameters provide the temporal variation of the meteorological condition surrounding the ship.

(3) Methods

Surface meteorological parameters were observed during the MR14-04 cruise from 8th July 2014 to 29th August 2014, except for the USA territorial waters. In this cruise, we used two systems for the observation.

i) MIRAI Surface Meteorological observation (SMet) system

Instruments of SMet system are listed in Table 2.3.1 and measured parameters are listed in Table 2.3.2. Data were collected and processed by KOAC-7800 weather data processor made by Koshin-Denki, Japan. The

data set consists of 6-second averaged data.

ii) Shipboard Oceanographic and Atmospheric Radiation (SOAR) measurement system

SOAR system designed by BNL (Brookhaven National Laboratory, USA) consists of major five parts.

- Portable Radiation Package (PRP) designed by BNL - short and long wave downward radiation.
- Analog meteorological data sampling with CR1000 logger manufactured by Campbell Inc. Canada - wind, pressure, and rainfall (by a capacitive rain gauge) measurement.
- Digital meteorological data sampling from individual sensors - air temperature, relative humidity and rainfall (by ORG (optical rain gauge)) measurement.
- Photosynthetically Available Radiation (PAR) sensor manufactured by Biospherical Instruments Inc. (USA) - PAR measurement.
- Scientific Computer System (SCS) developed by NOAA (National Oceanic and Atmospheric Administration, USA) - centralized data acquisition and logging of all data sets.

SCS recorded PRP data every 6 seconds, CR1000 data every 10 seconds, air temperature and relative humidity data every 2 seconds and ORG data every 5 seconds. SCS composed Event data (JamMet) from these data and ship's navigation data. Instruments and their locations are listed in Table 2.3.3 and measured parameters are listed in Table 2.3.4.

For the quality control as post processing, we checked the following sensors, before and after the cruise.

- Young rain gauge (SMet and SOAR)
Inspect of the linearity of output value from the rain gauge sensor to change input value by adding fixed quantity of test water.
- Barometer (SMet and SOAR)
Comparison with the portable barometer value, PTB220, VAISALA
- Thermometer (air temperature and relative humidity) (SMet and SOAR)
Comparison with the portable thermometer value, HMP41/45, VAISALA

(4) Preliminary results

Figs. 2.3-1 shows the time series of the following parameters;

Wind (SOAR)

Air temperature (SMet)

Relative humidity (SMet)

Precipitation (SOAR, rain gauge)

Short/long wave radiation (SOAR)

Pressure (SMet)

Sea surface temperature (SMet)

Significant wave height (SMet)

(5) Data archives

These meteorological data will be submitted to the Data Management Group (DMG) of JAMSTEC just after the cruise.

(6) Remarks (Times in UTC)

- i) Data acquisition was suspended in the territorial waters of USA.
- ii) The following periods, sea surface temperature of SMet data was available.
 - Leg 1: 01:39, 09 Jul. 2014 - 23:31, 14 Jul. 2014
 - Leg 2: 02:04, 17 Jul. 2014 - 12:30, 28 Aug. 2014
- iii) The following periods, navigation data (position, speed and course over ground) of SMet and JamMet were often invalid due to position fix error for loss of detected GPS satellites.
 - Leg 1: 14 Jul. to 15 Jul. 2014
 - Leg 2: 17 Jul. to 16 Aug. 2014
- iv) The following period, navigation data of SMet was invalid due to network server trouble.
 - Leg 2: 12:37, 23 Aug. 2014 - 12:44, 23 Aug. 2014
- v) The following period, ship gyro and LOG of JamMet were invalid due to communication error to network

server.

Leg 1: 07:57:06, 18:38:32; 11 Jul. 2014

Leg 2: 11:28:40, 08 Aug. 2014

19:21:00, 21 Aug. 2014

- vi) The following time, increasing of SMet capacitive rain gauge data were invalid due to test transmitting for VHF radio.

Leg 2: 14:23, 23:14; 19 Jul. 2014

05:18, 25 Jul. 2014

06:17, 26 Jul. 2014

06:06, 18:32; 27 Jul. 2014

18:13, 28 Jul. 2014

06:04, 17:19; 30 Jul. 2014

- vii) The following period, PRP data was invalid due to PC trouble.

Leg 1: 01:08, 09 Jul. 2014 - 01:25, 09 Jul. 2014

14:48, 09 Jul. 2014 - 14:54, 09 Jul. 2014

- viii) The following period, logging interval of PRP was longer than normal.

Leg 1: 08:50, 09 Jul. 2014 - 14:54, 09 Jul. 2014

- ix) The following period, ORG data was invalid due to sensor error.

Leg 2: 19:37:51 to 19:40:33, 27 Aug. 2014,

Table 2.3.1. Instruments and installation locations of MIRAI Surface Meteorological observation system.

Sensors	Type	Manufacturer	Location (altitude from surface)
Anemometer	KE-500	Koshin Denki, Japan	foremast (24 m)
Tair/RH	HMP155	Vaisala, Finland	
with 43408 Gill aspirated radiation shield		R.M. Young, USA	compass deck (21 m) starboard side and port side
Thermometer: SST	RFN2-0	Koshin Denki, Japan	4th deck (-1m, inlet -5m)
Barometer	Model-370	Setra System, USA	captain deck (13 m) weather observation room
Capacitive rain gauge	50202	R. M. Young, USA	compass deck (19 m)
Optical rain gauge	ORG-815DS	Osi, USA	compass deck (19 m)
Radiometer (short wave)	MS-802	Eko Seiki, Japan	radar mast (28 m)
Radiometer (long wave)	MS-202	Eko Seiki, Japan	radar mast (28 m)
Wave height meter	WM-2	Tsurumi-seiki, Japan	bow (10 m)

Table 2.3.2. Parameters of MIRAI Surface Meteorological observation system.

Parameter	Units	Remarks
1 Latitude	degree	
2 Longitude	degree	
3 Ship's speed	knot	Mirai log, DS-30 Furuno

4 Ship's heading	degree	Mirai gyro, TG-6000,TOKYO-KEIKI
5 Relative wind speed	m/s	6sec./10min. averaged
6 Relative wind direction	degree	6sec./10min. averaged
7 True wind speed	m/s	6sec./10min. averaged
8 True wind direction	degree	6sec./10min. averaged
9 Barometric pressure	hPa	adjusted to sea surface level 6sec. averaged
10 Air temperature (starboard side)	degC	6sec. averaged
11 Air temperature (port side)	degC	6sec. averaged
12 Dewpoint temperature (starboard side)	degC	6sec. averaged
13 Dewpoint temperature (port side)	degC	6sec. averaged
14 Relative humidity (starboard side)	%	6sec. averaged
15 Relative humidity (port side)	%	6sec. averaged
16 Sea surface temperature	degC	6sec. averaged
17 Rain rate (optical rain gauge)	mm/hr	hourly accumulation
18 Rain rate (capacitive rain gauge)	mm/hr	hourly accumulation
19 Down welling shortwave radiation	W/m ²	6sec. averaged
20 Down welling infra-red radiation	W/m ²	6sec. averaged
21 Significant wave height (bow)	m	hourly
22 Significant wave height (aft)	m	hourly
23 Significant wave period (bow)	second	hourly
24 Significant wave period (aft)	second	hourly

Table 2.3.3. Instruments and installation locations of SOAR system.

Sensors	Type	Manufacturer	Location (altitude from surface)
<i>Meteorological</i>			
Anemometer	05106	R.M. Young, USA	foremast (25 m)
Barometer with 61002 Gill pressure port	PTB210	Vaisala, Finland	
		R.M. Young, USA	foremast (23 m)
Capacitive rain gauge	50202	R.M. Young, USA	foremast (24 m)
Tair/RH	HMP155	Vaisala, Finland	
with 43408 Gill aspirated radiation shield		R.M. Young, USA	foremast (23 m)
Optical rain gauge	ORG-815DR	Osi, USA	foremast (24 m)
<i>PRP</i>			
Radiometer (short wave)	PSP	Epply Labs, USA	foremast (25 m)
Radiometer (long wave)	PIR	Epply Labs, USA	foremast (25 m)
Fast rotating shadowband radiometer		Yankee, USA	foremast (25 m)
<i>PAR</i>			
PAR sensor	PUV-510B	Biospherical Instruments Inc., USA	Navigation deck (18m)

Table 2.3.4. Parameters of SOAR system (JamMet).

Parameter	Units	Remarks
1 Latitude	degree	
2 Longitude	degree	
3 SOG	knot	
4 COG	degree	
5 Relative wind speed	m/s	
6 Relative wind direction	degree	
7 Barometric pressure	hPa	
8 Air temperature	degC	
9 Relative humidity	%	
10 Rain rate (optical rain gauge)	mm/hr	
11 Precipitation (capacitive rain gauge)	mm	reset at 50 mm
12 Down welling shortwave radiation	W/m ²	
13 Down welling infra-red radiation	W/m ²	
14 Defuse irradiance	W/m ²	
15 PAR	E/cm ² /sec	

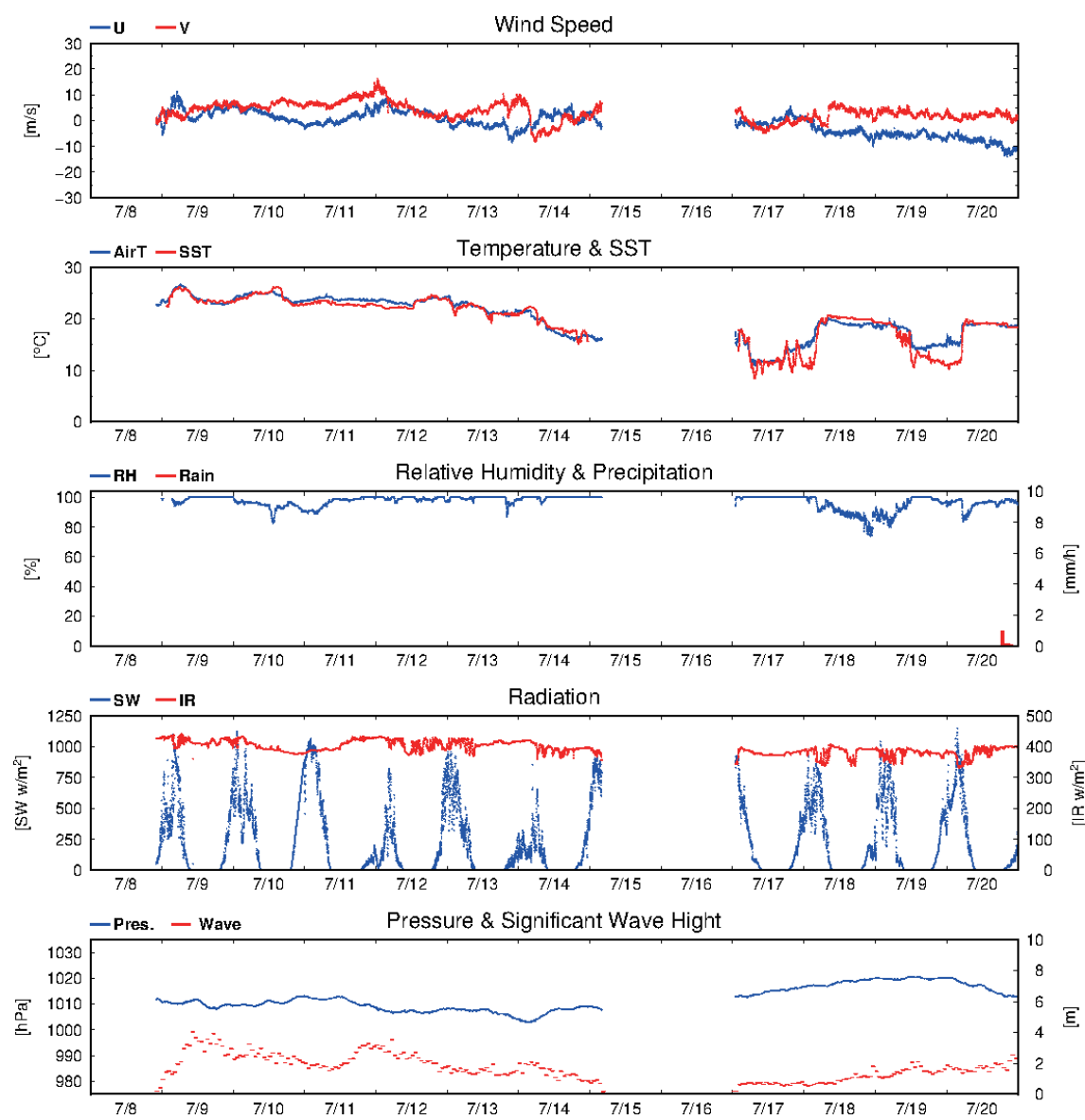


Figure 2.3.1. Time series of surface meteorological parameters during the MR14-04 cruise.

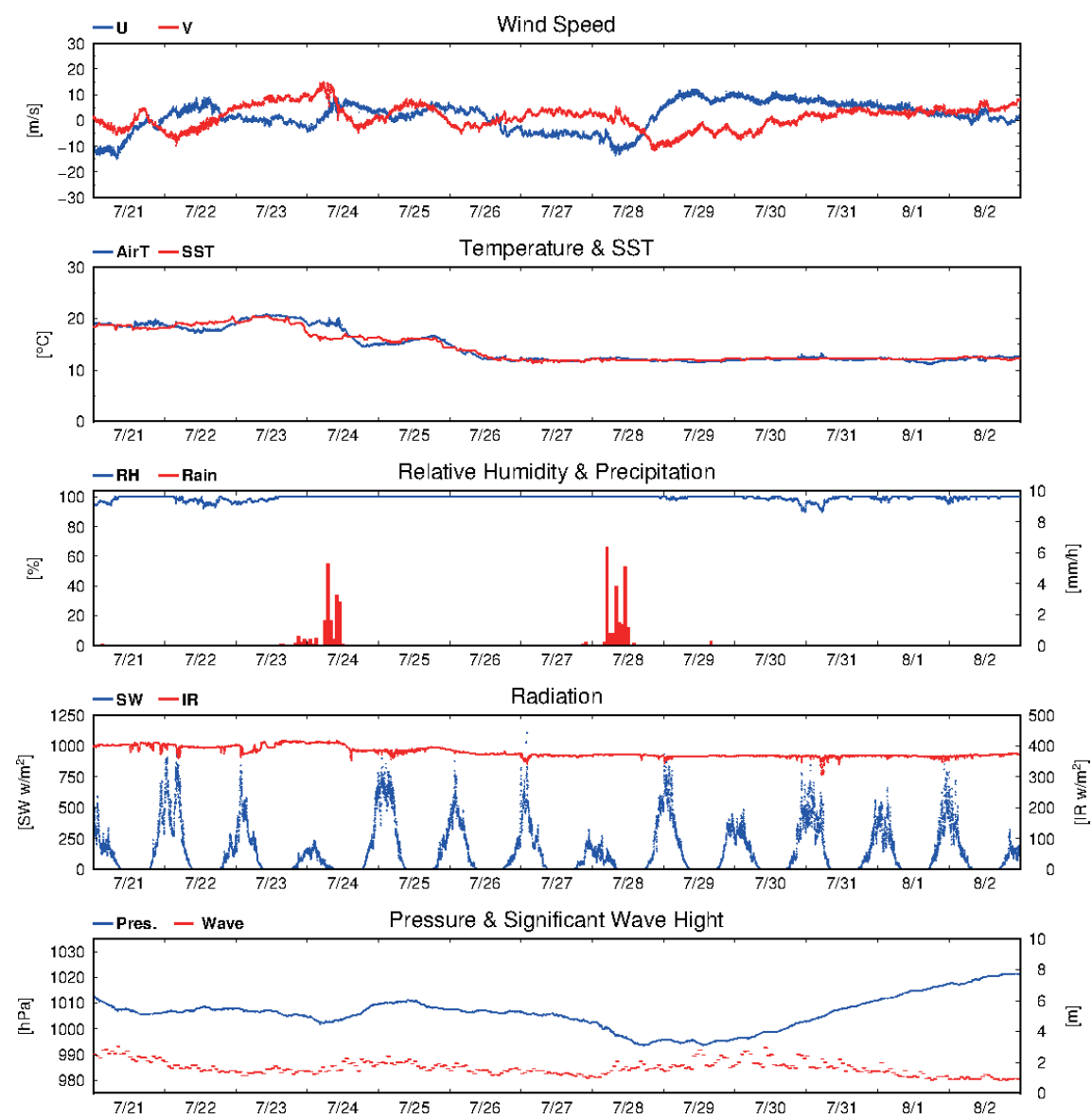


Fig. 2.3.1. (Continued)

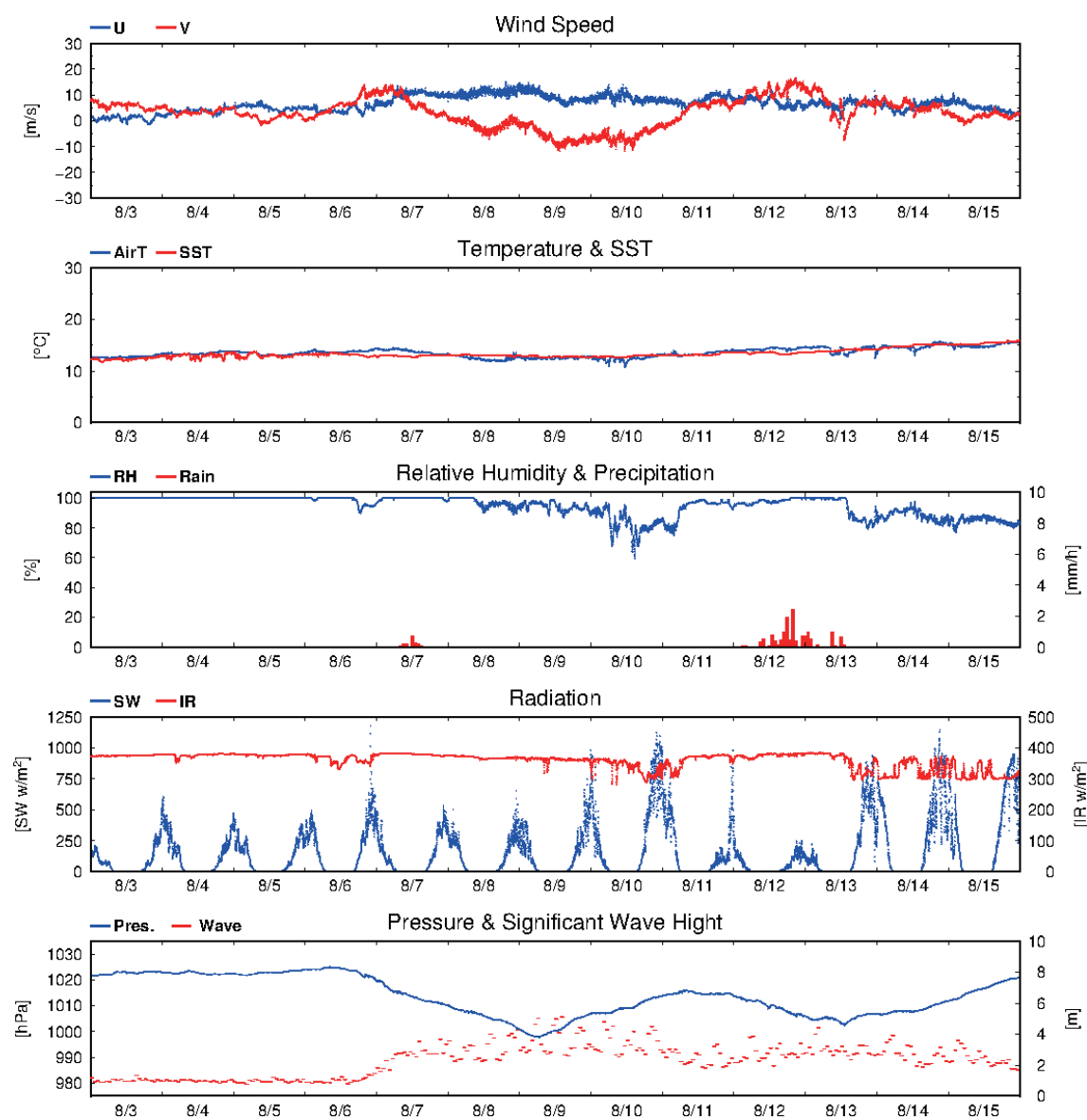


Figure 2.3.1. (Continued)

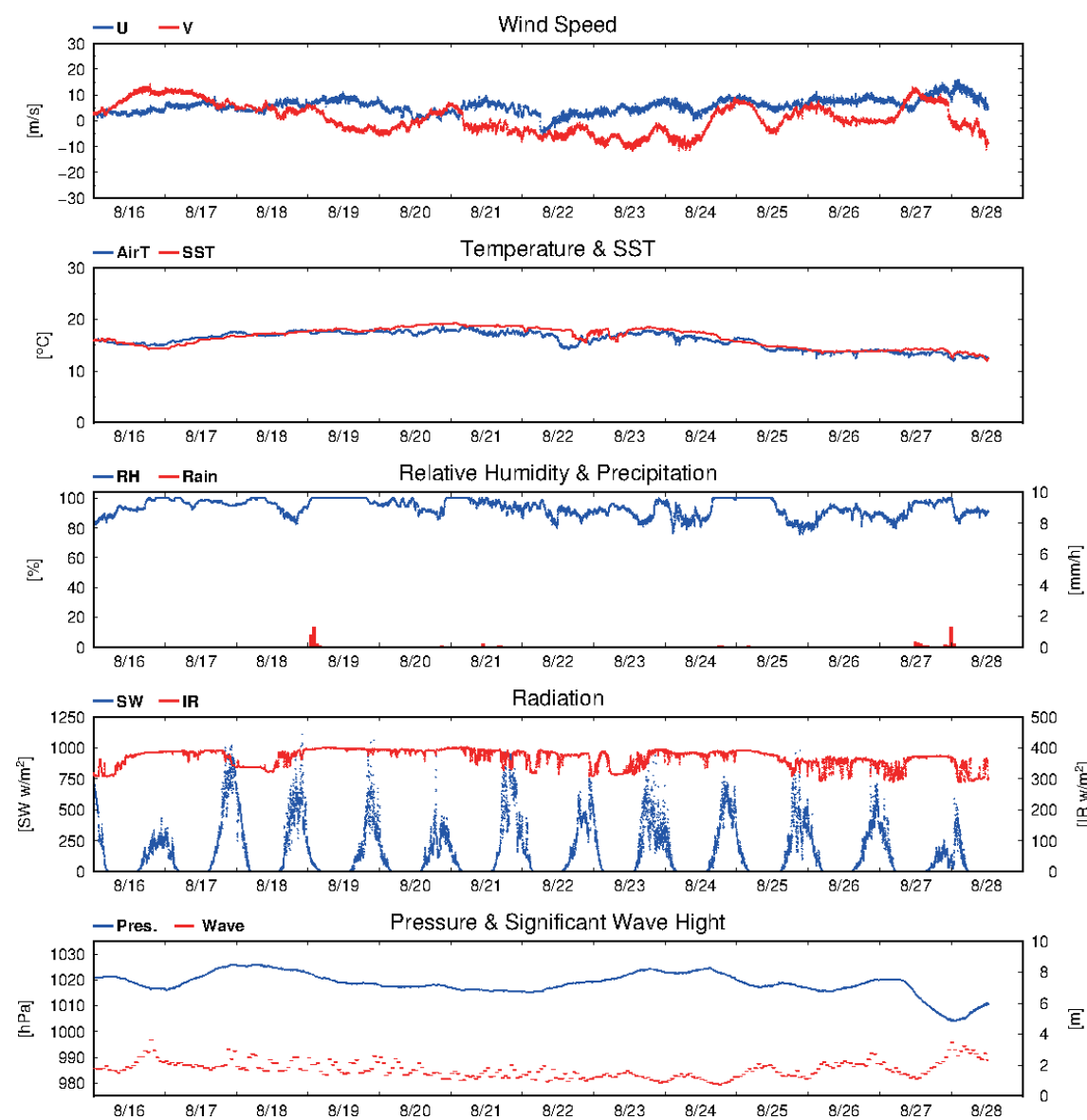


Figure 2.3.1. (Continued)

2.4 Thermo-Salinograph and Related Measurements

September 25, 2014

(1) Personnel

Hiroshi Uchida (JAMSTEC)

Keitaro Matsumoto (MWJ)

Katsunori Sagishima (MWJ)

Haruka Tamada (MWJ)

(2) Objectives

The objective is to collect sea surface salinity, temperature, dissolved oxygen, fluorescence, and nitrate data continuously along the cruise track.

(3) Materials and methods

The Continuous Sea Surface Water Monitoring System (Marine Works Japan Co, Ltd.) has six sensors and automatically measures salinity, temperature, dissolved oxygen, and fluorescence in sea surface water every one minute. This system is located in the sea surface monitoring laboratory and connected to shipboard LAN system. Measured data along with time and location of the ship were displayed on a monitor and stored in a desktop computer. The sea surface water was continuously pumped up to the laboratory from about 5 m water depth and flowed into the system through a vinyl-chloride pipe. The flow rate of the surface seawater was controlled to be about 1.2 L/min. Periods of measurement, maintenance and problems are listed in Table 2.4.1.

A chemical-free nitrate sensor was also used with the Continuous Sea Surface Water Monitoring System in leg 2. The nitrate sensor was attached using a flow cell next to the thermo-salinograph.

Software and sensors used in this system are listed below.

i. Software

Seamoni-kun Ver.1.50

ii. Sensors

Temperature and conductivity sensor

Model: SBE-45, SEA-BIRD ELECTRONICS, INC.

Serial number: 4552788-0319

Bottom of ship thermometer

Model: SBE 38, SEA-BIRD ELECTRONICS, INC.

Serial number: 3852788-0457

Dissolved oxygen sensor

Model: OPTODE 3835, Aanderaa Data Instruments, AS.

Serial number: 1519

Model: RINKO-II, JFE Advantech Co. Ltd.

Serial number: 0013

Fluorometer

Model: C3, TURNER DESIGNS

Serial number: 2300123

Nitrate sensor

Model: Deep SUNA, Satlantic, LP. (used only for leg 2)

Serial number: 0385

Table 2.4.1. Events of the Continuous Sea Surface Water Monitoring System operation.

System Date [UTC]	System Time [UTC]	Event
2014/07/09	02:32	Logging for leg 1 start
2014/07/14	23:30	Logging for leg 1 end
2014/07/17	02:50	Logging for leg 2 start
2014/07/28	23:52	Logging stop for filter cleaning
2014/07/29	00:48	Logging restart
2014/08/12	01:42	Logging stop for filter cleaning
2014/08/12	03:20	Logging restart
2014/08/22	02:27	Logging stop for filter cleaning
2014/08/22	03:27	Logging restart
2014/08/25	16:55	Logging stop for filter cleaning
2014/08/25	17:00	Logging restart
2014/08/28	12:29	Logging for leg 2 end

(4) Data Processing and Quality Control

The navigation data (latitude and longitude) for leg 2 was often invalid due to position fix error for loss of GPS satellites. The invalid navigation data were replaced by using the dataset “interpoGGA”. The “interpoGGA” was made using all available navigation data and was interpolated on a time interval of 1 second and low-pass filtered with a window of 20 seconds.

Data from the Continuous Sea Surface Water Monitoring System were obtained at 1 minute intervals. Data from the nitrate sensor were obtained at 1 minute intervals until 2014/07/18 03:50. However, the nitrate sensor frequently continued to show invalid data (-1.0) and needed to restart the system. Therefore, the time interval was changed to 2 minutes since then.

These data were processed as follows. Spikes in the temperature and salinity data were removed using a median filter with a window of 3 scans (3 minutes) when difference between the original data and the median

filtered data was larger than 0.1 °C for temperature and 0.5 for salinity. Data gaps were linearly interpolated when the gap was ≤ 7 minutes. Fluorometer data were low-pass filtered using a median filter with a window of 3 scans (3 minutes) to remove spikes. Raw data from the RINKO oxygen sensor, fluorometer and nitrate data were low-pass filtered using a Hamming filter with a window of 15 scans (15 minutes).

Salinity (S [PSU]), dissolved oxygen (O [$\mu\text{mol/kg}$]), fluorescence (Fl [RFU]), and nitrate (NRA [$\mu\text{mol/kg}$]) data were corrected using the water sampled data. Details of the measurement methods are described in Sections 3.2, 3.4, 3.5, and 3.8 for salinity, dissolved oxygen, nitrate and chlorophyll-a, respectively. Corrected salinity (S_{cor}), dissolved oxygen (O_{cor}), estimated chlorophyll *a* (Chl-a), and nitrate (NRA_{cor}) were calculated from following equations

$$S_{\text{cor}} [\text{PSU}] = c_0 + c_1 S + c_2 t$$

$$O_{\text{cor}} [\mu\text{mol/kg}] = c_0 + c_1 O + c_2 T + c_3 t$$

$$\text{Chl-a} [\mu\text{g/L}] = c_0 + c_1 \text{Fl}$$

$$\text{NRA}_{\text{cor}} [\mu\text{mol/kg}] = \text{NRA} + c_0 + c_1 t$$

where S is practical salinity, t is days from a reference time (2014/07/09 02:32 [UTC]), T is temperature in °C. The best fit sets of calibration coefficients (c_0 – c_3) were determined by a least square technique to minimize the deviation from the water sampled data. The calibration coefficients were listed in Table 2.4.2. Comparisons between the Continuous Sea Surface Water Monitoring System data and water sampled data are shown in from Figs. 2.4.1 to 2.4.4.

For fluorometer data, water sampled data obtained at night [PAR (Photosynthetically Available Radiation) $< 50 \mu\text{E}/(\text{m}^2 \text{sec})$, see Section 2.3] were used for the calibration, since sensitivity of the fluorometer to chlorophyll *a* is different at nighttime and daytime (Section 2.4 in Uchida et al., 2015). Sensitivity of the fluorometer to chlorophyll *a* may be also different between high and low temperature. Therefore, slope (c_1) of the calibration coefficients was changed for temperature range (Table 2.4.3). For temperature between 20.5 °C and 19.5 °C, chlorophyll *a* was estimated from weighted mean of the two equations as

$$\text{Chl-a} = \text{Chl-a}_1 f_2 + \text{Chl-a}_2 f_1$$

$$f_1 = 1 - (\text{TSG temperature} + 19.5 \text{ °C})$$

$$f_2 = 1 - f_1$$

where Chl- a_1 is chlorophyll a calculated by using the set of coefficients A, and Chl- a_2 is chlorophyll a calculated by using the set of coefficients B (Table 2.4.2).

Noise of the nitrate data tended to become large over time (Fig. 2.4.4). Dismounting of the flow cell improved the data quality probably because the optical windows were wiped and cleaned by the O rings of the flow cell. Data affected by the large noise were flagged as questionable data (Fig. 2.4.4).

(5) Reference

Uchida, H., K. Katsumata, and T. Doi (eds.) (2015): WHP P14S, S04I Revisit in 2012 Data Book, 187 pp., JAMSTEC.

Table 2.4.2. Calibration coefficients for the salinity, dissolved oxygen, and chlorophyll a , and nitrate.

c0	c1	c2	c3
<i>Salinity</i>			
-8.026137e-02	1.002264	4.381446e-04	
<i>Dissolved oxygen</i>			
5.929262	0.9575661	0.1590061	-5.164405e-02
<i>Chlorophyll a</i>			
4.845356e-02	0.1030891 (A: for TSG temperature ≥ 20.5 °C)		
4.845356e-02	5.411620e-02 (B: for TSG temperature < 19.5 °C)		
<i>Nitrate</i>			
-23.140	2.7154355 ($t \leq 14.76$)		
14.304	0.2678845 ($14.76 < t \leq 34.0$)		
-29.419	1.044715855 ($34.0 < t \leq 44.0$)		
-46.856	1.044715855 ($44.0 < t$)		

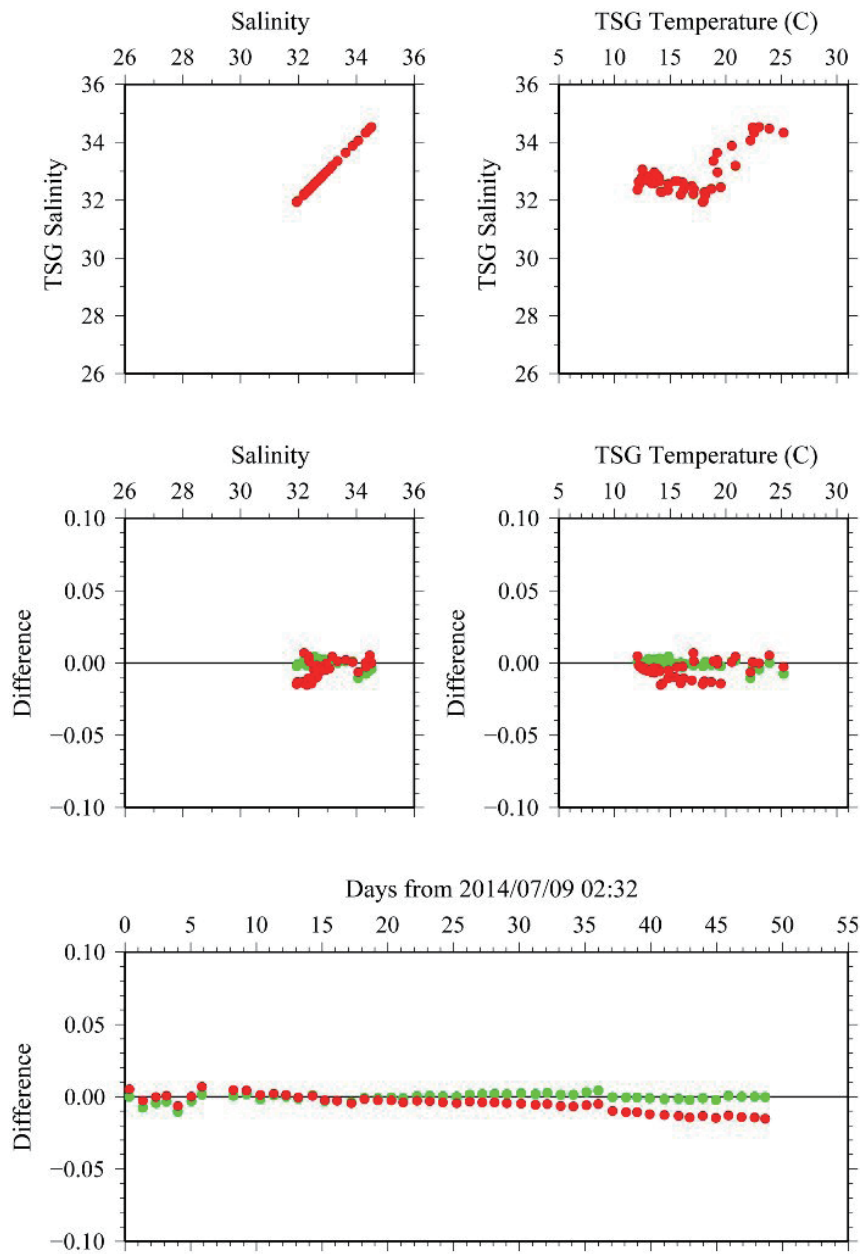


Figure 2.4.1. Comparison between TSG salinity (red: before correction, green: after correction) and sampled salinity.

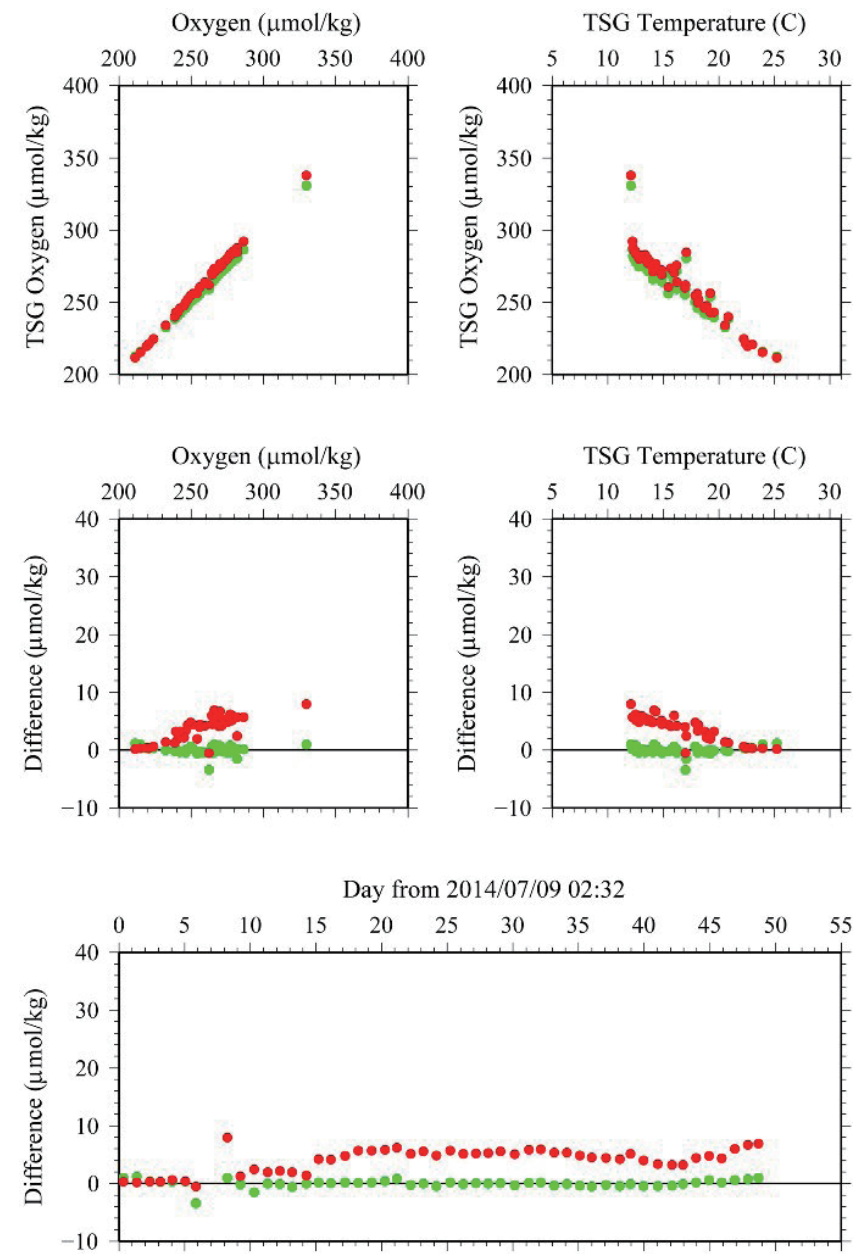


Figure 2.4.2. Comparison between TSG oxygen (red: before correction, green: after correction) and sampled oxygen.

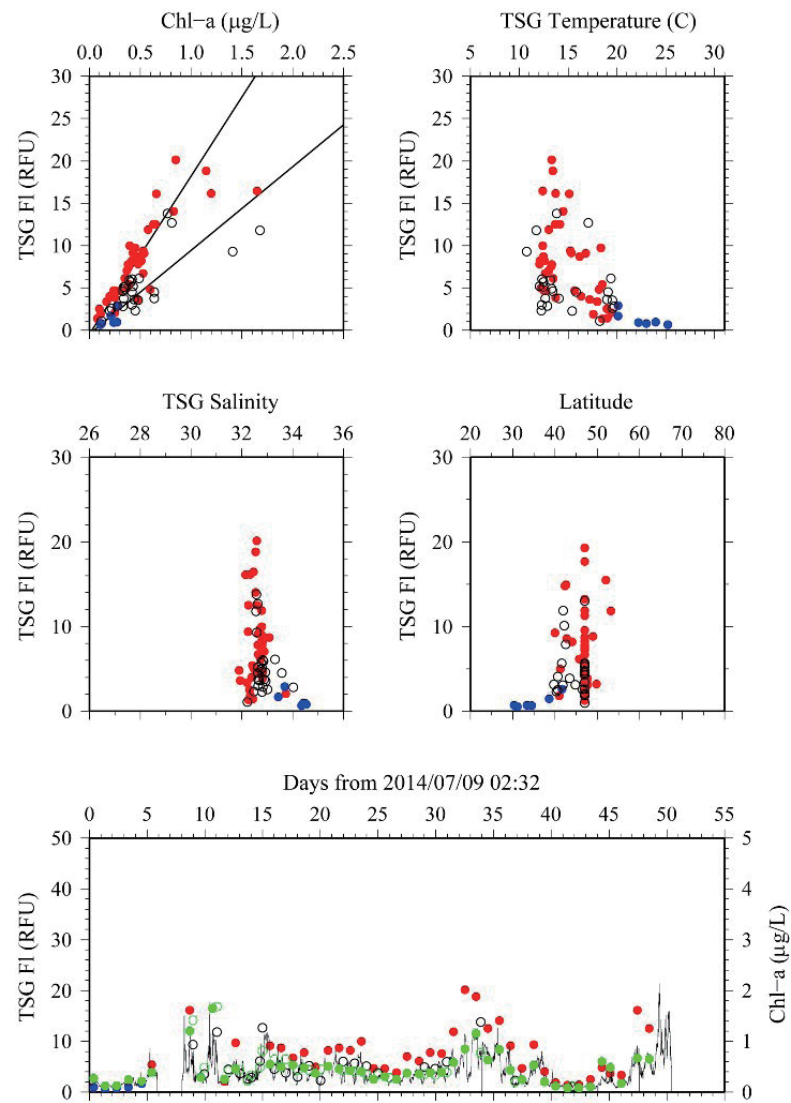


Figure 2.4.3. Comparison between TSG fluorescence and sampled chlorophyll *a*. Open circles indicate the daytime data. Blue dots indicate data obtained at temperature higher than or equal to 20 °C and red dots indicate data obtained at temperature lower than 20 °C. For bottom panel, blue or red dots indicate fluorescence and green dots indicate water sampled chlorophyll *a*. Line indicates chlorophyll *a* estimated from fluorometer.

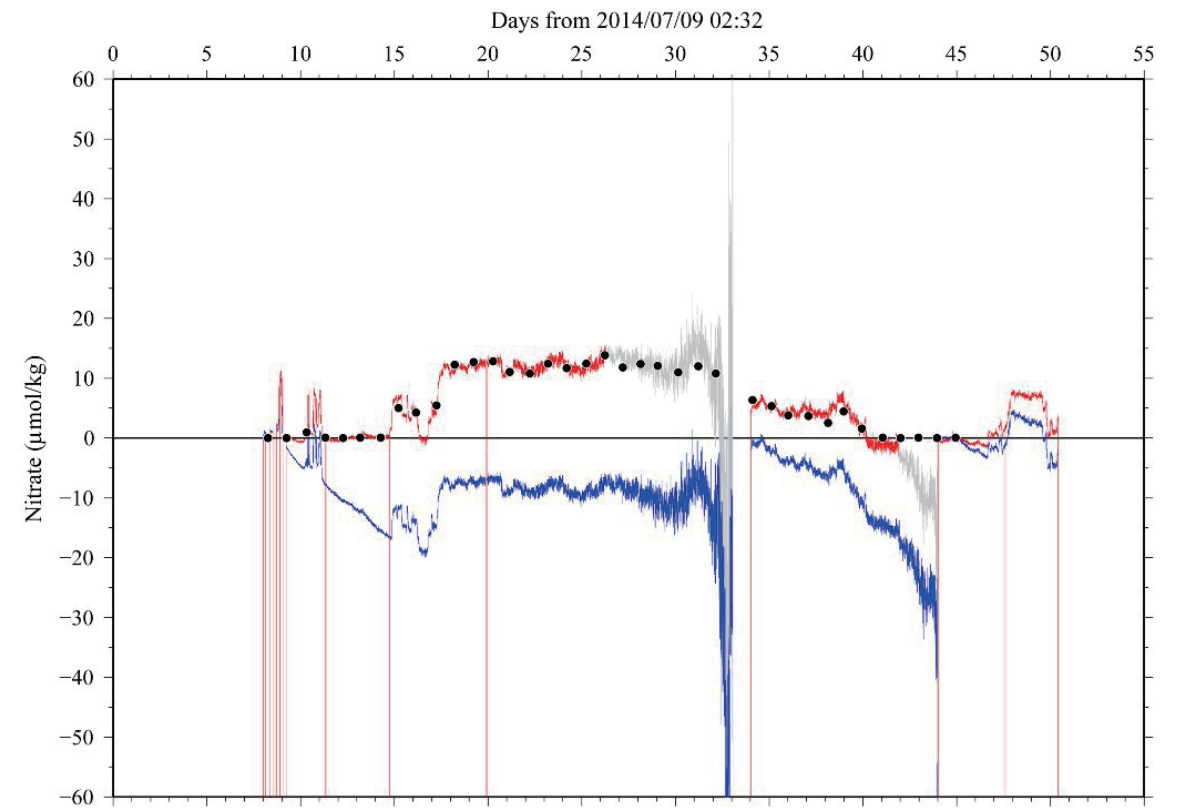


Figure 2.4.4. Comparison between TSG nitrate (blue line: before correction, red and gray lines: after correction) and sampled nitrate (dots). Gray lines indicate questionable data obtained during following periods: $26.3 < t \leq 34.0$ and $41.9 < t \leq 44.0$.

2.5 Underway pCO₂

February 1, 2017

(1) Personnel

Akihiko Murata	(JAMSTEC)
Yoshiko Ishikawa	(MWJ)
Atsushi Ono	(MWJ)

(2) Introduction

According to the latest report from Intergovernmental Panel on Climate Change, concentrations of CO₂ in the atmosphere have increased by 40% since pre-industrial times owing to human activities such as burning of fossil fuels, deforestation, and cement production. It is evaluated that the ocean has absorbed about 30% of the emitted anthropogenic CO₂. It is an urgent task to estimate as accurately as possible the absorption capacity of the oceans against the increased atmospheric CO₂, and to clarify the mechanism of the CO₂ absorption, because the magnitude of future global warming depends on the levels of CO₂ in the atmosphere.

The North Pacific is one of the regions where uncertainty of uptake of anthropogenic CO₂ is large. In this cruise, therefore, we were aimed at quantifying how much anthropogenic CO₂ is absorbed in the ocean interior of the North Pacific. For the purpose, we measured atmospheric and surface seawater partial pressures of CO₂ (pCO₂) along the extended WHP P10 and P01 lines at 149°E and 47°N, respectively, in the North Pacific.

(3) Apparatus and shipboard measurement

Continuous underway measurements of atmospheric and surface seawater pCO₂ were made with the CO₂ measuring system (Nippon ANS, Ltd) installed in the R/V *Mirai* of JAMSTEC. The system comprises of a non-dispersive infrared gas analyzer (Li-COR LI-7000), an air-circulation module and a showerhead-type equilibrator. To measure concentrations (mole fraction) of CO₂ in dry air (xCO₂a), air sampled from the bow

of the ship (approx. 30 m above the sea level) was introduced into the NDIR through a dehydrating route with an electric dehumidifier (kept at ~2 °C), a Perma Pure dryer (GL Sciences Inc.), and a chemical desiccant (Mg(ClO₄)₂). The flow rate of the air was 500 ml min⁻¹. To measure surface seawater concentrations of CO₂ in dry air (xCO₂s), the air equilibrated with seawater within the equilibrator was introduced into the NDIR through the same flow route as the dehydrated air used in measuring xCO₂a. The flow rate of the equilibrated air was 400 – 900 ml min⁻¹. The seawater was taken by a pump from the intake placed at the approx. 4.5 m below the sea surface. The flow rate of seawater in the equilibrator was 4000 – 5000 ml min⁻¹.

The CO₂ measuring system was set to repeat the measurement cycle such as 4 kinds of CO₂ standard gases (Table 2.5.1), xCO₂a (twice), xCO₂s (7 times). This measuring system was run automatically throughout the cruise by a PC control.

(4) Quality control

Concentrations of CO₂ of the standard gases are listed in Table 2.5.1, which were calibrated after cruise by the JAMSTEC primary standard gases. The CO₂ concentrations of the primary standard gases were calibrated by the Scripps Institution of Oceanography, La Jolla, CA, USA.

In actual shipboard observations, the signals of NDIR usually reveal a trend. The trends were adjusted linearly using the signals of the standard gases analyzed before and after the sample measurements.

Effects of water temperature increased between the inlet of surface seawater and the equilibrator on xCO₂s were adjusted based on Takahashi *et al.* (1993), although the temperature increases were slight, being ~0.3 °C.

We checked values of xCO₂a and xCO₂s by examining signals of the NDIR by plotting the xCO₂a and xCO₂s as a function of sequential day, longitude, sea surface temperature and sea surface salinity.

(5) Reference

Takahashi, T., J. Olafsson, J. G. Goddard, D. W. Chipman, and S. C. Southerland (1993) Seasonal variation of CO₂ and nutrients in the high-latitude surface oceans: a comparative study, *Global Biogeochem. Cycles*, 7, 843 – 878.

Table 2.5.1. Concentrations of CO₂ standard gases used during the North Pacific cruise.

Cylinder no.	Concentrations (ppmv)
CQB09459	249.59
CQB09354	299.03
CQB06574	398.90
CRC00732	448.90

2.6 Shipboard ADCP

November 21, 2016

(1) Personnel

Shinya Kouketsu	(JAMSTEC)	: Principal Investigator
Ryo Oyama	(Global Ocean Development Inc., GODI)	-leg1-
Souichiro Sueyoshi	(GODI)	-leg1-
Katsuhisa Maeno	(GODI)	-leg1-
Koichi Inagaki	(GODI)	-leg1-
Wataru Tokunaga	(GODI)	-leg2-
Kazuho Yoshida	(GODI)	-leg2-
Tetsuya Kai	(GODI)	-leg2-
Yutaro Murakami	(GODI)	-leg1, leg2-
Masanori Murakami	(MIRAI Crew)	-leg1, leg2-

(2) Objective

To obtain continuous measurement of the current profile along the ship's track.

(3) Methods

Upper ocean current measurements were made in the MR14-04 Leg1 and Leg2 cruises, using the hull-mounted Acoustic Doppler Current Profiler (ADCP) system. For most of its operation the instrument was configured for water-tracking mode. Bottom-tracking mode, interleaved bottom-ping with water-ping, was made to get the calibration data for evaluating transducer misalignment angle in the shallow water. The system consists of following components;

- i) R/V MIRAI has installed vessel-mount ADCP (acoustic frequency 76.8 kHz "Ocean Surveyor", Teledyne RD Instruments). It has a phased-array transducer with single ceramic assembly and creates 4 acoustic

beams electronically. We mounted the transducer head rotated to a ship-relative angle of 45 degrees azimuth from the keel.

- ii) For heading source, we use ship's gyro compass (TOKYO KEIKI, Japan), continuously providing heading to the ADCP system directory. Also we have Inertial Navigation System (PHINS, IXBLUE) which provide high-precision heading and attitude information are stored in ".N2R" data files.
- iii) DGPS system (Trimble SPS751 & StarFixXP) and GPS systems (Trimble 4000DS and FURUNO GP-36) providing position fixes. We selected the best system according to their positioning condition.
- iv) We used VmDas version 1.46.5 (TRDI) for data acquisition.
- v) To synchronize time stamp of pinging with GPS time, the clock of the logging computer is adjusted to GPS time every 5 minutes.
- vi) The sound speed at the transducer does affect the vertical bin mapping and vertical velocity measurement, is calculated from temperature, salinity (constant value; 35.0 psu) and depth (6.5 m; transducer depth) by equation in Medwin (1975).

Data was configured for 8-m intervals starting 23-m below the surface. Every ping was recorded as raw ensemble data (.ENR). Also, 60 seconds and 300 seconds averaged data were recorded as short term average (.STA) and long term average (.LTA) data, respectively. Major parameters for the measurement (Direct Command) are shown in Table 2.6.1. After the cruises, we plan to carry out the alignment correction and provide the processed data.

(4) Preliminary results

Fig.2.6.1 and 2.6.2 shows surface current profile along the ship's track, averaged four depth cells from 12th to 15th, about 110 m to 135 m with 60 minutes average.

(5) Data archive

These data obtained in this cruise will be submitted to the Data Management Group (DMG) of

JAMSTEC, and will be opened to the public via JAMSTEC home page.

Table 2.6.1. Major parameters

(6) Remarks (Times in UTC)

- i) Data acquisition was suspended in the territorial waters of USA.
- ii) During the Leg1 cruise, background signal under sail was large due to biofouling on the ship bottom window.
- iii) The following periods, data acquisition was suspended for system condition check.
 - Leg1: 23:29UTC 09 Jul. 2014 - 00:15UTC 10 Jul. 2014
 - 05:55UTC 10 Jul. 2014 - 06:48UTC 10 Jul. 2014
 - 03:42UTC 11 Jul. 2014 - 04:11UTC 11 Jul. 2014
 - 11:13UTC 12 Jul. 2014 - 11:20UTC 12 Jul. 2014
 - 00:42UTC 14 Jul. 2014 - 01:07UTC 14 Jul. 2014
- iv) The following periods, navigation data was often invalid due to GPS position fix error.
 - Leg1: 14 Jul. to 15 Jul. 2014
 - Leg2: 17 Jul. to 16 Aug. 2014

(7) Processed data

The processed data were corrected with the ADCP misalignment calculated by comparison between bottom track and ship velocities during the cruise. In this cruise, as there are many outliers in the GPS data, we did not use the data 3 times standard deviation far from the positions averaged in 5000 minutes. After that, by inverse method with the available beam velocities during 5 minutes, we obtained the velocity profiles and their estimation errors.

Bottom-Track Commands

BP = 001	Pings per Ensemble (almost less than 1300m depth)
	Leg1: 22:32UTC 08 Jul. 2014 - 03:08UTC 09 Jul. 2014
	16:44UTC 14 Jul. 2014 - 03:45UTC 14 Jul. 2014
	Leg2: 00:07UTC 17 Jul. 2014 - 14:21UTC 17 Jul. 2014
	14:49UTC 22 Aug. 2014 - 23:59UTC 22 Aug. 2014
	11:57UTC 28 Aug. 2014 - 12:30UTC 28 Aug. 2014

Environmental Sensor Commands

EA = +04500	Heading Alignment (1/100 deg)
EB = +00000	Heading Bias (1/100 deg)
ED = 00065	Transducer Depth (0 - 65535 dm)
EF = +001	Pitch/Roll Divisor/Multiplier (pos/neg) [1/99 - 99]
EH = 00000	Heading (1/100 deg)
ES = 35	Salinity (0-40 pp thousand)
EX = 00000	Coord Transform (Xform:Type; Tilts; 3Bm; Map)
EZ = 10200010	Sensor Source (C; D; H; P; R; S; T; U)
	C (1): Sound velocity calculates using ED, ES, ET (temp.)
	D (0): Manual ED
	H (2): External synchro
	P (0), R (0): Manual EP, ER (0 degree)
	S (0): Manual ES
	T (1): Internal transducer sensor
	U (0): Manual EU

Timing Commands

TE = 00:00:02.00 Time per Ensemble (hrs:min:sec.sec/100)
TP = 00:02.00 Time per Ping (min:sec.sec/100)

Water-Track Commands

WA = 255 False Target Threshold (Max) (0-255 count)
WB = 1 Mode 1 Bandwidth Control (0=Wid, 1=Med, 2=Nar)
WC = 120 Low Correlation Threshold (0-255)
WD = 111 100 000 Data Out (V; C; A; PG; St; Vsum; Vsum^2;#G;P0)
WE = 1000 Error Velocity Threshold (0-5000 mm/s)
WF = 0800 Blank After Transmit (cm)
WG = 001 Percent Good Minimum (0-100%)
WI = 0 Clip Data Past Bottom (0 = OFF, 1 = ON)
WJ = 1 Rcvr Gain Select (0 = Low, 1 = High)
WM = 1 Profiling Mode (1-8)
WN = 100 Number of depth cells (1-128)
WP = 00001 Pings per Ensemble (0-16384)
WS = 0800 Depth Cell Size (cm)
WT = 000 Transmit Length (cm) [0 = Bin Length]
WV = 0390 Mode 1 Ambiguity Velocity (cm/s radial)

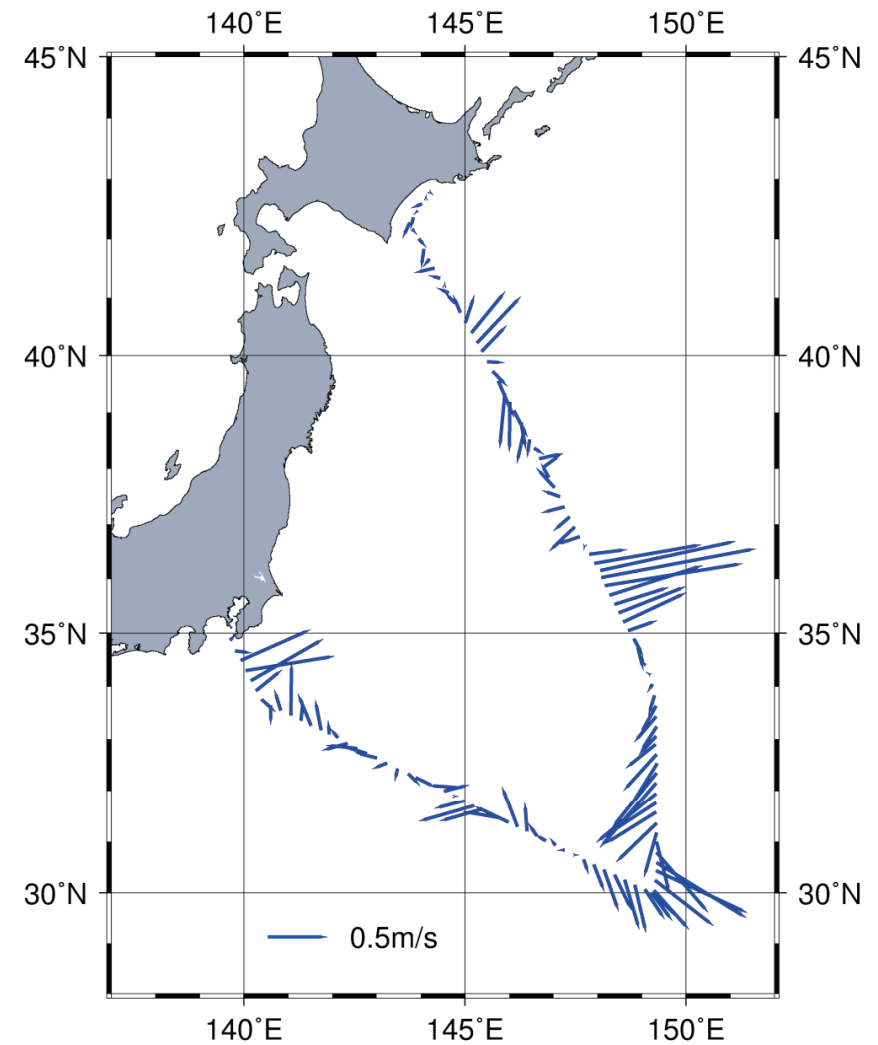


Figure 2.6.1. Current profile along the ship's track, about 110m to 136m depth, averaged every 60 minutes (Leg1).

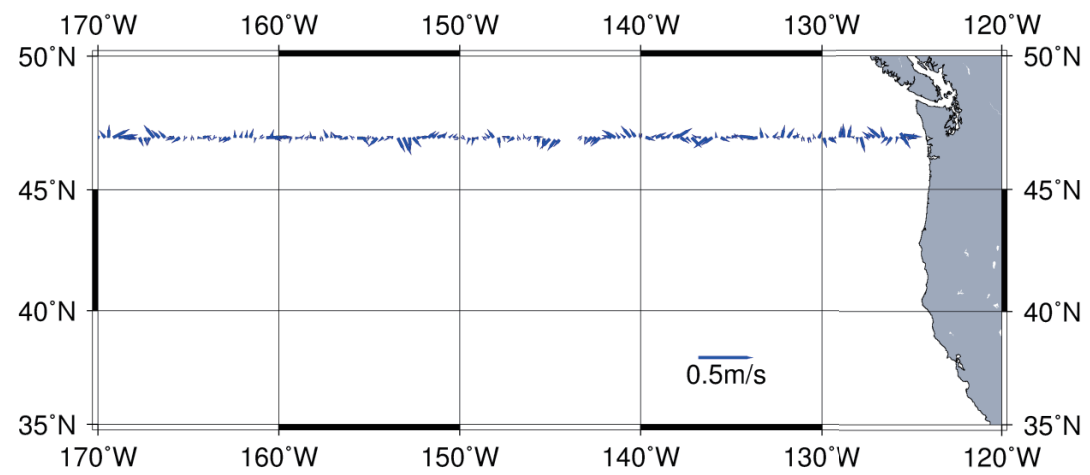
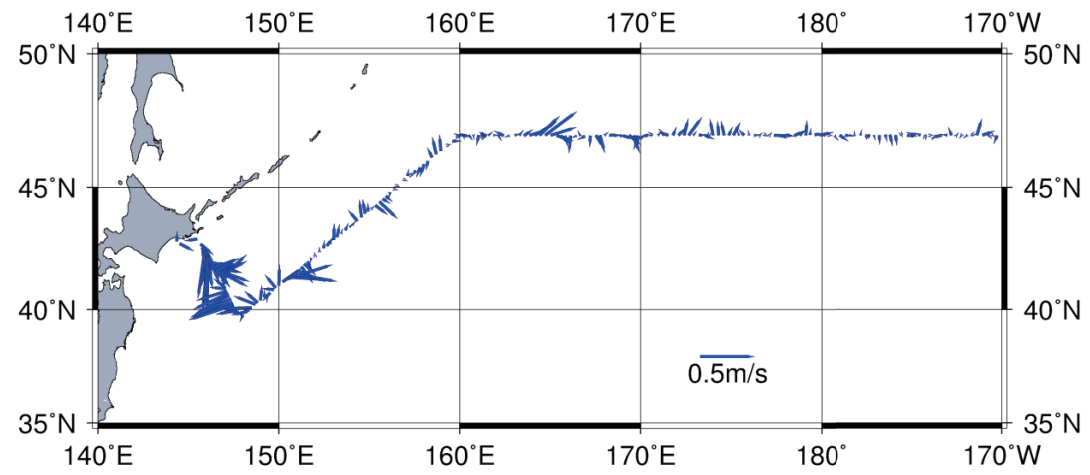


Figure 2.6.2. Current profile along the ship's track, about 110m to 135m depth, averaged every 60 minutes (Leg2).

2.7 XCTD

September 16, 2014

(1) Personnel

Hiroshi Uchida (JAMSTEC)
Ryo Oyama (GODI) (Leg 1)
Souichiro Sueyoshi (GODI) (Leg 1)
Katsuhisa Maeno (GODI) (Leg 1)
Koichi Inagaki (GODI) (Leg 1)
Yutaro Murakami (GODI) (Legs 1 and 2)
Wataru Tokunaga (GODI) (Leg 2)
Kazuho Yoshida (GODI) (Leg 2)
Tetsuya Kai (GODI) (Leg 2)

(2) Objectives

In this cruise, XCTD (eXpendable Conductivity, Temperature and Depth profiler) measurements were carried out to substitute for CTD measurements and to evaluate the fall rate equation and temperature by comparing with CTD (Conductivity, Temperature and Depth profiler) measurements.

(3) Instrument and Method

The XCTD used was XCTD-4 (Tsurumi-Seiki Co., Ltd., Yokohama, Kanagawa, Japan) with an MK-150N deck unit (Tsurumi-Seiki Co., Ltd.). The manufacturer's specifications are listed in Table 2.7.1. In this cruise, the XCTD probes were deployed by using 8-loading automatic launcher or hand launcher (Tsurumi-Seiki Co., Ltd.). For comparison with CTD, XCTD was deployed at about 10 minutes after the beginning of the down cast of the CTD (P10N_1, P10N_7, P10N_14, P10N_30, P01_77, P01_78, P01_80 and P01_81).

The fall-rate equation provided by the manufacturer was initially used to infer depth Z (m), $Z = at -$

bt^2 , where t is the elapsed time in seconds from probe entry into the water, and a (terminal velocity) and b (acceleration) are the empirical coefficients (Table 2.7.2).

(4) Data Processing and Quality Control

The XCTD data were processed and quality controlled based on a method by Uchida et al. (2011). Differences between XCTD and CTD depths were shown in Fig. 2.7.1. The terminal velocity error was estimated for the XCTD-4 (Table 2.7.2). The XCTD data were corrected for the depth error by using the estimated terminal velocities. Differences of temperature on pressure surfaces were examined by using side-by-side XCTD and CTD data (Fig. 2.7.2). The XCTD data used were corrected for the depth error. Average thermal bias below 900 dbar was 0.011 °C. Mean of the thermal biases of XCTD data estimated from five cruises was 0.014 ± 0.004 °C (Table 2.7.3). The XCTD data were corrected for the mean thermal bias (0.014 °C). Differences of salinity on pressure surfaces were examined by using side-by-side XCTD and CTD data (Fig. 2.7.3). The XCTD data used were corrected for the depth error and thermal bias. Average salinity bias was 0.013 ± 0.007 (Table 2.7.4). The XCTD data were corrected for the salinity bias. Temperature-salinity plot using the quality controlled XCTD data is shown in Fig. 2.7.4.

(5) References

- Kizu, S., H. Onishi, T. Suga, K. Hanawa, T. Watanabe, and H. Iwamiya (2008): Evaluation of the fall rates of the present and developmental XCTDs. *Deep-Sea Res I*, **55**, 571–586.
- Uchida, H., K. Shimada, and T. Kawano (2011): A method for data processing to obtain high-quality XCTD data. *J. Atmos. Oceanic Technol.*, **28**, 816–826.
- Uchida, H., A. Murata, and T. Doi (eds.) (2014): WHP P10 Revisit in 2011 Data Book, 179 pp., JAMSTEC.
- Uchida, H., K. Katsumata, and T. Doi (eds.) (2015): WHP P14S, S04I Revisit in 2012 Data Book, 187 pp., JAMSTEC.

Table 2.7.1. Manufacturer's specifications of XCTD-4.

Parameter	Range	Accuracy
Conductivity	0 ~ 60 mS cm ⁻¹	±0.03 mS cm ⁻¹
Temperature	-2 ~ 35 °C	±0.02 °C
Depth	0 ~ 1850 m	5 m or 2%, whichever is greater *

* Depth error is shown in Kizu et al (2008).

Table 2.7.2. Manufacturer's coefficients for the fall-rate equation.

Model	<i>a</i> (terminal velocity, m/s)	<i>b</i> (acceleration, m/s ²)	<i>e</i> (terminal velocity error, m/s)
XCTD-4	3.68081	0.00047	-0.0075

Table 2.7.3. Thermal biases of the XCTD temperature data.

Cruise	Average thermal bias (°C)	Depth range	Source
MR09-01	0.016	>= 1100 dbar	Uchida et al. (2011)
KH-02-3	0.019	>= 1100 dbar	Uchida et al. (2011)
MR11-08	0.014	>= 1100 dbar	Uchida et al. (2014)
MR12-05	0.009	>= 400 dbar	Uchida et al. (2015)
MR14-04	0.011	>= 900 dbar	This report
<i>Mean</i>	0.014 ± 0.004		

Table 2.7.4. Salinity bias of the XCTD data.

Cruise	Average salinity bias	Data
MR14-04	0.013 ± 0.007	Stations 1, 7, 14, 30, 77, 78, 80, 81

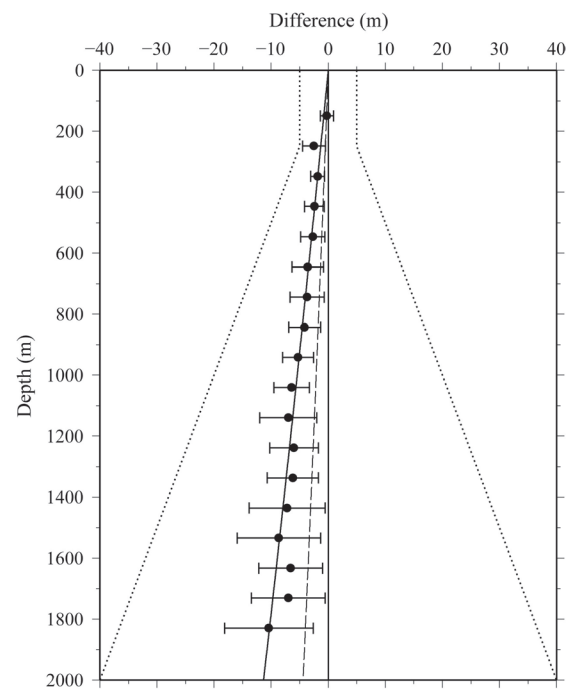


Figure 2.7.1. Differences between XCTD and CTD depths for XCTD-4. Differences were estimated with the same method as Uchida et al. (2011). Standard deviation of the estimates (horizontal bars) and the manufacturer's specification for XCTD depth error (dotted lines) are shown. The regressions for the data (solid line) and for the data obtained in the cruise MR12-05 (broken line) are also shown.

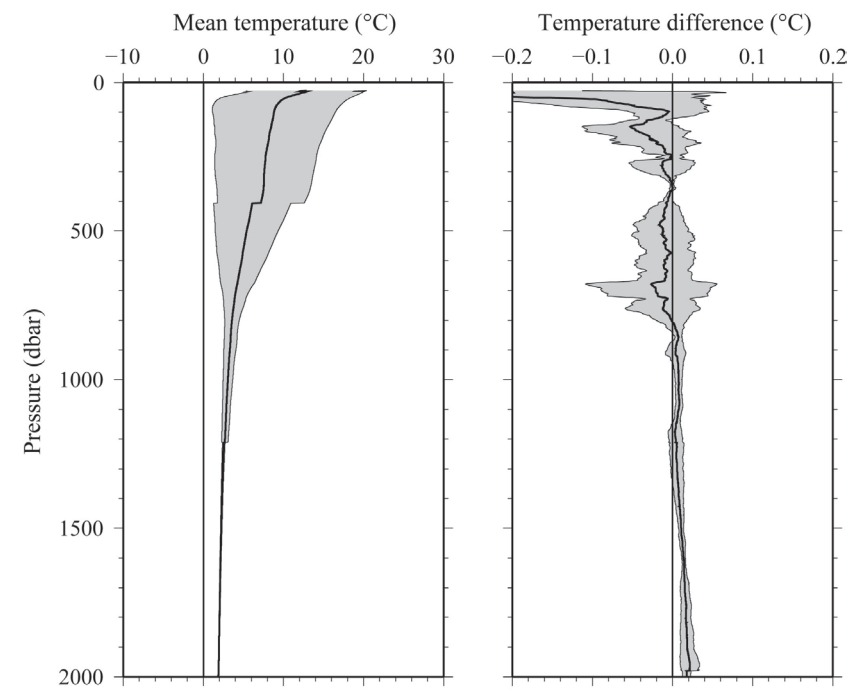


Figure 2.7.2. Comparison between XCTD and CTD temperature profiles. (a) Mean temperature of CTD profiles with standard deviation (shade) and (b) mean temperature difference with standard deviation (shade) between the XCTD and CTD. Mean profiles were low-pass filtered by a running mean with a window of 51 dbar.

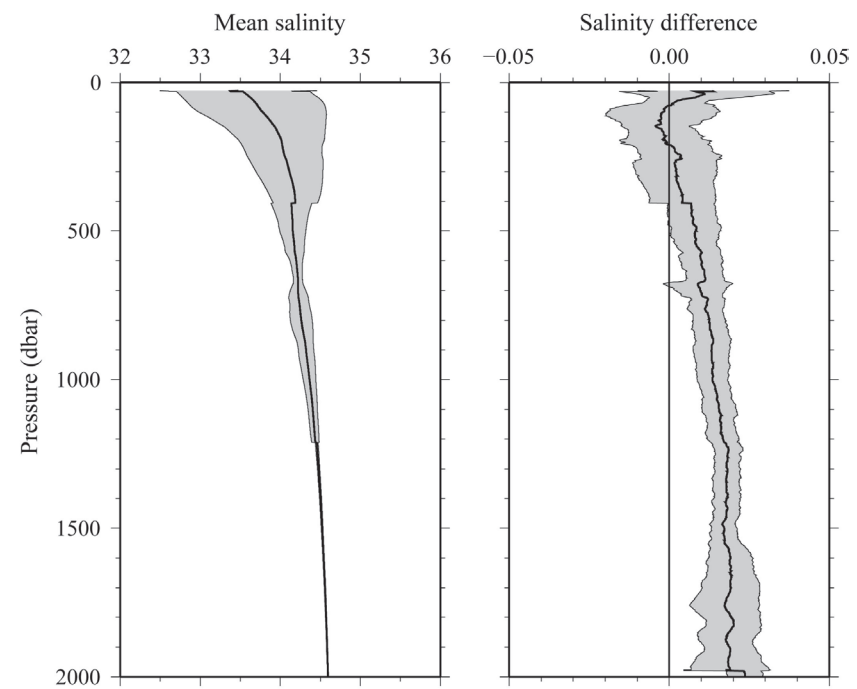


Figure 2.7.3. Comparison between XCTD and CTD salinity profiles. (a) Mean salinity of CTD profiles with standard deviation (shade) and (b) mean salinity difference with standard deviation (shade) between the XCTD and CTD. Mean profiles were low-pass filtered by a running mean with a window of 51 dbar.

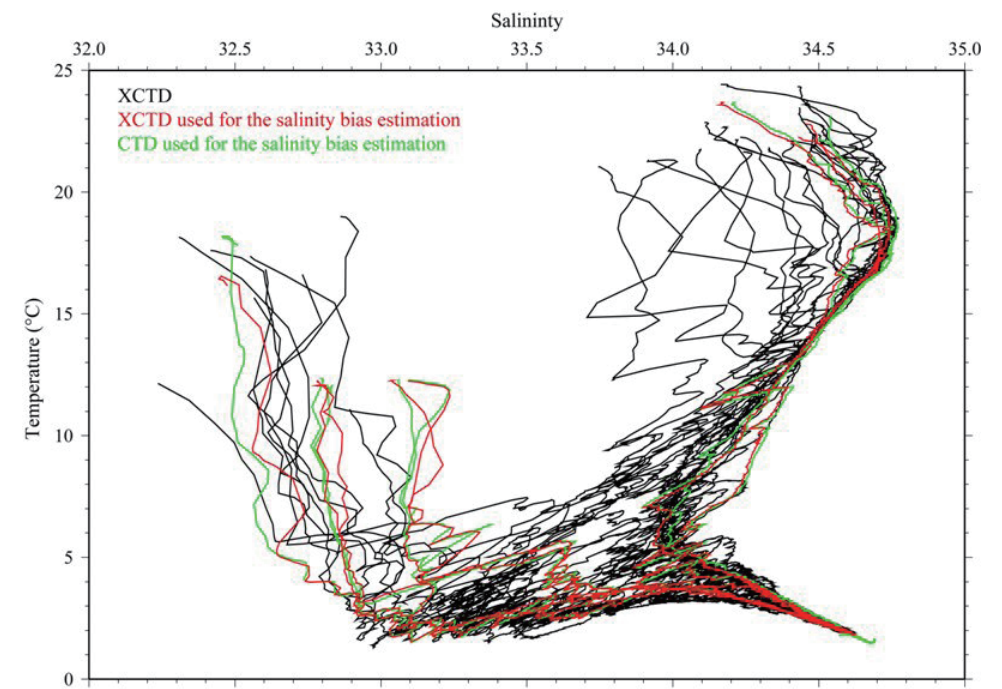


Figure 2.7.4. Comparison of temperature-salinity profiles of CTD (green lines) data used for the XCTD salinity bias estimation and salinity bias-corrected XCTD (red and black lines) data.

3 Hydrographic Measurements

3.1 CTDO₂ Measurements

April 20, 2015

(1) Personnel

Hiroshi Uchida (JAMSTEC)

Shinsuke Toyoda (MWJ)

Hiroshi Matsunaga (MWJ)

Rei Ito (MWJ)

Akira Watanabe (MWJ)

Kenichi Katayama (MWJ) (leg 1)

Tomoyuki Takamori (MWJ) (leg 2)

Michinari Sunamura (The University of Tokyo) (CDOM measurement)

(2) Winch arrangements

The CTD package was deployed by using 4.5 Ton Traction Winch System (Dynacon, Inc., Bryan, Texas, USA), which was renewed on the R/V Mirai in April 2014 (e.g. Fukasawa et al., 2004). Primary system components include a complete CTD Traction Winch System with up to 8500 m of 9.53 mm armored cable (Ocean Cable and Communications Co., Yokohama, Kanagawa, Japan).

(3) Overview of the equipment

The CTD system was SBE 911plus system (Sea-Bird Electronics, Inc., Bellevue, Washington, USA). The SBE 911plus system controls 36-position SBE 32 Carousel Water Sampler. The Carousel accepts 12-litre Niskin-X water sample bottles (General Oceanics, Inc., Miami, Florida, USA). The SBE 9plus was mounted horizontally in a 36-position carousel frame. SBE's temperature (SBE 3) and conductivity (SBE 4) sensor modules were used with the SBE 9plus underwater unit. The pressure sensor is mounted in the main housing of the underwater unit and is ported to outside through the oil-filled plastic capillary tube. A modular unit of

underwater housing pump (SBE 5T) flushes water through sensor tubing at a constant rate independent of the CTD's motion, and pumping rate (3000 rpm) remain nearly constant over the entire input voltage range of 12-18 volts DC. Flow speed of pumped water in standard TC duct is about 2.4 m/s. Two sets of temperature and conductivity modules were used. An SBE's dissolved oxygen sensor (SBE 43) was placed between the primary conductivity sensor and the pump module. Auxiliary sensors, a Deep Ocean Standards Thermometer (SBE 35), an altimeter (PSA-916T; Teledyne Benthos, Inc., North Falmouth, Massachusetts, USA), an oxygen optode (RINKO-III; JFE Advantech Co., Ltd, Kobe Hyogo, Japan), a fluorometer (Seapoint sensors, Inc., Kingston, New Hampshire, USA), a transmissometer (C-Star Transmissometer; WET Labs, Inc., Philomath, Oregon, USA), a Photosynthetically Active Radiation (PAR) sensor (Satlantic, LP, Halifax, Nova Scotia, Canada), a colored dissolved organic matter (ECO FL CDOM, WET Labs, Inc., Philomath, Oregon, USA), and an UV nitrate sensor (Deep SUNA, Satlantic, LP, Halifax, Nova Scotia, Canada) were also used with the SBE 9plus underwater unit. To minimize rotation of the CTD package, a heavy stainless frame (total weight of the CTD package without sea water in the bottles is about 1000 kg) was used with an aluminum plate (54 × 90 cm).

An additional set of SBE 911plus CTD system with 12-position SBE 32 was also used for four shallow casts (stations 73_4, 73_5, 124_2, and 124_3) for water sampling for phytoplankton incubation in leg 2. The SBE 9plus was mounted horizontally in a 12-position carousel frame. The 12-litre Niskin-X water sample bottles (General Oceanics, Inc.) were carefully cleaned and stored for the water sampling.

Summary of the system used in this cruise

36-position Carousel system

Deck unit:

SBE 11plus, S/N 11P54451-0872

Under water unit:

SBE 9plus, S/N 09P54451-117457 (pressure sensor S/N: 1027)

Temperature sensor:

SBE 3plus, S/N 4811 (primary)

SBE 3, S/N 1359 (secondary)

Conductivity sensor:

SBE 4, S/N 2435 (primary)

SBE 4, S/N 2854 (secondary)

Oxygen sensor:

SBE 43, S/N 0394 (stations from 001 to 057)

SBE 43, S/N 0330 (stations from 058 to 150)

JFE Advantech RINKO-III, S/N 0024 (foil batch no. 144002A)

Pump:

SBE 5T, S/N 4595 (primary)

SBE 5T, S/N 4598 (secondary)

Altimeter:

PSA-916T, S/N 1157

Deep Ocean Standards Thermometer:

SBE 35, S/N 0022

Fluorometer:

Seapoint Sensors, Inc., S/N 3618 (measurement range: 0-5 µg/L)

Transmissometer:

C-Star, S/N CST-1363DR

PAR:

Satlantic LP, S/N 0049

CDOM:

ECO FL CDOM, S/N 2014 (measurement range: 0-500 ppb)

Nitrate:

Deep SUNA, S/N 0385 (used only for stations 001_2, 007_1, 014_1, and 030_1)

Carousel Water Sampler:

SBE 32, S/N 0924 (stations from 001_1 to 001_2)

SBE 32, S/N 0391 (stations from 007_1 to 150_1)

Water sample bottle:

12-litre Niskin-X model 1010X (no TEFLON coating)

12-position Carousel system (used for water sampling for phytoplankton incubation)

Deck unit:

SBE 11plus, S/N 11P54451-0872

Under water unit:

SBE 9plus, S/N 09P27443-79511 (pressure sensor S/N: 0677)

Temperature sensor:

SBE 3, S/N 1524

Conductivity sensor:

SBE 4, S/N 1088

Pump:

SBE 5T, S/N 3118

Carousel Water Sampler:

SBE 32, S/N 0278

Water sample bottle:

12-litre Niskin-X model 1010X (TEFLON coating)

(4) Pre-cruise calibration

i. Pressure

The Paroscientific series 4000 Digiquartz high pressure transducer (Model 415K; Paroscientific, Inc., Redmond, Washington, USA) uses a quartz crystal resonator whose frequency of oscillation varies with pressure induced stress with 0.01 per million of resolution over the absolute pressure range of 0 to 15000 psia (0 to 10332 dbar). Also, a quartz crystal temperature signal is used to compensate for a wide range of temperature changes at the time of an observation. The pressure sensor has a nominal accuracy of 0.015 % FS (1.5 dbar), typical stability of 0.0015 % FS/month (0.15 dbar/month), and resolution of 0.001 % FS (0.1 dbar). Since the pressure sensor measures the absolute value, it inherently includes atmospheric pressure (about 14.7 psi). SEASOFT subtracts 14.7 psi from computed pressure automatically.

Pre-cruise sensor calibrations for linearization were performed at SBE, Inc.

S/N 1027, 4 February 2011

S/N 0677, 5 March 2014

The time drift of the pressure sensor is adjusted by periodic recertification corrections against a dead-weight piston gauge (Model 480DA, S/N 23906; Piston unit, S/N 079K; Weight set, S/N 3070; Bundenberg Gauge Co. Ltd., Irlam, Manchester, UK). The corrections are performed at JAMSTEC, Yokosuka, Kanagawa, Japan by Marine Works Japan Ltd. (MWJ), Yokohama, Kanagawa, Japan, usually once in a year in order to monitor sensor time drift and linearity.

S/N 1027, 9 April 2014

slope = 0.99995022

offset = -0.74973

S/N 0677, 9 April 2014

slope = 0.99972807

offset = -0.10585

ii. Temperature (SBE 3)

The temperature sensing element is a glass-coated thermistor bead in a stainless steel tube, providing a pressure-free measurement at depths up to 10500 (6800) m by titanium (aluminum) housing. The SBE 3 thermometer has a nominal accuracy of 1 mK, typical stability of 0.2 mK/month, and resolution of 0.2 mK at 24 samples per second. The premium temperature sensor, SBE 3plus, is a more rigorously tested and calibrated version of standard temperature sensor (SBE 3).

Pre-cruise sensor calibrations were performed at SBE, Inc.

S/N 4811, 18 January 2014

S/N 1359, 1 May 2014

S/N 1524, 12 November 2013

Pressure sensitivities of SBE 3s were corrected according to a method by Uchida et al. (2007), for the following sensors.

S/N 4811, -2.7192e-7 [°C/dbar]

S/N 1359, -1.8386e-7 [°C/dbar]

iii. Conductivity (SBE 4)

The flow-through conductivity sensing element is a glass tube (cell) with three platinum electrodes to provide in-situ measurements at depths up to 10500 (6800) m by titanium (aluminum) housing. The SBE 4 has a nominal accuracy of 0.0003 S/m, typical stability of 0.0003 S/m/month, and resolution of 0.00004 S/m at 24 samples per second. The conductivity cells have been replaced to newer style cells for deep ocean measurements.

Pre-cruise sensor calibrations were performed at SBE, Inc.

S/N 2435, 1 May 2014

S/N 2854, 1 May 2014

S/N 1088, 17 July 2013

The value of conductivity at salinity of 35, temperature of 15 °C (IPTS-68) and pressure of 0 dbar is

4.2914 S/m.

iv. Oxygen (SBE 43)

The SBE 43 oxygen sensor uses a Clark polarographic element to provide in-situ measurements at depths up to 7000 m. The range for dissolved oxygen is 120 % of surface saturation in all natural waters, nominal accuracy is 2 % of saturation, and typical stability is 2 % per 1000 hours.

Pre-cruise sensor calibration was performed at SBE, Inc.

S/N 0394, 29 April 2014

S/N 0330, 29 April 2014

v. Deep Ocean Standards Thermometer

Deep Ocean Standards Thermometer (SBE 35) is an accurate, ocean-range temperature sensor that can be standardized against Triple Point of Water and Gallium Melt Point cells and is also capable of measuring temperature in the ocean to depths of 6800 m. The SBE 35 was used to calibrate the SBE 3 temperature sensors in situ (Uchida et al., 2007; Uchida et al., 2015b).

Pre-cruise sensor linearization was performed at SBE, Inc.

S/N 0022, 4 March 2009

Then the SBE 35 is certified by measurements in thermodynamic fixed-point cells of the TPW (0.01 °C) and GaMP (29.7646 °C). The slow time drift of the SBE 35 is adjusted by periodic recertification corrections. Pre-cruise sensor calibration was performed at SBE, Inc. From the end of 2011, the SBE has been applying a NIST correction to the fixed-point cells used for the calibration.

S/N 0022, 3 September 2013 (slope and offset correction)

Slope = 1.000006

Offset = 0.000187

The time required per sample = $1.1 \times \text{NCYCLES} + 2.7$ seconds. The 1.1 seconds is total time per an acquisition cycle. NCYCLES is the number of acquisition cycles per sample and was set to 4. The 2.7 seconds

is required for converting the measured values to temperature and storing average in EEPROM.

vi. Altimeter

Benthos PSA-916T Sonar Altimeter (Teledyne Benthos, Inc.) determines the distance of the target from the unit by generating a narrow beam acoustic pulse and measuring the travel time for the pulse to bounce back from the target surface. It is rated for operation in water depths up to 10000 m. The PSA-916T uses the nominal speed of sound of 1500 m/s.

vii. Oxygen optode (RINKO)

RINKO (JFE Alec Co., Ltd.) is based on the ability of selected substances to act as dynamic fluorescence quenchers. RINKO model III is designed to use with a CTD system which accept an auxiliary analog sensor, and is designed to operate down to 7000 m.

Data from the RINKO can be corrected for the time-dependent, pressure-induced effect by means of the same method as that developed for the SBE 43 (Edwards et al., 2010). The calibration coefficients, H1 (amplitude of hysteresis correction), H2 (curvature function for hysteresis), and H3 (time constant for hysteresis) were determined empirically as follows.

H1 = 0.007 (for S/N 0024)

H2 = 5000 dbar

H3 = 2000 seconds

Outputs from RINKO are the raw phase shift data. The RINKO can be calibrated by the modified Stern-Volmer equation slightly modified from a method by Uchida et al. (2010):

$$O_2 (\mu\text{mol/l}) = [(V_0 / V)^E - 1] / K_{sv}$$

where V is voltage, V_0 is voltage in the absence of oxygen, K_{sv} is Stern-Volmer constant. The coefficient E corrects nonlinearity of the Stern-Volmer equation. The V_0 and the K_{sv} are assumed to be functions of temperature as follows.

$$K_{sv} = C_0 + C_1 \times T + C_2 \times T^2$$

$$V_0 = 1 + C_3 \times T$$

$$V = C_4 + C_5 \times V_b$$

where T is CTD temperature (°C) and V_b is raw output (volts). V_0 and V are normalized by the output in the absence of oxygen at 0°C. The oxygen concentration is calculated using accurate temperature data from the CTD temperature sensor instead of temperature data from the RINKO. The pressure-compensated oxygen concentration O_{2c} can be calculated as follows.

$$O_{2c} = O_2 (1 + C_{pP} / 1000)$$

where p is CTD pressure (dbar) and C_p is the compensation coefficient. Since the sensing foil of the optode is permeable only to gas and not to water, the optode oxygen must be corrected for salinity. The salinity-compensated oxygen can be calculated by multiplying the factor of the effect of salt on the oxygen solubility. The coefficients of the equation by García and Gordon (1992) were modified based on the laboratory experiment (Uchida et al., in prep.) and used for the compensation ($B_0 = -6.33568e-3$, $B_1 = -6.84389e-3$, $B_2 = -1.18326e-2$, $B_3 = -5.51960e-2$, $C_0 = 3.40543e-6$).

Pre-cruise sensor calibrations were performed at RCGC/JAMSTEC.

S/N 0024, 14 May 2014

viii. Fluorometer

The Seapoint Chlorophyll Fluorometer (Seapoint Sensors, Inc., Kingston, New Hampshire, USA) provides in-situ measurements of chlorophyll-a at depths up to 6000 m. The instrument uses modulated blue LED lamps and a blue excitation filter to excite chlorophyll-a. The fluorescent light emitted by the chlorophyll-a passes through a red emission filter and is detected by a silicon photodiode. The low level signal is then processed using synchronous demodulation circuitry, which generates an output voltage proportional to chlorophyll-a concentration.

ix. Transmissometer

The C-Star Transmissometer (WET Labs, Inc., Philomath, Oregon, USA) measures light transmittance at

a single wavelength (650 nm) over a known path (25 cm). In general, losses of light propagating through water can be attributed to two primary causes: scattering and absorption. By projecting a collimated beam of light through the water and placing a focused receiver at a known distance away, one can quantify these losses. The ratio of light gathered by the receiver to the amount originating at the source is known as the beam transmittance. Suspended particles, phytoplankton, bacteria and dissolved organic matter contribute to the losses sensed by the instrument. Thus, the instrument provides information both for an indication of the total concentrations of matter in the water as well as for a value of the water clarity.

Light transmission T_r (in %) and beam attenuation coefficient c_p are calculated from the sensor output (V in volt) as follows.

$$T_r = (c_0 + c_1 V) \times 100$$

$$c_p = - (1 / 0.25) \ln(T_r / 100)$$

The calibration coefficients were determined by using the data obtained in the R/V Mirai MR13-06 cruise.

x. PAR

Photosynthetically Active Radiation (PAR) sensors (Satlantic, LP, Halifax, Nova Scotia, Canada) provide highly accurate measurements of PAR (400 – 700 nm) for a wide range of aquatic and terrestrial applications. The ideal spectral response for a PAR sensor is one that gives equal emphasis to all photons between 400 – 700 nm. Satlantic PAR sensors use a high quality filtered silicon photodiode to provide a near equal spectral response across the entire wavelength range of the measurement.

Pre-cruise sensor calibration was performed at Satlantic, LP.

S/N 0049, 22 January 2009

xi. CDOM

The Environmental Characterization Optics (ECO) miniature fluorometer (WET Labs, Inc., Philomath, Oregon, USA) allows the user to measure relative Colored Dissolved Organic Matter (CDOM) concentrations by directly measuring the amount of fluorescence emission in a sample volume of water. The CDOM

fluorometer uses an UV LED to provide the excitation source. An interference filter is used to reject the small amount of out-of-band light emitted by the LED. The light from the source enters the water volume at an angle of approximately 55-60 degrees with respect to the end face of the unit. Fluoresced light is received by a detector positioned where the acceptance angle forms a 140-degree intersection with the source beam. An interference filter is used to discriminate against the scattered excitation light.

CDOM (Quinine Dihydrate Equivalent) concentration expressed in ppb can be derived using the equation as follows.

$$\text{CDOM} = \text{Scale Factor} * (\text{Output} - \text{Dark Counts})$$

Pre-cruise sensor calibration was performed at WET Labs.

S/N 2014, 21 September 2010

Dark Counts: 0.027 V

Scale Factor: 101 ppb/V

Maximum Output: 4.94 V

xii. Deep SUNA

The SUNA (Submersible Ultraviolet Nitrate Analyzer) is a chemical-free nitrate sensor (Satlantic, LP, Halifax, Nova Scotia, Canada). It is based on the ISUS (In Situ Ultraviolet Spectroscopy) technology developed at Monterey Bay Aquarium Research Institute (MBARI). The Deep SUNA housing is made from anodized aluminum. The housing is designed to withstand depths of up to 2000 m. The SUNA measures the concentration of dissolved nitrate in water. The sensor illuminates the water sample with its deuterium UV light source, and measures the throughput using its photo-spectrometer. The difference between this measurement and a prior baseline reference measurement of pure water constitutes an absorption spectrum.

Absorbance characteristics of natural water components are provided in the sensor calibration file. The Beer-Lambert Law for multiple absorbers establishes the relationship between the total measured absorbance and the concentrations of individual components. Based on this relationship, the sensor obtains a best estimate for the nitrate concentration using multi-variable linear regression.

The Deep SUNA was used with the CTD system as an auxiliary analog sensor at shallow casts in leg 1 (stations 001_2, 007_1, 014_1, and 030_1), since it is designed to operate down to 2000 m and it was used with the Continuous Sea Surface Water Monitoring System (see Section 2.4) in leg 2.

(5) Data collection and processing

i. Data collection

CTD system was powered on at least 20 minutes in advance of the data acquisition to stabilize the pressure sensor and was powered off at least two minutes after the operation in order to acquire pressure data on the ship's deck.

The package was lowered into the water from the starboard side and held 10 m beneath the surface in order to activate the pump. After the pump was activated, the package was lifted to the surface and lowered at a rate of 1.0 m/s to 200 m (or 300 m when significant wave height was high) then the package was stopped to operate the heave compensator of the crane. The package was lowered again at a rate of 1.2 m/s to the bottom. For the up cast, the package was lifted at a rate of 1.1 m/s except for bottle firing stops. As a rule, the bottle was fired after waiting from the stop for 30 seconds (20 seconds from station 049_1 to save the observation time) and the package was stayed at least 5 seconds for measurement of the SBE 35 at each bottle firing stops. For depths where vertical gradient of water properties were expected to be large, the bottle was exceptionally fired after waiting from the stop for 60 seconds (50 seconds from station 049_1 to save the observation time) to enhance exchanging the water between inside and outside of the bottle. At 200 m (or 300 m) from the surface, the package was stopped to stop the heave compensator of the crane.

Water samples were collected using a 36-bottle (or 12-bottles) SBE 32 Carousel Water Sampler with 12-litre Niskin-X bottles. Before a cast taken water for CFCs, the bottle frame and Niskin-X bottles were wiped with acetone.

Data acquisition software

SEASAVE-Win32, version 7.23.2

ii. Data collection problems

(a) Miss trip, miss fire, and remarkable leak

Niskin bottles did not trip correctly at the following stations.

Miss trip	Miss fire	Remarkable leak
140_1, #16	001_1, #6 001_2, #24	074_1 ~ 093_1, #3

Since all of the latch assemblies for the SBE 32 (S/N 0924) was defective, the SBE 32 was replaced from S/N 0924 to S/N 0391 after the station 001_2. Also, the latch assembly for #16 of S/N 0391 was replaced after the station 140_1. The bottle sampled salinity data were relatively lower (about 0.001) than the CTD salinity data for the bottle #3 at stations from 074 to 093. The drain cock of the bottle #3 was replaced after the station 094_1.

(b) Failure of insulation of the CTD winch armored cable

Failure of insulation of the CTD winch armored cable occurred at 2608 dbar of up cast of the station 041_1. Therefore, the up cast was aborted and the armored cable was cut 1620 m after the cast.

(c) Detachment of some sensors at deep casts deeper than 6000 m

Fluorometer, transmissometer, CDOM, LADCP, and Micro Rider were detached at stations 047_1, 046_1, 045_1, and 044_1, because of the withstand depth of 6000 m for these sensors. At stations 001_1, 080_1, 081_1, 088_1, and 089_1, the CTD package was lowered depths up to 6000 m without detachment of these sensors, although water depths of these stations were deeper than 6000 m.

(d) Noise of SBE 43 (S/N 0394)

Relatively large noise was found in the SBE 43 data at about 4762~4789 dbar of down cast. Therefore, the SBE 43 was replaced from S/N 0394 to S/N 0330 after the station 056_1.

(e) Noise of primary temperature and salinity data

The primary temperature and/or salinity data were noisy for down cast of following stations: 074_1 and 145_1. Therefore, the secondary temperature and salinity data were used for these stations for vertical profile (wct file). The primary temperature and/or salinity data were noisy for up cast of following stations: 050_1, 144_1, and 145_1. Therefore, the secondary temperature and salinity data were used for these stations for bottle data (seafile).

(f) Noise of transmissometer

The transmissometer data were (partly) noisy for down cast at following stations: 022_1, 043_1, 057_1, 065_1, 077_1, 079_1, 080_1, 089_1, 091_2, 092_1, 095_1, 097_1, 126_1, 130_1, 141_1, 142_1, and 145_1. Therefore, the up cast data were used for vertical profile data (wct file) for these stations instead using the down cast data.

iii. Data processing

SEASOFT consists of modular menu driven routines for acquisition, display, processing, and archiving of oceanographic data acquired with SBE equipment. Raw data are acquired from instruments and are stored as unmodified data. The conversion module DATCNV uses instrument configuration and calibration coefficients to create a converted engineering unit data file that is operated on by all SEASOFT post processing modules. The following are the SEASOFT and original software data processing module sequence and specifications used in the reduction of CTD data in this cruise.

Data processing software

SBEDataProcessing-Win32, version 7.23.2

DATCNV converted the raw data to engineering unit data. DATCNV also extracted bottle information where scans were marked with the bottle confirm bit during acquisition. The duration was set to 4.4 seconds, and the offset was set to 0.0 second. The hysteresis correction for the SBE 43 data (voltage) was applied for both profile and bottle information data.

TCORP (original module, version 1.1) corrected the pressure sensitivity of the SBE 3 for both profile and bottle information data.

RINKOCOR (original module, version 1.0) corrected the time-dependent, pressure-induced effect (hysteresis) of the RINKO for both profile data.

RINKOCORROS (original module, version 1.0) corrected the time-dependent, pressure-induced effect (hysteresis) of the RINKO for bottle information data by using the hysteresis-corrected profile data.

BOTTLESUM created a summary of the bottle data. The data were averaged over 4.4 seconds (or 1 second for the bottle fired without stop).

ALIGNCTD converted the time-sequence of sensor outputs into the pressure sequence to ensure that all calculations were made using measurements from the same parcel of water. For a SBE 9plus CTD with the ducted temperature and conductivity sensors and a 3000-rpm pump, the typical net advance of the conductivity relative to the temperature is 0.073 seconds. So, the SBE 11plus deck unit was set to advance the primary and the secondary conductivity for 1.73 scans ($1.75/24 = 0.073$ seconds). Oxygen data are also systematically delayed with respect to depth mainly because of the long time constant of the oxygen sensor and of an additional delay from the transit time of water in the pumped plumbing line. This delay was compensated by 6 seconds advancing the SBE 43 oxygen sensor output (voltage) relative to the temperature data. Delay of the RINKO data was also compensated by 1 second advancing sensor output (voltage) relative to the temperature data. Delay of the transmissometer data was also compensated by 2 seconds advancing sensor output (voltage) relative to the temperature data.

WILDEDIT marked extreme outliers in the data files. The first pass of WILDEDIT obtained an accurate estimate of the true standard deviation of the data. The data were read in blocks of 1000 scans. Data greater than 10 standard deviations were flagged. The second pass computed a standard deviation over the same 1000 scans excluding the flagged values. Values greater than 20 standard deviations were marked bad. This process was applied to pressure, temperature, conductivity, and SBE 43 output.

CELLTM used a recursive filter to remove conductivity cell thermal mass effects from the measured conductivity. Typical values used were thermal anomaly amplitude $\alpha = 0.03$ and the time constant $1/\beta =$

7.0.

FILTER performed a low pass filter on pressure with a time constant of 0.15 seconds. In order to produce zero phase lag (no time shift) the filter runs forward first then backwards.

WFILTER performed as a median filter to remove spikes in fluorometer, transmissometer, and CDOM data. A median value was determined by 49 scans of the window.

SECTIONU (original module, version 1.1) selected a time span of data based on scan number in order to reduce a file size. The minimum number was set to be the start time when the CTD package was beneath the sea-surface after activation of the pump. The maximum number was set to be the end time when the depth of the package was 1 dbar below the surface. The minimum and maximum numbers were automatically calculated in the module.

LOOPEDIT marked scans where the CTD was moving less than the minimum velocity of 0.0 m/s (traveling backwards due to ship roll).

DESPIKE (original module, version 1.0) removed spikes of the data. A median and mean absolute deviation was calculated in 1-dbar pressure bins for both down- and up-cast, excluding the flagged values. Values greater than 4 mean absolute deviations from the median were marked bad for each bin. This process was performed 2 times for temperature, conductivity, SBE 43, and RINKO output.

DERIVE was used to compute oxygen (SBE 43).

BINAVG averaged the data into 1-dbar pressure bins. The center value of the first bin was set equal to the bin size. The bin minimum and maximum values are the center value plus and minus half the bin size. Scans with pressures greater than the minimum and less than or equal to the maximum were averaged. Scans were interpolated so that a data record exist every dbar.

BOTTOMCUT (original module, version 0.1) deleted the deepest pressure bin when the averaged scan number of the deepest bin was smaller than the average scan number of the bin just above.

DERIVE was re-used to compute salinity, potential temperature, and density (σ_θ).

SPLIT was used to split data into the down cast and the up cast.

Remaining spikes in the CTD data were manually eliminated from the 1-dbar-averaged data. The data

gaps resulting from the elimination were linearly interpolated with a quality flag of 6.

(6) Post-cruise calibration

i. Pressure

The CTD pressure sensor offset in the period of the cruise was estimated from the pressure readings on the ship deck. For best results the Paroscientific sensor was powered on for at least 20 minutes before the operation. In order to get the calibration data for the pre- and post-cast pressure sensor drift, the CTD deck pressure was averaged over first and last one minute, respectively. Then the atmospheric pressure deviation from a standard atmospheric pressure (14.7 psi) was subtracted from the CTD deck pressure to check the pressure sensor time drift. The atmospheric pressure was measured at the captain deck (20 m high from the base line) and sub-sampled one-minute interval as a meteorological data. Time series of the CTD deck pressure is shown in Fig. 3.1.1. The CTD pressure sensor offset was estimated from the deck pressure. Mean of the pre- and the post-casts data over the whole period gave an estimation of the pressure sensor offset (-0.04 dbar) from the pre-cruise calibration. The post-cruise correction of the pressure data is not deemed necessary for the pressure sensor.

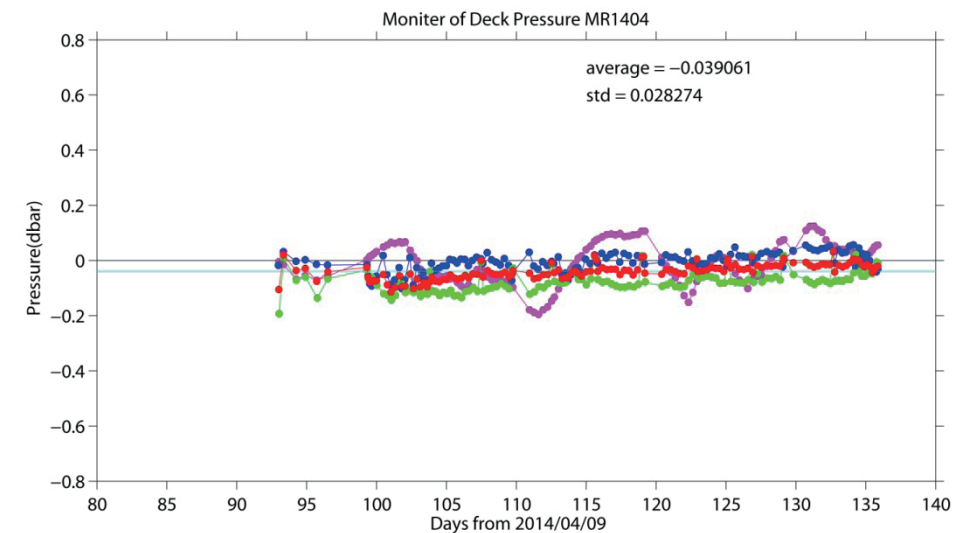


Figure 3.1.1. Time series of the CTD deck pressure. Atmospheric pressure deviation (magenta dots) from a standard atmospheric pressure was subtracted from the CTD deck pressure. Blue and green dots indicate pre- and post-cast deck pressures, respectively. Red dots indicate averages of the pre- and the post-cast deck pressures.

ii. Temperature

The CTD temperature sensors (SBE 3) were calibrated with the SBE 35 under the assumption that discrepancies between SBE 3 and SBE 35 data were due to pressure sensitivity, the viscous heating effect, and time drift of the SBE 3, according to a method by Uchida et al. (2007).

Post-cruise sensor calibration for the SBE 35 was performed at SBE, Inc in February 2015.

S/N 0022, 4 February 2015 (2nd step: fixed point calibration)

Slope = 1.000007

Offset = 0.000246

Offset of the SBE 35 data from the pre-cruise calibration was estimated to be smaller than 0.1 mK for temperature smaller than 4.5°C. So the post-cruise correction of the SBE 35 temperature data was not deemed

necessary for the SBE 35.

The CTD temperature was preliminary calibrated as

$$\text{Calibrated temperature} = T - (c_0 \times P + c_1 \times t + c_2)$$

where T is CTD temperature in °C, P is pressure in dbar, t is time in days from pre-cruise calibration date of the CTD temperature and c_0 , c_1 , and c_2 are calibration coefficients. The coefficients were determined using the data for the depths deeper than 1950 dbar.

The primary temperature data were basically used for the post-cruise calibration. The secondary temperature sensor was also calibrated and used instead of the primary temperature data when the data quality of the primary temperature data was bad. The calibration coefficients are listed in Table 3.1.1. The results of the post-cruise calibration for the CTD temperature are summarized in Table 3.1.2 and shown in Figs. 3.1.2 and 3.1.3.

Table 3.1.1. Calibration coefficients for the CTD temperature sensors.

Serial number	c_0 (°C/dbar)	c_1 (°C/day)	c_2 (°C)
4811	-1.29748e-8	4.02418e-6	-0.0003
1359	1.67653e-8	5.20248e-6	-0.0002

Table 3.1.2. Difference between the CTD temperature and the SBE 35 after the post-cruise calibration. Mean and standard deviation (Sdev) are calculated for the data below and above 950 dbar. Number of data used is also shown.

Serial number	Pressure ≥ 950 dbar			Pressure < 950 dbar		
	Number	Mean (mK)	Sdev (mK)	Number	Mean (mK)	Sdev (mK)
4811	1544	-0.0	0.2	2756	-0.1	11.7
1359	1546	0.0	0.2	2774	0.3	9.1

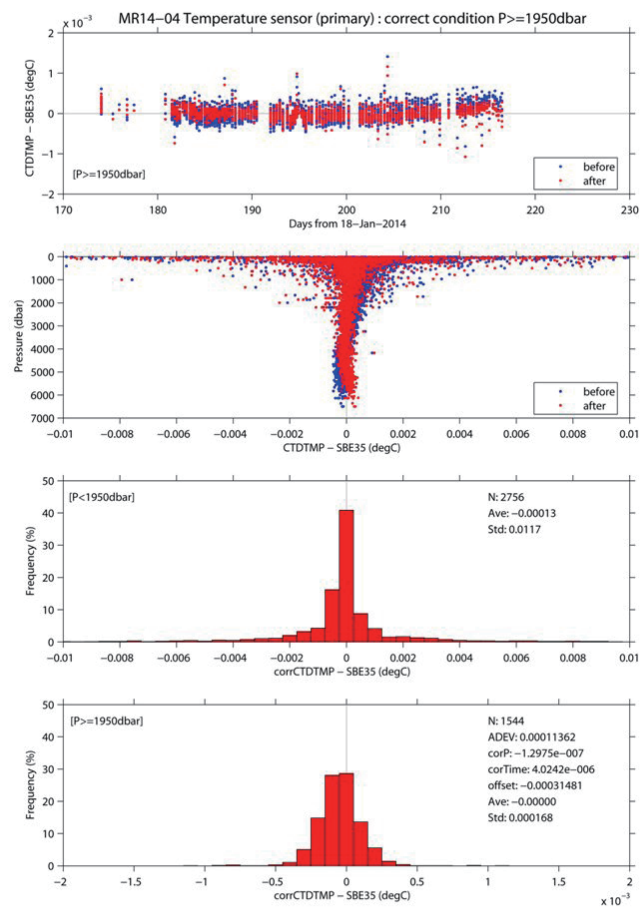


Figure 3.1.2. Difference between the CTD temperature (primary) and the SBE 35. Blue and red dots indicate before and after the post-cruise calibration using the SBE 35 data, respectively. Lower two panels show histogram of the difference after the calibration.

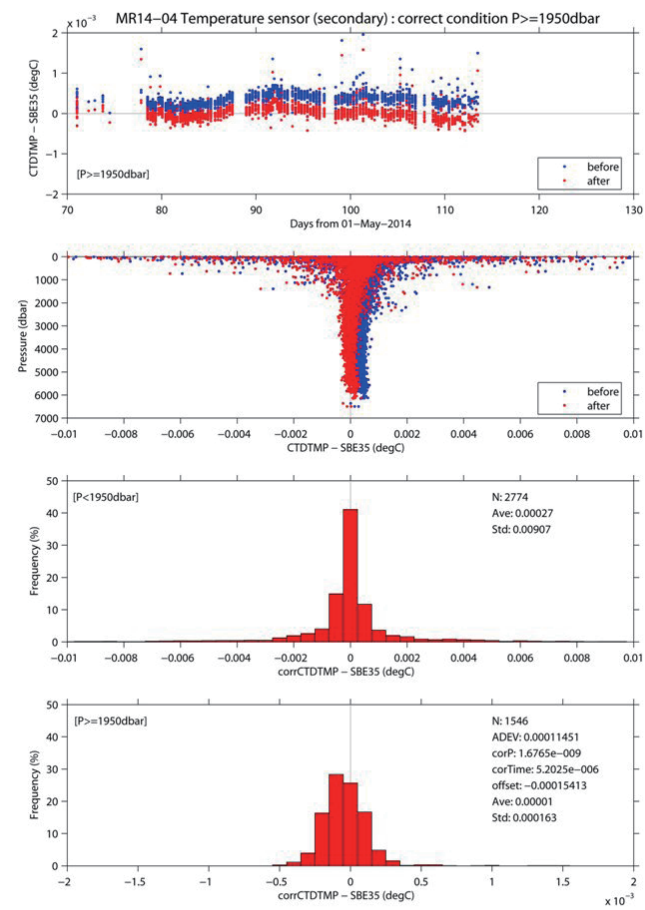


Figure 3.1.3. Same as Fig. 3.1.2, but for secondary temperature sensor.

iii. Salinity

The discrepancy between the CTD conductivity and the conductivity calculated from the bottle salinity data with the CTD temperature and pressure data is considered to be a function of conductivity, pressure and time. The CTD conductivity was calibrated as

$$\text{Calibrated conductivity} = c_0 \times C + c_1 \times P + c_2 \times C \times P + c_3 \times t + c_4$$

where C is CTD conductivity in S/m, P is pressure in dbar, t is time in days from 11 July 2009, 00:58 (UTC) and c_0 , c_1 , c_2 , c_3 and c_4 are calibration coefficients. The best fit sets of coefficients were determined by a least square technique to minimize the deviation from the conductivity calculated from the bottle salinity data.

The primary conductivity data created by the software module ROSSUM were basically used after the post-cruise calibration for the temperature data. The secondary conductivity sensor was also calibrated and used instead of the primary conductivity data when the data quality of the primary temperature or conductivity data was bad. The calibration coefficients are listed in Table 3.1.3. The results of the post-cruise calibration for the CTD salinity are summarized in Table 3.1.4 and shown in Figs. 3.1.4 and 3.1.5.

Table 3.1.3. Calibration coefficients for the CTD conductivity sensors.

Serial Number	c_0	c_1 [S/(m dbar)]	c_2 (1/dbar)	c_3 [S/(m day)]	c_4 (S/m)
2435	-7.51283e-5	2.42062e-7	-6.89235e-8	-5.29014e-7	1.93028e-4
2854	-2.18278e-4	-1.62860e-7	5.27345e-8	1.50084e-6	5.46236e-4

Table 3.1.4. Difference between the CTD salinity and the bottle salinity after the post-cruise calibration. Mean and standard deviation (Sdev) (in 10^{-3}) are calculated for the data below and above 1950 dbar. Number of data used is also shown.

Serial number	Pressure \geq 1950 dbar			Pressure < 1950 dbar		
	Number	Mean	Sdev	Number	Mean	Sdev
2435	1574	0.0	0.4	2105	-0.9	7.3
2854	1580	0.0	0.5	2140	-0.9	7.5

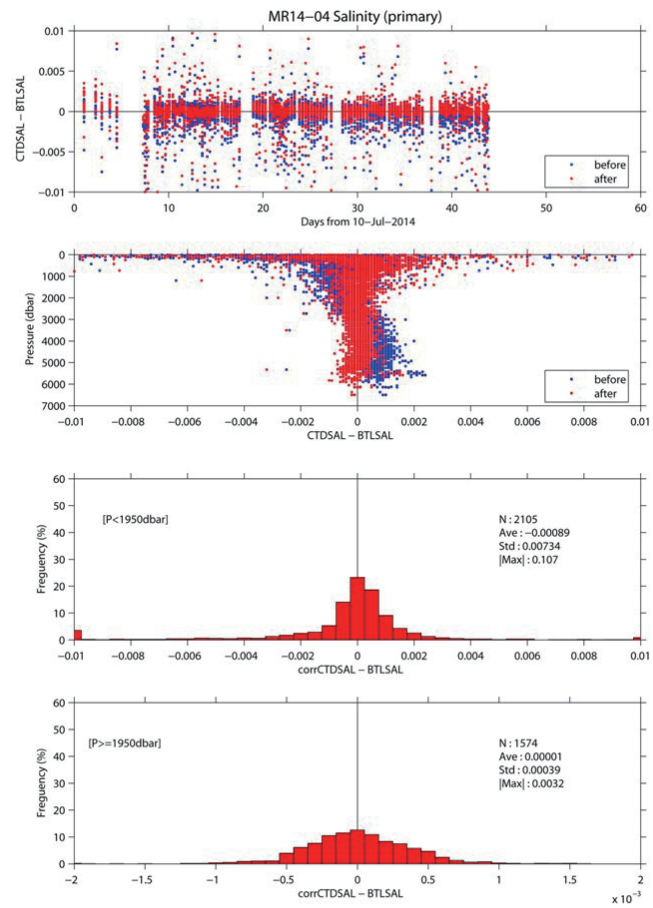


Figure 3.1.4. Difference between the CTD salinity (primary) and the bottle salinity. Blue and red dots indicate before and after the post-cruise calibration, respectively. Lower two panels show histogram of the difference after the calibration.

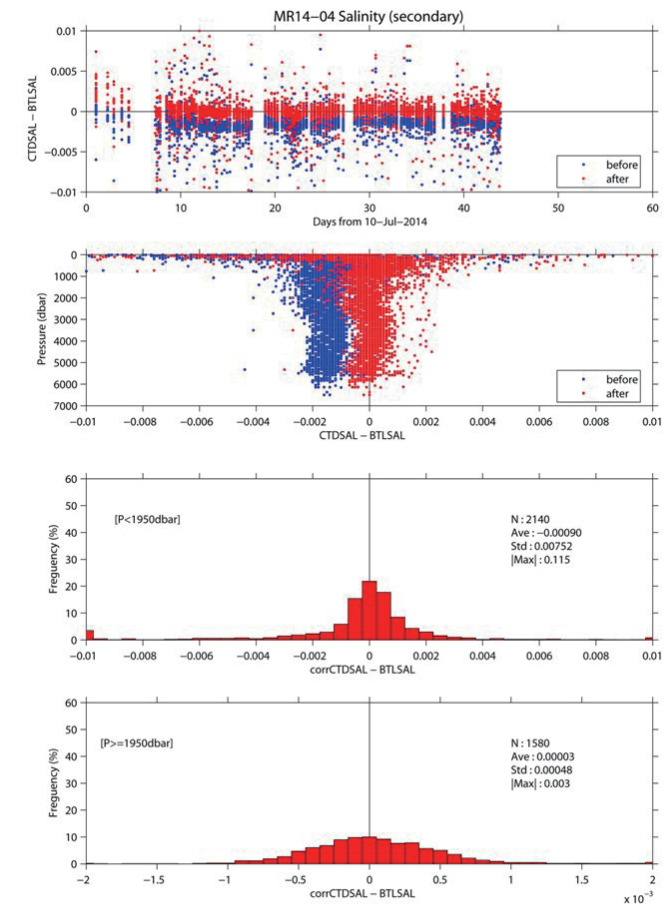


Figure 3.1.5. Same as Fig. 3.1.4, but for secondary salinity.

iv. Oxygen

The RINKO oxygen optode (S/N 0024) was calibrated and used as the CTD oxygen data, since the RINKO has a fast time response. The pressure-hysteresis corrected RINKO data was calibrated by the modified Stern-Volmer equation, basically according to a method by Uchida et al. (2010) with slight modification:

$$[O_2] (\mu\text{mol/l}) = [(V_0 / V)^{1.1} - 1] / K_{sv}$$

and

$$K_{sv} = C_0 + C_1 \times T + C_2 \times T^2$$

$$V_0 = 1 + C_3 \times T$$

$$V = C_4 + C_5 \times V_b + C_6 \times t + C_7 \times t \times V_b$$

where V_b is the RINKO output (voltage), V_0 is voltage in the absence of oxygen, T is temperature in °C, and t is exciting time (days) integrated from the first CTD cast for each leg. Time drift of the RINKO output was corrected. The calibration coefficients were determined by minimizing the sum of absolute deviation with a weight from the bottle oxygen data. The revised quasi-Newton method (DMINF1) was used to determine the sets.

The post-cruise calibrated temperature and salinity data were used for the calibration. The calibration coefficients are listed in Table 3.1.5. The results of the post-cruise calibration for the RINKO oxygen are summarized in Table 3.1.6 and shown in Fig. 3.1.6.

Table 3.1.5. Calibration coefficients for the RINKO oxygen sensors.

Coefficient	S/N 0024
c_0	4.08789e-3
c_1	1.58333e-4
c_2	2.10854e-6
c_3	-1.14204e-3
c_4	-0.109961
c_5	0.356093
c_6	-2.55873e-4
c_7	3.13918e-4
c_p	0.014

Table 3.1.6. Difference between the RINKO oxygen and the bottle oxygen after the post-cruise calibration.

Mean and standard deviation (Sdev) are calculated for the data below and above 1950 dbar. Number of data used is also shown.

Serial number	Pressure \geq 1950 dbar			Pressure < 1950 dbar		
	Number	Mean	Sdev	Number	Mean	Sdev
	[$\mu\text{mol/kg}$]			[$\mu\text{mol/kg}$]		
0024	1571	-0.03	0.30	2100	0.01	1.50

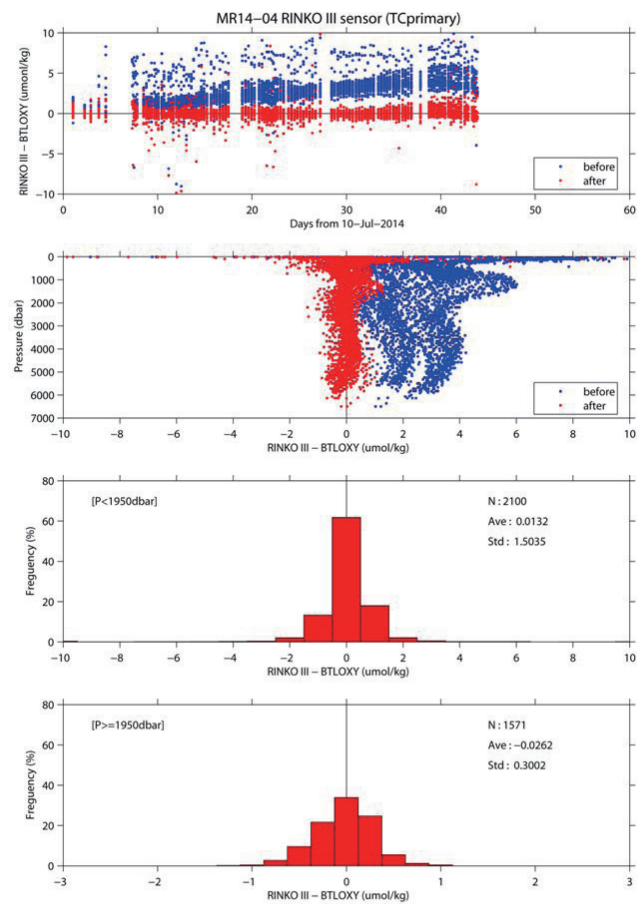


Figure 3.1.6. Difference between the CTD oxygen and the bottle oxygen for leg 1. Blue and red dots indicate before and after the post-cruise calibration, respectively. Lower two panels show histogram of the difference after the calibration.

Correction of down cast RINKO profiles for pressure hysteresis

Data from the RINKO can be corrected for the time-dependent, pressure-induced effect by means of the same method as that developed for the SBE 43 (Edwards et al., 2010). The calibration coefficients, H1 (amplitude of hysteresis correction), H2 (curvature function for hysteresis), and H3 (time constant for hysteresis) were empirically determined before the R/V Mirai cruise MR12-05 and used for the cruises MR12-05 and MR14-04 as follows:

$$H1 = 0.007 \text{ (for serial no. 0024)}$$

$$H2 = 5000 \text{ dbar}$$

$$H3 = 2000 \text{ seconds.}$$

However, it was found that magnitude of the time-dependent, pressure-induced hysteresis was changed in time (Fig. 3.1.7). Although to determine the calibration coefficients (H1, H2, and H3) and to reprocess from the raw RINKO data is the best way for correction of the hysteresis, it is actually quite time-consuming to reprocess. Therefore, the discrepancy between the down and up cast profiles for depths deeper than 300 dbar were simply corrected by using a model as a function of pressure and the maximum pressure of the cast as follows:

$$O_{cor} = O + C \times (p_{max} - 300) / (6500.0 - 300.0) \times \sin(\pi / (p_{max} - 300.0) \times (P - 300.0))$$

where O is the RINKO oxygen in $\mu\text{mol/kg}$ before the correction, P is pressure in dbar, p_{max} is maximum pressure of the CTD cast, and C is correction factor. The correction factor C was estimated to be 0.3, 0.5 and 0.7 for MR12-05 leg 2, MR12-05 leg 3, and MR14-04 cruise, respectively.

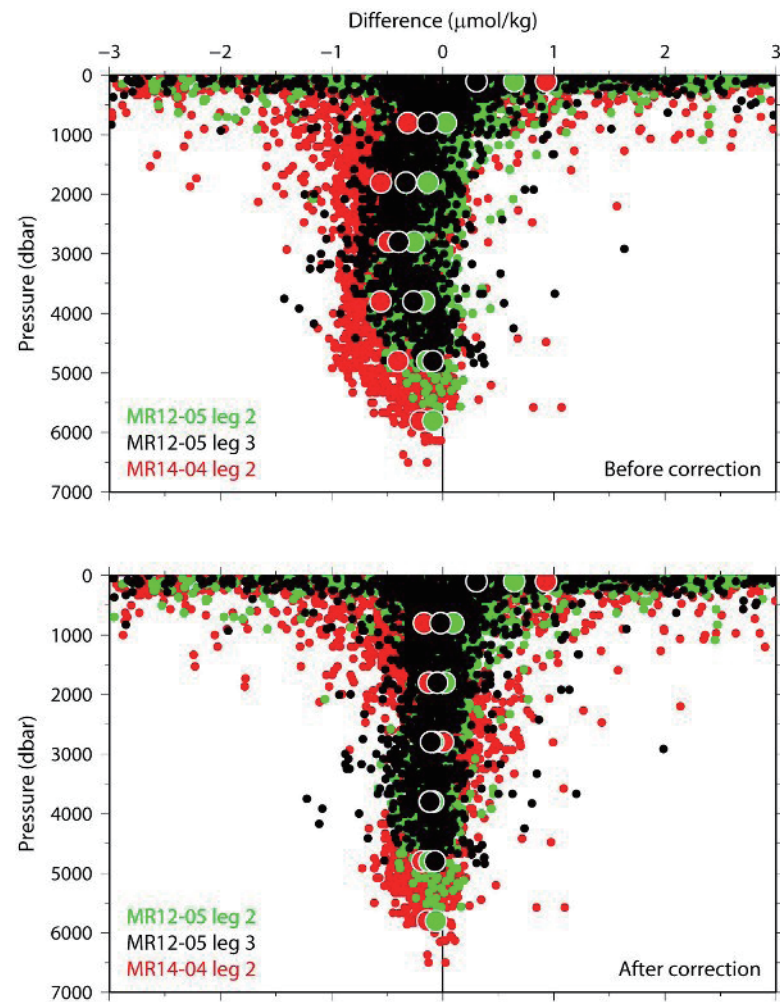


Figure 3.1.7. Difference between down and up cast CTD oxygen. Data at depths shallower than 300 dbar were compared on the same pressure surface and data at depths deeper than 300 dbar were compared on the same density surface (potential density with a reference pressure of 2500 dbar). Large dots indicate median value estimated from the data obtained at depths shallower than 300 dbar or at depths deeper than 300 dbar at 1000-dbar intervals.

v. Fluorometer

The CTD fluorometer (FLUOR in $\mu\text{g/L}$) was calibrated by comparing with the bottle sampled chlorophyll-*a* as

$$\text{FLUOR}_c = c_0 + c_1 \times \text{FLUOR}$$

where c_0 and c_1 are calibration coefficients. The CTD fluorometer data is slightly noisy so that the up cast profile data which was averaged over one decibar agree with the bottle sampled data better than the discrete CTD fluorometer data obtained at bottle-firing stop. Therefore, the CTD fluorometer data at water sampling depths extracted from the up cast profile data were compared with the bottle sampled chlorophyll-*a* data. The bottle sampled data obtained at dark condition [PAR (Photosynthetically Available Radiation) $< 50 \mu\text{E}/(\text{m}^2 \text{ sec})$, see Section 2.3] were used for the calibration, since sensitivity of the fluorometer to chlorophyll *a* is different at nighttime and daytime (Section 2.4 in Uchida et al., 2015a). Sensitivity of the fluorometer to chlorophyll *a* may be also different between high and low temperature (see Section 2.4). Therefore, the slopes (c_1) of the calibration coefficients are determined for three groups of stations: stations south of 38.8°N in leg 1 (001, 007, 014, and 022), the closest station to the coast (036), and other stations (Fig. 3.1.8). For the last group of stations, sensitivity of the fluorometer to chlorophyll *a* change at about $0.3 \mu\text{g/L}$ of the fluorometer data, so that the slope (c_1) is changed for the fluorometer data larger than $0.3 \mu\text{g/L}$. The calibration coefficients are listed in Table 3.1.7. The results of the post-cruise calibration for the fluorometer are summarized in Table 3.1.8 and shown in Fig. 3.1.9.

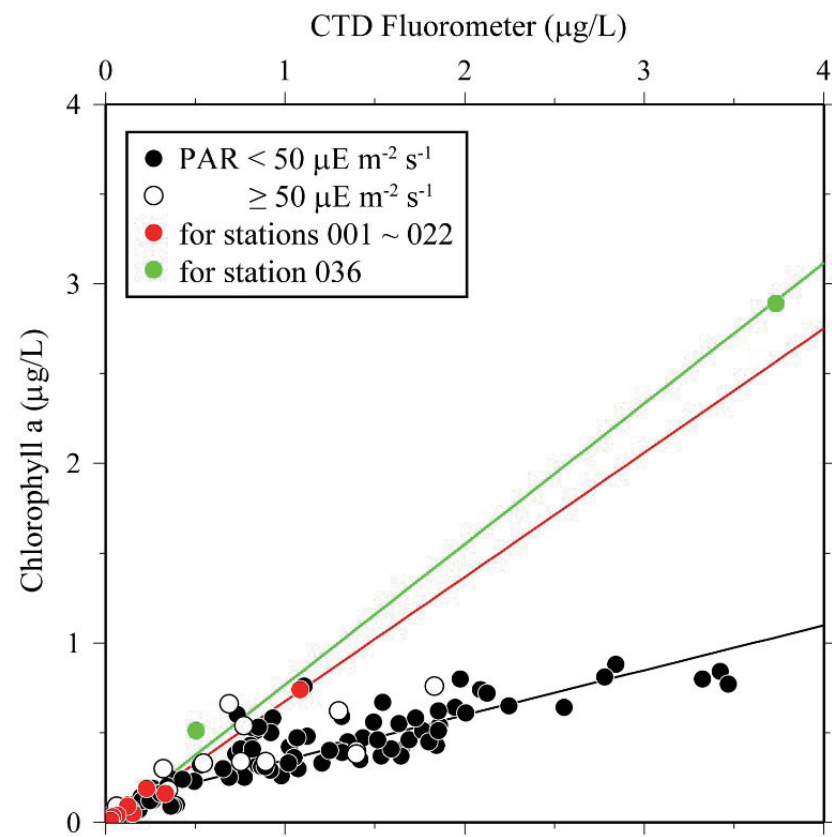


Figure 3.1.8. Comparison of the CTD fluorometer and the bottle sampled chlorophyll-*a*. The regression lines are also shown.

Table 3.1.7. Calibration coefficients for the CTD fluorometer.

Stations	c_0	c_1	Note
001, 007, 014, 022	-1.64441e-2	0.691796	
036	-1.64441e-2	0.783024	
Other stations	-1.64441e-2	0.630088	Fluorometer data ≤ 0.3 g/L
	9.75510e-2	0.250104	Fluorometer data > 0.3 g/L

Table 3.1.8. Difference between the CTD fluorometer and the bottle chlorophyll-*a* after the post-cruise calibration. Mean, standard deviation (Sdev), and number of data used are shown. Data obtained at daytime are also used in this calculation.

Number	Mean	Sdev
221	-0.00 µg/L	0.08 µg/L

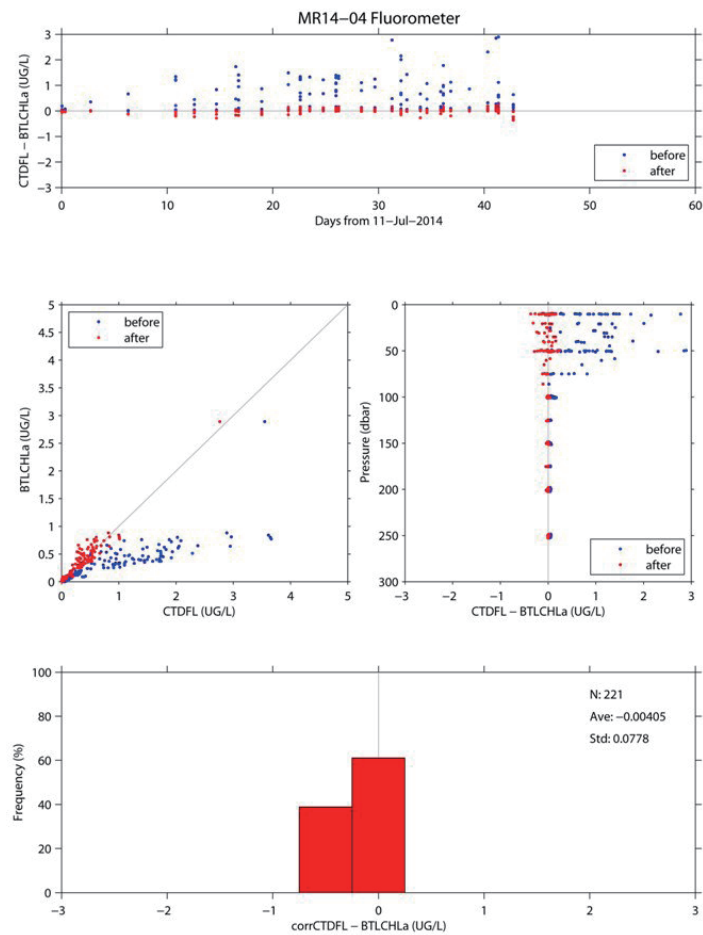


Figure 3.1.9. Comparison of the CTD fluorometer and the bottle sampled chlorophyll-*a*. Blue and red dots indicate before and after the post-cruise calibration, respectively. Lower panel shows histogram of the difference after the calibration. Data obtained at daytime are also shown in this figure.

vi. Transmissometer

The transmissometer (T_r in %) is calibrated as

$$T_r = (V - V_d) / (V_r - V_d) \times 100$$

where V is the measured signal (voltage), V_d is the dark offset for the instrument, and V_r is the signal for clear water. V_d can be obtained by blocking the light path. V_d and V_{air} , which is the signal for air, were measured on deck before each cast after wiping the optical windows with ethanol. V_d was constant (0.0012) during the cruise. V_r is estimated from the measured maximum signal in the deep ocean at each cast. Since the transmissometer drifted in time (Fig. 3.1.10), V_r is expressed as

$$V_r = c_0 + c_1 \times t + c_2 \times t^2$$

where t is working time (in days) of the transmissometer, and c_0 , c_1 , and c_2 are calibration coefficients.

The calibration coefficients are listed in Table 3.1.9. For stations 066 and 097, V_r shifted though V_d was same as others. Therefore, V_r was individually estimated as to be 4.6166 and 4.6044 for stations 066 and 097, respectively. In addition, the transmissometer data for station 141_1 was also corrected with an offset of +0.0055 volts.

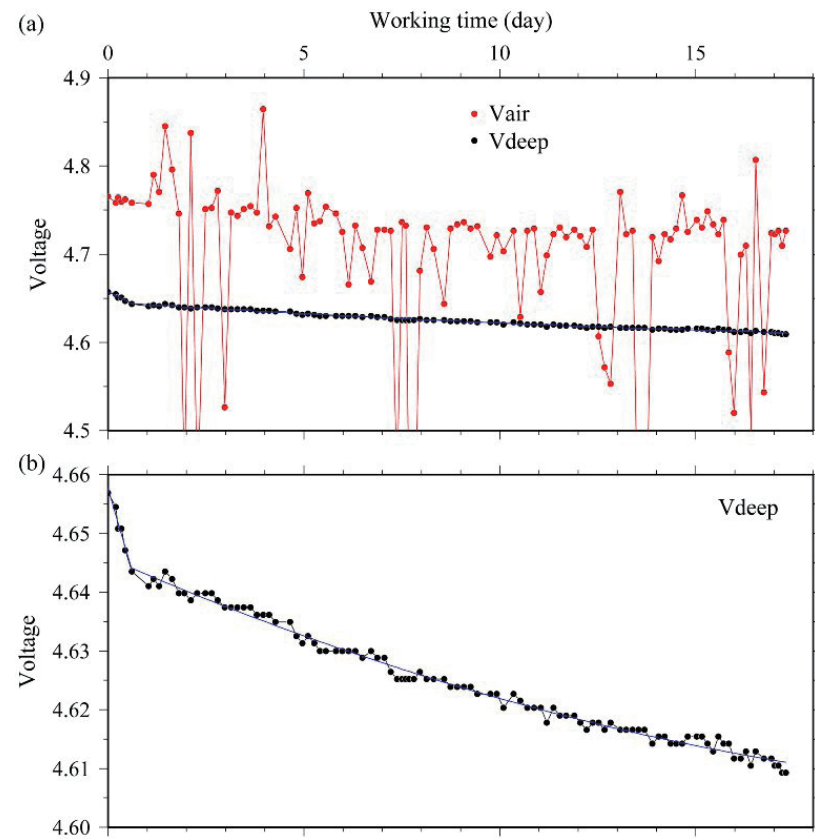


Figure 3.1.10. Time series of an output signal (voltage) from transmissometer at on deck before CTD casts (Vair) and deep ocean (Vdeep). The black solid line indicates the modeled signal in the deep clear ocean.

Table 3.1.9. Calibration coefficients for the CTD transmissometer.

Leg	c_0	c_1	c_2	V_d
1	4.65763	-2.28408e-2	-	0.0012
2	4.64582	-2.91438e-3	5.23667e-5	0.0012

vii. PAR

The PAR sensor was calibrated with an offset correction. The offset was estimated from the data measured in the deep ocean during the cruise. The corrected data (PARc) is calculated from the raw data (PAR) as follows:

$$\text{PARc} [\mu\text{E m}^{-2} \text{ s}^{-1}] = \text{PAR} - 0.046.$$

viii. CDOM

The CDOM sensor wasn't calibrated, since the reference data (see Section 3.9) was not adequate for the in-situ calibration. The data were low-pass filtered by a running mean with a window of 15 seconds (about 13 m), since the data was noisy (Fig. 3.1.11). Moreover, the data were flagged as 4 (bad measurement) for depths deeper than about 4500 m due to large shift of the data (Fig. 3.1.11).

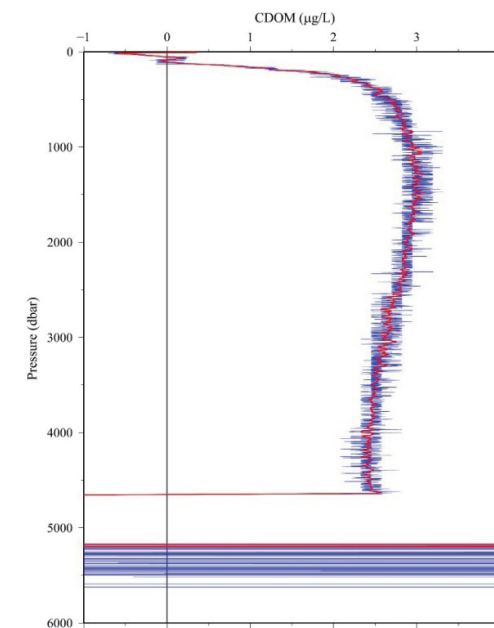


Figure 3.1.11. An example of vertical profile of the CDOM sensor (station 100). Blue line shows original data and red line shows low-pass filtered data.

ix. Deep SUNA

The down and up cast profile from the Deep SUNA showed relatively large difference (Fig. 3.1.12). Maximum difference between the down and up cast data was about 0.084 volts and it corresponded to 4 $\mu\text{mol/kg}$ of nitrate (Fig. 3.1.13). Since average of the down and up cast data at same pressure surface showed better linearity against the bottle sampled nitrate data (Fig. 3.1.13), nitrate from the Deep SUNA (NRA in $\mu\text{mol/kg}$) was estimated from the average data (NRAVave in volts) by comparing with the bottle sampled nitrate data as

$$\text{NRA} = c_0 + c_1 \times \text{NRAVave}$$

where c_0 and c_1 are calibration coefficients. The calibration coefficients are listed in Table 3.1.10. The average of the down and up cast data was used for the bottle sampled data (seafile) and profile data (wct file).

Table 3.1.10. Calibration coefficients for the Deep SUNA.

number of comparison	c_0	c_1	Sdev
43	-5.84651	22.7101	0.53 $\mu\text{mol/kg}$

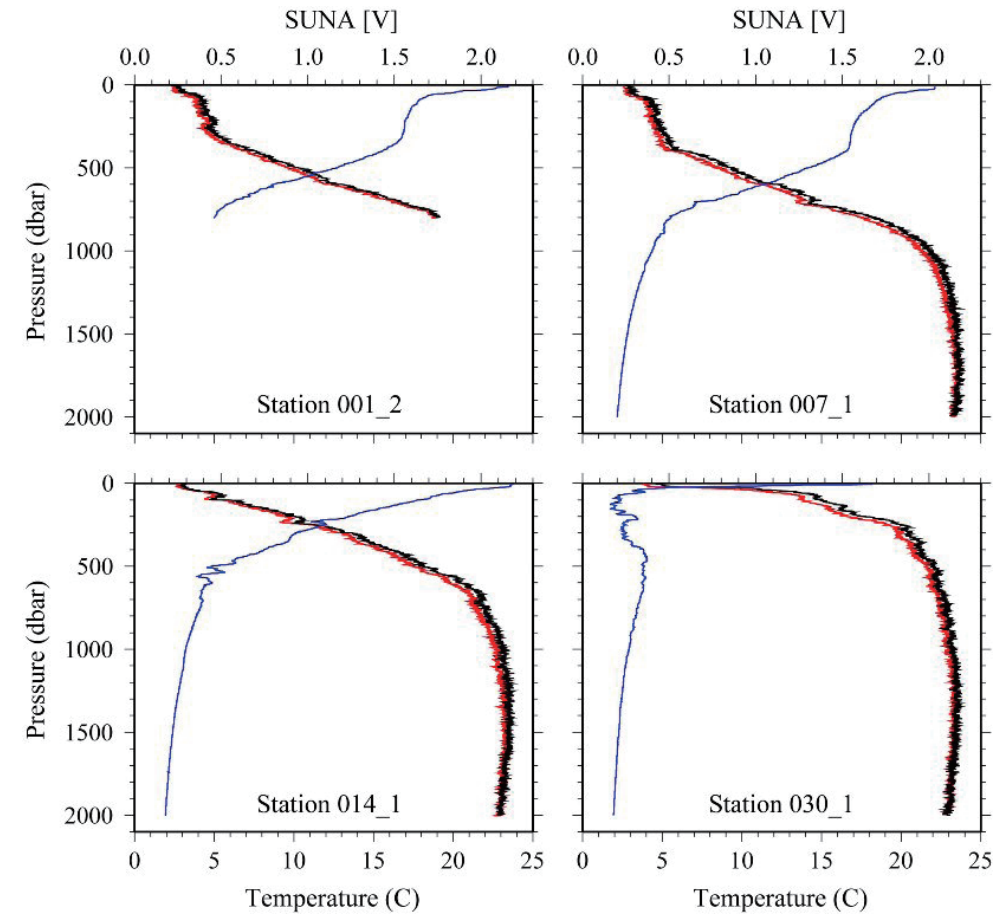


Figure 3.1.12. Vertical profiles of raw data (voltage) of the Deep SUNA (red line: down cast, black line: up cast) and temperature (blue line).

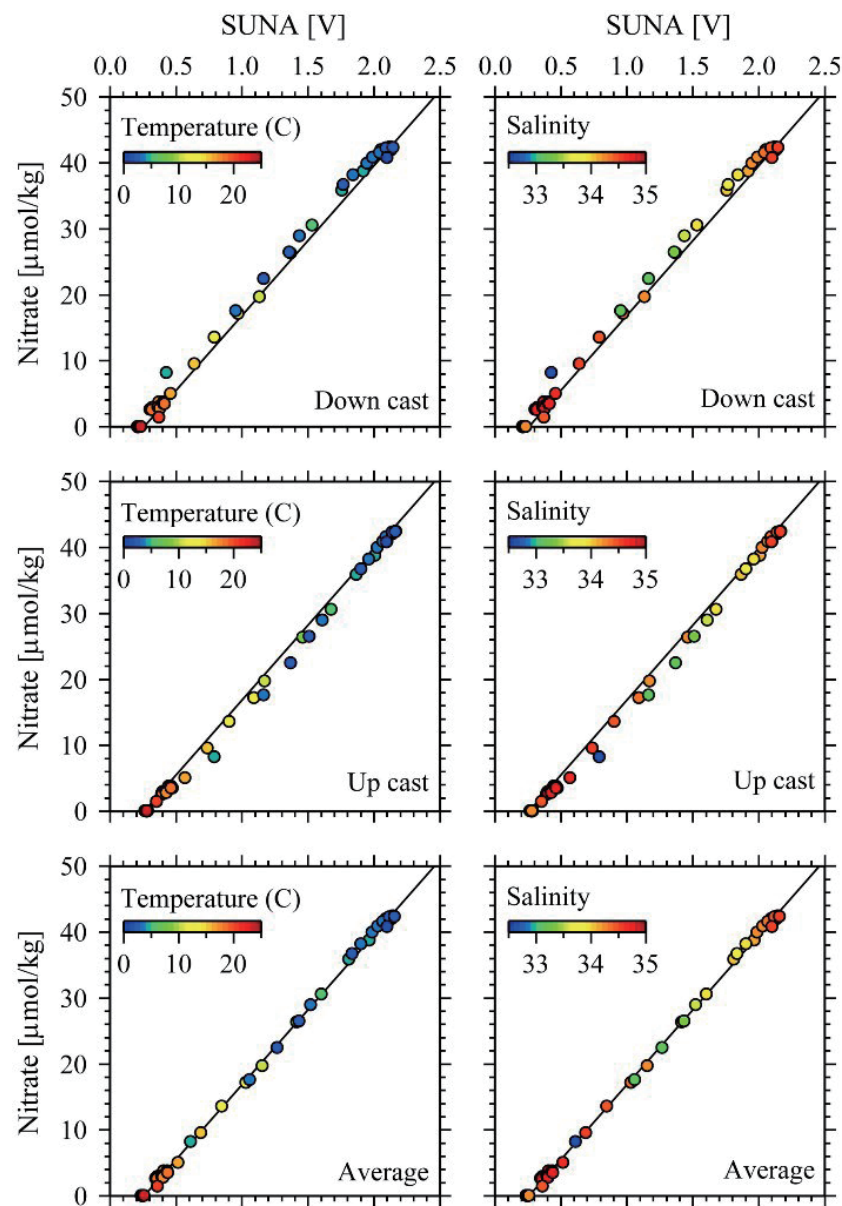


Figure 3.1.13. Comparison of the Deep SUNA output (voltage) and the bottle sampled nitrate. Upper panels are for down cast, middle panels are for up cast, and lower panels are for average of the down and up cast for the Deep SUNA data. The regression lines for the average data are shown.

(7) References

- Edwards, B., D. Murphy, C. Janzen and N. Larson (2010): Calibration, response, and hysteresis in deep-sea dissolved oxygen measurements, *J. Atmos. Oceanic Technol.*, 27, 920–931.
- Fukasawa, M., T. Kawano and H. Uchida (2004): Blue Earth Global Expedition collects CTD data aboard Mirai, BEAGLE 2003 conducted using a Dynacon CTD traction winch and motion-compensated crane, *Sea Technology*, 45, 14–18.
- García, H. E. and L. I. Gordon (1992): Oxygen solubility in seawater: Better fitting equations. *Limnol. Oceanogr.*, 37 (6), 1307–1312.
- Uchida, H., G. C. Johnson, and K. E. McTaggart (2010): CTD oxygen sensor calibration procedures, The GO-SHIP Repeat Hydrography Manual: A collection of expert reports and guidelines, IOCCP Rep., No. 14, ICPO Pub. Ser. No. 134.
- Uchida, H., K. Katsumata, and T. Doi (eds.) (2015a): WHP P14S, S04I Revisit in 2012 Data Book, 187 pp., JAMSTEC.
- Uchida, H., T. Nakano, J. Tamba, J.V. Widiatmo, K. Yamazawa, S. Ozawa and T. Kawano (2015b): Deep ocean temperature measurements with an uncertainty of 0.7 mK, *J. Atmos. Oceanic Technol.*, 32, 2199–2210.
- Uchida, H., K. Ohya, S. Ozawa, and M. Fukasawa (2007): In situ calibration of the Sea-Bird 9plus CTD thermometer, *J. Atmos. Oceanic Technol.*, 24, 1961–1967.

3.2 Bottle Salinity

September 10, 2014

(1) Personnel

Hiroshi Uchida (JAMSTEC)

Tatsuya Tanaka (MWJ)

Sonoka Wakatsuki (MWJ)

(2) Objectives

Bottle salinities were measured to calibrate CTD salinity data.

(3) Instrument and Method

Salinity measurement was conducted basically based on a method by Kawano (2010).

i. Salinity Sample Collection

The bottles in which the salinity samples were collected and stored were 250 ml brown borosilicate glass bottles with screw caps (PTFE packing). Each bottle was rinsed three times with sample water and was filled to the shoulder of the bottle. The caps were also thoroughly rinsed. Salinity samples were stored more than 24 hours in the same laboratory as the salinity measurement was made.

ii. Instruments and Methods

Salinity of water samples was measured with a salinometer (Autosal model 8400B; Guildline Instruments Ltd., Ontario, Canada; S/N 62827), which was modified by adding an peristaltic-type intake pump (Ocean Scientific International Ltd., Hampshire, UK) and two platinum thermometers (Guildline Instruments Ltd., model 9450). One thermometer monitored an ambient temperature and the other monitored a salinometer's bath temperature. The resolution of the thermometers was 0.001 °C. The measurement system was almost

same as Aoyama et al. (2002). The salinometer was operated in the air-conditioned laboratory of the ship at a bath temperature of 24 °C.

The ambient temperature varied from approximately 22.5 to 24.5 °C, while the bath temperature was stable and varied within ± 0.002 °C. A measure of a double conductivity ratio of a sample was taken as a median of 31 readings. Data collection was started after 10 seconds and it took about 10 seconds to collect 31 readings by a personal computer. Data were sampled for the sixth and seventh filling of the cell. In case where the difference between the double conductivity ratio of this two fillings was smaller than 0.00002, the average value of the two double conductivity ratios was used to calculate the bottle salinity with the algorithm for practical salinity scale, 1978 (UNESCO, 1981). When the difference was greater than or equal to the 0.00003, we measured another additional filling of the cell. In case where the double conductivity ratio of the additional filling did not satisfy the criteria above, we measured other additional fillings of the cell within 10 fillings in total. In case where the number of fillings was 10 and those fillings did not satisfy the criteria above, the median of the double conductivity ratios of five fillings were used to calculate the bottle salinity.

The measurement was conducted about from 3 to 18 hours per day and the cell was cleaned with soap (50 times diluted solution of S-CLEAN WO-23 [Neutral], Sasaki Chemical Co. Ltd., Kyoto, Japan) after the measurement for each day. A total of 4584 water samples were measured during the cruise.

(4) Results

i. Standard Seawater

Standardization control was set to 512. The value of STANDBY was 5392 or 5393 \pm 0001 and that of ZERO was 0.00000 or -0.00001. We used IAPSO Standard Seawater batch P156 whose conductivity ratio is 0.99984 (double conductivity ratio is 1.99968) as the standard for salinity measurement. We measured 188 bottles of the Standard Seawater during the cruise. History of double conductivity ratio measurement of the Standard Seawater is shown in Fig. 3.2.1.

Time drift of the salinometer was corrected by using the Standard Seawater measurements. Linear time drift of the salinometer was estimated from the Standard Seawater measurement by using the least square

method (thin black line in Fig. 3.2.1). No remarkable time drift was estimated from the Standard Seawater measurement. The average of double conductivity ratio was 1.99968 and the standard deviation was 0.00001, which is equivalent to 0.0003 in salinity.

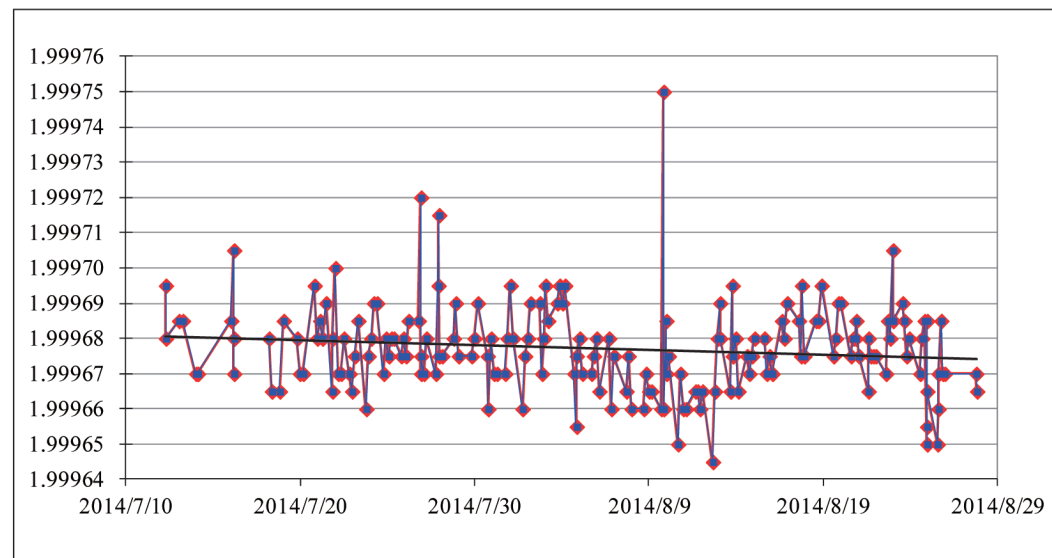


Figure 3.2.1. History of double conductivity ratio measurement of the Standard Seawater (P156). Horizontal and vertical axes represent date and double conductivity ratio, respectively. Blue dots indicate raw data and red dots indicate corrected data.

ii. Sub-Standard Seawater

We also used sub-standard seawater which was deep-sea water filtered by pore size of 0.45 μm and stored in a 20 liter cubitainer made of polyethylene and stirred for at least 24 hours before measuring. It was measured every 6 samples in order to check the possible sudden drift of the salinometer. During the whole measurements, there was no detectable sudden drift of the salinometer.

iii. Replicate Samples

We took 675 pairs of replicate samples collected from the same Niskin bottle. Histogram of the absolute difference between replicate samples is shown in Fig. 3.2.2. The root-mean-square of the absolute difference was 0.0002.

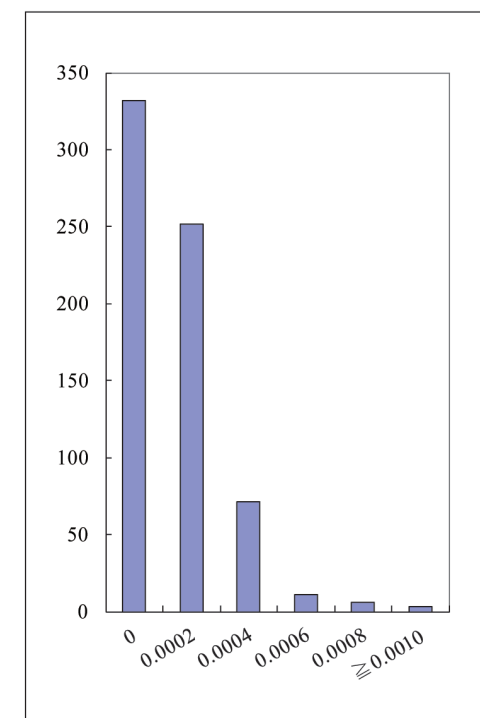


Figure 3.2.2. Histogram of the absolute difference between replicate samples. Horizontal axis is absolute difference in salinity and vertical axis is frequency.

iv. Duplicate Samples

We took 37 pairs of duplicate samples collected from the different Niskin bottle at same depth. Histogram of the absolute difference between duplicate samples is shown in Fig. 3.2.3. The root-mean-square of the absolute difference was 0.0003.

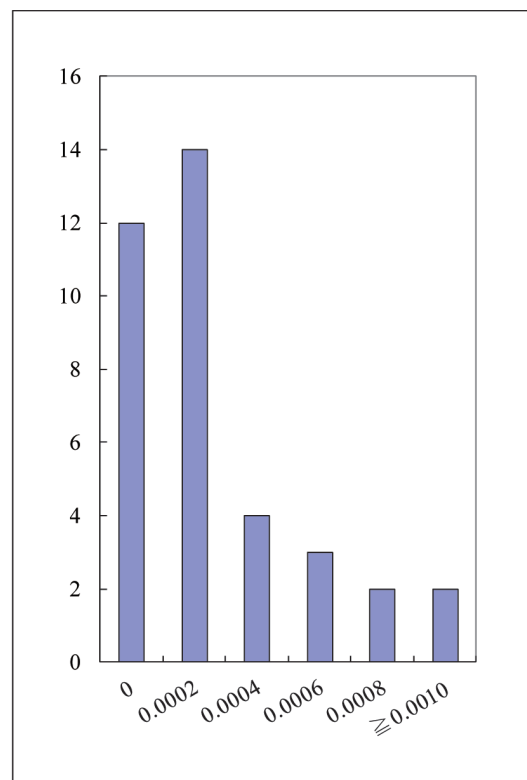


Fig. 3.2.3. Histogram of the absolute difference between duplicate samples. Horizontal axis is absolute difference in salinity and vertical axis is frequency.

(5) References

- Aoyama, M., T. Joyce, T. Kawano and Y. Takatsuki (2002): Standard seawater comparison up to P129. Deep-Sea Research, I, Vol. 49, 1103-1114.
- Kawano (2010): Salinity. The GO-SHIP Repeat Hydrography Manual: A collection of Expert Reports and Guidelines, IOCCP Report No. 14, ICPO Publication Series No. 134, Version 1.
- UNESCO (1981): Tenth report of the Joint Panel on Oceanographic Tables and Standards. UNESCO Tech. Papers in Mar. Sci., 36, 25 pp.

3.3 Density

November 25, 2014

(1) Personnel

Hiroshi Uchida (JAMSTEC)

(2) Objectives

The objective of this study is to collect absolute salinity (also called “density salinity”) data, and to evaluate an algorithm to estimate absolute salinity provided along with TEOS-10 (the International Thermodynamic Equation of Seawater 2010) (IOC et al., 2010).

(3) Materials and methods

Seawater densities were measured during the cruise with an oscillation-type density meter (DMA 5000M, serial no. 80570578, Anton-Paar GmbH, Graz, Austria) with a sample changer (Xsample 122, serial no. 80548492, Anton-Paar GmbH). The sample changer was used to load samples automatically from up to ninety-six 12-mL glass vials.

The water samples were collected in 100-mL aluminum bottles (Mini Bottle Can, Daiwa Can Company, Japan). The bottles were stored at room temperature (~23 °C) upside down usually for 12 to 24 hours to make the temperature of the sample equal to the room temperature. The water sample was filled in a 12-mL glass vial and the glass vial was sealed with Parafilm M (Pechiney Plastic Packaging, Inc., Menasha, Wisconsin, USA) immediately after filling. Densities of the samples were measured at 20 °C by the density meter two times for each bottle and averaged to estimate the density. When the difference between the two measurements was greater than 0.002, additional measurements were conducted until two samples satisfying the above criteria were obtained.

Time drift of the density meter was monitored by periodically measuring the density of ultra-pure water (Milli-Q water, Millipore, Billerica, Massachusetts, USA) prepared from Yokosuka (Japan) tap water in

October 2012. The true density at 20 °C of the Milli-Q water was estimated to be 998.2042 kg m⁻³ from the isotopic composition ($\delta D = -8.76 \text{ ‰}$, $\delta^{18}O = -56.86 \text{ ‰}$) and International Association for the Properties of Water and Steam (IAPWS)-95 standard. An offset correction was applied to the measured density by using the Milli-Q water measurements ($\rho_{\text{Milli-Q}}$) with a slight modification of the density dependency (Uchida et al., 2011). The offset (ρ_{offset}) of the measured density (ρ) was reevaluated in November 2014 as follows:

$$\rho_{\text{offset}} = (\rho_{\text{Milli-Q}} - 998.2042) - (\rho - 998.2042) \times 0.000411 \text{ [kg m}^{-3}\text{]}.$$

The offset correction was verified by measuring Reference Material for Density in Seawater (prototype Dn-RM1 and Pre 18) developing with Marine Works Japan, Ltd., Kanagawa, Japan, and produced by Kanso Technos Co., Ltd., Osaka, Japan, along with the Milli-Q water.

Density salinity can be back calculated from measured density and temperature (20 °C) with TEOS-10.

(4) Results

Results of density measurements of the Reference Material for Density in Seawater (Dn-RM1 and Pre 18) were shown in Table 3.3.1 and Table 3.3.2. Mean densities of the Dn-RM1 and Pre 18 were in good agreement with the measurements before the reevaluation of the offset of density measurements (Table 3.3.2).

A total of 16 pairs of replicate samples were measured. The root-mean square of the absolute difference of replicate samples was 0.0008 g/kg.

The measured density salinity anomalies (δS_A) are shown in Fig. 3.3.1. The measured δS_A well agree with calculated δS_A from Pawlowicz et al. (2011) which exploits the correlation between δS_A and nutrient concentrations and carbonate system parameters based on mathematical investigation using a model relating composition, conductivity and density of arbitrary seawaters.

(5) References

IOC, SCOR and IAPSO (2010): The international thermodynamic equation of seawater – 2010: Calculation and use of thermodynamic properties. Intergovernmental Oceanographic Commission, Manuals and Guides No. 56, United Nations Educational, Scientific and Cultural Organization (English), 196 pp.

Pawlowicz, R., D. G. Wright and F. J. Millero (2011): The effects of biogeochemical processes on ocean conductivity/salinity/density relationships and the characterization of real seawater. *Ocean Science*, 7, 363–387.

Uchida, H., T. Kawano, M. Aoyama and A. Murata (2011): Absolute salinity measurements of standard seawaters for conductivity and nutrients. *La mer*, 49, 237–244.

Table 3.3.1. Result of density measurements of the Reference Material for Density in Seawater (prototype Dn-RM1).

Date	Stations (sample no.)	Mean density of Dn-RM1 (kg/m ³)	Note
------	--------------------------	--	------

Leg 1

2014/07/11	001	1024.2625	
2014/07/12	007,014	1024.2649	
2014/07/14	022,030	1024.2645	

Leg 2

2014/07/18	036,037,038,040	1024.2641	
2014/07/19	045	1024.2627	
2014/07/20	043	1024.2622	
2014/07/21	051	1024.2643	
2014/07/25	060	1024.2617	
2014/07/27	067	1024.2632	
2014/07/29	073	1024.2621	
2014/08/01	079	1024.2619	

2014/08/03	089	1024.2615	
2014/08/05	095	1024.2613	
2014/08/07	101	1024.2621	
2014/08/11	110	1024.2625	
2014/08/14	120	1024.2618	
2014/08/16	128	1024.2631	
2014/08/17	151	1024.2620	
2014/08/20	136	1024.2623	
2014/08/22	140,143	1024.2639	Stn. 140 #16: Miss trip (flag 4)
2014/08/23	145,147	1024.2621	
2014/08/24	148,149,150	1024.2618	

Average: 1024.2627 ± 0.0010

Table 3.3.2. Comparison of density measurement of the Reference Material for Density in Seawater (prototype Dn-RM1 and Pre 18).

Date	Serial no.	Density [kg/m ³]	Note
<i>Measurements on this cruise</i>			
<i>Pre 18</i>			
2014/07/23	270	1024.2222	
2014/08/18	150	1024.2216	
2014/08/18	309	1024.2219	
2014/08/20	370	1024.2223	
2014/08/22	289	1024.2223	
		Average: 1024.2221 ± 0.0003	
<i>Dn-RM1</i>			
2014/07/11- 2014/08/24		1024.2627 ± 0.0010	See Table 3.3.1
<i>Recent measurements before this cruise</i>			
<i>Pre 18</i>			
2014/03/27- 2014/04/06		1024.2216 ± 0.0012	4 bottles
<i>Dn-RM1</i>			
2014/04/03-06		1024.2623 ± 0.0007	8 bottles

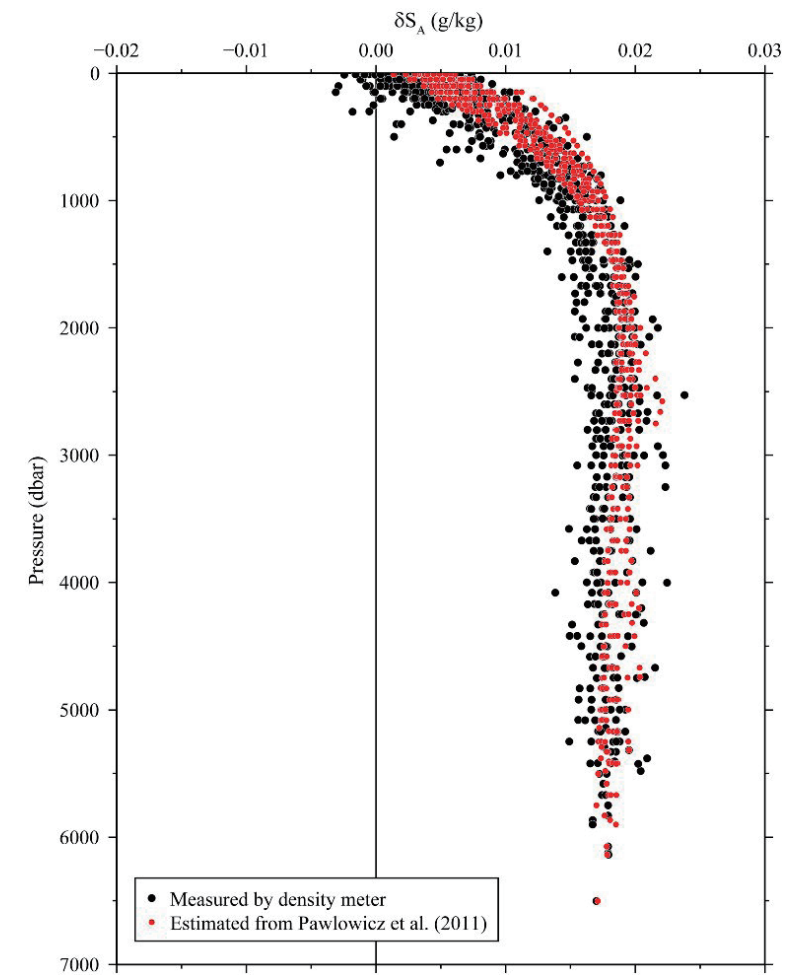


Figure 3.3.1. Vertical distribution of density salinity anomaly measured by the density meter. Absolute Salinity anomaly estimated from nutrients and carbonate parameters (Pawlowicz et al., 2011) are also shown for comparison.

3.4 Oxygen

August 26, 2014

(1) Personnel

Yuichiro Kumamoto ¹⁾, Misato Kuwahara ²⁾, Keitaro Matsumoto ²⁾, Katsunori Sagishima ²⁾, and Haruka Tamada ²⁾

1) Japan Agency for Marine-Earth Science and Technology

2) Marine Works Japan Co. Ltd

(2) Objectives

Dissolved oxygen is one of good tracers for the ocean circulation. Climate models predict a decline in oceanic dissolved oxygen concentration and a consequent expansion of the oxygen minimum layers under global warming conditions, which results mainly from decreased interior advection and ongoing oxygen consumption by remineralization. The mechanism of the decrease, however, is still unknown. During MR14-04 cruise, we measured dissolved oxygen concentration from surface to bottom layers at all the hydrocast stations in the North Pacific Ocean. All the stations reoccupied the WOCE Hydrographic Program P10N (Leg-1) and P01 (Leg-2) stations in the 1990s. Our purpose is to evaluate temporal change in dissolved oxygen concentration in the North Pacific Ocean during the past decades.

(3) Reagents

Pickling Reagent I: Manganous chloride solution (3M)

Pickling Reagent II: Sodium hydroxide (8M) / sodium iodide solution (4M)

Sulfuric acid solution (5M)

Sodium thiosulfate (0.025M)

Potassium iodate (0.001667M): Wako Pure Chemical Industries, Ltd., volumetric standard, reference material for iodometry, Lot No.TLG0272, Purity: 99.97 ± 0.04 %

CSK standard of potassium iodate: Lot TLM1372, Wako Pure Chemical Industries Ltd., 0.0100N

(4) Instruments

Burette for sodium thiosulfate and potassium iodate;

APB-620 and APB-510 manufactured by Kyoto Electronic Co. Ltd. / 10 cm³ of titration vessel

Detector;

Automatic photometric titrator, DOT-01X manufactured by Kimoto Electronic Co. Ltd.

(5) Seawater sampling

Following procedure is based on a determination method in the WHP Operations Manual (Dickson, 1996). Seawater samples were collected from 12-liters Niskin sampler bottles attached to the CTD-system. Seawater for bottle oxygen measurement was transferred from the Niskin sampler bottle to a volume calibrated glass flask (ca. 100 cm³). Three times volume of the flask of seawater was overflowed. Sample temperature was measured using a thermometer (ARO-PR, JFE Advantech Co. Ltd.) that was calibrated with a standard thermometer (SBE 3plus, Sea-Bird Electronics, Inc.). Then two reagent solutions (Reagent I, II) of 0.5 cm³ each were added immediately into the sample flask and the stopper was inserted carefully into the flask. The sample flask was then shaken vigorously to mix the contents and to disperse the precipitate finely throughout. After the precipitate has settled at least halfway down the flask, the flask was shaken again to disperse the precipitate. The sample flasks containing pickled samples were stored in a laboratory until they were titrated.

(6) Sample measurement

At least two hours after the re-shaking, the pickled samples were measured on board. A magnetic stirrer bar and 1 cm³ sulfuric acid solution were added into the sample flask and stirring began. Samples were titrated by sodium thiosulfate solution whose molarity was determined by potassium iodate solution. Temperature of sodium thiosulfate during titration was recorded by a thermometer. We measured dissolved

oxygen concentration using two sets of the titration apparatus, named DOT-7 and DOT-8. Dissolved oxygen concentration ($\mu\text{mol kg}^{-1}$) was calculated by the sample temperature during the sampling, CTD salinity, flask volume, and titrated volume of the sodium thiosulfate solution.

(7) Standardization

Concentration of sodium thiosulfate titrant (ca. 0.025M) was determined by potassium iodate solution. Pure potassium iodate was dried in an oven at 130°C. 1.7835 g potassium iodate weighed out accurately was dissolved in deionized water and diluted to final volume of 5 dm³ in a calibrated volumetric flask (0.001667M). 10 cm³ of the standard potassium iodate solution was added to a flask using a volume-calibrated dispenser. Then 90 cm³ of deionized water, 1 cm³ of sulfuric acid solution, and 0.5 cm³ of pickling reagent solution II and I were added into the flask in order. Amount of titrated volume of sodium thiosulfate (usually 5 times measurements average) gave the molarity of the sodium thiosulfate titrant. Table 3.4.1 shows result of the standardization during this cruise. Coefficient of variation (C.V.) for the standardizations was $0.02 \pm 0.01 \%$ (n = 36), c.a. $0.05 \mu\text{mol kg}^{-1}$.

(8) Determination of the blank

The oxygen in the pickling reagents I (0.5 cm³) and II (0.5 cm³) was assumed to be 3.8×10^{-8} mol (Murray *et al.*, 1968). The blank from the presence of redox species apart from oxygen in the reagents (the pickling reagents I, II, and the sulfuric acid solution) was determined as follows. 1 and 2 cm³ of the standard potassium iodate solution were added to two flasks respectively. Then 100 cm³ of deionized water, 1 cm³ of sulfuric acid solution, and 0.5 cm³ of pickling reagent solution II and I each were added into the two flasks in order. The blank was determined by difference between the two times of the first (1 cm³ of KIO₃) titrated volume of the sodium thiosulfate and the second (2 cm³ of KIO₃) one. The results of 3 times blank determinations were averaged (Table 3.4.1). The averaged blank values for DOT-7 and DOT-8 were 0.000 ± 0.001 (standard deviation, S.D., n=18) and 0.000 ± 0.001 (S.D., n=18) cm³, respectively.

Table 3.4.1. Results of the standardization (End point, E.P.) and the blank determinations (cm³).

Date(UTC)	KIO ₃ No.	Na ₂ S ₂ O ₃ No.	DOT-7		DOT-8		Stations
			E.P.	blank	E.P.	blank	
2014/7/10	K1404B01	T1406A	3.957	-0.002	3.960	-0.002	001, 007, 014, 022, 030
2014/7/16	K1404B02	T1406C	3.956	0.000	3.961	-0.001	036, 037, 038, 039, 040, 047, 046, 045, 044, 041, 042, 043, 048, 049, 050, 051, 052, 053, 054
2014/7/22	K1404B03	T1406D	3.957	0.000	3.963	-0.001	055, 056, 057, 058, 059, 060, 061, 062, 063, 064, 065, 066, 067, 068
2014/7/26	K1404B04	T1406D	3.958	0.001	3.962	0.001	069, 070, 071, 072, 073, 074, 075, 076, 077, 078
2014/7/30	K1404B05	T1406E	3.958	0.001	3.958	0.000	079, 080, 081, 082, 083, 084, 085, 086, 087, 088, 089, 090, 091, 092, 093, 094, 095, 096, 097
2014/8/5	K1404B06	T1406E	3.956	0.000	3.962	-0.001	098, 099, 100, 101, 102, 103, 104
2014/8/8	K1404B07	T1406F	3.957	0.001	3.958	-0.001	105, 106, 107, 108, 109, 110, 111, 112, 113, 114, 115, 116, 117, 118
2014/8/13	K1404B09	T1406F	3.955	0.002	3.959	0.000	119, 120, 121, 122, 123, 124, 125, 126, 127, 128, 151
2014/8/17	K1404C01	T1406G	3.956	0.001	3.958	0.000	129, 130, 131, 132, 133, 134, 135, 136
2014/8/20	K1404C02	T1406G	3.955	0.000	3.958	0.000	137, 138, 139, 140, 141, 142, 143, 144, 145, 146, 147, 148, 149, 150

(9) Replicate sample measurement

From a routine CTD cast at all the stations, a pair of replicate samples was collected at four layers of 50, 400, 1800, and 3500 dbars. The total number of the replicate sample pairs in good measurement (flagged 2) was 447 (Fig. 3.4.1). The standard deviation of the replicate measurement was $0.12 \mu\text{mol kg}^{-1}$ calculated by a procedure (SOP23) in DOE (1994).

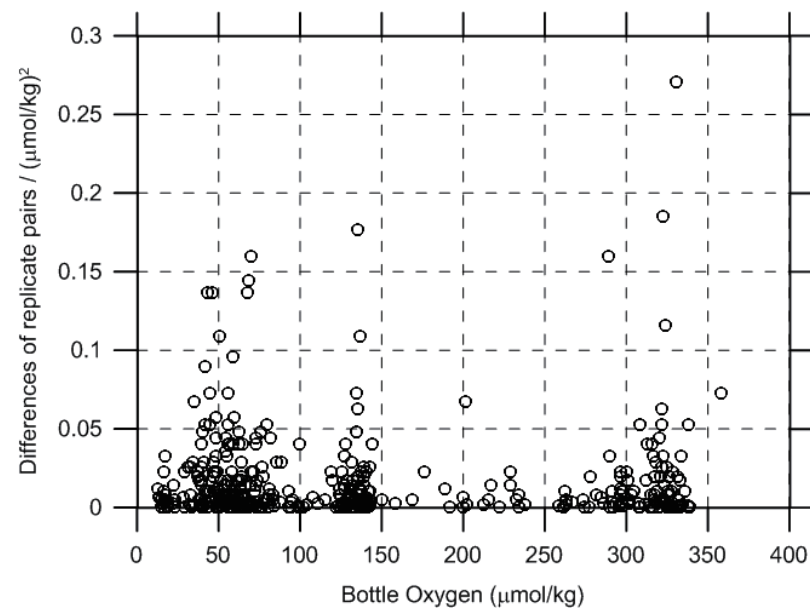


Figure 3.4.1. Oxygen difference between measurements of a replicate pair against oxygen concentration (Data from Stn. 139-1 #35: 0.79 and Stn. 146-1 #35: 4.00 ($\mu\text{mol kg}^{-1}$)² are not shown in this figure).

(10) Duplicate sample measurement

During the Leg-2 duplicate sampling were taken for all the Niskin bottles (36 bottles, Table 3.4.2). The standard deviation of the duplicate measurements were calculated to be $0.09 \mu\text{mol kg}^{-1}$, which were equivalent with that of the replicate measurements ($0.12 \mu\text{mol kg}^{-1}$, see section 9).

(11) CSK standard measurements

The CSK standard is a commercial potassium iodate solution (0.0100 N) for analysis of dissolved oxygen. We titrated the CSK standard solution (Lot TLM1372) against our KIO_3 standards as samples before and during the cruise (Table 3.4.3). A good agreement among them confirms that there was no systematic shift in our oxygen analyses between preparation of our KIO_3 standards onshore and the sample measurements on board.

(12) Quality control flag assignment

Quality flag values were assigned to oxygen measurements using the code defined in Table 0.2 of WHP Office Report WHPO 91-1 Rev.2 section 4.5.2 (Joyce *et al.*, 1994). Measurement flags of 2 (good), 3 (questionable), 4 (bad), and 5 (missing) have been assigned (Table 3.4.4). For the choice between 2, 3, or 4, we basically followed a flagging procedure as listed below:

- Bottle oxygen concentration at the sampling layer was plotted against sampling pressure. Any points not lying on a generally smooth trend were noted.
- Difference between bottle oxygen and CTD oxygen was then plotted against sampling pressure. If a datum deviated from a group of plots, it was flagged 3.
- Vertical sections against pressure and potential density were drawn. If a datum was anomalous on the section plots, datum flag was degraded from 2 to 3, or from 3 to 4.
- If there was problem in the measurement, the datum was flagged 4.
- If the bottle flag was 4 (did not trip correctly), a datum was flagged 4 (bad). In case of the bottle flag 3 (leaking) or 5 (unknown problem), a datum was flagged based on steps a, b, c, and d.

Table 3.4.2. Results of duplicate sample measurements.

	Leg	Stations	Duplicated Niskin #	Niskins	Duplicated Pres.(db)	Dissolved oxygen (µmol/kg)	
1	2	042	2-9	X12J02, 03,	4000	150.62	150.54
				04, 05, 06,		150.56	150.63
				07, 08 ,09		150.68	150.53
						150.49	150.44
2	2	048	1, (2)	X12J01	5575	160.04	159.98
3	2	049	(4), 10	X12J10	5330	159.42	159.25
4	2	051	(4), 11	X12J11	5250	159.90	160.04
5	2	052	(5), 12	X12J12	5080	159.06	159.29
6	2	053	(4), 13	X12113	5170	160.64	160.54
7	2	055	(4), 14	X12J14	5330	160.77	160.72
8	2	056	(3), 15	X12J15	5420	163.02	162.98
9	2	057	(3), 16	X12J16	5500	160.68	160.60
10	2	059	(4), 17	X12J17	5170	159.17	159.10
11	2	061	(5), 18	X12J18	5080	157.19	157.17
12	2	062	(4), 19	X12J19	5170	157.33	157.42
13	2	063	(5), 20	X12J20	5000	157.24	157.34
14	2	064	(4), 21	X12J21	5330	157.35	157.23
15	2	065	(4), 22	X12J22	5170	158.59	158.63
16	2	066	(4), 23	X12J23	5250	157.28	157.20
17	2	068	(4), 24	X12J24	5170	157.09	157.13
18	2	069	(6), 25	X12J25	4750	157.17	157.05
19	2	070	(6), 26	X12J26	4830	156.52	156.46
20	2	071	(6), 27	X12J27	4670	155.65	155.44

21	2	072	(5), 28	X12J28	5000	157.30	157.11
22	2	074	(3), 29	X12J29	5420	159.10	159.25
23	2	075	(3), 30	X12J30	5500	157.10	157.05
24	2	082	(5), 31	X12J31	5080	156.15	155.97
25	2	083	(8), 32	X12J32	4170	150.07	149.90
26	2	086	(9), 33	X12J33	3920	147.63	147.43
27	2	090	(3), 34	X12J34	5500	155.63	155.68
28	2	094	(3), 35	X12J35	5580	154.33	154.23
29	2	096	(3), 36	X12J36	5500	152.86	152.84
30	2	106	(2), 3	X12J03	5580	152.84	152.63
31	2	107	(2), 3	X12J03	5420	151.88	151.69

Table 3.4.3. Results of the CSK standard (Lot TLM1372) measurements.

Date (UTC)	KIO ₃ ID No.	DOT-5		-		Remarks
		Conc. (N)	error (N)	-	-	
2014/05/13	K1404A01	0.010012	0.000005			Onshore lab.
2014/05/14	K1404C12	0.010013	0.000003			Onshore lab.
2014/05/15	K1404I12	0.010010	0.000002			Onshore lab.
		DOT-7		DOT-8		
		Conc. (N)	error (N)	Conc. (N)	error (N)	
2014/06/09	K1404A09	0.010009	0.000004	0.010005	0.000003	MR14-03
2014/07/10	K1404B01	0.010005	0.000003	0.010004	0.000005	MR14-04 Leg-1
2014/08/17	K1404C01	0.010007	0.000004	0.010006	0.000003	MR14-04 Leg-2

Table 3.4.4. Summary of assigned quality control flags.

Flag	Definition	Number*
2	Good	3714
3	Questionable	1
4	Bad	4
5	Not report (missing)	2
Total		3721

*Replicate samples (n = 447) were not included.

DOE (1994) Handbook of methods for the analysis of the various parameters of the carbon dioxide system in sea water; version 2. A.G. Dickson and C. Goyet (eds), ORNL/CDIAC-74.

Joyce, T., and C. Corry, eds., C. Corry, A. Dessier, A. Dickson, T. Joyce, M. Kenny, R. Key, D. Legler, R. Millard, R. Onken, P. Saunders, M. Stalcup (1994) Requirements for WOCE Hydrographic Programme Data Reporting, WHPO Pub. 90-1 Rev. 2, May 1994 Woods Hole, Mass., USA.

Murray, C.N., J.P. Riley, and T.R.S. Wilson (1968) The solubility of oxygen in Winkler reagents used for determination of dissolved oxygen, Deep-Sea Res., 15, 237-238.

References

Dickson, A. (1996) Determination of dissolved oxygen in sea water by Winkler titration, in WHPO Pub. 91-1 Rev. 1, November 1994, Woods Hole, Mass., USA.

3.5 Nutrients

October 14, 2016 (ver.2.2)

(1) Personnel

Michio AOYAMA (JAMSTEC / Fukushima University, Principal Investigator)

Leg 1

Yasuhiro ARII (Department of Marine Science, Marine Works Japan Ltd.)

Minoru KAMATA (Department of Marine Science, Marine Works Japan Ltd.)

Tomomi SONE (Department of Marine Science, Marine Works Japan Ltd.)

Leg 2

Yasuhiro ARII (Department of Marine Science, Marine Works Japan Ltd.)

Kenichiro SATO (Department of Marine Science, Marine Works Japan Ltd.)

Elena HAYASHI (Department of Marine Science, Marine Works Japan Ltd.)

(2) Objectives

The objectives of nutrients analyses during the R/V Mirai MR1404 cruise, WOCE P1 revisited cruise in 2014, in the North Pacific Ocean are as follows;

- Describe the present status of nutrients concentration with excellent comparability.
- The determinants are nitrate, nitrite, silicate, phosphate and Ammonium.
- Study the temporal and spatial variation of nutrients concentration based on the previous high quality experiments data of WOCE previous P1 cruises in 2007, GEOSECS, IGY and so on.
- Study of temporal and spatial variation of nitrate: phosphate ratio, so called Redfield ratio.
- Obtain more accurate estimation of total amount of nitrate, silicate and phosphate in the interested area.
- Provide more accurate nutrients data for physical oceanographers to use as tracers of water mass movement.

(3) Summary of nutrients analysis

We made 129 QuAAtro 2-HR runs for the samples at 118 casts, 113 stations in MR1404. The total amount of layers of the seawater sample reached up to 3918 for MR1404. We made duplicate measurement at all layers, except for ammonium samples.

(4) Instrument and Method

(4.1) Analytical detail using QuAAtro 2-HR systems (BL-Tech)

We applied three units of QuAAtro in this cruise. Unit 1 and Unit 2 were put for R/V Mirai equipment. Unit 3 was carried on R/V Mirai. Configurations of all three units are completely same for four parameters, Nitrate, Nitrite, Silicate and Phosphate, while Unit 3 has ammonium measurement channel as channel 5.

Nitrate + nitrite and nitrite were analyzed according to the modification method of Grasshoff (1970). The sample nitrate was reduced to nitrite in a cadmium tube inside of which was coated with metallic copper. The sample streamed with its equivalent nitrite was treated with an acidic, sulfanilamide reagent and the nitrite forms nitrous acid which reacted with the sulfanilamide to produce a diazonium ion. N-1-Naphthylethylene-diamine added to the sample stream then coupled with the diazonium ion to produce a red, azo dye. With reduction of the nitrate to nitrite, both nitrate and nitrite reacted and were measured; without reduction, only nitrite reacted. Thus, for the nitrite analysis, no reduction was performed and the alkaline buffer was not necessary. Nitrate was computed by difference.

The silicate method was analogous to that described for phosphate. The method used was essentially that of Grasshoff et al. (1983), wherein silicomolybdic acid was first formed from the silicate in the sample and added molybdic acid; then the silicomolybdic acid was reduced to silicomolybdous acid, or "molybdenum blue" using ascorbic acid as the reductant. The analytical methods of the nutrients, nitrate, nitrite, silicate and phosphate, during this cruise were same as the methods used in (Kawano et al. 2009).

The phosphate analysis was a modification of the procedure of Murphy and Riley (1962). Molybdic acid was added to the seawater sample to form phosphomolybdic acid which was in turn reduced to phosphomolybdous acid using L-ascorbic acid as the reductant.

The details of modification of analytical methods for four parameters, Nitrate, Nitrite, Silicate and Phosphate, used in this cruise are also compatible with the methods described in nutrients section in GO-SHIP repeat hydrography manual (Hydes et al., 2010), while an analytical method of ammonium is compatible with Determination of ammonia in seawater using a vaporization membrane permeability method (Kimura, 2000). The flow diagrams and reagents for each parameter are shown in Figures 3.5.1 to 3.5.5.

(4.2) Nitrate Reagents

Imidazole (buffer), 0.06 M (0.4 % w/v)

Dissolve 4 g imidazole, $C_3H_4N_2$, in 1000 ml DIW, add 2 ml concentrated HCl and 0.2 ml 1% $CuSO_4$ solution. After mixing, 1 ml Triton™ X-100 (50 % solution in ethanol) is added.

Sulfanilamide, 0.06 M (1 % w/v) in 1.2 M HCl

Dissolve 10 g sulfanilamide, $4-NH_2C_6H_4SO_3H$, in 900 ml of DIW, add 100 ml concentrated HCl. After mixing, 2 ml Triton™ X-100 (50 % solution in ethanol) is added.

N-1-Naphthylethylene-diamine dihydrochloride, 0.004 M (0.1 % w/v)

Dissolve 1 g NED, $C_{10}H_7NHCH_2CH_2NH_2 \cdot 2HCl$, in 1000 ml of DIW and add 10 ml concentrated HCl. After mixing, 1 ml Triton™ X-100 (50 % solution in ethanol) is added.

Stored in a dark bottle.

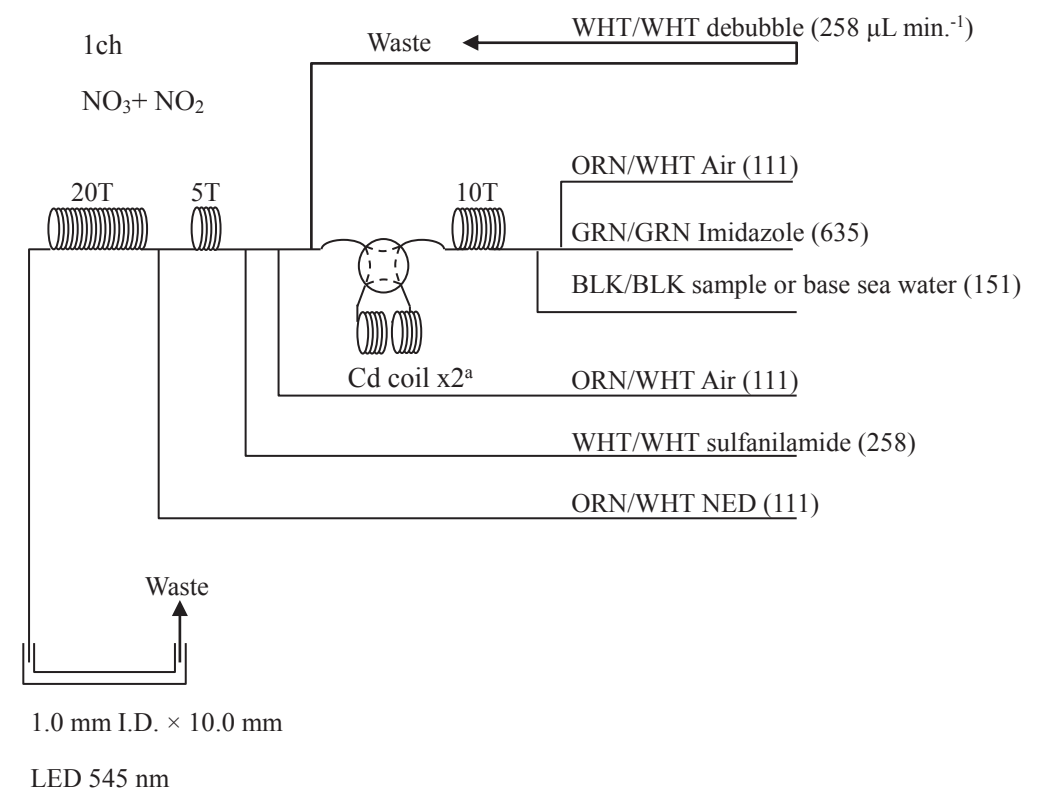


Figure 3.5.1. NO₃ + NO₂ (1ch.) Flow diagram.

note a: 5turn Cd coil were doubled during MR1404 cruise

(4.3) Nitrite Reagents

Sulfanilamide, 0.06 M (1% w/v) in 1.2 M HCl

Dissolve 10 g sulfanilamide, $4\text{-NH}_2\text{C}_6\text{H}_4\text{SO}_3\text{H}$, in 900 ml of DIW, add 100 ml concentrated HCl. After mixing, 2 ml Triton™ X-100 (50% solution in ethanol) is added.

N-1-Naphthylethylene-diamine dihydrochloride, 0.004 M (0.1% w/v)

Dissolve 1 g NED, $\text{C}_{10}\text{H}_7\text{NHCH}_2\text{CH}_2\text{NH}_2 \cdot 2\text{HCl}$, in 1000 ml of DIW and add 10 ml concentrated HCl. After mixing, 1 ml Triton™ X-100 (50% solution in ethanol) is added. This reagent was stored in a dark bottle.

(4.4) Silicate Reagents

Molybdic acid, 0.06 M (2% w/v)

Dissolve 15 g disodium Molybdate(VI) dihydrate, $\text{Na}_2\text{MoO}_4 \cdot 2\text{H}_2\text{O}$, in 980 ml DIW, add 8 ml concentrated H_2SO_4 . After mixing, 20 ml sodium dodecyl sulphate (15% solution in water) is added.

Oxalic acid, 0.6 M (5% w/v)

Dissolved 50 g oxalic acid anhydrous, HOOC:COOH , in 950 ml of DIW.

Ascorbic acid, 0.01 M (3% w/v)

Dissolved 2.5g L(+)-ascorbic acid, $\text{C}_6\text{H}_8\text{O}_6$, in 100 ml of DIW. This reagent was freshly prepared at every day.

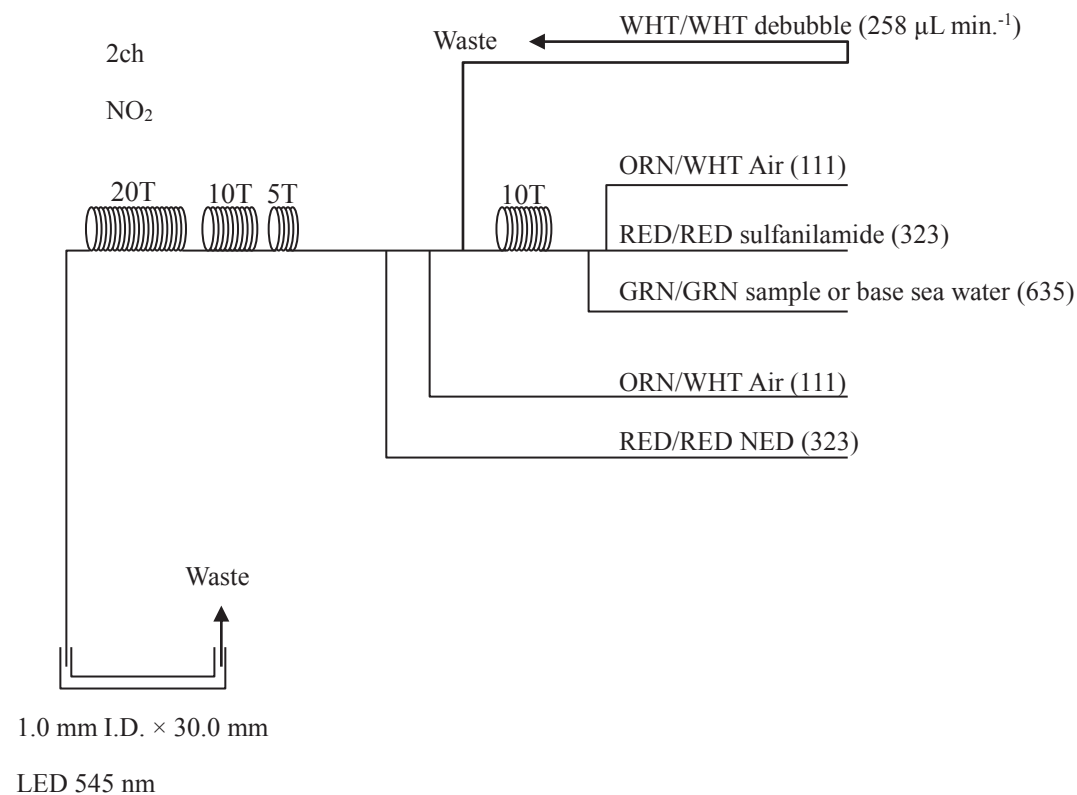


Figure 3.5.2. NO₂ (2ch.) Flow diagram.

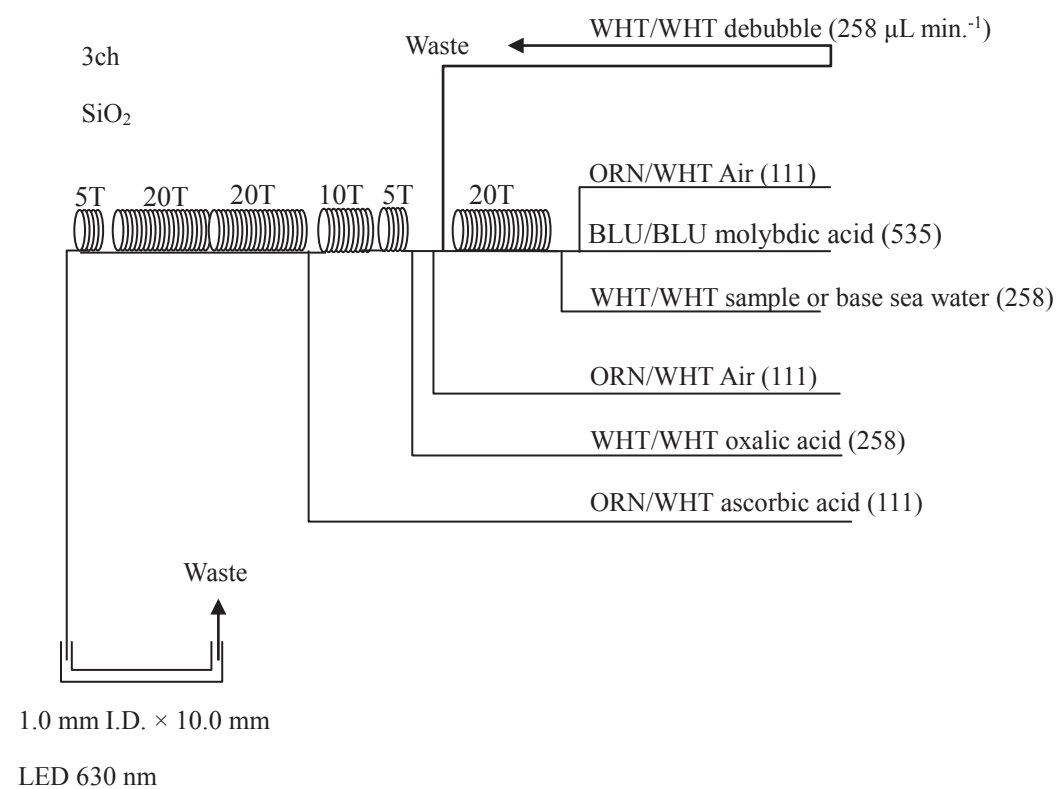


Figure 3.5.3. SiO₂ (3ch.) Flow diagram.

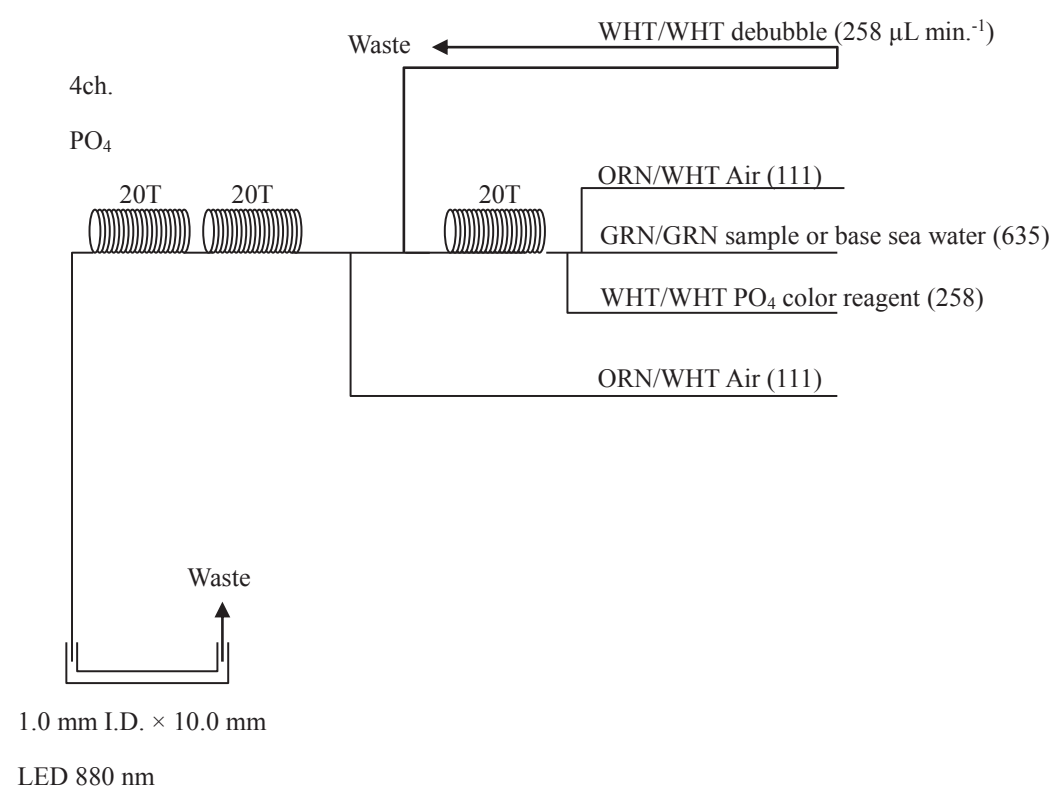


Figure 3.5.4. PO₄ (4ch.) Flow diagram.

(4.5) Phosphate Reagents

Stock molybdate solution, 0.03 M (0.8% w/v)

Dissolved 8 g disodium molybdate(VI) dihydrate, Na₂MoO₄•2H₂O, and 0.17 g antimony potassium tartrate, C₈H₄K₂O₁₂Sb₂•3H₂O, in 950 ml of DIW and added 50 ml concentrated H₂SO₄.

Mixed Reagent

Dissolved 1.2 g L(+)-ascorbic acid, C₆H₈O₆, in 150 ml of stock molybdate solution. After mixing, 3 ml sodium dodecyl sulphate (15% solution in water) was added. This reagent was freshly prepared before every measurement.

(4.6) Ammonium Reagents

EDTA

Dissolve 41 g EDTA (ethylenediaminetetraacetic acid tetrasodium salt), C₁₀H₁₂N₂O₈Na₄•4H₂O, and 2 g boric acid, H₃BO₃, in 200 ml of DIW. After mixing, 1 ml Triton™ X-100 (30% solution in DIW) is added. This reagent is prepared at a week about.

NaOH

Dissolve 5 g sodium hydroxide, NaOH, and 16 g EDTA in 100 ml of DIW. This reagent is prepared at a week about.

Stock Nitroprusside

Dissolved 0.25 g sodium pentacyanonitrosylferrate(II), $\text{Na}_2[\text{Fe}(\text{CN})_5\text{NO}]$, in 100 ml of DIW and add 0.2 ml 1N H_2SO_4 . Stored in a dark bottle and prepared at a month about.

Nitroprusside solution

Mixed 4 ml stock nitroprusside and 5 ml 1N H_2SO_4 in 500 ml of DIW. After mixing, 2 ml Triton™ X-100 (30% solution in DIW) is added. This reagent is stored in a dark bottle and prepared at every 2 or 3 days.

Alkaline phenol

Dissolved 10 g phenol, $\text{C}_6\text{H}_5\text{OH}$, 5 g sodium hydroxide and citric acid, $\text{C}_6\text{H}_8\text{O}_7$, in 200 ml DIW. Stored in a dark bottle and prepared at a week about.

NaClO solution

Mixed 3 ml sodium hypochlorite solution, NaClO, in 47 ml DIW. Stored in a dark bottle and freshly prepared before every measurement. This reagent is prepared 0.3% available chlorine.

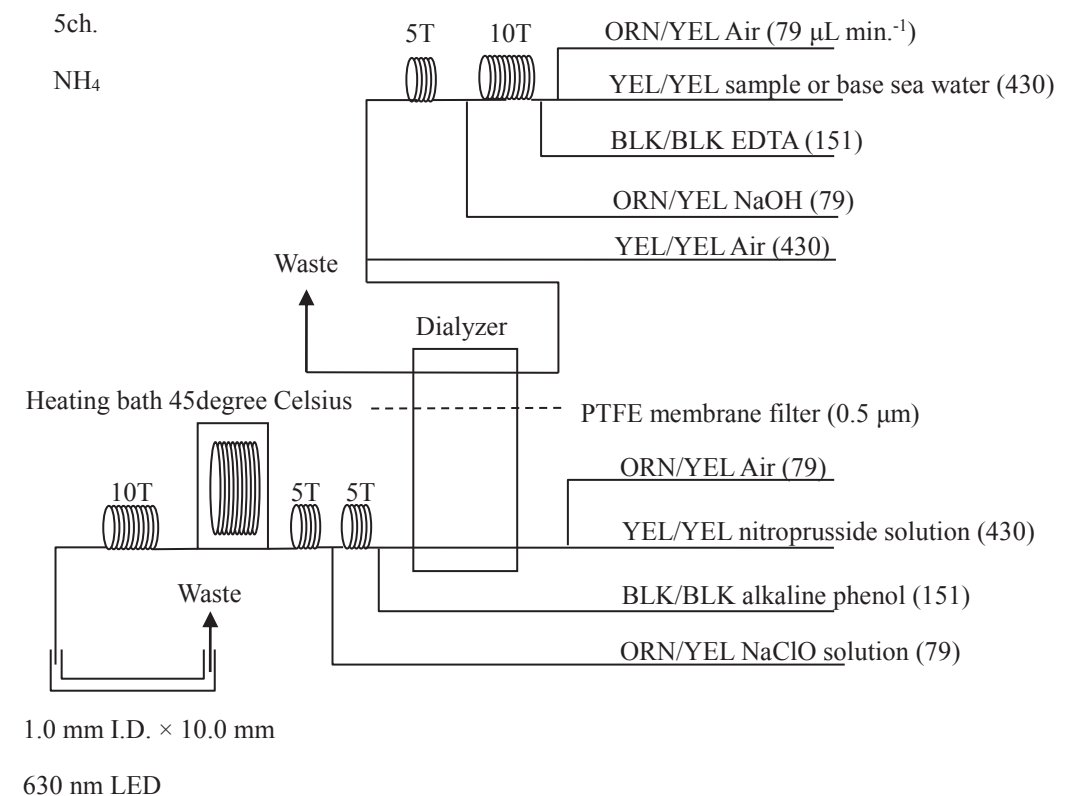


Figure 3.5.5. NH₄ (5ch.) Flow diagram.

(4.7) Sampling procedures

Sampling of nutrients followed that oxygen, salinity and trace gases. Samples were drawn into two of virgin 10 ml polyacrylates vials without sample drawing tubes. These were rinsed three times before filling and then vials were capped immediately after the drawing. The vials were put into water bath adjusted to ambient temperature, 24 ± 2 degree Celsius, in about 30 minutes before use to stabilize the temperature of samples in MR1404.

No transfer was made and the vials were set an auto sampler tray directly. Samples were analyzed after collection basically within 24 hours in principal.

7 casts among 29 casts of samples for ammonium were drawn into a virgin 50 ml PE tubes and frozen using liquid nitrogen after the water sampling immediately. After that, these samples were stored in deep freezer, -70 degree Celsius. Frozen samples were thawed using water bath, 40 degree Celsius, and put on room temperature just before the measurement. Samples were transferred into the virgin 10 ml vial due to set an auto sampler tray directly. However we observed concentrations changes of ammonium for frozen samples stated above 7casts, we measured samples of remaining 22 casts as NOT frozen.

(4.8) Data processing

Raw data from QuAAtro 2-HR was treated as follows:

- Checked baseline shift.
- Checked the shape of each peak and positions of peak values taken, and then changed the positions of peak values taken if necessary.
- Carry-over correction and baseline drift correction were applied to peak heights of each samples followed by sensitivity correction.
- Baseline correction and sensitivity correction were done basically using liner regression.
- Loaded pressure and salinity from CTD data to calculate density of seawater. In case of bucket sample, we generally used bottle salinity from AUTOSAL, while in case of MBC cast we used surface CTD data.
- Calibration curves to get nutrients concentration were assumed second order equations.

(5) Nutrients standards

(5.1) Volumetric laboratory ware of in-house standards

All volumetric glass ware and polymethylpentene (PMP) ware were gravimetrically calibrated. These volumetric flasks were gravimetrically calibrated at the temperature of using in the laboratory within 4 K.

Volumetric flasks

Volumetric flasks of Class quality (Class A) are used because their nominal tolerances are 0.05 % or less over the size ranges likely to be used in this work. Class A flasks are made of borosilicate glass, and the standard solutions were transferred to plastic bottles as quickly as possible after they are made up to volume and well mixed in order to prevent excessive dissolution of silicate from the glass. High quality plastic (polymethylpentene, PMP, or polypropylene) volumetric flasks were gravimetrically calibrated and used only within 4 K of the calibration temperature.

The computation of volume contained by glass flasks at various temperatures other than the calibration temperatures were done by using the coefficient of linear expansion of borosilicate crown glass.

Because of their larger temperature coefficients of cubical expansion and lack of tables constructed for these materials, the plastic volumetric flasks were gravimetrically calibrated over the temperature range of intended use and used at the temperature of calibration within 4 K. The weights obtained in the calibration weightings were corrected for the density of water and air buoyancy.

Pipettes and pipettors

All pipettes have nominal calibration tolerances of 0.1 % or better. These were gravimetrically calibrated in order to verify and improve upon this nominal tolerance.

(5.2) Reagents, general considerations

Specifications

For nitrate standard, “potassium nitrate 99.995 suprapur®” provided by Merck, Lot. B0771365211, CAS

No. 7757-91-1, was used.

For nitrite standard, “sodium nitrite” provided by Wako, Lot. HLK7554, CAS No. 7632-00-0, was used. The assay of nitrite salts was determined according JIS K8019 and the result of the assay was 98.53%. We use that value to adjust the weights taken.

For phosphate standard, “potassium dihydrogen phosphate anhydrous 99.995 suprapur®” provided by Merck, Lot. B0691108204, CAS No.: 7778-77-0, was used.

For the silicate standard, we use “Silicon standard solution SiO₂ in NaOH 0.5 mol/l CertiPUR®” provided by Merck, CAS No. 1310-73-2, of which lot number is HC382250 are used. The silicate concentration is certified by NIST-SRM3150 with the uncertainty of 0.5 %. HC382250 was certified as 1001 mg L⁻¹.

Treatment of silicate standard due to high alkalinity

Since the silicon standard solution Merck CertiPUR® is in NaOH 0.5 mol/l, we need to dilute and neutralize to avoid make precipitation of MgOH₂ etc. When we make B standard, silicon standard solution is diluted by factor 12 with pure water and neutralized by HCl 1.0 mol L⁻¹ to be about 7. After that B standard solution is used to prepare C standards.

Ultra pure water

Ultra pure water (Milli-Q water) freshly drawn was used for preparation of reagents, standard solutions and for measurement of reagent and system blanks.

Low-Nutrient Seawater (LNSW)

Surface water having low nutrient concentration was taken and filtered using 0.20 µm pore size capsule cartridge filter. This water is stored in 20 liter cubitainer with paper box. The concentrations of nutrient of this water were measured carefully in October 2014.

(5.3) Concentrations of nutrients for A, B and C standards

Concentrations of nutrients for A, B and C standards are set as shown in Table 3.5.1. The C standard is prepared according recipes as shown in Table 3.5.2. All volumetric laboratory tools were calibrated prior the cruise as stated in chapter (5.1). Then the actual concentration of nutrients in each fresh standard was calculated based on the ambient, solution temperature and determined factors of volumetric laboratory wares.

The calibration curves for each run were obtained using 6 levels, C-1, C-2, C-3, C-4, C-5 and C-6. C-1, C-2, C-3, C-4 and C-5 were the reference material of nutrients in seawater and C-6 was in-house standard.

Table 3.5.1. Nominal concentrations of nutrients for A, B and C standards.

	A	B	C-1	C-2	C-3	C-4	C-5	C-6	C-7	C-8
NO ₃ (µM)	22500	900	BY	BU	CA	BW	BZ	54	-	-
NO ₂ (µM)	4000	20	BY	BU	CA	BW	BZ	1.2	-	-
SiO ₂ (µM)	35000	2760	BY	BU	CA	BW	BZ	166	-	-
PO ₄ (µM)	3000	60	BY	BU	CA	BW	BZ	3.7	-	-
NH ₄ (µM)	4000	200	-	-	-	-	-	6.0	2.0	0

Table 3.5.2. Working calibration standard recipes.

C std.	B-1 std.	B-2 std.	B-3 std.
C-6	25 ml	25 ml	15 ml
C-7	-	-	5 ml
C-8	-	-	0 ml

B-1 std.: Mixture of nitrate, silicate and phosphate

B-2 std.: Nitrite

B-3 std.: Ammonium

(5.4) Renewal of in-house standard solutions.

In-house standard solutions as stated in paragraph (5.2) were renewed as shown in Table 3.5.3(a) to (c).

Table 3.5.3(a). Timing of renewal of in-house standards.

NO_3 , NO_2 , SiO_2 , PO_4 , NH_4	Renewal
A-1 std. (NO_3)	maximum a month
A-2 std. (NO_2)	maximum a month
A-3 std. (SiO_2)	commercial prepared solution
A-4 std. (PO_4)	maximum a month
A-5 std. (NH_4)	maximum a month
B-1 std. (mixture of A-1, A-3 and A-4 std.)	maximum 8 days
B-2 std. (dilute A-2 std.)	maximum 8 days
B-3 std. (dilute A-4 std.)	maximum 8 days

Table 3.5.3(b). Timing of renewal of in-house standards.

Working standards	Renewal
C-6 std. (mixture of B-1 and B-2 std.)	
C-7 std. (dilute B-3 std.)	every 24 hours
C-8 (LNSW)	

Table 3.5.3(c). Timing of renewal of in-house standards for reduction estimation.

Reduction estimation	Renewal
D-1 std. (3600 $\mu\text{M NO}_3$)	maximum 8 days
43 $\mu\text{M NO}_3$	when C Std. renewed
47 $\mu\text{M NO}_2$	when C Std. renewed

(6) Reference material of nutrients in seawater

To get the more accurate and high quality nutrients data to achieve the objectives stated above, huge numbers of the bottles of the reference material of nutrients in seawater (hereafter RMNS) are prepared (Aoyama et al., 2006, 2007, 2008, 2009). In the previous worldwide expeditions, such as WOCE cruises, the higher reproducibility and precision of nutrients measurements were required (Joyce and Corry, 1994). Since no standards were available for the measurement of nutrients in seawater at that time, the requirements were described in term of reproducibility. The required reproducibility was 1%, 1 to 2%, 1 to 3% for nitrate, phosphate and silicate, respectively. Although nutrient data from the WOCE one-time survey was of unprecedented quality and coverage due to much care in sampling and measurements, the differences of nutrients concentration at crossover points are still found among the expeditions (Aoyama and Joyce, 1996, Mordy et al., 2000, Gouretski and Jancke, 2001). For instance, the mean offset of nitrate concentration at deep waters was 0.5 $\mu\text{mol kg}^{-1}$ for 345 crossovers at world oceans, though the maximum was

1.7 $\mu\text{mol kg}^{-1}$ (Gouretski and Jancke, 2001). At the 31 crossover points in the Pacific WHP one-time lines, the WOCE standard of reproducibility for nitrate of 1 % was fulfilled at about half of the crossover points and the maximum difference was 7 % at deeper layers below 1.6 degree Celsius in potential temperature (Aoyama and Joyce, 1996).

During the period from 2003 to 2010, RMNS were used to keep comparability of nutrients measurement among the 8 cruises of CLIVAR project (Sato et al., 2010), MR1005 cruise for Arctic research (Aoyama et al., 2010) and MR1006 cruise for “Change in material cycles and ecosystem by the climate change and its feedback” (Aoyama et al., 2011).

(6.1) RMNSs for this cruise

RMNS lots BY, BU, CA, BW and BZ, which cover full range of nutrients concentrations in the North Pacific Ocean are prepared for MR1404. 87 sets of BY, BU, CA, BW and BZ are prepared.

59 bottles of RMNS lot BV are prepared for this cruise. Lot BV was analyzed at all stations to keep the comparability. These RMNS assignment were completely done based on random number. The RMNS bottles were stored at a room in the ship, REAGENT STORE, where the temperature was maintained around 20 - 24 degree Celsius.

(6.2) Assigned concentration for RMNSs

We assigned nutrients concentrations for RMNS lots BY, BU, CA, BW, BZ, and BV as shown in Table 3.5.4.

(6.3) Homogeneity of RMNSs

The homogeneity of lot BV used in MR1404 cruise and analytical precisions are shown in Table 3.5.5. These are for the assessment of the magnitude of homogeneity of the RMNS bottles those are used during this cruise. As shown in Table 3.5.5, the homogeneity of RMNS lot BV for nitrate, phosphate and silicate are the same magnitude of analytical precision derived from fresh raw seawater in January 2009.

Table 3.5.4. Assigned concentration of RMNSs.

	unit: $\mu\text{mol kg}^{-1}$			
	Nitrate	Phosphate [†]	Silicate ^{††}	Nitrite
BY*	0.07	0.041	1.58	0.03
BU**	3.96	0.348	20.79	0.07
CA*	19.65	1.423	36.57	0.07
BW*	24.59	1.545	59.67	0.08
BZ*	43.40	3.059	160.65	0.21
BV**	35.32	2.512	102.10	0.06

* The values are assigned for this cruise on 5 March 2014.

** The values are assigned for MR1205 cruise on 7 November 2012.

† The values of phosphate are re-assigned on 28 October 2014 due to correct by LNSW offset.

†† The values of silicate are re-assigned on June 2016 by one of Merck KGaA silicon standard solution 1000 mg L^{-1} Si traceable to National Institute of Standards and Technology (NIST) SRM of silicon standard solution (SRM3150).

Table 3.5.5. The homogeneity of lot BV derived from simultaneous samples measurements and analytical precision onboard R/V Mirai in MR1404 and offshore laboratory at YOKOSUKA in 2012.

	Nitrate	Phosphate	Silicate
	CV %	CV %	CV %
BV (on board)*	0.12	0.15	0.12
BV (laboratory)**	0.10	0.12	0.08
Precision (on board)	0.09	0.08	0.07
Precision (laboratory)	0.16	0.07	0.08

*: N = 125

**: N = 30

(7) Quality control

(7.1) Precision of nutrients analyses during the cruise

Precision of nutrients analyses during this cruise was evaluated based on the 7 to 11 measurements, which are measured every 8 to 13 samples, during a run at the concentration of C-6 std. Summary of precisions are shown as Table 3.5.6 and Figures 3.5.6 to 3.5.8, the precisions for each parameter are generally good considering the analytical precisions during the R/V Mirai cruises conducted in 2009 - 2014. During this cruise, analytical precisions were 0.09% for nitrate, 0.08% for phosphate and 0.07% for silicate in terms of median of precision, respectively.

An improvement of analytical precisions of all parameters was estimated that replacement roller of the pump that improvement as shown Table 3.5.6. The reason of relative poor precision observed was contamination of the sample line tube.

Table 3.5.6. Summary of precision based on the replicate analyses for all unit.

	Nitrate	Nitrite	Silicate	Phosphate	Ammonium
	CV %	CV %	CV %	CV %	CV %
Median	0.09	0.14	0.07	0.08	0.22
Mean	0.09	0.15	0.09	0.09	0.24
Maximum	0.31	0.54	0.27	0.31	0.49
Minimum	0.03	0.04	0.02	0.02	0.03
N	125	125	125	125	25

Table 3.5.6(a). Summary of precision based on the replicate analyses for unit 1.

	Nitrate	Nitrite	Silicate	Phosphate	Ammonium
	CV %	CV %	CV %	CV %	CV %
Median	0.08	0.13	0.07	0.07	0.23
Mean	0.10	0.14	0.09	0.08	0.23
Maximum	0.31	0.34	0.27	0.31	0.33
Minimum	0.03	0.05	0.03	0.02	0.16
N	63	63	63	63	5

Table 3.5.6(b). Summary of precision based on the replicate analyses for unit 2.

	Nitrate	Nitrite	Silicate	Phosphate	Ammonium
	CV %	CV %	CV %	CV %	CV %
Median	0.07	0.14	0.06	0.08	0.22
Mean	0.07	0.18	0.07	0.08	0.25
Maximum	0.14	0.54	0.12	0.14	0.49
Minimum	0.03	0.04	0.04	0.02	0.03
N	17	17	17	17	20

Table 3.5.6(c). Summary of precision based on the replicate analyses for unit 3.

	Nitrate	Nitrite	Silicate	Phosphate	Ammonium
	CV %	CV %	CV %	CV %	CV %
Median	0.10	0.14	0.09	0.08	-
Mean	0.10	0.15	0.09	0.09	-
Maximum	0.22	0.29	0.21	0.24	-
Minimum	0.03	0.05	0.02	0.03	-
N	46	46	46	46	-

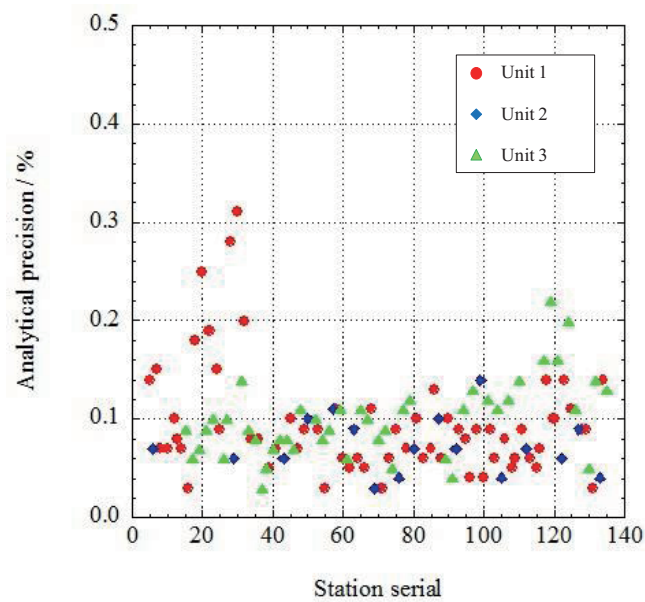


Figure 3.5.6. Time series of precision of nitrate in MR1404

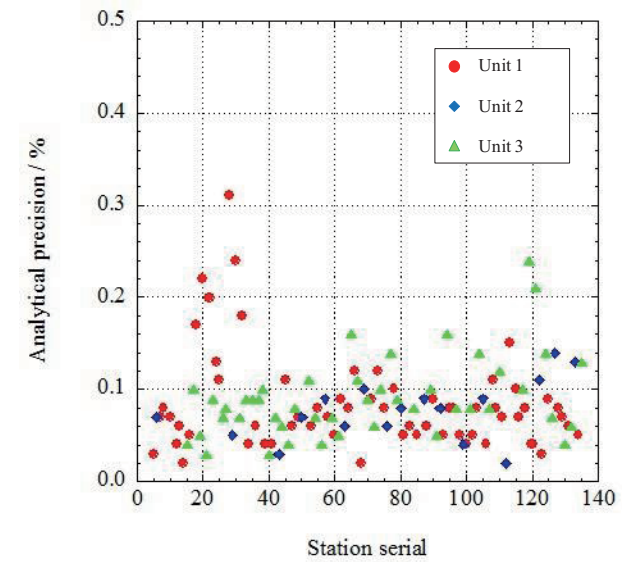


Figure 3.5.7. Time series of precision of phosphate in MR1404.

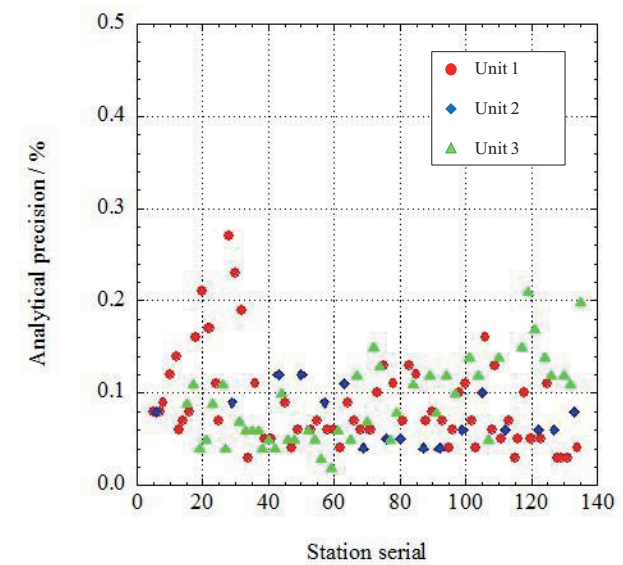


Figure 3.5.8. Time series of precision of silicate in MR1404.

(7.2) RMNS lot. BV measurement during this cruise

RMNS lot. BV was measured every run to keep the comparability. The results of lot. BV during this cruise are shown as Figures 3.5.9 to 3.5.11. Error bars represent analytical precision in figure 3.5.6 to 3.5.8.

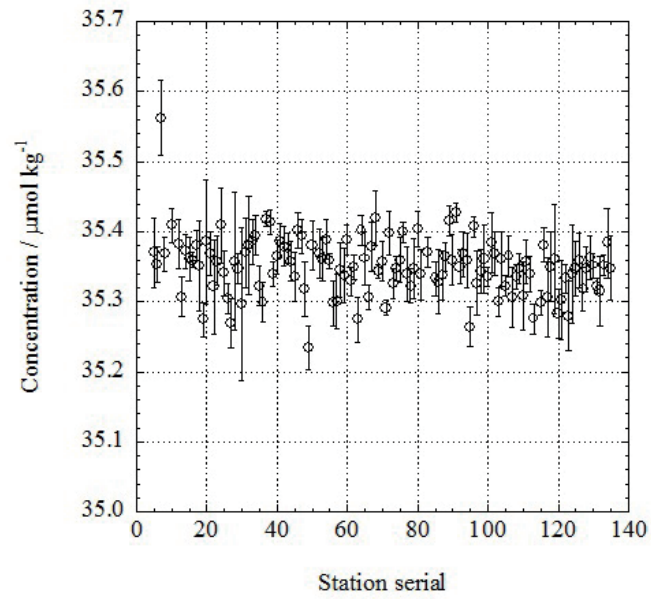


Figure 3.5.9. Time series of RMNS-BV of nitrate in MR1404.

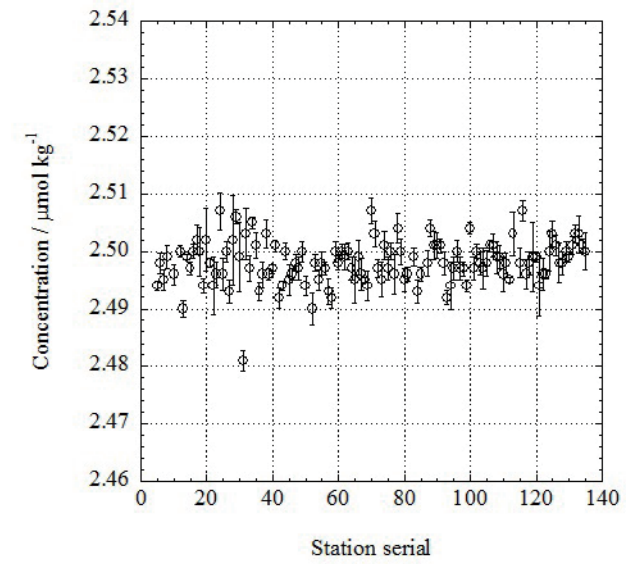


Figure 3.5.10. Time series of RMNS-BV of phosphate in MR1404.

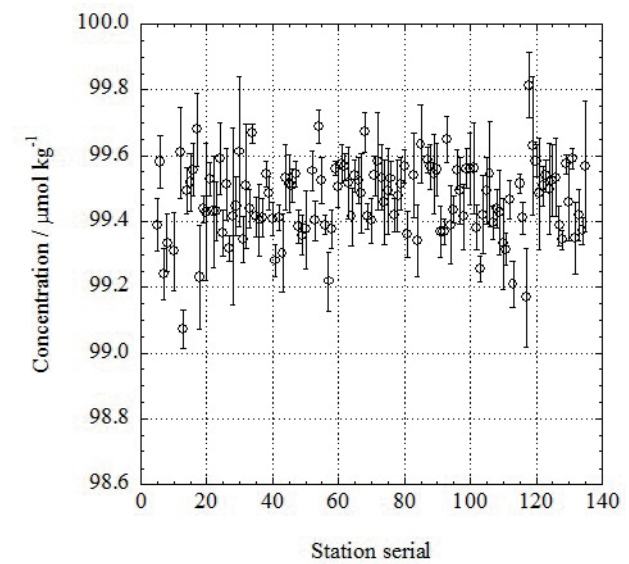


Figure 3.5.11. Time series of RMNS-BV of silicate in MR1404.

(7.3) Carryover

We can also summarize the magnitudes of carryover throughout the cruise. These are small enough within acceptable levels as shown in Table 3.5.7 and Figures 3.5.12 to 3.5.14. The carryover in silicate had a bias by equipment. It was 0.1%, mean value, at Unit 1 and Unit 2, R/V Mirai equipment. The other hand, it was 0.2%, mean value, at Unit 3. We carried out the maintenance for Unit 3 by cleaning of the glass coils and changing for new transmission tube before the stn. 144. The bias was clearly solved by the maintenance.

Table 3.5.7. Summary of carry over throughout MR1404.

	Nitrate	Nitrite	Silicate	Phosphate	Ammonium
	CV %	CV %	CV %	CV %	CV %
Median	0.14	0.07	0.11	0.17	0.55
Mean	0.14	0.09	0.13	0.18	0.55
Maximum	0.22	0.40	0.34	0.41	0.92
Minimum	0.00	0.00	0.05	0.02	0.22
N	125	125	125	125	25

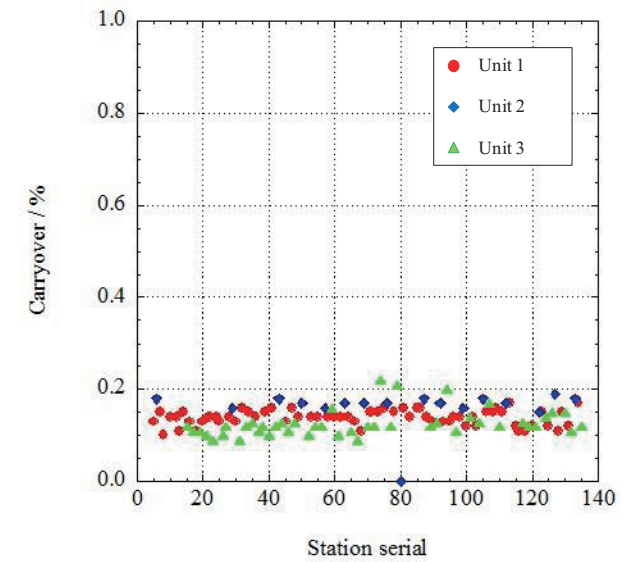


Figure 3.5.12. Time series of carryover of nitrate in MR1404.

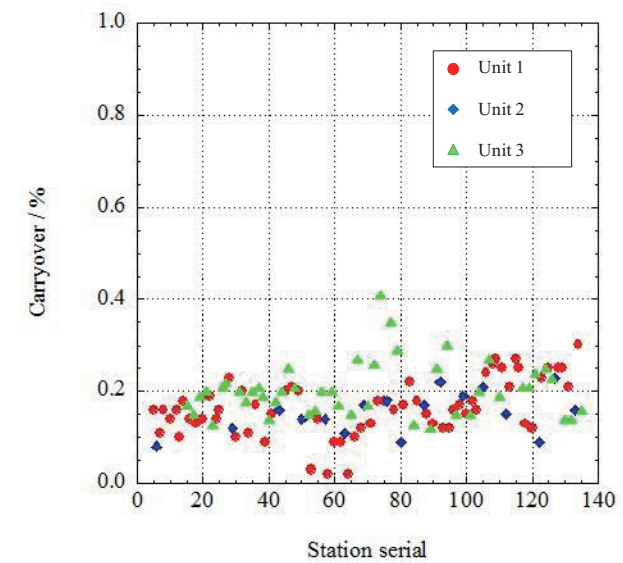


Figure 3.5.13. Time series of carryover of phosphate in MR1404.

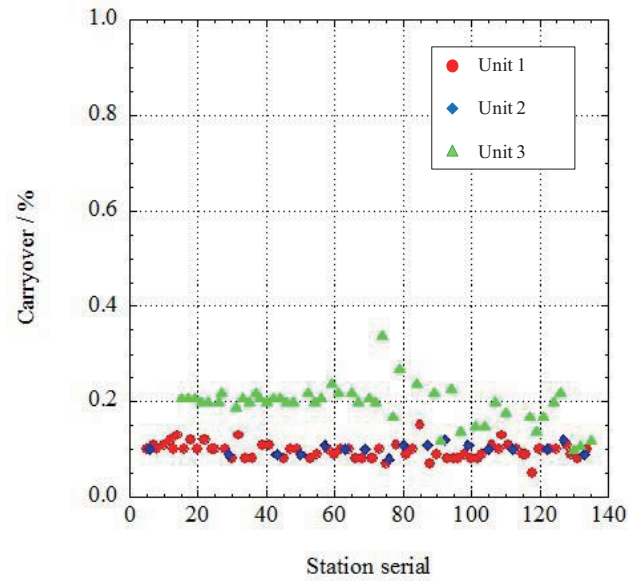


Figure 3.5.14. Time series of carryover of silicate in MR1404.

(7.4) Estimation of uncertainty of phosphate, nitrate and silicate concentrations

Empirical equations, eq. (1), (2) and (3) to estimate uncertainty of measurement of phosphate, nitrate and silicate are used based on measurements of 60 sets of RMNSs during this cruise. Empirical equations, eq. (4) and (5) to estimate uncertainty of measurement of nitrite and ammonium are used based on duplicate measurements of the samples. These empirical equations are as follows, respectively.

Phosphate Concentration C_p in $\mu\text{mol kg}^{-1}$:

$$\text{Uncertainty of measurement of phosphate (\%)} = 0.035031 + 0.35937 \times (1 / C_p) \quad - (1)$$

where C_p is phosphate concentration of sample.

Nitrate Concentration C_{no_3} in $\mu\text{mol kg}^{-1}$:

$$\text{Uncertainty of measurement of nitrate (\%)} = 0.10084 + 1.0963 \times (1 / C_{no_3}) + 0.042373 \times (1 / C_{no_3}) \times (1 / C_{no_3}) \quad - (2)$$

where C_{no_3} is nitrate concentration of sample.

Silicate Concentration C_s in $\mu\text{mol kg}^{-1}$:

$$\text{Uncertainty of measurement of silicate (\%)} = 0.063921 + 7.3785 \times (1 / C_s) + 5.4241 \times (1 / C_s) \times (1 / C_s) \quad - (3)$$

where C_s is silicate concentration of sample.

Nitrite Concentration C_{no_2} in $\mu\text{mol kg}^{-1}$:

$$\text{Uncertainty of measurement of nitrite (\%)} = -0.1648 + 0.2457 \times (1 / C_{no_2}) - 0.00050611 \times (1 / C_{no_2}) \times (1 / C_{no_2}) \quad - (4)$$

where C_a is ammonium concentration of sample.

Ammonium Concentration C_a in $\mu\text{mol kg}^{-1}$:

$$\text{Uncertainty of measurement of ammonium (\%)} = 1.8748 + 1.5641 \times (1 / C_a) - 0.009571 \times (1 / C_a) \times (1 / C_a) \quad - (5)$$

where C_a is ammonium concentration of sample.

(8) Problems / improvements occurred and solutions

(8.1) LNSW offset

LNSW was assigned concentration of each parameter before the cruise. We found an offset for concentration of phosphate, $-0.03 \mu\text{mol L}^{-1}$ between this year assign and past, as a result to assess the value of the reagent blank. We corrected assign values of RMNSs from this cruise.

(8.2) Contamination of ammonium from the air in the laboratory

In ammonium data, we could find a contamination from the air in the laboratory in this cruise leg2. We made a closed supply system of the LNSW from the 20 liter cubitainer to auto sampler due to avoid the contamination from the air. We could not find the contamination on and after using this system.

(8.3) Contamination of nitrite from the LNSW bottle

In nitrite data, we could find a contamination. But we could not calculate an origin of the contamination. As the result of the maintenance and cleaning of the equipment, the origin was the contamination of the LNSW bottle. We applied the closed supply system as same as the contamination of ammonium on and after cleared this problem,.

(8.4) Remove of the dilution line at phosphate measurement

Karel Bakker at NIOZ suggested us to remove the dilution line at phosphate measurement to improve the peak shape in Spring 2013, therefore we had removed dilution line since MR1304 R/V Mirai cruise. As a result of this, precision of phosphate measurement becomes drastically excellent up to 0.08% in terms of median of 127 runs.

(8.5) Usage of a power pipettor

We have applied a power pipettor to avoid a bias by operators since this cruise, when made calibration standards for nutrients analysis. The power pipettor was gravimetrically calibrated according to paragraph (5.1) before the cruise.

(8.6) Improvement of reduction rate at nitrate measurement

We added a 5 turn Cu-Cd coil to previously used a 5 turn Cu-Cd coil in nitrate measurement flow line and also added CuSO_4 in the imidazole solution to get a stable and high redaction rate in this cruise. As a result, we achieved a good stable and high reduction rate which was 99.0% in terms of median of 126 runs during this

cruise.

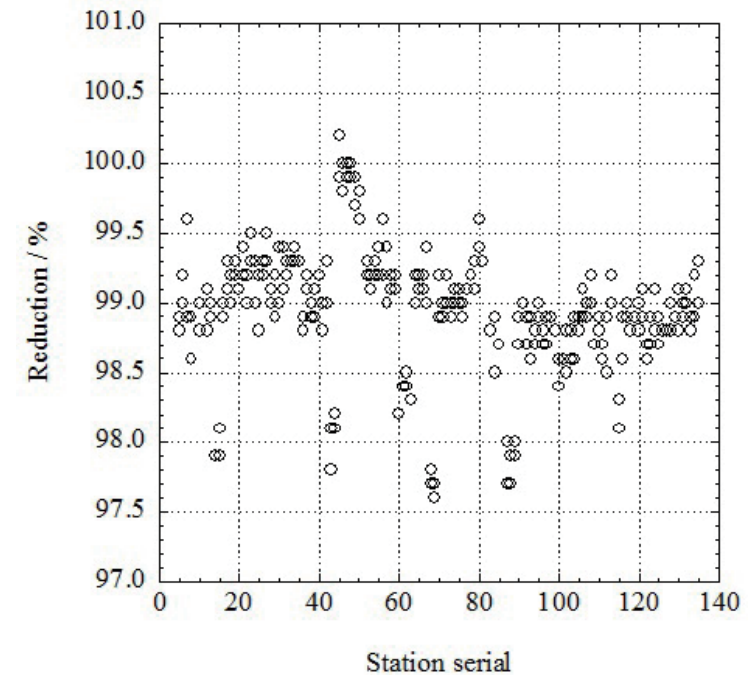


Figure 3.5.15. Time series of reduction of nitrate in MR1404.

(9) Data archive

All data will be submitted to JAMSTEC Data Management Office (DMO) and is currently under its control.

References

Aminot, A. and Kerouel, R. 1991. Autoclaved seawater as a reference material for the determination of nitrate and phosphate in seawater. *Anal. Chim. Acta*, 248: 277-283.

- Aminot, A. and Kirkwood, D.S. 1995. Report on the results of the fifth ICES intercomparison exercise for nutrients in sea water, ICES coop. Res. Rep. Ser., 213.
- Aminot, A. and Kerouel, R. 1995. Reference material for nutrients in seawater: stability of nitrate, nitrite, ammonia and phosphate in autoclaved samples. *Mar. Chem.*, 49: 221-232.
- Aoyama M., and Joyce T.M. 1996, WHP property comparisons from crossing lines in North Pacific. In Abstracts, 1996 WOCE Pacific Workshop, Newport Beach, California.
- Aoyama, M., 2006: 2003 Intercomparison Exercise for Reference Material for Nutrients in Seawater in a Seawater Matrix, Technical Reports of the Meteorological Research Institute No.50, 91pp, Tsukuba, Japan.
- Aoyama, M., Susan B., Minhan, D., Hideshi, D., Louis, I. G., Kasai, H., Roger, K., Nurit, K., Doug, M., Murata, A., Nagai, N., Ogawa, H., Ota, H., Saito, H., Saito, K., Shimizu, T., Takano, H., Tsuda, A., Yokouchi, K., and Agnes, Y. 2007. Recent Comparability of Oceanographic Nutrients Data: Results of a 2003 Intercomparison Exercise Using Reference Materials. *Analytical Sciences*, 23: 1151-1154.
- Aoyama M., J. Barwell-Clarke, S. Becker, M. Blum, Braga E. S., S. C. Coverly, E. Czobik, I. Dahllorf, M. H. Dai, G. O. Donnell, C. Engelke, G. C. Gong, Gi-Hoon Hong, D. J. Hydes, M. M. Jin, H. Kasai, R. Kerouel, Y. Kiyomono, M. Knockaert, N. Kress, K. A. Kroglund, M. Kumagai, S. Leterme, Yarong Li, S. Masuda, T. Miyao, T. Moutin, A. Murata, N. Nagai, G. Nausch, M. K. Ngirchchol, A. Nybakk, H. Ogawa, J. van Ooijen, H. Ota, J. M. Pan, C. Payne, O. Pierre-Duplessix, M. Pujo-Pay, T. Raabe, K. Saito, K. Sato, C. Schmidt, M. Schuett, T. M. Shammon, J. Sun, T. Tanhua, L. White, E.M.S. Woodward, P. Worsfold, P. Yeats, T. Yoshimura, A. Youenou, J. Z. Zhang, 2008: 2006 Intercomparison Exercise for Reference Material for Nutrients in Seawater in a Seawater Matrix, Technical Reports of the Meteorological Research Institute No. 58, 104pp.
- Aoyama, M., Nishino, S., Nishijima, K., Matsushita, J., Takano, A., Sato, K., 2010a. Nutrients, In: R/V Mirai Cruise Report MR10-05. JAMSTEC, Yokosuka, pp. 103-122.
- Aoyama, M., Matsushita, J., Takano, A., 2010b. Nutrients, In: MR10-06 preliminary cruise report. JAMSTEC, Yokosuka, pp. 69-83
- Gouretski, V.V. and Jancke, K. 2001. Systematic errors as the cause for an apparent deep water property variability: global analysis of the WOCE and historical hydrographic data · REVIEW ARTICLE, *Progress In Oceanography*, 48: Issue 4, 337-402.
- Grasshoff, K., Ehrhardt, M., Kremling K. et al. 1983. *Methods of seawater analysis*. 2nd rev. Weinheim: Verlag Chemie, Germany, West.
- Hydes, D.J., Aoyama, M., Aminot, A., Bakker, K., Becker, S., Coverly, S., Daniel, A., Dickson, A.G., Grosso, O., Kerouel, R., Ooijen, J. van, Sato, K., Tanhua, T., Woodward, E.M.S., Zhang, J.Z., 2010. Determination of Dissolved Nutrients (N, P, Si) in Seawater with High Precision and Inter-Comparability Using Gas-Segmented Continuous Flow Analysers, In: *GO-SHIP Repeat Hydrography Manual: A Collection of Expert Reports and Guidelines*. IOCCP Report No. 14, ICPO Publication Series No 134.
- Joyce, T. and Corry, C. 1994. Requirements for WOCE hydrographic programmed data reporting. WHPO Publication, 90-1, Revision 2, WOCE Report No. 67/91.
- Kawano, T., Uchida, H. and Doi, T. WHP P01, P14 REVISIT DATA BOOK, (Ryoin Co., Ltd., Yokohama, 2009).
- Kimura, 2000. Determination of ammonia in seawater using a vaporization membrane permeability method. 7th auto analyzer Study Group, 39-41.

3.6 Carbon Items (C_T , A_T and pH)

November 18, 2016

(1) Personnel

Akihiko Murata (JAMSTEC)

Yoshihiro Shinoda (JAMSTEC)

Tomonori Watai (MWJ)

Yoshiko Ishikawa (MWJ)

Atsushi Ono (MWJ)

Emi Deguchi (MWJ)

(2) Objectives

Concentrations of CO_2 in the atmosphere are now increasing at a rate of about 2.0 ppmv y^{-1} owing to human activities such as burning of fossil fuels, deforestation, and cement production. It is an urgent task to estimate as accurately as possible the absorption capacity of the oceans against the increased atmospheric CO_2 , and to clarify the mechanism of the CO_2 absorption, because the magnitude of the anticipated global warming depends on the levels of CO_2 in the atmosphere, and because the ocean currently absorbs 1/3 of the 6 Gt of carbon emitted into the atmosphere each year by human activities.

The North Pacific is one of the regions where uncertainty of uptake of anthropogenic CO_2 is large. In this cruise, therefore, we were aimed at quantifying how much anthropogenic CO_2 was absorbed in the ocean interior of the North Pacific. For the purpose, we measured CO_2 -system parameters such as dissolved inorganic carbon (C_T), total alkalinity (A_T) and pH along the extended WHP P10 and P01 lines at $149^\circ E$ and $47^\circ N$, respectively, in the North Pacific.

(3) Apparatus

i. C_T

Measurement of C_T was made with two total CO_2 measuring systems (called as Systems C and D, respectively; Nippon ANS, Inc.), which were slightly different from each other. The systems comprised of a seawater dispensing system, a CO_2 extraction system and a coulometer. In this cruise, we used coulometers, Seacat2000 and Model23000 for Systems C and D, respectively, both of which were constructed by Nippon ANS. Each of the two systems had almost a same specification as follows:

The seawater dispensing system has an auto-sampler (6 ports), which dispenses seawater from a 300 ml borosilicate glass bottle into a pipette of about 15 ml volume by PC control. The pipette is kept at $20^\circ C$ by a water jacket, in which water from a water bath set at $20^\circ C$ is circulated. CO_2 dissolved in a seawater sample is extracted in a stripping chamber of the CO_2 extraction system by adding phosphoric acid ($\sim 10\% \text{ v/v}$) of about 2 ml. The stripping chamber is approx. 25 cm long and has a fine frit at the bottom. The acid is added to the stripping chamber from the bottom of the chamber by pressurizing an acid bottle for a given time to push out the right amount of acid. The pressurizing is made with nitrogen gas (99.9999 %). After the acid is transferred to the stripping chamber, a seawater sample kept in a pipette is introduced to the stripping chamber by the same method as in adding an acid. The seawater reacted with phosphoric acid is stripped of CO_2 by bubbling the nitrogen gas through a fine frit at the bottom of the stripping chamber. The CO_2 stripped in the chamber is carried by the nitrogen gas (flow rates is 140 ml min^{-1}) to the coulometer through a dehydrating module. The modules of Systems C and D consist of two electric dehumidifiers (kept at $\sim 4^\circ C$) and a chemical desiccant ($Mg(ClO_4)_2$).

The measurement sequence such as system blank (phosphoric acid blank), 1.865 % CO_2 gas in a nitrogen base, sea water samples (6) is programmed to repeat. The measurement of 1.865 % CO_2 gas is made to monitor response of coulometer solutions purchased from UIC, Inc. or laboratory-made.

ii. A_T

Measurement of A_T was made based on spectrophotometry using a custom-made system (Nippon ANS, Inc.). The system comprises of a water dispensing unit, an auto-syringe (Hamilton) for hydrochloric acid, a spectrophotometer (TM-UV/VIS C10082CAH, Hamamatsu Photonics), and a light source (Mikropack), which are automatically controlled by a PC. The water dispensing unit has a water-jacketed pipette (42.2663 mL at 25°C) and a titration cell, which is also controlled at 25°C.

A seawater of approx. 42 ml is transferred from a sample bottle (DURAN® glass bottle, 100 ml) into the pipette by pressurizing the sample bottle (nitrogen gas), and is introduced into the titration cell. The seawater is used to rinse the titration cell. Then, Milli-Q water is introduced into the titration cell, also for rinse. A seawater of approx. 42 ml is weighted again by the pipette, and is transferred into the titration cell. Then, for seawater blank, absorbances are measured at three wavelengths (730, 616 and 444 nm). After the measurement, an acid titrant, which is a mixture of approx. 0.05 M HCl in 0.65 M NaCl and 38 μ M bromocresol green (BCG) is added into the titration cell. The volume of the acid titrant is changed between 1.980 mL and 2.200 mL according to estimated values of A_T . The seawater + acid titrant solution is stirred for over 9 minutes with bubbling by nitrogen gas in the titration cell. Then, absorbances at the three wavelengths are measured.

Calculation of A_T is made by the following equation:

$$A_T = (-[H^+]_T V_{SA} + M_A V_A) / V_S,$$

where M_A is the molarity of the acid titrant added to the seawater sample, $[H^+]_T$ is the total excess hydrogen ion concentration in the seawater, and V_S , V_A and V_{SA} are the initial seawater volume, the added acid titrant volume, and the combined seawater plus acid titrant volume, respectively. $[H^+]_T$ is calculated from the measured absorbances based on the following equation (Yao and Byrne, 1998):

$$\text{pH}_T = -\log[H^+]_T = 4.2699 + 0.002578(35 - S) + \log((R - 0.00131)/(2.3148 - 0.1299R)) - \log(1 - 0.001005S),$$

where S is the sample salinity, and R is the absorbance ratio calculated as:

$$R = (A_{616} - A_{730}) / (A_{444} - A_{730}),$$

where A_i is the absorbance at wavelength i nm.

The HCl in the acid titrant is standardized on land. The concentrations of BCG were estimated to be approx. 2.0×10^{-6} M in sample seawater.

iii. pH

Measurement of pH was made by a pH measuring system (Nippon ANS, Inc.). For the detection of pH, spectrophotometry is adopted. The system comprises of a water dispensing unit and a spectrophotometer (Bio 50 Scan, Varian). For an indicator, *m*-cresol purple (2 mM), which is purified based on Patsavas et al. (2013), is used.

Seawater is transferred from borosilicate glass bottle (250 ml) to a sample cell in the spectrophotometer. The length and volume of the cell are 8 cm and 13 ml, respectively, and the sample cell is kept at 25.00 ± 0.05 °C in a thermostated compartment. First, absorbance of seawater only is measured at three wavelengths (730, 578 and 434 nm). Then the indicator is injected and circulated for about 4 minutes to mix the indicator and seawater sufficiently. After the pump is stopped, the absorbance of seawater + indicator is measured at the same wavelengths. The pH is calculated based on the following equation (Liu et al., 2011):

$$\text{pH}_T = -\log(K_T^2 e_2) + \log\left(\frac{R - e_1}{1 - R(e_3/e_2)}\right),$$

where $-\log(K_T^2 e_2) = a + (b/T) + c \times \ln T - d \times T$; $a = -246.64209 + 0.315971 \times S + 2.86855 \times 10^{-4} \times S^2$; $b = 7229.23864 - 7.098137 \times S - 0.057034 \times S^2$; $c = 44.493382 - 0.052711 \times S$; $d = 0.007762$; $e_1 = -0.007762 + 4.5174 \times 10^{-5} T$; $e_3/e_2 = -0.020813 + 2.60262 \times 10^{-4} \times T + 1.0436 \times 10^{-4} \times (S - 35)$. The T and S indicate temperature in K and salinity, respectively. The K_T^2 is the dissociation constant of HI, which is a protonated species of sulfonephthalein indicators. The R is the ratio of sulfonephthalein absorbances ($= A_{578}/A_{434}$) at wavelengths of 578 nm and 434 nm.

(4) Shipboard measurement

(4.1) Sampling

i. C_T

All seawater samples were collected from depth with 12 liter Niskin bottles basically at every other station. The seawater samples for C_T were taken with a plastic drawing tube (PFA tubing connected to silicone rubber tubing) into a 250 ml DURAN[®] glass bottle. The glass bottle was filled with seawater smoothly from the bottom following a rinse with sample seawater of 2 full, bottle volumes. The glass bottle was closed by an inner cap loosely, which was fitted tightly to the bottle mouth after mercuric chloride was added.

At a chemical laboratory on ship, a volume of about 3mL seawater was removed with a plastic pipette from sampling bottles to have a headspace of approx. 1 % of the bottle volume. A saturated mercuric chloride of 100 μ l was added to poison seawater samples. The seawater samples were kept at 5°C in a refrigerator until analysis. A few hours just before analysis, the seawater samples were kept at 20°C in a water bath.

ii. A_T

All seawater samples were collected from depth using 12 liter Niskin bottles at the same stations as for C_T . The seawater samples for A_T were taken with a plastic drawing tube (PFA tubing connected to silicone rubber tubing) into DURAN glass bottles of 100 ml. The glass bottle was filled with seawater smoothly from the bottom after rinsing it with sample seawater of 2 full, bottle volume.

The samples were stored at about 5°C in a refrigerator. A few hours before analysis, the seawater samples were kept at 25 °C in a water bath.

iii. pH

All seawater samples were collected from depth with 12 liter Niskin bottles at the same stations as for C_T and A_T . The seawater samples for pH were taken with a plastic drawing tube (PFA tubing connected to silicone rubber tubing) into a 250 ml borosilicate glass bottle. The glass bottle was filled with seawater smoothly from the bottom following a rinse with sample seawater of 2 full, bottle volumes. The glass bottle

was closed by a stopper, which was fitted to the bottle mouth gravimetrically without additional force.

A few hours just before analysis, the seawater samples were kept at 25°C in a water bath.

(4.2) Analyses

i. C_T

At the start of each leg, we calibrated the measuring systems by blank and 5 kinds of Na_2CO_3 solutions (nominally 500, 1000 1500, 2000, 2500 $\mu\text{mol/L}$). As it was empirically known that coulometers do not show a stable signal (low repeatability) with fresh (low absorption of carbon) coulometer solutions. Therefore, we measured 1.865% CO_2 gas repeatedly until the measurements became stable. Then we started the calibration.

The measurement sequence such as system blank (phosphoric acid blank), 1.865% CO_2 gas in a nitrogen base, seawater samples (6) was programmed to repeat. The measurement of 1.865% CO_2 gas was made to monitor response of coulometer solutions (from UIC, Inc. or in-house made). For every renewal of coulometer solutions, certified reference materials (CRMs, batch 136, certified value = 2021.15 $\mu\text{mol kg}^{-1}$) provided by Prof. A. G. Dickson of Scripps Institution of Oceanography were analyzed. In addition, in-house reference materials (RM) (batch QRM Q30 and Q31) were measured at the initial, intermediate and end times of a coulometer solution's lifetime.

The preliminary values were reported in a data sheet on the ship. Repeatability and vertical profiles of C_T based on raw data for each station helped us check performances of the measuring systems.

In the cruise, we finished all the analyses for C_T on board the ship.

ii. A_T

We analyzed reference materials (RM), which were produced for C_T measurement by JAMSTEC, but were efficient also for the monitor of A_T measurement. In addition, certified reference materials (CRM, batches 136, certified value = 2246.74 $\mu\text{mol kg}^{-1}$) were analyzed periodically to monitor systematic differences of measured A_T . The reported values of A_T were set to be comparable to the certified value of the batch 136.

The preliminary values were reported in a data sheet on ship. Repeatability calculated from replicate

samples and vertical profiles of A_T based on raw data for each station helped us check performance of the measuring system.

In the cruise, we finished all the analyses for A_T on board the ship.

iii. pH

For an indicator solution, purified *m*-cresol purple (2 mM) was used. The indicator solution was produced on board a ship, and retained in a 1000 ml DURAN[®] laboratory bottle. The absorbance ratios of the indicator solution were kept between 1.4 and 1.6 by adding acid or alkali solution appropriately.

It is difficult to mix seawater with an indicator solution sufficiently under no headspace condition. However, by circulating the mixed solution with a peristaltic pump, a well-mixed condition came to be attained rather shortly, leading to a rapid stabilization of absorbance. We renewed a TYGON[®] tube of a peristaltic pump periodically, when a tube deteriorated. We measured absorbances at 25°C.

Absorbances of seawater only and seawater + indicator solutions were measured 5 times each after stable absorbances were attained, and the averaged values were used for the calculation of pH.

The preliminary values of pH were reported in a data sheet on the ship. Repeatability calculated from replicate samples and vertical profiles of pH based on raw data for each station helped us check performance of the measuring system.

We finished all the analyses for pH on board the ship.

(5) Quality control

i. C_T

We conducted quality control of the data after return to a laboratory on land. With calibration factors, which had been determined on board a ship based on blank and 5 kinds of Na_2CO_3 solutions, we calculated C_T of CRM (batches 136), and plotted the values as a function of sequential day, separating legs and the systems used. There were no statistically-significant trends of CRM measurements.

The repeatability of measurements was estimated to be $0.7 \mu\text{mol kg}^{-1}$, which was calculated from 230 differences of replicate measurements.

ii. A_T

Temporal changes of A_T , which originate from analytical problems, were monitored by measuring A_T of CRM. We found no abnormal measurements during the cruises.

The repeatability of measurements was estimated to be $1.1 \mu\text{mol kg}^{-1}$, which was calculated from 210 differences of replicate measurements.

iii. pH

It is recommended that correction for pH change resulting from addition of indicator solutions is made (Dickson et al., 2007). To check the perturbation of pH due to the addition, we measured absorbance ratios by doubling the volume of indicator solution and added it to a replicate seawater sample. We corrected absorbance ratios based on an empirical method (Dickson et al., 2007), although the perturbations were small. The correction was made by subtracting 0.0019 from measured absorbances. The repeatability of measurements was estimated to be 0.0005 pH unit, which was calculated from 272 differences of replicate measurements.

We evaluated accuracy of pH values by comparing the corrected values with those computed from measured C_T and A_T . Averaged differences (computed – measured) of pH values were 0.011 ± 0.008 ($n = 1957$).

References

- Clayton T. D. and R. H. Byrne (1993) Spectrophotometric seawater pH measurements: total hydrogen ion concentration scale calibration of m-cresol purple and at-sea results. *Deep-Sea Research* 40, 2115-2129.
- Dickson, A. G., C. L. Sabine and J. R. Christian eds. (2007) *Guide to best practices for ocean CO₂ measurements*, PICES Special Publication 3, 191 pp.
- Liu, X., M. C. Patsavas and R. H. Byrne (2011) Purification and characterization of meta-cresol purple for spectrophotometric seawater pH measurements. *Environmental Science and Technology*, 45, 4862-4868.
- Patsavas, M. C., R. H. Byrne and X. Liu (2013) Purification of meta-cresol purple and cresol red by flash chromatography: Procedures for ensuring accurate spectrophotometric seawater pH measurements. *Marine Chemistry*, 150, 19-24.
- Yao, W. and R. B. Byrne (1998) Simplified seawater alkalinity analysis: Use of linear array spectrometers. *Deep-Sea Research* 45, 1383-1392.

3.7 Chlorophyll *a*

December 16, 2016

(1) Personnel

Kosei Sasaoka (JAMSTEC) (Leg 2)

Hiroshi Uchida (JAMSTEC) (Legs 1, 2)

Kanta Chida (Rakuno Gakuen University) (Legs 1, 2)

Takuya Takahashi (Rakuno Gakuen University) (Legs 1, 2)

Keitaro Matsumoto (MWJ) (Legs 1, 2)

Katsunori Sagishima (MWJ) (Legs 1, 2)

Haruka Tamada (MWJ) (Legs 1, 2)

Misato Kuwahara (MWJ) (Legs 1)

(2) Objectives

Chlorophyll *a* is one of the most convenient indicators of phytoplankton stock, and has been used extensively for the estimation of phytoplankton abundance in various aquatic environments. In this study, we investigated horizontal and vertical distribution of phytoplankton along the P01 section in the North Pacific. The chlorophyll *a* data is also utilized for calibration of fluorometers, which were installed in the surface water monitoring and CTD profiler system.

(3) Instrument and Method

Seawater samples were collected in 250 ml brown Nalgene bottles without head-space (500 ml bottles for samples from the surface water monitoring system). The whole samples were gently filtrated by low vacuum pressure (<0.02 MPa) through Whatman GF/F filter (diameter 25 mm) in the dark room. Whole volume of each sampling bottle was precisely measured in advance. After filtration, phytoplankton pigments were immediately extracted in 7 ml of N,N-dimethylformamide (DMF), and samples were stored at -20°C under

the dark condition to extract chlorophyll *a* more than 24 hours. Chlorophyll *a* concentrations were measured by the Turner fluorometer (10-AU-005, TURNER DESIGNS), which was previously calibrated against a pure chlorophyll *a* (Sigma-Aldrich Co., LLC) (Fig. 3.7.1). To estimate the chlorophyll *a* concentrations, we applied to the fluorometric “Non-acidification method” (Welschmeyer, 1994).

(4) Results

Vertical profiles of chlorophyll *a* concentrations along the P10N (Leg 1) and P01 (Leg 2) sections during the cruise are shown in Figure 3.7.2. and Figure 3.7.3. respectively. Cross section of chlorophyll *a* concentrations along the P01 line (Leg 2) is shown in Figure 3.7.4. To estimate the measurement precision, 41-pairs of replicate samples were obtained from hydrographic casts. All pairs of the replicate samples were collected in 250 ml bottles. Standard deviation calculated from 41-pairs of the replicate samples was 0.008 µg/L, although absolute difference values between 36-pairs of the replicate samples were smaller than 0.01 µg/L.

(5) Reference

Welschmeyer, N. A. (1994): Fluorometric analysis of chlorophyll *a* in the presence of chlorophyll *b* and pheopigments. *Limnol. Oceanogr.*, 39, 1985-1992.

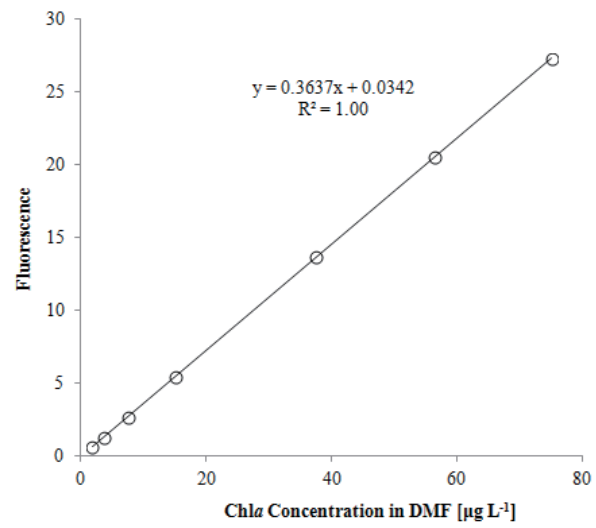


Figure 3.7.1. Relationships between pure chlorophyll *a* concentrations and fluorescence light intensity.

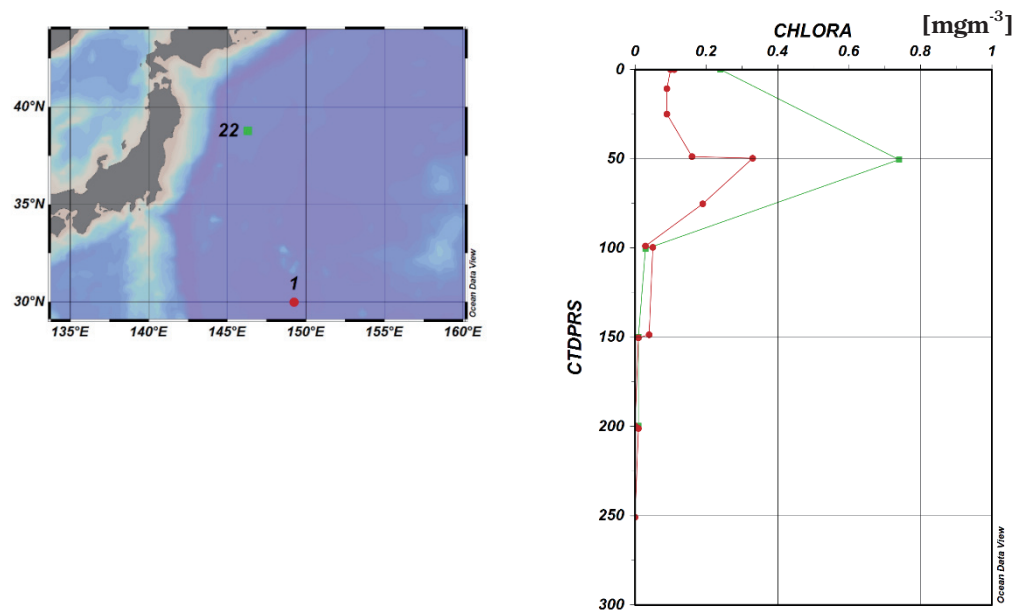


Figure 3.7.2. Vertical profiles of chlorophyll *a* concentrations along the P10N section (Leg 1) obtained from hydrographic casts.

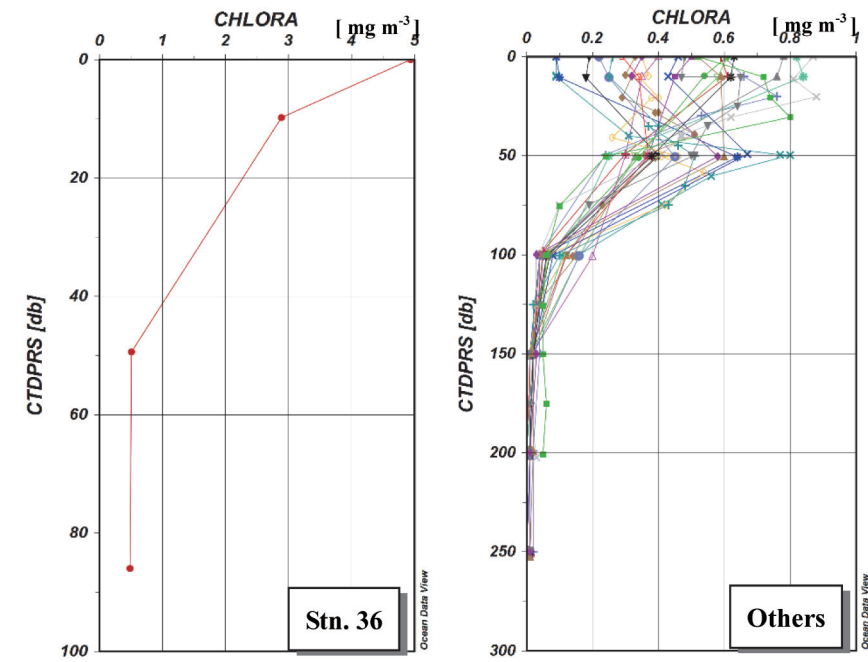


Figure 3.7.3. Vertical profiles of chlorophyll *a* concentrations along the P01 section (Leg 2) obtained from hydrographic casts.

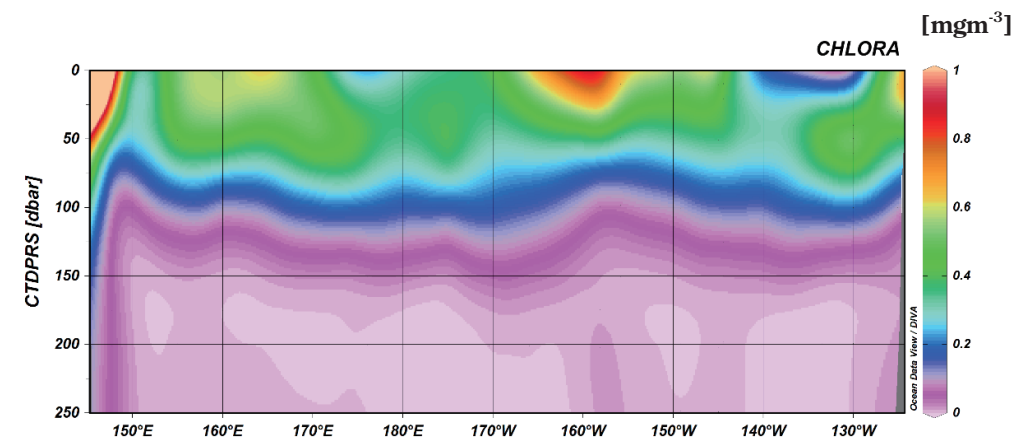


Figure 3.7.4. Cross section of chlorophyll *a* concentrations along the P01-line (Leg 2) obtained from hydrographic casts.

3.8 Absorption Coefficients of Particulate Matter and Colored Dissolved Organic Matter (CDOM)

September 12, 2014

(1) Personnel

Kosei Sasaoka (JAMSTEC) (Leg 2)

(2) Objectives

Absorption coefficients of particulate matter (phytoplankton and non-phytoplankton particles, defined as 'detritus') and colored dissolved organic matter (CDOM) play an important role in determining the optical properties of seawater. In particular, light absorption by phytoplankton is a fundamental process of photosynthesis, and their chlorophyll *a* (Chl-*a*) specific coefficient, a_{ph}^* , can be essential factors for bio-optical models to estimate primary productivities. Absorption coefficients of CDOM are also important parameters to validate and develop the bio-optical algorithms for ocean color sensors, because the absorbance spectrum of CDOM overlaps that of Chl-*a*. The global colored detrital and dissolved materials (CDOM) distribution appears regulated by a coupling of biological, photochemical, and physical oceanographic processes all acting on a local scale, and greater than 50% of blue light absorption is controlled by CDOM (Siegel et al., 2002). Additionally, some investigators have reported that CDOM emerges as a unique tracer for diagnosing changes in biogeochemistry and the overturning circulation, similar to dissolved oxygen (e.g., Nelson et al., 2010). The objectives of this study are to understand the east-west variability of light absorption by phytoplankton and CDOM along the P01 section in the North Pacific.

(3) Methods

Seawater samples for absorption coefficient of total particulate matter ($a_p(\lambda)$) were performed using Niskin bottles and a bucket above 100m depth along the P01 section (Fig. 3.8.1, Table 3.8.1). Samples were collected in 3000ml dark bottles and filtered (500 – 3000 ml) through 25-mm What-man GF/F glass-fiber

filters under a gentle vacuum (< 0.013 MPa) on board in the dark room. After filtration, the optical density of total particulate matter on filter ($OD_{fp}(\lambda)$) between 350 and 750 nm at a rate of 1.0 nm was immediately measured by an UV-VIS recording spectrophotometer (UV-2400, Shimadzu Co.), and absorption coefficient was determined from the OD according to the quantitative filter technique (QFT) (Mitchell, 1990). A blank filter with filtered seawater was used as reference. All spectra were normalized to 0.0 at 750nm to minimize difference between sample and reference filter. To determine the optical density of non-pigment detrital particles ($OD_{fd}(\lambda)$), the filters were then soaked in methanol for a few hours and rinsed with filtered seawater to extract and remove the pigments (Kishino et al., 1985), and its absorption coefficient was measured again by UV-2400. These measured optical densities on filters ($OD_{fp}(\lambda)$ and $OD_{fd}(\lambda)$) were converted to optical densities in suspensions ($OD_{sp}(\lambda)$ and $OD_{sd}(\lambda)$) using the pathlength amplification factor of Cleveland and Weidemann (1993) as follows:

$$OD_{sp}(\lambda) = 0.378 OD_{fp}(\lambda) + 0.523 OD_{fp}(\lambda)^2 \text{ and}$$

$$OD_{sd}(\lambda) = 0.378 OD_{fd}(\lambda) + 0.523 OD_{fd}(\lambda)^2.$$

The absorption coefficient of total particles ($a_p(\lambda)$ (m^{-1})) and non-pigment detrital particles ($a_d(\lambda)$ (m^{-1})) are computed from the corrected optical densities ($OD_s(\lambda)$):

$$a_p(\lambda) = 2.303 \times OD_{sp}(\lambda) / L \quad (L = V / S), \text{ and}$$

$$a_d(\lambda) = 2.303 \times OD_{sd}(\lambda) / L \quad (L = V / S),$$

Where S is the clearance area of the filter (m^2) and V is the volume filtered (m^3). Absorption coefficient of phytoplankton ($a_{ph}(\lambda)$) was obtained by subtracting $a_d(\lambda)$ from $a_p(\lambda)$ as follows:

$$a_{ph}(\lambda) = a_p(\lambda) - a_d(\lambda).$$

Finally, we calculated Chl-*a* normalized specific absorption spectra (a_{ph}^*) to divide a_{ph} by Chl-*a* concentrations obtained from same hydrographic casts.

Seawater samples for absorption coefficient of CDOM ($a_y(\lambda)$) were collected in 250ml bottles using Niskin bottles and a bucket from surface to bottom (Fig. 3.8.1, Table 3.8.1). CDOM samples were filtered using 0.2 μm Nuclepore polycarbonate filters on board. Optical densities of the CDOM ($OD_y(\lambda)$) in this filtered seawater were recorded against UV-2400 in the range from 300 to 800 nm using 10-cm pathlength

glass cells. Milli-Q water was used as a base line. A blank (Milli-Q water versus Milli-Q water) was subtracted from each wavelength of the spectrum. The absorption coefficient of CDOM ($a_y(\lambda)$ (m^{-1})) was calculated from measured optical densities ($OD_y(\lambda)$) as follows:

$$a_y(\lambda) = 2.303 \times OD_y(\lambda) / L \quad (L \text{ is the cuvette path-length (m)}).$$

(4) Preliminary results

Some examples of Chl-*a* normalized specific absorption spectra (a_{ph}^*) were shown in Fig.3.8.2. Cross section of CDOM (as absorption coefficient at 325 nm, unit = m^{-1}) along the P01 section were shown in Fig. 3.8.3.

(5) References

- Cleveland, J.S. and Weidemann, A.D., 1993, Quantifying absorption by aquatic particles: a multiple scattering correction for glass fiber filters, *Limnology and Oceanography*, 38, 1321-1327.
- Kishino, M., Takahashi, M., Okami, N. and Ichimura, S., 1985, Estimation of the spectral absorption coefficients of phytoplankton in the sea, *Bulletin of Marine Science*, 37, 634-642.
- Mitchell, B.G., 1990, Algorithms for determining the absorption coefficient of aquatic particulates using the quantitative filter technique (QFT), *Ocean Optics X*, SPIE 1302, 137-148.
- Nelson, N. B., D. A. Siegel, C. A. Carlson, and C. M. Swan, 2010, Tracing global biogeochemical cycles and meridional overturning circulation using chromophoric dissolved organic matter, *Geophys. Res. Lett.*, 37, L03610, doi:10.1029/2009GL042325.
- Siegel, D.A., Maritorena, S., Nelson, N.B., Hansell, D.A., Lorenzi-Kayser, M., 2002, Global distribution and dynamics of colored dissolved and detrital organic materials. *J. Geophys. Res.*, 107, C12, 3228, doi:10.1029/2001JC000965.

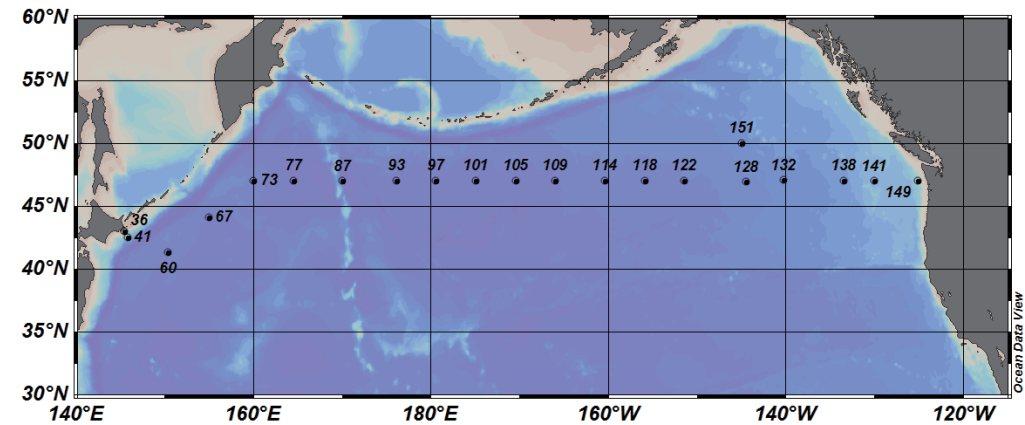


Fig. 3.8.1. Location of sampling stations for absorption coefficients of phytoplankton and CDOM along the P01 section during MR14-04.

Table 3.8.1. List of sampling stations for absorption coefficients of phytoplankton and CDOM during MR14-04.

Station	Date (UTC)	Time (UTC)	Latitude	Longitude	Sampling type	Cast No.	Sampling depth (db)	
							Particle absorbance	CDOM absorbance
36	07/17/2014	7:28	42.97 N	145.45 E	CTD + Bucket	1	0, 10, 50, 86	0, 10, 50, 86
41	07/19/2014	15:56	42.48 N	145.84 E	CTD + Bucket	2	none	Bottom-10, 2930, 1930, 970, 470, 200, 100, 50, 10, 0
60	07/23/2014	13:34	41.27 N	150.39 E	CTD + Bucket	1	0, 10, 50, 100	Bottom-10, 5000, 4000, 3000, 2000, 1000, 500, 200, 100, 50, 10, 0
67	07/25/2014	15:59	44.09 N	155.02 E	CTD + Bucket	2	0, 10, 50, 100	Bottom-10, 5080, 4080, 3080, 2070, 1070, 530, 200, 100, 50, 10, 0
73	07/21/2014	11:59	47.01 N	160.02 E	CTD + Bucket	1	0, 10, 50, 100	Bottom-10, 5000, 3000, 2000, 1000, 800, 500, 200, 100, 50, 10, 0
77	07/29/2014	22:47	47.00 N	164.51 E	CTD + Bucket	1	0, 10, 50, 100	Bottom-10, 4920, 2930, 1930, 970, 770, 470, 200, 100, 50, 10, 0
87	08/01/2014	11:06	46.98 N	170.00 E	CTD + Bucket	1	0, 10, 50, 100	Bottom-10, 3000, 2000, 1000, 800, 500, 200, 100, 50, 10, 0
93	08/03/2014	12:05	47.00 N	176.09 E	CTD + Bucket	1	0, 10, 50, 100	Bottom-10, 5000, 3000, 2000, 1000, 800, 500, 200, 100, 50, 10, 0
97	08/04/2014	18:25	46.99 N	179.43 W	CTD + Bucket	1	0, 10, 50	Bottom-10, 5080, 3080, 2070, 1070, 830, 530, 200, 100, 50, 10, 0
101	08/06/2014	5:30	47.00 N	174.95 W	CTD + Bucket	3	0, 10, 50, 100	Bottom-10, 4920, 2930, 1930, 970, 770, 470, 200, 100, 50, 10, 0
105	08/08/2014	9:33	47.00 N	170.42 W	CTD + Bucket	1	0, 10, 50	Bottom-10, 5000, 3000, 2000, 1000, 800, 500, 200, 100, 50, 10, 0
109	08/09/2014	15:55	47.01 N	165.98 W	CTD + Bucket	1	0, 10, 50, 100	Bottom-10, 5080, 3080, 2070, 1070, 830, 530, 200, 100, 50, 10, 0
114	08/11/2014	6:33	46.99 N	160.36 W	CTD + Bucket	1	0, 10, 50, 100	Bottom-10, 5000, 3000, 2000, 1000, 800, 500, 200, 100, 50, 10, 0
118	08/12/2014	16:39	46.99 N	155.85 W	CTD + Bucket	1	0, 10, 50, 100	Bottom-10, 5080, 3080, 2070, 1070, 830, 530, 200, 100, 50, 10, 0
122	08/13/2014	23:25	47.00 N	151.40 W	CTD + Bucket	2	0, 10, 50, 100	Bottom-10, 4920, 2930, 1930, 970, 770, 470, 200, 100, 50, 10, 0
128	08/15/2014	21:25	46.90 N	144.44 W	CTD + Bucket	1	0, 10, 50, 100	Bottom-10, 2930, 1930, 970, 770, 470, 280, 200, 100, 50, 10, 0
151	08/16/2014	20:20	50.00 N	144.99 W	CTD + Bucket	1	0, 10, 50, 100	Bottom-10, 3000, 2000, 1000, 800, 500, 300, 200, 100, 50, 10, 0
132	08/18/2014	14:48	47.03 N	140.23 W	CTD + Bucket	1	0, 10, 50, 100	Bottom-10, 3000, 2000, 1000, 800, 500, 300, 200, 100, 50, 10, 0
138	08/20/2014	8:35	46.99 N	133.47 W	CTD + Bucket	1	0, 10, 50, 100	Bottom-10, 3000, 2000, 1000, 800, 500, 300, 200, 100, 50, 10, 0
141	08/21/2014	3:25	46.98 N	130.03 W	CTD + Bucket	1	0, 10, 50, 100	Bottom-10, 2000, 1000, 800, 500, 300, 200, 100, 50, 10, 0
149	08/22/2014	18:29	47.00 N	125.06 W	CTD + Bucket	1	0, 10, 20, 30, 50, 100	Bottom-10, 970, 770, 470, 280, 200, 100, 50, 30, 20, 10, 0

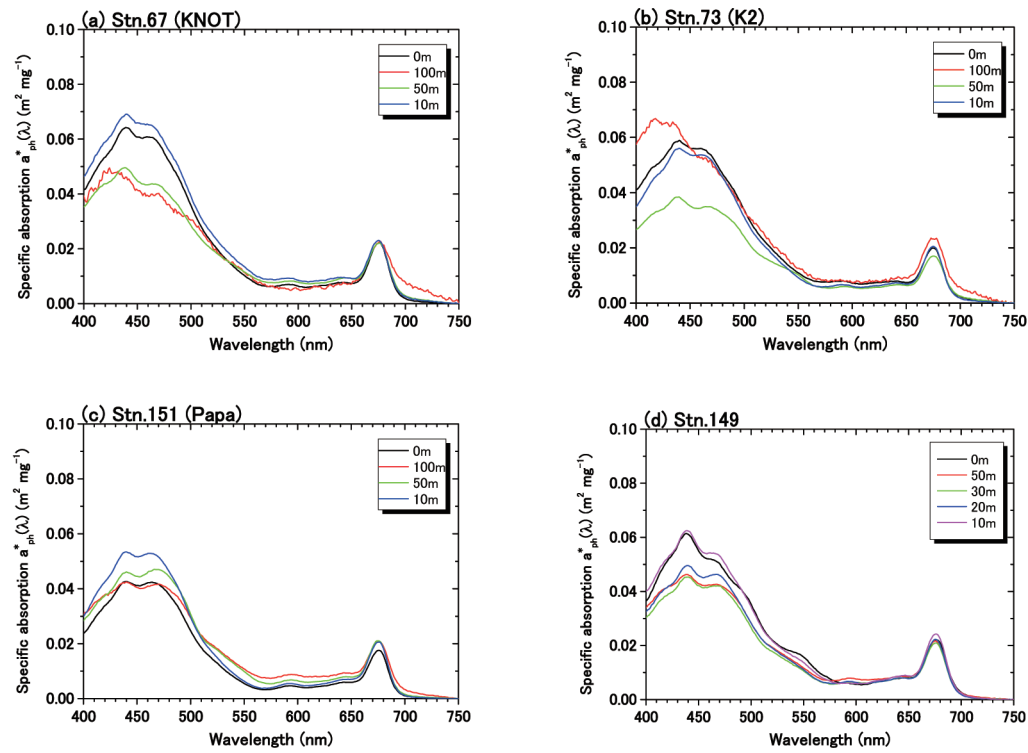


Fig.3.8.2. Examples of chlorophyll-specific phytoplankton absorption coefficient spectra ($a^*_{ph}(\lambda)$) at 400-750 nm, (a) Stn.KNOT, (b) Stn. K2, (c) Stn. Papa, (d) Stn. 149. All spectra were normalized to 0.0 at 750nm.

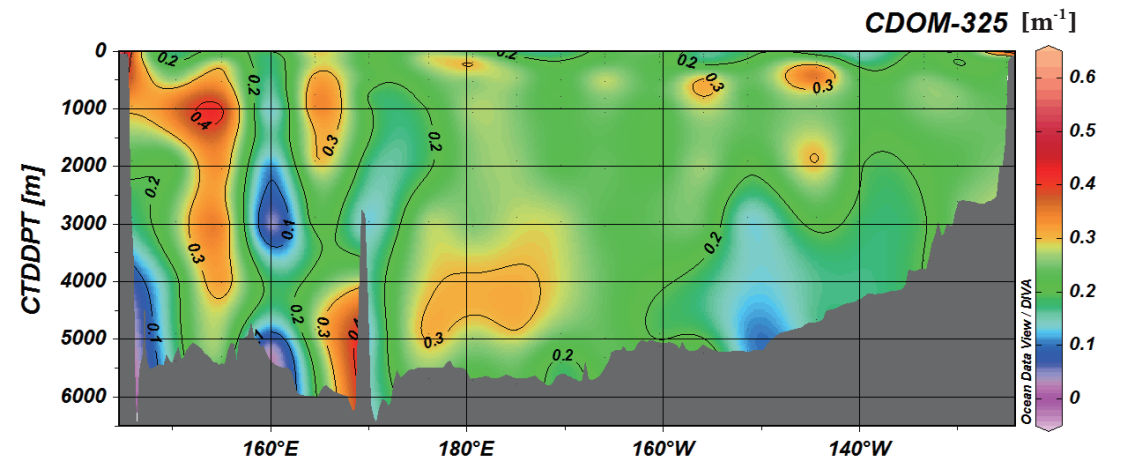


Fig.3.8.3. Contours showing distribution of CDOM (as absorption coefficient at 325 nm, unit = m^{-1}) along the P01 section during MR14-04.

3.9 Calcium

September 16, 2014

(1) Personnel

Yoshihiro Shinoda (JAMSTEC)

(2) Objectives

According to the recent IPCC report, concentrations of CO₂ in the atmosphere have increased by 40% since pre-industrial times, primarily from fossil fuel emissions and secondarily from net land use change emissions. The ocean has absorbed about 30% of the emitted anthropogenic carbon dioxide, causing ocean acidification. Ocean acidification is characterized by an increase of H⁺ (i.e., a decrease of pH) and a concurrent decrease of carbonate ion concentration (CO₃²⁻). The decrease of CO₃²⁻ is unfavorable to marine calcifying organisms, which utilize CO₃²⁻, together with Ca²⁺, to produce their calcium carbonate (CaCO₃) shells and skeletons. To evaluate dissolution and precipitation of calcium carbonate, we measured directly the concentration of calcium in the sea water in the subarctic region of the North Pacific.

(3) Reagents

NH ₃ /NH ₄ buffer:	0.4 mol/l NH ₄ Cl/ 0.4 mol/l NH ₃ buffer
Zincon solution:	0.004 mol/l Zincon, 0.0925g Zincon was dissolved 0.8 ml 1M NaOH and was diluted to 50 ml
EGTA titrant:	0.02 mol/l EGTA, 3.80g EGTA was dissolved 30 ml 1M NaOH and was diluted to 500 ml
Zn/EGTA solution:	0.004 mol/l ZnSO ₄ / 0.004 mol/l EGTA
STD solution:	40ml 1000mg/l Ca standard solution was diluted to 100ml

(4) Apparatus

Measurement of calcium was made by a modified Dissolved Oxygen Titrator DOT-01 (Kimoto Electronic Co. Ltd.). Bandpass filter was replaced to f₀=620nm. The system comprises of a light source, photodiode detectors, auto-burette and control unit.

Seawater of approx. 10ml is transferred from a sample bottle (60ml HDPE bottle) into 100 ml tall beaker by transfer pipet. A magnetic stirrer bar was added into beaker. 5ml NH₃/NH₄buffer, 1ml Zincon solution, 1ml Zn/EGTA solution and about 60ml H₂O were added into the beaker. The seawater samples were titrated by the EGTA titrant. The EGTA titrant was calibrated by measuring STD solution.

(5) Performances

The system worked well no troubles. The repeatability was estimated to 0.0089±0.0076 (n=20 pairs) mmol kg⁻¹.

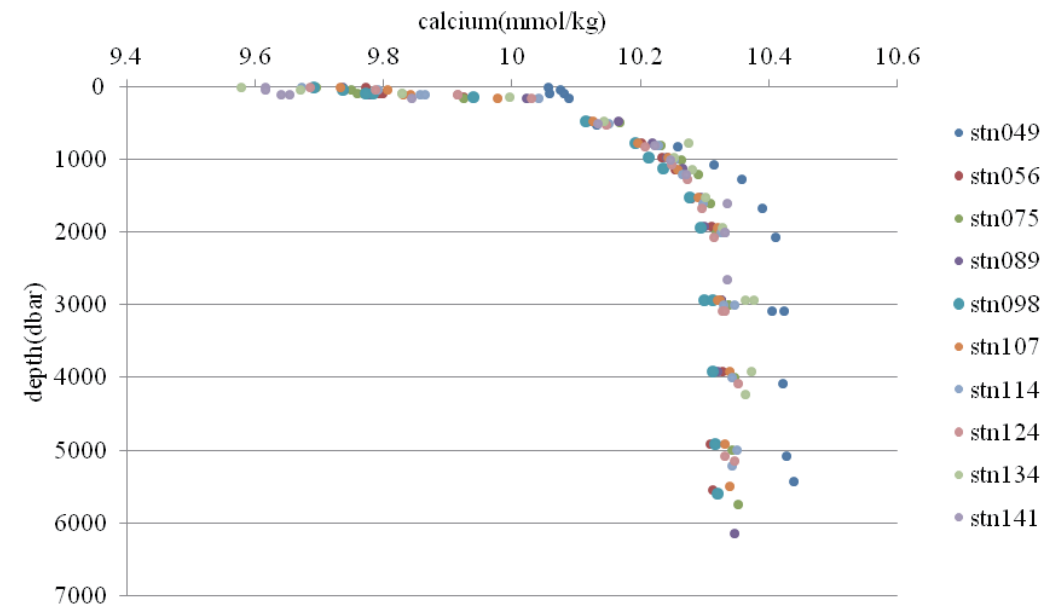


Fig. 3.9.1. Vertical profiles of calcium.

3.10 Dissolved Organic Carbon

February 9, 2017

(1) Personnel

Takeshi Yoshimura¹, Dennis A. Hansell², and Andrew Margolin²

¹Central Research Institute of Electric Power Industry

²Rosenstiel School of Marine and Atmospheric Science, University of Miami

(2) Background and objectives

For several years, the Hansell Laboratory has pursued opportunities to determine the global ocean distribution of dissolved organic carbon (DOC), which plays a significant role in marine carbon cycle. In the Pacific, in collaboration with Prof. Craig Carlson at the Univ. of California Santa Barbara, we have measured DOC on several of the CLIVAR Repeat Hydrography lines, including P16 (north and south), P06, P02, and P18 (<http://yyy.rsmas.miami.edu/groups/biogeochem/Data.html>). On the map given at that website, the major gaps in coverage of the global ocean are readily apparent, including the NW and the NE Pacific Ocean. P10N and P01 are well located for filling these critical gaps as they cover the distal end of the global ocean thermohaline circulation cell. Ultimately our goal is to evaluate the cause of DOC concentration gradients in the deep Pacific, but those gradients must first be established by surveys such as P01. Gradients indicate sources and sinks for refractory DOC (RDOC) in the deep layers, processes that are not understood at the present. RDOC has been implicated by paleoceanographers as the source of carbon responsible for climate hyperthermals of the Paleocene/Eocene epochs (45–50M ybp), but we know too little about RDOC in the modern ocean to confirm or refute that role. To fill the gaps in global coverage of DOC, we collected seawater samples at the stations on P10N and P01 lines during the MR14-04 cruise.

(3) Samplings

Seawater samples were collected in P10N (Leg. 1) and P01 line (Leg. 2) at all of the stations and layers where inorganic carbon parameters were measured in the main subject of this cruise. Water was collected directly into 60 mL polycarbonate bottles from the 12-L Niskin bottles attached to a CTD system. The bottles were then stored frozen until analysis at our laboratory at the University of Miami. Total number of the samples collected was approximately 2100.

(4) Sample analyses and data managements

The frozen samples were returned to the laboratory and thawed for analysis by high temperature catalytic oxidation using a Shimadzu TOC analyzer. The method used was described in a chapter in the methods manual by Dickson et al. (2007). The method: An acidified water sample is sparged with oxygen to remove inorganic carbon. The water is then injected onto a combustion column packed with platinum-coated alumina beads held at 680°C. Non-purgeable organic carbon compounds are combusted and converted to CO₂, which is detected by a non-dispersive infrared detector (NDIR). The instrument was a Shimadzu TOC-L with ASI-V auto sampler.

Instrument conditions were as follows:

Combustion temperature	680°C
Carrier gas	UHP Oxygen
Carrier flow rate	50 ml min ⁻¹
Sample sparge time	2.0 min
Minimum number of injections	3
Maximum number of injections	5
Number of washes	2
Standard deviation maximum	0.10 ppm
CV maximum	2.0%
Injection volume	100 µL

Trace-impurity analyzed concentrated hydrochloric acid is used to acidify samples prior to analysis. Approximately 0.1% by volume of the concentrated acid is added to each sample prior to analysis to lower the pH of the sample to $\text{pH} < 2$. At this pH and with sparging, all inorganic carbon species are converted to CO_2 and removed from the sample. The system is calibrated using potassium hydrogen phthalate in Milli-Q[®] water. System performance is verified daily using Consensus Reference Water (www.rsmas.miami.edu/groups/biogeochem/CRM.html). This reference water is deep Sargasso Sea water (DSR) that has been acidified and sealed in 10 ml ampoules, the concentrations of which have been determined by the consensus of up to six expert and independent laboratories. Low Carbon Water (LCW) that has gone through the same acidification, sealing process, and consensus verification program as the DSR, and has an agreed upon carbon concentration of $1\text{--}2 \mu\text{mol C L}^{-1}$, is also analyzed and used to determine the instrument blank. After verifying proper operation of the instrument, samples are placed on an auto sampler for analysis. The run starts with a QW (Q Water) blank and a reference seawater analysis. Then six samples are analyzed, followed by another QW blank and reference sea water. This sequence is repeated until all samples for that run are analyzed. The run ends with a QW blank, reference water, and a QW blank that had not been acidified. This last blank verifies that the hydrochloric acid used to acidify the samples is not contaminated. QW blanks and reference water samples are used to evaluate system performance during the analytical run. If a problem is detected with the blanks or reference waters, the samples are reanalyzed.

On a daily basis, CRM is analyzed to verify system performance. If the value of the CRM does not fall within the expected range, samples are not analyzed until the expected performance has been established. The QW blanks and reference seawater samples analyzed with the samples are used for quality assurance and quality control (QA/QC). By evaluating the performance of these reference waters, instrument drift and performance can be evaluated. If a problem is detected with either drift or performance, the samples are reanalyzed.

(5) Reference

Dickson, A.G., Sabine, C.L. and Christian, J.R. (Eds.) 2007. Guide to best practices for ocean CO_2 measurements. PICES Special Publication 3, 191 pp.

3.11 Lowered Acoustic Doppler Current Profiler (LADCP)

November 17, 2016

(1) Personnel

Shinya Kouketsu (JAMSTEC) (Principal Investigator, Leg 2)

Hiroshi Uchida (JAMSTEC) (Legs 1 and 2)

(2) Overview of the equipment

An acoustic Doppler current profiler (ADCP) was integrated with the CTD/RMS package. The lowered ADCP (LADCP), Workhorse Monitor WHM300 (Teledyne RD Instruments, San Diego, California, USA), which has 4 downward facing transducers with 20-degree beam angles, rated to 6000 m. The LADCP makes direct current measurements at the depth of the CTD, thus providing a full profile of velocity. The LADCP was powered during the CTD casts by a 48 volts battery pack. The LADCP unit was set for recording internally prior to each cast. After each cast the internally stored observed data was uploaded to the computer on-board. By combining the measured velocity of the sea water and bottom with respect to the instrument, and shipboard navigation data during the CTD cast, the absolute velocity profile were obtained (e.g. Visbeck, 2002). However, in some stations, the shipboard ADCP profiles were not obtained due to GPS problems, and the estimation errors of the velocity estimations of lowered ADCP were slightly large at the stations. Furthermore, the first cast at station 1, the data process software did not work well due to small echo intensities in the deep layers.

The instrument used in this cruise was as follows.

Teledyne RD Instruments, WHM300

S/N 20754(CPU firmware ver. 50.40)

(3) Data collection

In this cruise, data were collected with the following configuration.

Bin size: 4.0 m

Number of bins: 25

Pings per ensemble: 1

Ping interval: 1.0 sec

At the following stations, the CTD cast was carried out without the LADCP, because the maximum pressure was beyond the pressure-proof of the LADCP (6000 m).

Stations from P01_44 to P01_46

Reference

Visbeck, M. (2002): Deep velocity profiling using Lowered Acoustic Doppler Current Profilers: Bottom track and inverse solutions. *J. Atmos. Oceanic Technol.*, **19**, 794-807.

Station Summary

R/V MIRAI CRUISE MR1404 LEG1

SHIP/CRS EXPCODE	WOCE SECT	STNNBR	CASTNO	CAST TYPE	DATE	UTC TIME	EVENT CODE	LATITUDE	POSITION LONGITUDE	NAV	UNC DEPTH	COR DEPTH	HT ABOVE BOTTOM	WIRE OUT	MAX PRESS	NO. OF BOTTLES	PARAMETERS	COMMENTS
49NZ20140709		901	1	UNK	070914	1500	DE	33 3.99 N	142 2.21 E	GPS	-9	8939						RADIOSONDE #1
49NZ20140709		902	1	UNK	071014	0513	DE	31 39.97 N	145 19.16 E	GPS	-9	6045						HYVIS #1
49NZ20140709	P10N	1	1	ROS	071014	2326	BE	29 58.78 N	149 15.23 E	GPS	-9	6198						
49NZ20140709	P10N	1	1	BUC	071014	2335	UN	29 58.81 N	149 15.28 E	GPS	-9	6197					1,3-6,20,30,31,33,34,82,90,100,102,103,106	22.9C
49NZ20140709	P10N	1	1	XCT	071014	2339	DE	29 58.82 N	149 15.30 E	GPS	-9	6196			431			
																		TSK XCTD-4 #14015331, FAILED
49NZ20140709	P10N	1	1	ROS	071114	0058	BO	29 58.86 N	149 15.50 E	GPS	-9	6198	79	5986	6128	35	1,3-6,20,23,24,26,30,31,33,34,43,82,90,92,100,102-104,106,113	#2 CHLORA MAX, #6 MISS FIRE, LADCP SOUNDING
49NZ20140709	P10N	1	1	ROS	071114	0352	EN	29 58.77 N	149 15.96 E	GPS	-9	6189						
49NZ20140709	P10N	1	1	FLT	071114	0426	DE	29 59.06 N	149 16.20 E	GPS	-9	6190						
																		ARGO #OINI3JAP-ARL-60/ID131532 (FOR PHOTOGRAPHY BY JBC)
49NZ20140709	P10N	1	1	FLT	071114	0458	RE	29 58.87 N	149 16.32 E	GPS	-9	6181						
49NZ20140709	P10N	1	1	BIO	071114	0514	BE	29 58.78 N	149 16.45 E	GPS	-9	6177						ORI NET
49NZ20140709	P10N	1	1	BIO	071114	0715	EN	29 55.74 N	149 14.12 E	GPS	-9	6192						
49NZ20140709	P10N	1	2	ROS	071114	0759	BE	29 57.48 N	149 15.04 E	GPS	-9	6191						
49NZ20140709	P10N	1	2	BUC	071114	0807	UN	29 57.44 N	149 15.13 E	GPS	-9	6205					3-6,22,30,31,33,34,82,89,91,100-104,106,108,112,113	23.6C
49NZ20140709	P10N	1	2	ROS	071114	0820	BO	29 57.37 N	149 15.27 E	GPS	-9	6180	-9	790	802	35	3-6,22,30,31,33,34,82,89,91,100-104,106,108,112,113	#1 CHLORA MAX, #24 MISS FIRE
49NZ20140709	P10N	1	2	ROS	071114	0906	EN	29 57.39 N	149 15.76 E	GPS	-9	6167						
49NZ20140709	P10N	903	1	UNK	071114	1200	DE	30 29.74 N	149 20.08 E	GPS	-9	6136						RADIOSONDE #2
49NZ20140709	P10N	2	1	XCT	071114	1204	DE	30 30.09 N	149 20.14 E	GPS	-9	6139			2031			TSK XCTD-4 #14015333
49NZ20140709	P10N	3	1	XCT	071114	1536	DE	31 10.03 N	149 20.22 E	GPS	-9	6045			1979			TSK XCTD-4 #14015334
49NZ20140709	P10N	904	1	UNK	071114	1800	DE	31 37.74 N	149 19.41 E	GPS	-9	5416						RADIOSONDE #3
49NZ20140709	P10N	4	1	XCT	071114	1902	DE	31 49.97 N	149 19.64 E	GPS	-9	5672			2031			TSK XCTD-4 #14015332
49NZ20140709	P10N	5	1	XCT	071114	2234	DE	32 29.72 N	149 20.06 E	GPS	-9	5943			2031			TSK XCTD-4 #14046637
49NZ20140709	P10N	905	1	UNK	071214	0000	DE	32 44.67 N	149 19.75 E	GPS	-9	5997						RADIOSONDE #4
49NZ20140709	P10N	906	1	UNK	071214	0051	DE	32 52.82 N	149 18.02 E	GPS	-9	6026						HYVIS #2
49NZ20140709	P10N	6	1	XCT	071214	0220	DE	33 9.27 N	149 19.72 E	GPS	-9	6115			2031			TSK XCTD-4 #14046640
49NZ20140709	P10N	907	1	UNK	071214	0426	DE	33 33.00 N	149 19.34 E	GPS	-9	6143						HYVIS #3
49NZ20140709	P10N	7	1	ROS	071214	0539	BE	33 44.16 N	149 19.35 E	GPS	-9	6168						
49NZ20140709	P10N	7	1	BUC	071214	0547	UN	33 44.11 N	149 19.35 E	GPS	-9	6172					1,3-6,20,22,30,31,33,82,89-91,102,103,106	22.4C
49NZ20140709	P10N	7	1	XCT	071214	0552	DE	33 44.10 N	149 19.35 E	GPS	-9	6171			1236			TSK XCTD-4 #14046643
49NZ20140709	P10N	908	1	UNK	071214	0600	DE	33 44.07 N	149 19.34 E	GPS	-9	6170						RADIOSONDE #5
49NZ20140709	P10N	7	1	ROS	071214	0618	BO	33 43.96 N	149 19.31 E	GPS	-9	6169	-9	1976	2002	36	1,3-6,20,22-24,26,30,31,33,43,82,89-92,102,103,106	
49NZ20140709	P10N	7	1	ROS	071214	0726	EN	33 43.67 N	149 19.29 E	GPS	-9	6172						
49NZ20140709	P10N	8	1	XCT	071214	0943	DE	34 10.02 N	149 13.03 E	GPS	-9	6174			2031			TSK XCTD-4 #14046645
49NZ20140709	P10N	909	1	UNK	071214	1000	DE	34 11.93 N	149 12.29 E	GPS	-9	6153						RADIOSONDE #6
49NZ20140709	P10N	9	1	XCT	071214	1138	DE	34 29.82 N	149 1.34 E	GPS	-9	6138			2031			TSK XCTD-4 #14046642
49NZ20140709	P10N	910	1	UNK	071214	1200	DE	34 32.37 N	148 59.92 E	GPS	-9	6132						RADIOSONDE #7
49NZ20140709	P10N	10	1	XCT	071214	1323	DE	34 47.83 N	148 53.58 E	GPS	-9	6142			2031			TSK XCTD-4 #14046641
49NZ20140709	P10N	911	1	UNK	071214	1400	DE	34 52.53 N	148 50.22 E	GPS	-9	6125						RADIOSONDE #8
49NZ20140709	P10N	912	1	UNK	071214	1500	DE	35 2.55 N	148 41.91 E	GPS	-9	6078						RADIOSONDE #9
49NZ20140709	P10N	11	1	XCT	071214	1518	DE	35 5.09 N	148 39.62 E	GPS	-9	6069			2031			TSK XCTD-4 #14046639

R/V MIRAI CRUISE MR1404 LEG2

SHIP/CRS EXPCODE	WOCE SECT	STNNBR	CASTNO	CAST TYPE	DATE	UTC TIME	EVENT CODE	LATITUDE	POSITION LONGITUDE	NAV	UNC DEPTH	COR DEPTH	HT ABOVE BOTTOM	WIRE OUT	MAX PRESS	NO. OF BOTTLES	PARAMETERS	COMMENTS
49NZ20140717	P01	36	1	BUC	071714	0720	UN	42 58.41 N	145 27.22 E	GPS	-9	96					1,3,4,5,6,20,31,33,34,90,98,99,102	9.0C
49NZ20140717	P01	36	1	ROS	071714	0721	BE	42 58.41 N	145 27.20 E	GPS	-9	97						
49NZ20140717	P01	36	1	ROS	071714	0727	BO	42 58.41 N	145 27.12 E	GPS	-9	96	10	82	86	6	1-8,20,23,24,26,27,31,33,34,43,90,92,93,98,99,102	
49NZ20140717	P01	36	1	ROS	071714	0737	EN	42 58.42 N	145 27.04 E	GPS	-9	95						
49NZ20140717	P01	37	1	ROS	071714	0933	BE	42 53.42 N	145 31.20 E	GPS	-9	349						
49NZ20140717	P01	37	1	BUC	071714	0941	UN	42 53.46 N	145 31.20 E	GPS	-9	380					1,3-6,102	12.6C
49NZ20140717	P01	37	1	ROS	071714	0944	BO	42 53.46 N	145 31.20 E	GPS	-9	381	10	344	350	12	1-8,20,23,24,26,27,31,33,34,43,90,92,93,98,99,102	
49NZ20140717	P01	37	1	ROS	071714	1014	EN	42 53.38 N	145 31.17 E	GPS	-9	351						
49NZ20140717	P01	38	1	ROS	071714	1205	BE	42 51.39 N	145 32.41 E	GPS	-9	911						
49NZ20140717	P01	38	1	BUC	071714	1213	UN	42 51.41 N	145 32.39 E	GPS	-9	907					1,3-6,20,102	11.5C
49NZ20140717	P01	38	1	ROS	071714	1227	BO	42 51.42 N	145 32.37 E	GPS	-9	899	8	893	905	13	1-8,20,23,24,26,27,43,92,93,101,102	
49NZ20140717	P01	38	1	ROS	071714	1318	EN	42 51.43 N	145 32.27 E	GPS	-9	898						
49NZ20140717	P01	39	1	ROS	071714	1524	BE	42 48.80 N	145 35.60 E	GPS	-9	1532						
49NZ20140717	P01	39	1	BUC	071714	1534	UN	42 48.77 N	145 35.66 E	GPS	-9	1541					1-8,20,23,24,26,27,43,93,102	12.9C
49NZ20140717	P01	39	1	ROS	071714	1558	BO	42 48.68 N	145 35.69 E	GPS	-9	1544	11	1524	1546		17 1-8,27,93,101,102	
49NZ20140717	P01	39	1	ROS	071714	1702	EN	42 48.49 N	145 35.80 E	GPS	-9	1587						
49NZ20140717	P01	40	1	ROS	071714	1855	BE	42 38.39 N	145 42.04 E	GPS	-9	2444						
49NZ20140717	P01	40	1	BUC	071714	1903	UN	42 38.38 N	145 42.11 E	GPS	-9	2453					1,3-6,20,82,102,103,106	11.0C
49NZ20140717	P01	40	1	ROS	071714	1938	BO	42 38.29 N	145 42.37 E	GPS	-9	2474	9	2454	2493	21	1-8,20,23,24,26,27,30,43,82,92,93,101-103,106	
49NZ20140717	P01	40	1	ROS	071714	2108	EN	42 38.23 N	145 42.73 E	GPS	-9	2495						
49NZ20140717	P01	41	1	ROS	071714	2333	BE	42 29.39 N	145 50.32 E	GPS	-9	3149						
49NZ20140717	P01	41	1	BUC	071714	2345	UN	42 29.37 N	145 50.25 E	GPS	-9	3149					1,3-6,102	12.8C
49NZ20140717	P01	41	1	ROS	071814	0029	BO	42 29.36 N	145 49.99 E	GPS	-9	3145	8	3135	3183	0		
																		CAST ABORT DUE TO CTD CABLE TROUBLE
49NZ20140717	P01	41	1	ROS	071814	0148	EN	42 29.43 N	145 49.43 E	GPS	-9	3133						
																		CUT CTD CABLE (1620M) AFTER THE CAST
49NZ20140717	P01	925	1	UNK	071814	0555	BE	41 51.91 N	146 19.13 E	GPS	-9	6698						
																		3-AXIS MAGNETMETER CALIBRATION
49NZ20140717	P01	925	1	UNK	071814	0620	EN	41 51.35 N	146 19.53 E	GPS	-9	7088						
49NZ20140717	P01	47	1	ROS	071814	1103	BE	41 38.64 N	146 29.35 E	GPS	-9	6026						
																		WITHOUT LADCP/MR/FL/TX/CDOM
49NZ20140717	P01	47	1	BUC	071814	1111	UN	41 38.15 N	146 30.06 E	GPS	-9	6025					1,3-6,20,30,82,102,106	20.5C
49NZ20140717	P01	47	1	ROS	071814	1236	BO	41 38.50 N	146 30.88 E	GPS	-9	6035	9	6007	6153	36	1-8,20,23,24,26,27,30,43,82,93,102,106	
49NZ20140717	P01	47	1	ROS	071814	1529	EN	41 38.60 N	146 32.62 E	GPS	-9	6029						
49NZ20140717	P01	46	1	ROS	071814	1744	BE	41 42.64 N	146 24.97 E	GPS	-9	6521						
																		WITHOUT LADCP/MR/FL/TX/CDOM
49NZ20140717	P01	46	1	BUC	071814	1754	UN	41 42.63 N	146 25.16 E	GPS	-9	6502					1,3-6,102	20.0C
49NZ20140717	P01	46	1	ROS	071814	1922	BO	41 42.89 N	146 25.82 E	GPS	-9	6512	-9	6345	6502	36	1-8,27,93,102	
49NZ20140717	P01	46	1	ROS	071814	2216	EN	41 42.81 N	146 26.76 E	GPS	-9	6484						
49NZ20140717	P01	45	1	ROS	071914	0000	BE	41 52.07 N	146 18.95 E	GPS	-9	6697						
																		WITHOUT LADCP/MR/FL/TX/CDOM
49NZ20140717	P01	45	1	BUC	071914	0009	UN	41 52.10 N	146 18.99 E	GPS	-9	6699					1,3-6,20,30,82,100,102-104,106	19.4C
49NZ20140717	P01	45	1	ROS	071914	0138	BO	41 52.42 N	146 19.16 E	GPS	-9	6760	-9	6348	6501	36	1-8,20,23,24,26,27,30,43,82,92,93,102-104,106	
49NZ20140717	P01	45	1	ROS	071914	0436	EN	41 53.43 N	146 20.66 E	GPS	-9	6773						
49NZ20140717	P01	44	1	ROS	071914	0642	BE	41 58.90 N	146 14.67 E	GPS	-9	6294						

														WITHOUT LADCP/MR/FL/TX/CDOM								
49NZ20140717	P01	44	1	BUC	071914	0652	UN	41	58.89	N	146	14.75	E	GPS	-9	6300				1,3-6,102	18.6C	
49NZ20140717	P01	44	1	ROS	071914	0825	BO	41	59.41	N	146	15.04	E	GPS	-9	6187	10	6245	6372	36	1-8,27,93,102	
49NZ20140717	P01	44	1	ROS	071914	1115	EN	41	59.94	N	146	16.51	E	GPS	-9	6169						
49NZ20140717	P01	41	2	ROS	071914	1501	BE	42	29.18	N	145	50.04	E	GPS	-9	3153						
49NZ20140717	P01	41	2	BUC	071914	1511	UN	42	29.08	N	145	50.02	E	GPS	-9	3154					1,3-6,98,102	12.4C
49NZ20140717	P01	41	2	ROS	071914	1556	BO	42	28.92	N	145	50.20	E	GPS	-9	3163	10	3144	3197	25	1-8,27,93,98,102	
49NZ20140717	P01	41	2	ROS	071914	1737	EN	42	28.83	N	145	50.36	E	GPS	-9	3170						
49NZ20140717	P01	42	1	ROS	071914	1910	BE	42	17.09	N	146	3.31	E	GPS	-9	4175						
49NZ20140717	P01	42	1	BUC	071914	1919	UN	42	17.14	N	146	3.26	E	GPS	-9	4163					1,3-6,20,31,33,43,102	12.0C
49NZ20140717	P01	42	1	ROS	071914	2019	BO	42	17.15	N	146	2.96	E	GPS	-9	4153	10	4135	4214	36	1-8,23,24,26,27,31,33,43,92,93,101,102	
RRROM #2 TO #9 DUPL BTLS																						
49NZ20140717	P01	42	1	ROS	071914	2220	EN	42	17.25	N	146	2.88	E	GPS	-9	4134						
49NZ20140717	P01	43	1	ROS	072014	0028	BE	42	10.77	N	146	4.99	E	GPS	-9	5066						
49NZ20140717	P01	43	1	BUC	072014	0036	UN	42	10.78	N	146	5.00	E	GPS	-9	5056					1,3-6,20,30,82,102,106	11.2C
49NZ20140717	P01	43	1	ROS	072014	0148	BO	42	10.83	N	146	4.88	E	GPS	-9	5040	9	5035	5142	34	1-8,20,23,24,26,27,30,43,82,92,93,101,102,106	
49NZ20140717	P01	43	1	ROS	072014	0405	EN	42	11.29	N	146	4.41	E	GPS	-9	4959						
49NZ20140717	P01	48	1	ROS	072014	0907	BE	41	21.56	N	146	41.27	E	GPS	-9	5475						
49NZ20140717	P01	48	1	BUC	072014	0916	UN	41	21.69	N	146	41.36	E	GPS	-9	5479					1,3-6,102	19.1C
49NZ20140717	P01	48	1	ROS	072014	1035	BO	41	22.56	N	146	42.18	E	GPS	-9	5480	12	5494	5576	36	1-8,27,93,102	#1=#8 DUPL BTLS
49NZ20140717	P01	48	1	ROS	072014	1300	EN	41	24.08	N	146	44.12	E	GPS	-9	5481						
49NZ20140717	P01	49	1	ROS	072014	1446	BE	41	7.72	N	146	53.08	E	GPS	-9	5338						
49NZ20140717	P01	49	1	BUC	072014	1456	UN	41	7.78	N	146	53.07	E	GPS	-9	5334					1,3-6,20,31,33,90,102	18.3C
49NZ20140717	P01	49	1	ROS	072014	1612	BO	41	8.17	N	146	53.31	E	GPS	-9	5336	10	5316	5430	35	1-8,20,23,24,26,27,31,33,43,90,93,97,101,102	#4=#10 DUPL BTLS
49NZ20140717	P01	49	1	ROS	072014	1833	EN	41	8.80	N	146	53.80	E	GPS	-9	5335						
49NZ20140717	P01	50	1	ROS	072014	2104	BE	40	51.81	N	147	3.96	E	GPS	-9	4778						
49NZ20140717	P01	50	1	BUC	072014	2114	UN	40	51.85	N	147	3.95	E	GPS	-9	4763					1,3-6,30,82,102,103,106	18.5C
49NZ20140717	P01	50	1	ROS	072014	2220	BO	40	52.13	N	147	4.01	E	GPS	-9	4830	10	4685	4768	36	1-8,27,30,82,93,101-103,106	
49NZ20140717	P01	50	1	ROS	072114	0025	EN	40	53.26	N	147	3.86	E	GPS	-9	5001					FURUNO GPS	
49NZ20140717	P01	50	1	FLT	072114	0032	DE	40	53.39	N	147	4.03	E	GPS	-9	4998					ARGO S3A RINKO #7251	
49NZ20140717	P01	50	2	FLT	072114	0034	DE	40	53.39	N	147	4.08	E	GPS	-9	4998					ARGO S3A RINKO #7252	
49NZ20140717	P01	51	1	ROS	072114	0227	BE	40	37.64	N	147	12.70	E	GPS	-9	5289						
49NZ20140717	P01	51	1	BUC	072114	0236	UN	40	37.72	N	147	12.61	E	GPS	-9	5292						
49NZ20140717	P01	51	1	ROS	072114	0353	BO	40	38.11	N	147	12.30	E	GPS	-9	5302	10	5304	5382	35	1,3-6,20,31,33,43,102	18.9C
49NZ20140717	P01	51	1	ROS	072114	0608	EN	40	38.67	N	147	11.67	E	GPS	-9	5301					1-8,23,24,26,27,31,33,43,92,93,101,102	#4=#11 DUPL BTLS
49NZ20140717	P01	52	1	ROS	072114	0833	BE	40	22.97	N	147	22.78	E	GPS	-9	5278						
49NZ20140717	P01	52	1	BUC	072114	0842	UN	40	23.00	N	147	22.69	E	GPS	-9	5275					1,3-6,102	18.8C
49NZ20140717	P01	52	1	ROS	072114	0956	BO	40	23.39	N	147	21.93	E	GPS	-9	5279	9	5291	5365	34	1-8,27,93,101,102	#5=#12 DUPL BTLS
49NZ20140717	P01	52	1	ROS	072114	1214	EN	40	23.89	N	147	20.65	E	GPS	-9	5273						
49NZ20140717	P01	53	1	ROS	072114	1409	BE	40	8.01	N	147	33.45	E	GPS	-9	5294						
49NZ20140717	P01	53	1	BUC	072114	1417	UN	40	7.97	N	147	33.39	E	GPS	-9	5293						
49NZ20140717	P01	53	1	ROS	072114	1531	BO	40	7.87	N	147	33.00	E	GPS	-9	5293	9	5266	5381	35	1,3-6,102	18.3C
49NZ20140717	P01	53	1	ROS	072114	1748	EN	40	7.60	N	147	32.71	E	GPS	-9	5295					1-8,27,93,101,102	#4=#13 DUPL BTLS
49NZ20140717	P01	54	1	ROS	072114	1915	BE	39	56.81	N	147	42.83	E	GPS	-9	5234						
49NZ20140717	P01	54	1	BUC	072114	1923	UN	39	56.82	N	147	42.80	E	GPS	-9	5234						
49NZ20140717	P01	54	1	ROS	072114	1929	BO	39	56.83	N	147	42.79	E	GPS	-9	5236	-9	491	502	35	3-6,30-34,82,100-104,106-112	18.1C
49NZ20140717	P01	54	1	ROS	072114	2009	EN	39	56.83	N	147	42.62	E	GPS	-9	5238					3-6,30-34,82,100-104,106-113	FOR BGC
49NZ20140717	P01	54	1	BIO	072114	2024	BE	39	56.83	N	147	42.60	E	GPS	-9	5234						
49NZ20140717	P01	54	1	BIO	072114	2209	EN	39	56.87	N	147	41.82	E	GPS	-9	5234					NORPAC NET #1	
49NZ20140717	P01	54	2	ROS	072114	2228	BE	39	56.93	N	147	41.94	E	GPS	-9	5235						
49NZ20140717	P01	54	2	BUC	072114	2236	UN	39	56.93	N	147	41.91	E	GPS	-9	5235					1,3-6,20,30,31,33,102	18.4C
49NZ20140717	P01	54	2	ROS	072114	2348	BO	39	57.21	N	147	41.80	E	GPS	-9	5246	9	5224	5329	34	1-8,12,13,20,23,24,26,27,30,31,33,43,82,93,101-103,106	
49NZ20140717	P01	54	2	ROS	072214	0202	EN	39	57.38	N	147	41.96	E	GPS	-9	5249						

49NZ20140717	P01	55	1	ROS	072214	0421	BE	39	41.64	N	147	55.15	E	GPS	-9	5346						
49NZ20140717	P01	55	1	BUC	072214	0431	UN	39	41.64	N	147	55.11	E	GPS	-9	5346			1,3-6,102	19.3C		
49NZ20140717	P01	55	1	ROS	072214	0546	BO	39	41.58	N	147	54.82	E	GPS	-9	5343	10	5317	5439	35	1-8,27,93,102	#4=#14 DUPL BTLS
49NZ20140717	P01	55	1	ROS	072214	0801	EN	39	41.57	N	147	54.55	E	GPS	-9	5345						
49NZ20140717	P01	56	1	ROS	072214	1049	BE	40	1.24	N	148	24.15	E	GPS	-9	5459						
49NZ20140717	P01	56	1	BUC	072214	1057	UN	40	1.20	N	148	24.07	E	GPS	-9	5457				1,3-6,102	19.2C	
49NZ20140717	P01	56	1	ROS	072214	1216	BO	40	0.91	N	148	23.23	E	GPS	-9	5446	9	5480	5553	36	1-8,20,23,24,26,27,43,93,97,102	#3=#15 DUPL BTLS
49NZ20140717	P01	56	1	ROS	072214	1437	EN	40	0.44	N	148	22.44	E	GPS	-9	5426						
49NZ20140717	P01	57	1	ROS	072214	1724	BE	40	19.36	N	148	52.39	E	GPS	-9	5455						
49NZ20140717	P01	57	1	BUC	072214	1732	UN	40	19.42	N	148	52.33	E	GPS	-9	5462				1,3-6,102	19.3C	
49NZ20140717	P01	57	1	ROS	072214	1851	BO	40	19.50	N	148	52.23	E	GPS	-9	5458	11	5435	5558	36	1-8,27,93,102	#3=#16 DUPL BTLS
49NZ20140717	P01	57	1	ROS	072214	2109	EN	40	19.34	N	148	52.28	E	GPS	-9	5457						
49NZ20140717	P01	58	1	ROS	072214	2345	BE	40	37.45	N	149	22.79	E	GPS	-9	5344						
49NZ20140717	P01	58	1	BUC	072214	2353	UN	40	37.44	N	149	22.79	E	GPS	-9	5344				1,3-6,20,30,82,102,103	19.4C	
49NZ20140717	P01	58	1	ROS	072314	0109	BO	40	37.44	N	149	22.97	E	GPS	-9	5343	10	5333	5448	34	1-8,23,24,26,27,30,43,82,93,102,103	
49NZ20140717	P01	58	1	ROS	072314	0325	EN	40	37.17	N	149	23.77	E	GPS	-9	5302						
49NZ20140717	P01	59	1	ROS	072314	0552	BE	40	55.82	N	149	51.78	E	GPS	-9	5378						
49NZ20140717	P01	59	1	BUC	072314	0600	UN	40	55.86	N	149	51.79	E	GPS	-9	5373				1,3-6,102	20.5C	
49NZ20140717	P01	59	1	ROS	072314	0718	BO	40	55.74	N	149	51.92	E	GPS	-9	5374	10	5357	5470	35	1-8,27,93,102	#4=#17 DUPL BTLS
49NZ20140717	P01	59	1	ROS	072314	0930	EN	40	55.87	N	149	52.25	E	GPS	-9	5369						
49NZ20140717	P01	60	1	ROS	072314	1206	BE	41	15.85	N	150	21.70	E	GPS	-9	5383						
49NZ20140717	P01	60	1	BUC	072314	1215	UN	41	15.87	N	150	21.88	E	GPS	-9	5386				1,3-6,20,31,33,34,90,98,99,102	20.1C	
49NZ20140717	P01	60	1	ROS	072314	1334	BO	41	16.08	N	150	23.20	E	GPS	-9	5382	12	5501	5481	36	1-8,20,23,24,26,27,31,33,34,43,90,92,93,98,99,102	
49NZ20140717	P01	60	1	ROS	072314	1557	EN	41	17.22	N	150	24.97	E	GPS	-9	5123						
49NZ20140717	P01	61	1	ROS	072314	1814	BE	41	33.73	N	150	52.54	E	GPS	-9	5219						
49NZ20140717	P01	61	1	BUC	072314	1823	UN	41	33.74	N	150	52.61	E	GPS	-9	5213				1,3-6,102	19.1C	
49NZ20140717	P01	61	1	ROS	072314	1936	BO	41	33.65	N	150	53.04	E	GPS	-9	5210	10	5186	5298	34	1-8,27,93,102	#5=#18 DUPL BTLS
49NZ20140717	P01	61	1	ROS	072314	2150	EN	41	33.33	N	150	54.07	E	GPS	-9	5209						
49NZ20140717	P01	62	1	ROS	072414	0044	BE	41	56.36	N	151	28.26	E	GPS	-9	5162						
49NZ20140717	P01	62	1	BUC	072414	0052	UN	41	56.39	N	151	28.33	E	GPS	-9	5165				1,3-6,20,102	17.0C	
49NZ20140717	P01	62	1	ROS	072414	0205	BO	41	56.30	N	151	28.67	E	GPS	-9	5158	9	5136	5246	35	1-8,20,23,24,26,27,43,93,	#4=#19 DUPL BTLS
49NZ20140717	P01	62	1	ROS	072414	0415	EN	41	56.24	N	151	28.78	E	GPS	-9	5160						
49NZ20140717	P01	63	1	ROS	072414	0722	BE	42	19.83	N	152	5.47	E	GPS	-9	5121						
49NZ20140717	P01	63	1	BUC	072414	0731	UN	42	19.87	N	152	5.49	E	GPS	-9	5119				1,3-6,102	16.1C	
49NZ20140717	P01	63	1	ROS	072414	0843	BO	42	20.01	N	152	5.97	E	GPS	-9	5116	10	5116	5207	34	1-8,27,93	#5=#20 DUPL BTLS
49NZ20140717	P01	63	1	ROS	072414	1054	EN	42	19.92	N	152	7.11	E	GPS	-9	5127						
49NZ20140717	P01	64	1	ROS	072414	1338	BE	42	40.86	N	152	41.02	E	GPS	-9	5308						
49NZ20140717	P01	64	1	BUC	072414	1347	UN	42	40.87	N	152	41.09	E	GPS	-9	5307				1,3-6,20,31,33,102	16.7C	
49NZ20140717	P01	64	1	ROS	072414	1503	BO	42	40.67	N	152	41.39	E	GPS	-9	5305	11	5291	5401	35	1-8,20,23,24,26,27,31,33,43,93,102	#4=#21 DUPL BTLS
49NZ20140717	P01	64	1	ROS	072414	1717	EN	42	40.34	N	152	42.46	E	GPS	-9	5295						
49NZ20140717	P01	65	1	ROS	072414	2032	BE	43	4.87	N	153	19.41	E	GPS	-9	5160						
49NZ20140717	P01	65	1	BUC	072414	2039	UN	43	4.86	N	153	19.38	E	GPS	-9	5162				1,3-6,102	16.3C	
49NZ20140717	P01	65	1	ROS	072414	2150	BO	43	4.88	N	153	19.45	E	GPS	-9	5163	10	5139	5254	35	1-8,27,93,102	#4=#22 DUPL BTLS
49NZ20140717	P01	65	1	ROS	072414	2358	EN	43	4.86	N	153	19.50	E	GPS	-9	5166						
49NZ20140717	P01	66	1	ROS	072514	0357	BE	43	33.99	N	154	10.28	E	GPS	-9	5445						
49NZ20140717	P01	66	1	BUC	072514	0406	UN	43	33.97	N	154	10.34	E	GPS	-9	5446				1,3-6,20,102	15.6C	
49NZ20140717	P01	66	1	ROS	072514	0524	BO	43	33.98	N	154	10.67	E	GPS	-9	5437	10	5432	5547	35	1-8,20,23,24,26,27,43,93,102	#4=#23 DUPL BTLS
49NZ20140717	P01	66	1	ROS	072514	0732	EN	43	34.11	N	154	11.74	E	GPS	-9	5467						
49NZ20140717	P01	67	1	ROS	072514	1116	BE	44	4.88	N	154	58.94	E	GPS	-9	5349						
49NZ20140717	P01	67	1	ROS	072514	1136	BO	44	5.04	N	154	59.23	E	GPS	-9	5335	-9	837	833	36	22,89,91	FOR RN
49NZ20140717	P01	67	1	ROS	072514	1215	EN	44	5.15	N	154	59.69	E	GPS	-9	5324						
49NZ20140717	P01	67	1	BIO	072514	1227	BE	44	5.14	N	154	59.80	E	GPS	-9	5320					NORPAC NET #2	
49NZ20140717	P01	67	1	BIO	072514	1423	EN	44	5.27	N	155	0.50	E	GPS	-9	5316						
49NZ20140717	P01	67	2	ROS	072514	1433	BE	44	5.24	N	155	0.61	E	GPS	-9	5310						
49NZ20140717	P01	67	2	BUC	072514	1443	UN	44	5.25	N	155	0.67	E	GPS	-9	5307				1,3-6,20,22,31,33,34,82,89-91,98,99,102,103,106	16.1C	

49NZ20140717	P01	67	2	ROS	072514	1558	BO	44	5.16	N	155	0.92	E	GPS	-9	5308	9	5293	5405	36	1-8,12,13,20,23,24,26,27,34,43,82,90,92,93,98,99,102,103,106	STATION KNOT	
49NZ20140717	P01	67	2	ROS	072514	1810	EN	44	5.10	N	155	1.66	E	GPS	-9	5311							
49NZ20140717	P01	68	1	ROS	072514	2201	BE	44	34.57	N	155	47.80	E	GPS	-9	5140							
49NZ20140717	P01	68	1	BUC	072514	2209	UN	44	34.65	N	155	47.82	E	GPS	-9	5138					1,3-6,102		14.6C
49NZ20140717	P01	68	1	ROS	072514	2320	BO	44	35.05	N	155	47.55	E	GPS	-9	5146	9	5142	5233	35	1-8,27,93,102		#4=#24 DUPL BTLS
49NZ20140717	P01	68	1	ROS	072614	0130	EN	44	35.31	N	155	47.72	E	GPS	-9	5137							
49NZ20140717	P01	69	1	ROS	072614	0522	BE	45	4.40	N	156	38.28	E	GPS	-9	4768							
49NZ20140717	P01	69	1	BUC	072614	0530	UN	45	4.39	N	156	38.27	E	GPS	-9	4766					1,3-6,20,102		13.8C
49NZ20140717	P01	69	1	ROS	072614	0637	BO	45	4.28	N	156	38.27	E	GPS	-9	4783	9	4752	4853	33	1-8,20,23,24,26,27,43,102		#6=#25 DUPL BTLS
49NZ20140717	P01	69	1	ROS	072614	0833	EN	45	3.87	N	156	38.10	E	GPS	-9	4803							
49NZ20140717	P01	70	1	ROS	072614	1249	BE	45	33.71	N	157	28.96	E	GPS	-9	5031							
49NZ20140717	P01	70	1	BUC	072614	1259	UN	45	33.67	N	157	28.75	E	GPS	-9	5039					1,3-6,102		12.4C
49NZ20140717	P01	70	1	ROS	072614	1409	BO	45	33.64	N	157	28.07	E	GPS	-9	5038	8	5036	5128	33	1-6,27,93,102		#6=#26 DUPL BTLS
49NZ20140717	P01	70	1	ROS	072614	1618	EN	45	33.41	N	157	26.79	E	GPS	-9	5036							
49NZ20140717	P01	71	1	ROS	072614	2022	BE	46	3.94	N	158	19.56	E	GPS	-9	4838							
49NZ20140717	P01	71	1	BUC	072614	2035	UN	46	3.97	N	158	19.58	E	GPS	-9	4832					1,3-6,20,31,33,102		12.1C
49NZ20140717	P01	71	1	ROS	072614	2142	BO	46	4.22	N	158	19.68	E	GPS	-9	4837	10	4823	4916	33	1-8,20,23,24,26,27,31,33,43,93,102		#6=#27 DUPL BTLS
49NZ20140717	P01	71	1	ROS	072614	2343	EN	46	4.86	N	158	20.24	E	GPS	-9	4840							
49NZ20140717	P01	72	1	ROS	072714	0341	BE	46	33.36	N	159	13.66	E	GPS	-9	5126							
49NZ20140717	P01	72	1	BUC	072714	0349	UN	46	33.41	N	159	13.65	E	GPS	-9	5121					1,3-6,102		11.4C
49NZ20140717	P01	72	1	ROS	072714	0500	BO	46	33.54	N	159	13.69	E	GPS	-9	5109	10	5095	5205	34	1-8,27,93,102		#5=#25 DUPL BTLS
49NZ20140717	P01	72	1	ROS	072714	0702	EN	46	33.55	N	159	13.78	E	GPS	-9	5122							
49NZ20140717	P01	73	1	ROS	072714	1038	BE	47	0.46	N	160	1.25	E	GPS	-9	5195							OCEAN STATION K2
49NZ20140717	P01	73	1	BUC	072714	1046	UN	47	0.36	N	160	1.36	E	GPS	-9	5202					1,3-6,20,31,33,34,43,82,90,98,99,102		11.5C
49NZ20140717	P01	73	1	ROS	072714	1158	BO	47	0.56	N	160	1.31	E	GPS	-9	5197	8	5182	5292	36	1-8,12,13,20,23,24,26,27,31,33,34,43,82,90,92,98,99,102		
49NZ20140717	P01	73	1	ROS	072714	1409	EN	47	1.05	N	160	1.13	E	GPS	-9	5189							
49NZ20140717	P01	73	1	BIO	072714	1421	BE	47	1.11	N	160	1.11	E	GPS	-9	5188							NORPAC NET #3
49NZ20140717	P01	73	1	BIO	072714	1612	EN	47	1.79	N	160	0.73	E	GPS	-9	5189							
49NZ20140717	P01	73	2	ROS	072714	1623	BE	47	1.88	N	160	0.66	E	GPS	-9	5194							FOR RN
49NZ20140717	P01	73	2	ROS	072714	1642	BO	47	2.03	N	160	0.64	E	GPS	-9	5191	-9	821	831	36	22,89,91		
49NZ20140717	P01	73	2	ROS	072714	1721	EN	47	2.38	N	160	0.78	E	GPS	-9	5187							
49NZ20140717	P01	73	3	ROS	072714	1808	BE	47	0.64	N	160	1.13	E	GPS	-9	5188							FOR BGC
49NZ20140717	P01	73	3	ROS	072714	1821	BO	47	0.73	N	160	1.15	E	GPS	-9	5190	-9	525	534	34	3-6,30,31-34,82,100-104,106-113,		
49NZ20140717	P01	73	3	ROS	072714	1903	EN	47	0.96	N	160	1.30	E	GPS	-9	5187							
49NZ20140717	P01	73	4	ROS	072714	1957	BE	47	0.89	N	160	1.38	E	GPS	-9	5188							
																							FOR BIO, 12L CLEAN NISKIN x12 CTD/CWS
49NZ20140717	P01	73	4	ROS	072714	2001	BO	47	0.91	N	160	1.40	E	GPS	-9	5188	-9	46	50	12	64		
49NZ20140717	P01	73	4	ROS	072714	2007	EN	47	0.93	N	160	1.43	E	GPS	-9	5191							
49NZ20140717	P01	73	5	ROS	072714	2056	BE	47	0.58	N	160	1.40	E	GPS	-9	5194							FOR BIO, 12L CLEAN NISKIN x12 CTD/CWS
49NZ20140717	P01	73	5	ROS	072714	2100	BO	47	0.58	N	160	1.42	E	GPS	-9	5194	-9	46	51	12	64		
49NZ20140717	P01	73	5	ROS	072714	2106	EN	47	0.59	N	160	1.51	E	GPS	-9	5197							
49NZ20140717	P01	926	1	UNK	072814	0622	BE	46	58.22	N	161	26.64	E	GPS	-9	5657							
																							3-AXIS MAGNETMETER CALIBRATION
49NZ20140717	P01	926	1	UNK	072814	0649	EN	46	58.00	N	161	25.97	E	GPS	-9	5650							
49NZ20140717	P01	74	1	ROS	072814	2205	BE	46	59.97	N	161	9.28	E	GPS	-9	5429							
49NZ20140717	P01	74	1	BUC	072814	2214	UN	46	59.95	N	161	9.25	E	GPS	-9	5452					1,3-6,102		12.0C
49NZ20140717	P01	74	1	ROS	072814	2330	BO	46	59.98	N	161	8.93	E	GPS	-9	5459	11	5441	5561	36	1-8,27,93		#3=#29 DUPL BTLS
49NZ20140717	P01	74	1	ROS	072914	0142	EN	47	0.08	N	161	7.79	E	GPS	-9	5281							
49NZ20140717	P01	75	1	ROS	072914	0548	BE	46	59.48	N	162	15.42	E	GPS	-9	5651							
49NZ20140717	P01	75	1	BUC	072914	0602	UN	46	59.44	N	162	15.28	E	GPS	-9	5645					1,3-6,20,31,33,102		12.1C
49NZ20140717	P01	75	1	ROS	072914	0714	BO	46	59.14	N	162	14.97	E	GPS	-9	5626	10	5626	5741	36	1-8,20,23,24,26,27,31,33,43,93,97,102		#3=#30 DUPL BTLS

49NZ20140717	P01	87	1	BUC	080114	0956	UN	46	58.97	N	169	59.74	E	GPS	-9	4921					1,3-6,20,31,33,34,90,98,99,102	12.1C	
49NZ20140717	P01	87	1	ROS	080114	1106	BO	46	58.86	N	169	59.75	E	GPS	-9	4923	9	4901	5006	36	1-8,20,23,24,26,27,31,33,34,43,90,93,98,99,102,106		
49NZ20140717	P01	87	1	ROS	080114	1307	EN	46	58.59	N	169	59.85	E	GPS	-9	4946							
49NZ20140717	P01	88	1	ROS	080114	1502	BE	46	59.77	N	170	28.22	E	GPS	-9	6335							
49NZ20140717	P01	88	1	BUC	080114	1510	UN	46	59.78	N	170	28.29	E	GPS	-9	6336						1,3-6,102	12.1C
49NZ20140717	P01	88	1	ROS	080114	1634	BO	46	59.69	N	170	28.48	E	GPS	-9	6334	63	5996	6137	36	1-8,27,93,102	LADCP SOUNDING	
49NZ20140717	P01	88	1	ROS	080114	1905	EN	46	59.49	N	170	28.43	E	GPS	-9	6335							
49NZ20140717	P01	89	1	ROS	080114	2253	BE	47	0.10	N	171	36.80	E	GPS	-9	6060							
49NZ20140717	P01	89	1	BUC	080114	2301	UN	47	0.06	N	171	36.82	E	GPS	-9	6049						1,3-6,20,102	12.2C
49NZ20140717	P01	89	1	ROS	080214	0024	BO	46	59.91	N	171	37.05	E	GPS	-9	6022	23	6004	6138	36	1-8,20,23,24,26,27,43,93,97,102		
49NZ20140717	P01	89	1	ROS	080214	0248	EN	46	59.81	N	171	37.22	E	GPS	-9	6027							
49NZ20140717	P01	90	1	ROS	080214	0641	BE	46	59.98	N	172	43.04	E	GPS	-9	5626							
49NZ20140717	P01	90	1	BUC	080214	0649	UN	47	0.04	N	172	43.05	E	GPS	-9	5615						1,3-8,102	12.5C
49NZ20140717	P01	90	1	ROS	080214	0809	BO	47	0.20	N	172	43.23	E	GPS	-9	5606	10	5596	5719	36	1-8,27,93,102	#3=#34 DUPL BTLS	
49NZ20140717	P01	90	1	ROS	080214	1029	EN	47	0.12	N	172	43.86	E	GPS	-9	5632							
49NZ20140717	P01	91	1	ROS	080214	1415	BE	47	0.34	N	173	49.54	E	GPS	-9	5807							
49NZ20140717	P01	91	1	ROS	080214	1431	BO	47	0.35	N	173	49.54	E	GPS	-9	5813	-9	523	531	36	3-6,30-34,82,100-104,106-113	FOR BGC	
49NZ20140717	P01	91	1	ROS	080214	1512	EN	47	0.32	N	173	49.65	E	GPS	-9	5809							
49NZ20140717	P01	91	1	BIO	080214	1522	BE	47	0.31	N	173	49.70	E	GPS	-9	5807							
49NZ20140717	P01	91	1	BIO	080214	1712	EN	47	0.35	N	173	50.20	E	GPS	-9	5713						NORPAC NET #4	
49NZ20140717	P01	91	2	ROS	080214	1723	BE	47	0.33	N	173	50.28	E	GPS	-9	5715							
49NZ20140717	P01	91	2	ROS	080214	1743	BO	47	0.34	N	173	50.41	E	GPS	-9	5712	-9	820	831	36	22,89,91	FOR RN	
49NZ20140717	P01	91	2	ROS	080214	1819	EN	47	0.26	N	173	50.60	E	GPS	-9	5723							
49NZ20140717	P01	91	3	ROS	080214	1906	BE	47	0.32	N	173	49.81	E	GPS	-9	5804							
49NZ20140717	P01	91	3	BUC	080214	1915	UN	47	0.30	N	173	49.85	E	GPS	-9	5803						1,3-6,20,31,33,102,106	12.1C
49NZ20140717	P01	91	3	ROS	080214	2037	BO	47	0.35	N	173	50.02	E	GPS	-9	5784	10	5775	5910	36	1-8,12,13,20,23,24,26,27,31,33,43,93,102,106		
49NZ20140717	P01	91	3	ROS	080214	2255	EN	47	0.27	N	173	50.46	E	GPS	-9	5734							
49NZ20140717	P01	92	1	ROS	080314	0245	BE	47	0.31	N	174	57.70	E	GPS	-9	5676							
49NZ20140717	P01	92	1	BUC	080314	0254	UN	47	0.30	N	174	57.77	E	GPS	-9	5674						1,3-6,102	12.0C
49NZ20140717	P01	92	1	ROS	080314	0413	BO	47	0.31	N	174	58.01	E	GPS	-9	5680	10	5648	5779	36	1-8,27,93,102		
49NZ20140717	P01	92	1	ROS	080314	0635	EN	47	0.25	N	174	57.97	E	GPS	-9	5672							
49NZ20140717	P01	93	1	ROS	080314	1038	BE	46	59.76	N	176	5.54	E	GPS	-9	5691							
49NZ20140717	P01	93	1	BUC	080314	1045	UN	46	59.76	N	176	5.52	E	GPS	-9	5692						1,3-6,20,31,33,34,98,99,102	12.1C
49NZ20140717	P01	93	1	ROS	080314	1205	BO	46	59.81	N	176	5.64	E	GPS	-9	5693	10	5669	5803	35	1-8,20,23,24,26,27,31,33,34,43,93,98,99,102		
49NZ20140717	P01	93	1	ROS	080314	1427	EN	46	59.96	N	176	6.31	E	GPS	-9	5694							
49NZ20140717	P01	94	1	ROS	080314	1804	BE	46	59.73	N	177	10.73	E	GPS	-9	5680							
49NZ20140717	P01	94	1	BUC	080314	1815	UN	46	59.71	N	177	10.82	E	GPS	-9	5677						1,3-6,102	12.0C
49NZ20140717	P01	94	1	ROS	080314	1933	BO	46	59.60	N	177	11.39	E	GPS	-9	5683	10	5669	5786	36	1-8,27,93,102	#3=#35 DUPL BTLS	
49NZ20140717	P01	94	1	ROS	080314	2154	EN	46	59.40	N	177	11.90	E	GPS	-9	5697							
49NZ20140717	P01	95	1	ROS	080414	0137	BE	46	59.95	N	178	17.52	E	GPS	-9	5752							
49NZ20140717	P01	95	1	BUC	080414	0146	UN	46	59.95	N	178	17.60	E	GPS	-9	5750						1,3-6,20,31,33,102	13.4C
49NZ20140717	P01	95	1	ROS	080414	0307	BO	46	59.84	N	178	18.28	E	GPS	-9	5760	10	5754	5865	36	1-8,20,23,24,26,27,31,33,43,92,102		
49NZ20140717	P01	95	1	ROS	080414	0532	EN	46	59.17	N	178	18.82	E	GPS	-9	5733							
49NZ20140717	P01	96	1	ROS	080414	0926	BE	47	0.66	N	179	26.76	E	GPS	-9	5619							
49NZ20140717	P01	96	1	BUC	080414	0933	UN	47	0.67	N	179	26.78	E	GPS	-9	5611						1,3-8,102	12.2C
49NZ20140717	P01	96	1	ROS	080414	1051	BO	47	0.65	N	179	26.96	E	GPS	-9	5640	11	5600	5729	36	1-8,27,93,102	#3=#36 DUPL BTLS	
49NZ20140717	P01	96	1	ROS	080414	1310	EN	47	0.56	N	179	27.24	E	GPS	-9	5678							
49NZ20140717	P01	97	1	ROS	080414	1656	BE	46	59.58	N	179	25.73	W	GPS	-9	5720							
49NZ20140717	P01	97	1	BUC	080414	1704	UN	46	59.52	N	179	25.72	W	GPS	-9	5720						1,3-6,20,30,31,33,34,82,98-100,102-104,106	13.4C
49NZ20140717	P01	97	1	ROS	080414	1825	BO	46	59.15	N	179	25.58	W	GPS	-9	5740	10	5724	5846	36	1-8,20,23,24,26,27,30,31,33,34,43,82,93,98-100,102-104,106		
49NZ20140717	P01	97	1	ROS	080414	2048	EN	46	58.90	N	179	25.35	W	GPS	-9	5742							
49NZ20140717	P01	98	1	ROS	080514	0038	BE	46	59.88	N	178	18.42	W	GPS	-9	5500							
49NZ20140717	P01	98	1	BUC	080514	0047	UN	46	59.88	N	178	18.42	W	GPS	-9	5503						1,3-8,20,90,102	12.8C
49NZ20140717	P01	98	1	ROS	080514	0204	BO	46	59.90	N	178	18.08	W	GPS	-9	5494	9	5484	5603	35	1-8,20,23,24,26,27,43,90,93,97,102		
49NZ20140717	P01	98	1	ROS	080514	0421	EN	46	59.67	N	178	17.47	W	GPS	-9	5576							

49NZ20140717	P01	99	1	ROS	080514	0804	BE	46	59.97	N	177	12.87	W	GPS	-9	5719					
49NZ20140717	P01	99	1	BUC	080514	0811	UN	46	59.96	N	177	12.85	W	GPS	-9	5717			1,3-6,20,31,33,102	13.2C	
49NZ20140717	P01	99	1	ROS	080514	0930	BO	46	59.83	N	177	12.87	W	GPS	-9	5710	9	5687	5820	36	1-8,20,23,24,26,27,31,33,43,93,102
49NZ20140717	P01	99	1	ROS	080514	1153	EN	46	59.64	N	177	12.90	W	GPS	-9	5698					
49NZ20140717	P01	99	1	FLT	080514	1201	DE	46	59.77	N	177	12.61	W	GPS	-9	5688					ARGO NAVIS #F0349
49NZ20140717	P01	100	1	ROS	080514	1553	BE	47	0.80	N	176	2.67	W	GPS	-9	5632					
49NZ20140717	P01	100	1	BUC	080514	1601	UN	47	0.78	N	176	2.60	W	GPS	-9	5632				1,3-6,102	12.4C
49NZ20140717	P01	100	1	ROS	080514	1720	BO	47	0.63	N	176	2.25	W	GPS	-9	5628	9	5612	5740	35	1-8,27,93,102
49NZ20140717	P01	100	1	ROS	080514	1941	EN	47	0.51	N	176	1.84	W	GPS	-9	5627					
49NZ20140717	P01	101	1	ROS	080514	2318	BE	47	0.32	N	174	57.29	W	GPS	-9	5788					FOR BGC
49NZ20140717	P01	101	1	ROS	080514	2331	BO	47	0.28	N	174	57.30	W	GPS	-9	5790	-9	465	472	36	3-6,30-34,82,100-104,106-113
49NZ20140717	P01	101	1	ROS	080614	0010	EN	47	0.22	N	174	57.21	W	GPS	-9	5788					
49NZ20140717	P01	101	1	BIO	080614	0026	BE	47	0.21	N	174	57.22	W	GPS	-9	5793					NORPAC NET #5
49NZ20140717	P01	101	1	BIO	080614	0207	EN	46	59.92	N	174	57.07	W	GPS	-9	5795					
49NZ20140717	P01	101	2	ROS	080614	0219	BE	46	59.92	N	174	57.06	W	GPS	-9	5797					FOR RN
49NZ20140717	P01	101	2	ROS	080614	0237	BO	46	59.87	N	174	57.03	W	GPS	-9	5792	-9	760	770	36	22,89,91
49NZ20140717	P01	101	2	ROS	080614	0312	EN	46	59.80	N	174	56.95	W	GPS	-9	5794					
49NZ20140717	P01	101	3	ROS	080614	0404	BE	47	0.29	N	174	57.36	W	GPS	-9	5786					
49NZ20140717	P01	101	3	BUC	080614	0410	UN	47	0.29	N	174	57.33	W	GPS	-9	5787				1,3-6,20,31,33,34,98,99,102	13.3C
49NZ20140717	P01	101	3	ROS	080614	0530	BO	47	0.14	N	174	57.24	W	GPS	-9	5796	11	5769	5901	36	1-8,12,13,20,23,24,26,27,31,33,34,43,92,98,99,102
49NZ20140717	P01	101	3	ROS	080614	0758	EN	46	59.96	N	174	57.02	W	GPS	-9	5787					
49NZ20140717	P01	927	1	UNK	080614	0809	BE	46	59.75	N	174	56.22	W	GPS	-9	5791					

3-AXIS MAGNETMETER CALIBRATION

49NZ20140717	P01	927	1	UNK	080614	0838	EN	46	59.74	N	174	55.80	W	GPS	-9	5784					
49NZ20140717	P01	102	1	ROS	080714	0902	BE	46	60.00	N	173	47.60	W	GPS	-9	5723					
49NZ20140717	P01	102	1	BUC	080714	0912	UN	46	59.93	N	173	47.45	W	GPS	-9	5728				1,3-6,102	12.9C
49NZ20140717	P01	102	1	ROS	080714	1030	BO	46	59.59	N	173	47.16	W	GPS	-9	5724	8	5710	5835	36	1-8,27,93,102
49NZ20140717	P01	102	1	ROS	080714	1253	EN	46	59.21	N	173	46.97	W	GPS	-9	5574					
49NZ20140717	P01	103	1	ROS	080714	1635	BE	46	59.61	N	172	42.37	W	GPS	-9	5786					
49NZ20140717	P01	103	1	BUC	080714	1644	UN	46	59.56	N	172	42.37	W	GPS	-9	5789				1,3-6,20,31,33,90,102	13.2C
49NZ20140717	P01	103	1	ROS	080714	1805	BO	46	59.35	N	172	42.26	W	GPS	-9	5795	10	5771	5907	36	1-8,20,23,24,26,27,31,33,43,90,93,102
49NZ20140717	P01	103	1	ROS	080714	2028	EN	46	59.11	N	172	42.03	W	GPS	-9	5802					
49NZ20140717	P01	104	1	ROS	080814	0027	BE	47	0.56	N	171	33.54	W	GPS	-9	5712					
49NZ20140717	P01	104	1	BUC	080814	0037	UN	47	0.56	N	171	33.55	W	GPS	-9	5726				1,3-6,102	13.3C
49NZ20140717	P01	104	1	ROS	080814	0156	BO	47	0.50	N	171	33.55	W	GPS	-9	5731	10	5695	5830	36	1-8,27,93,102
49NZ20140717	P01	104	1	ROS	080814	0420	EN	47	0.30	N	171	33.26	W	GPS	-9	5764					
49NZ20140717	P01	105	1	ROS	080814	0810	BE	46	59.91	N	170	25.60	W	GPS	-9	5500					
49NZ20140717	P01	105	1	BUC	080814	0819	UN	46	59.88	N	170	25.58	W	GPS	-9	5448				1,3-8,20,30,31,33,34,82,98,99,102,103,106	13.1C
49NZ20140717	P01	105	1	ROS	080814	0933	BO	46	59.73	N	170	25.49	W	GPS	-9	5407	10	5406	5530	36	1-8,20,23,24,26,27,30,31,33,34,43,82,93,98,99,102,103,106
49NZ20140717	P01	105	1	ROS	080814	1145	EN	46	59.21	N	170	25.54	W	GPS	-9	5532					
49NZ20140717	P01	106	1	ROS	080814	1533	BE	46	59.61	N	169	20.63	W	GPS	-9	5617					
49NZ20140717	P01	106	1	BUC	080814	1541	UN	46	59.49	N	169	20.64	W	GPS	-9	5613				1,3-6,102	13.1C
49NZ20140717	P01	106	1	ROS	080814	1701	BO	46	59.43	N	169	20.66	W	GPS	-9	5617	10	5595	5725	36	1-8,27,93,102
49NZ20140717	P01	106	1	ROS	080814	1920	EN	46	59.07	N	169	20.65	W	GPS	-9	5622					
49NZ20140717	P01	106	1	FLT	080814	1927	DE	46	59.16	N	169	20.58	W	GPS	-9	5619					ARGO NAVIS #F0350
49NZ20140717	P01	107	1	ROS	080814	2321	BE	46	59.91	N	168	12.71	W	GPS	-9	5408					
49NZ20140717	P01	107	1	BUC	080814	2330	UN	46	59.89	N	168	12.69	W	GPS	-9	5402				1,3-6,20,31,33,102	13.1C
49NZ20140717	P01	107	1	ROS	080914	0045	BO	46	59.72	N	168	12.53	W	GPS	-9	5395	8	5378	5503	36	1-8,20,23,24,26,27,31,33,43,93,97,102
49NZ20140717	P01	107	1	ROS	080914	0300	EN	46	58.80	N	168	12.37	W	GPS	-9	5377					
49NZ20140717	P01	108	1	ROS	080914	0657	BE	46	59.96	N	167	4.92	W	GPS	-9	5428					
49NZ20140717	P01	108	1	BUC	080914	0705	UN	46	59.90	N	167	4.92	W	GPS	-9	5419				1,3-6,102	12.7C
49NZ20140717	P01	108	1	ROS	080914	0820	BO	46	59.79	N	167	5.05	W	GPS	-9	5425	10	5401	5522	34	1-8,27,93,102
49NZ20140717	P01	108	1	ROS	080914	1031	EN	46	59.66	N	167	5.06	W	GPS	-9	5425					
49NZ20140717	P01	109	1	ROS	080914	1429	BE	47	0.58	N	165	58.93	W	GPS	-9	5338					

49NZ20140717	P01	128	1	BIO	081614	0126	EN	46	54.42	N	144	26.17	W	GPS	-9	4677
49NZ20140717	P01	128	2	ROS	081614	0138	BE	46	54.41	N	144	26.14	W	GPS	-9	4677
49NZ20140717	P01	128	2	ROS	081614	0155	BO	46	54.40	N	144	26.06	W	GPS	-9	4674
49NZ20140717	P01	128	2	ROS	081614	0229	EN	46	54.34	N	144	26.02	W	GPS	-9	4672
49NZ20140717	P01	928	1	UNK	081614	0236	BE	46	54.17	N	144	26.20	W	GPS	-9	4678

FOR RN

-9 760 771 36 22,89,91

3-AXIS MAGNETMETER CALIBRATION

49NZ20140717	P01	928	1	UNK	081614	0310	EN	46	54.20	N	144	25.92	W	GPS	-9	4672
49NZ20140717	P01	128	3	ROS	081614	0322	BE	46	53.93	N	144	25.98	W	GPS	-9	4675
49NZ20140717	P01	128	3	ROS	081614	0334	BO	46	53.88	N	144	25.82	W	GPS	-9	4679
49NZ20140717	P01	128	3	ROS	081614	0415	EN	46	53.73	N	144	25.54	W	GPS	-9	4674
49NZ20140717	PAPA	151	1	ROS	081614	1912	BE	49	59.87	N	144	59.70	W	GPS	-9	4256
49NZ20140717	PAPA	151	1	BUC	081614	1921	UN	49	59.83	N	144	59.55	W	GPS	-9	4256
49NZ20140717	PAPA	151	1	ROS	081614	2020	BO	49	59.70	N	144	59.14	W	GPS	-9	4253
49NZ20140717	PAPA	151	1	ROS	081614	2208	EN	49	59.48	N	144	58.96	W	GPS	-9	4255
49NZ20140717	PAPA	151	1	BIO	081614	2219	BE	49	59.43	N	144	58.91	W	GPS	-9	4256
49NZ20140717	PAPA	151	1	BIO	081714	0009	EN	49	59.39	N	144	58.40	W	GPS	-9	4258
49NZ20140717	P01	129	1	ROS	081714	1701	BE	47	0.86	N	143	29.76	W	GPS	-9	4598
49NZ20140717	P01	129	1	BUC	081714	1710	UN	47	0.83	N	143	29.73	W	GPS	-9	4596
49NZ20140717	P01	129	1	ROS	081714	1813	BO	47	0.78	N	143	29.57	W	GPS	-9	4598
49NZ20140717	P01	129	1	ROS	081714	2007	EN	47	0.80	N	143	29.45	W	GPS	-9	4593
49NZ20140717	P01	130	1	ROS	081714	2346	BE	47	0.48	N	142	26.29	W	GPS	-9	4504
49NZ20140717	P01	130	1	BUC	081714	2355	UN	47	0.49	N	142	26.24	W	GPS	-9	4500
49NZ20140717	P01	130	1	ROS	081814	0057	BO	47	0.41	N	142	26.08	W	GPS	-9	4501
49NZ20140717	P01	130	1	ROS	081814	0254	EN	47	0.23	N	142	25.59	W	GPS	-9	4505
49NZ20140717	P01	131	1	ROS	081814	0634	BE	46	59.30	N	141	21.22	W	GPS	-9	4412
49NZ20140717	P01	131	1	BUC	081814	0643	UN	46	59.26	N	141	21.14	W	GPS	-9	4412
49NZ20140717	P01	131	1	ROS	081814	0744	BO	46	59.27	N	141	21.15	W	GPS	-9	4416
49NZ20140717	P01	131	1	ROS	081814	0942	EN	46	59.24	N	141	21.11	W	GPS	-9	4412
49NZ20140717	P01	132	1	ROS	081814	1339	BE	47	1.57	N	140	13.65	W	GPS	-9	4336
49NZ20140717	P01	132	1	BUC	081814	1347	UN	47	1.58	N	140	13.65	W	GPS	-9	4336
49NZ20140717	P01	132	1	ROS	081814	1448	BO	47	1.66	N	140	13.58	W	GPS	-9	4333
49NZ20140717	P01	132	1	ROS	081814	1635	EN	47	1.67	N	140	13.46	W	GPS	-9	4332
49NZ20140717	P01	133	1	ROS	081814	2027	BE	46	59.66	N	139	3.91	W	GPS	-9	4231
49NZ20140717	P01	133	1	BUC	081814	2035	UN	46	59.62	N	139	3.84	W	GPS	-9	4231
49NZ20140717	P01	133	1	ROS	081814	2134	BO	46	59.57	N	139	3.76	W	GPS	-9	4230
49NZ20140717	P01	133	1	ROS	081814	2320	EN	46	59.28	N	139	3.56	W	GPS	-9	4232
49NZ20140717	P01	134	1	ROS	081914	0300	BE	46	59.58	N	137	57.93	W	GPS	-9	4172
49NZ20140717	P01	134	1	BUC	081914	0308	UN	46	59.51	N	137	57.81	W	GPS	-9	4171
49NZ20140717	P01	134	1	ROS	081914	0407	BO	46	59.46	N	137	57.78	W	GPS	-9	4171
49NZ20140717	P01	134	1	ROS	081914	0557	EN	46	59.19	N	137	57.77	W	GPS	-9	4174
49NZ20140717	P01	135	1	ROS	081914	0946	BE	46	59.57	N	136	51.36	W	GPS	-9	4177
49NZ20140717	P01	135	1	BUC	081914	0955	UN	46	59.55	N	136	51.33	W	GPS	-9	4175
49NZ20140717	P01	135	1	ROS	081914	1053	BO	46	59.53	N	136	51.25	W	GPS	-9	4176
49NZ20140717	P01	135	1	ROS	081914	1242	EN	46	59.51	N	136	51.21	W	GPS	-9	4174
49NZ20140717	P01	136	1	ROS	081914	1630	BE	47	0.02	N	135	44.00	W	GPS	-9	4141
49NZ20140717	P01	136	1	ROS	081914	1649	BO	46	59.92	N	135	43.96	W	GPS	-9	4143
49NZ20140717	P01	136	1	ROS	081914	1723	EN	46	59.78	N	135	43.96	W	GPS	-9	4143
49NZ20140717	P01	136	2	ROS	081914	1808	BE	46	60.00	N	135	44.13	W	GPS	-9	4141
49NZ20140717	P01	136	2	BUC	081914	1817	UN	46	59.95	N	135	44.12	W	GPS	-9	4142
49NZ20140717	P01	136	2	ROS	081914	1916	BO	46	59.80	N	135	44.16	W	GPS	-9	4143
49NZ20140717	P01	136	2	ROS	081914	2104	EN	46	59.62	N	135	44.17	W	GPS	-9	4148
49NZ20140717	P01	137	1	ROS	082014	0058	BE	47	1.24	N	134	37.10	W	GPS	-9	3998
49NZ20140717	P01	137	1	BUC	082014	0106	UN	47	1.22	N	134	37.12	W	GPS	-9	3996
49NZ20140717	P01	137	1	ROS	082014	0201	BO	47	1.17	N	134	37.12	W	GPS	-9	3997

FOR BGC

-9 464 473 36 3-6,30-34,82,100-104,106-113

OCEAN STATION PAPA
14.5C

1,3-6,20,31,33,34,98,99,102
9 4238 4317 30 1-8,20,23,24,26,27,31,33,34,43,92,93,98,99,102

NORPAC NET #8

1,3-6,102
8 4571 4667 31 1-8,27,102

16.5C

1,3-6,20,31,33,102
10 4484 4574 30 1-8,20,23,24,26,27,31,33,43,93,102

16.9C

1,3-6,102
9 4389 4480 31 1-8,27,93,102

17.5C

1,3-6,20,31,33,34,90,98,99,102,106
9 4309 4399 32 1-8,20,23,24,26,27,31,33,34,43,90,98,99,102,106

17.4C

1,3-6,102
10 4209 4293 29 1-8,27,93,102

17.7C

1,3-6,20,31,33,102
10 4151 4235 30 1-8,20,23,24,26,27,31,33,43,93,97,102

18.0C

1,3-6,102
10 4154 4237 29 1-8,27,93,102

18.3C

FOR RN

-9 819 831 36 22,89,91

1,3-6,20,30,82,102-104,106
9 4123 4203 35 1-8,12,13,20,23,24,26,27,30,43,82,92,93,100,102-104,106

17.8C

1,3-6,102
10 3973 4052 29 1-8,27,93,102

18.2C

49NZ20140717	P01	148	1	ROS	082214	1516	BO	47	0.12	N	125	30.73	W	GPS	-9	1752	10	1732	1756	18	1-8,20,23,24,26,27,43,92,93,102	
49NZ20140717	P01	148	1	ROS	082214	1618	EN	47	0.02	N	125	30.60	W	GPS	-9	1752						
49NZ20140717	P01	149	1	ROS	082214	1801	BE	46	59.94	N	125	3.52	W	GPS	-9	999						
49NZ20140717	P01	149	1	BUC	082214	1808	UN	46	59.93	N	125	3.55	W	GPS	-9	1009					1,3-6,20,31,33,34,43,98,99,102	16.3C
49NZ20140717	P01	149	1	ROS	082214	1829	BO	46	59.89	N	125	3.62	W	GPS	-9	1049	31	1012	1026	17	1-8,20,23,24,26,27,31,33,34,43,98,99,102	LADCP SOUNDING
49NZ20140717	P01	149	1	ROS	082214	1915	EN	46	59.79	N	125	3.73	W	GPS	-9	1080						
49NZ20140717	P01	150	1	ROS	082214	2051	BE	46	56.31	N	124	59.05	W	GPS	-9	283						
49NZ20140717	P01	150	1	BUC	082214	2053	UN	46	56.30	N	124	59.05	W	GPS	-9	284					1,3-6,20,90,102	16.1C
49NZ20140717	P01	150	1	ROS	082214	2101	BO	46	56.31	N	124	59.04	W	GPS	-9	281	13	289	294	7	1-8,20,23,24,26,27,43,90,102	
49NZ20140717	P01	150	1	ROS	082214	2119	EN	46	56.30	N	124	59.04	W	GPS	-9	283						
49NZ20140717		930	1	UNK	082414	2259	BE	51	3.65	N	138	32.35	W	GPS	-9	3249						
																						3-AXIS MAGNETMETER CALIBRATION
49NZ20140717		930	1	UNK	082414	2324	EN	51	3.81	N	138	32.85	W	GPS	-9	3082						

Water sample parameters:

Number	Parameter	Mnemonic	Mnemonic for expected error
1	Salinity	SALNTY	
2	Oxygen	OXYGEN	
3	Silicate	SILCAT	SILUNC *1
4	Nitrate	NITRAT	NRAUNC *1
5	Nitrite	NITRIT	NRIUNC *1
6	Phosphate	PHSPHT	PHPUNC *1
7	Freon-11	CFC-11	
8	Freon-12	CFC-12	
9	Tritium		
10	Helium		
11	He-3/He-4		
12	14Carbon	DELC14	C14ERR
13	13Carbon	DELC13	C13ERR
14	Kr-85		
15	Argon		
16	Ar-39		
17	Neon		
18	Ra-228		
19	Ra-226		
20	Ratio of O18 to O16	O18/O16	
21	Sr-90		
22	Cesium-137	CS-137	CS137ER *2
23	Total carbon	TCARBN	
24	Total alkalinity	ALKALI	
25	pCO2		
26	pH	PH	
27	Freon-113	CFC113	
28	Carbon tetrachloride	CCL4	
29	Iodate/Iodide		
30	Ammonium	NH4	
31	Methane	CH4	
32	Dissolved organic nitrogen	DON	
33	Nitrous oxide	N2O	
34	Chlorophyll-a	CHLORA	
35	Pheophytin		
36	Halocarbons		
37	Biogenic sulfur compounds	DMS	
38	Hydrocarbons		
39	Barium		
40	Particulate organic carbon	POC	
41	Particulate organic nitrogen	PON	
42	Abundance of bacteria	BACT	
43	Dissolved organic carbon	DOC	
44	Carbon monoxide		

Number	Parameter	Mnemonic	Mnemonic for expected error
45	Nitrogen (gas)		
46	Total organic carbon	TOC	
47	Plutonium	PLUTO	PLUTOER *2
48	Primary productivity		
64	Incubation		
81	Particulate organic matter	POM	
82	15N-Nitrate	15NO3	
83	Particulate inorganic matter	PIM	
84	Dissolved organic phosphate		
85	Ratio of O-17 to O-16	O17/O16	
86	Flowcytometry		
87	Genetic analysis		
88	Nitrogen fixation		
89	Cesium-134	CS-134	CS134ER
90	Perfluoroalkyl substances	PFAS	
91	Iodine-129	I-129	
92	Density salinity	DNSSAL	
93	Sulfur hexafluoride	SF6	
94	Isoprene		
95	Pigment		
96	Microscope		
97	Calcium		
98	Colored dissolved organic matter	CDOM	
99	Absorption coefficients of particulate matter	AP	
100	Nitrification		
101	13C-CH4		
102	Prokaryotic abundance		
103	Fluorescence in situ hybridization		
104	Prokaryotic activity		
105	Viral production		
106	Microbial diversity		
107	N2O 15N-isotope		
108	Nitrogen fixation		
109	NH4 15N-isotope		
110	Urea		
111	NO2 15N-isotope		
112	Coenzyme F430		
113	Chlorophyll 15N-isotope		

Figure captions

- Figure 1 Station locations for (a) WHP P10N and (b) WHP P01 revisit in 2014 cruise with bottom topography.
- Figure 2 Bathymetry measured by Multi Narrow Beam Echo Sounding system.
- Figure 3 Surface wind measured at 25 m above sea level. Wind data is averaged over 6-hour.
- Figure 4 (a) Sea surface temperature ($^{\circ}\text{C}$), (b) sea surface salinity (psu), (c) sea surface oxygen ($\mu\text{mol}/\text{kg}$), and (d) sea surface chlorophyll a (mg/m^3) measured by the Continuous Sea Surface Water Monitoring System.
- Figure 5 Difference in the partial pressure of CO_2 between the ocean and the atmosphere, $\Delta p\text{CO}_2$.
- Figure 6 Surface current at 100 m depth measured by ship board acoustic Doppler current profiler (ADCP).
- Figure 7 Potential temperature ($^{\circ}\text{C}$) cross sections calculated by using CTD temperature and salinity data calibrated by bottle salinity measurements. Vertical exaggeration of the 0-6500 m section is 1000:1, and expanded section of the upper 1000 m is made with a vertical exaggeration of 2500:1.
- Figure 8 CTD salinity (psu) cross sections calibrated by bottle salinity measurements. Vertical exaggeration is same as Fig. 7.
- Figure 9 Absolute salinity (g/kg) cross sections calculated by using CTD salinity data. Vertical exaggeration is same as Fig. 7.
- Figure 10 Density (upper: σ_0 , lower: σ_t) (kg/m^3) cross sections calculated by using CTD temperature and salinity data. Vertical exaggeration of the 0-1500 m and 1500-6500 m section are 2500:1 and 1000:1, respectively. (a) EOS-80 and (b) TEOS-10 definition.
- Figure 11 Neutral density (γ^n) (kg/m^3) cross sections calculated by using CTD temperature and salinity data. Vertical exaggeration is same as Fig. 7.
- Figure 12 CTD oxygen ($\mu\text{mol}/\text{kg}$) cross sections. Vertical exaggeration is same as Fig. 7.
- Figure 13 CTD chlorophyll a (mg/m^3) cross section. Vertical exaggeration of the upper 1000 m section is same as Fig. 7.
- Figure 14 CTD beam attenuation coefficient (m^{-1}) cross sections. Vertical exaggeration is same as Fig. 7.
- Figure 15 Bottle sampled dissolved oxygen ($\mu\text{mol}/\text{kg}$) cross sections. Data with quality flags of 2 were plotted. Vertical exaggeration is same as Fig. 7.
- Figure 16 Silicate ($\mu\text{mol}/\text{kg}$) cross sections. Data with quality flags of 2 were plotted. Vertical exaggeration is same as Fig. 7.
- Figure 17 Nitrate ($\mu\text{mol}/\text{kg}$) cross sections. Data with quality flags of 2 were plotted. Vertical exaggeration is same as Fig. 7.
- Figure 18 Nitrite ($\mu\text{mol}/\text{kg}$) cross section. Data with quality flags of 2 were plotted. Vertical exaggeration of the upper 1000 m section is same as Fig. 7.

Figure 19 Phosphate ($\mu\text{mol/kg}$) cross sections. Data with quality flags of 2 were plotted. Vertical exaggeration is same as Fig. 7.

Figure 20 Dissolved inorganic carbon ($\mu\text{mol/kg}$) cross sections. Data with quality flags of 2 were plotted. Vertical exaggeration is same as Fig. 7.

Figure 21 Total alkalinity ($\mu\text{mol/kg}$) cross sections. Data with quality flags of 2 were plotted. Vertical exaggeration is same as Fig. 7.

Figure 22 pH cross sections. Data with quality flags of 2 were plotted. Vertical exaggeration is same as Fig. 7.

Figure 23 Dissolved organic carbon ($\mu\text{mol/kg}$) cross sections. Data with quality flags of 2 were plotted. Vertical exaggeration is same as Fig. 7.

Figure 24 Cross sections of current velocity (cm/s) normal to the cruise track measured by LADCP (eastward or northward is positive). Vertical exaggeration is same as Fig. 7.

Figure 25 Difference in potential temperature ($^{\circ}\text{C}$) between results from the WOCE revisit cruise in 2007 and the revisit in 2014. Red and blue areas show areas where potential temperature increased and decreased in the revisit cruise, respectively. On white areas differences in temperature do not exceed the detection limit of 0.002°C . Vertical exaggeration is same as Fig. 7.

Figure 26 Same as Fig. 25, but for salinity (psu). CTD salinity data with SSW batch correction¹ were used. On white areas differences in salinity do not exceed the detection limit of 0.002 psu.

Figure 27 Same as Fig. 25, but for dissolved oxygen ($\mu\text{mol/kg}$). CTD oxygen data were used. On white areas differences in dissolved oxygen do not exceed the detection limit of $2 \mu\text{mol/kg}$.

Note

1. As for the traceability of SSW to Kawano's value (Kawano et al., 2006), the offset for the batches P148 (WOCE P01 revisit in 2007) and P156 (WOCE P01 revisit in 2014) are 0.0000 and 0.0004, respectively. The offset values for the recent batches are listed in Table A1 (Uchida et al., in preparation).

Table A1. SSW batch to batch differences from P145 to P159 (Uchida et al., in preparation). The difference of P145 is reevaluated.

Batch no.	Production date	K15	Sp	Batch to batch difference ($\times 10^{-3}$)	
				Mantyla's standard	Kawano's standard
P145	2004/07/15	0.99981	34.9925	-2.3	-1.0
P146	2005/05/12	0.99979	34.9917	-2.8	-1.5
P147	2006/06/06	0.99982	34.9929	-1.9	-0.6
P148	2006/10/01	0.99982	34.9929	-1.3	0.0
P149	2007/10/05	0.99984	34.9937	-0.6	0.7
P150	2008/05/22	0.99978	34.9913	-0.6	0.7
P151	2009/05/20	0.99997	34.9984	-1.7	-0.4
P152	2010/05/05	0.99981	34.9926	-1.3	0.0
P153	2011/03/08	0.99979	34.9918	-0.9	0.4
P154	2011/10/20	0.99990	34.9961	-0.7	0.6
P155	2012/09/19	0.99981	34.9925	-1.2	0.1
P156	2013/07/23	0.99984	34.9937	-0.9	0.4
P157	2014/05/15	0.99985	34.9941	-2.0	-0.7
P158	2015/03/25	0.99970	34.9883	-1.5	-0.2
P159	2015/12/15	0.99988	34.9953	-1.6	-0.3

Reference

Kawano, T., M. Aoyama, T. Joyce, H. Uchida, Y. Takatsuki and M. Fukasawa (2006): The latest batch-to-batch difference table of standard seawater and its application to the WOCE onetime sections, *J. Oceanogr.*, 62, 777–792.

Figure 1a
Station locations for WHP P10N

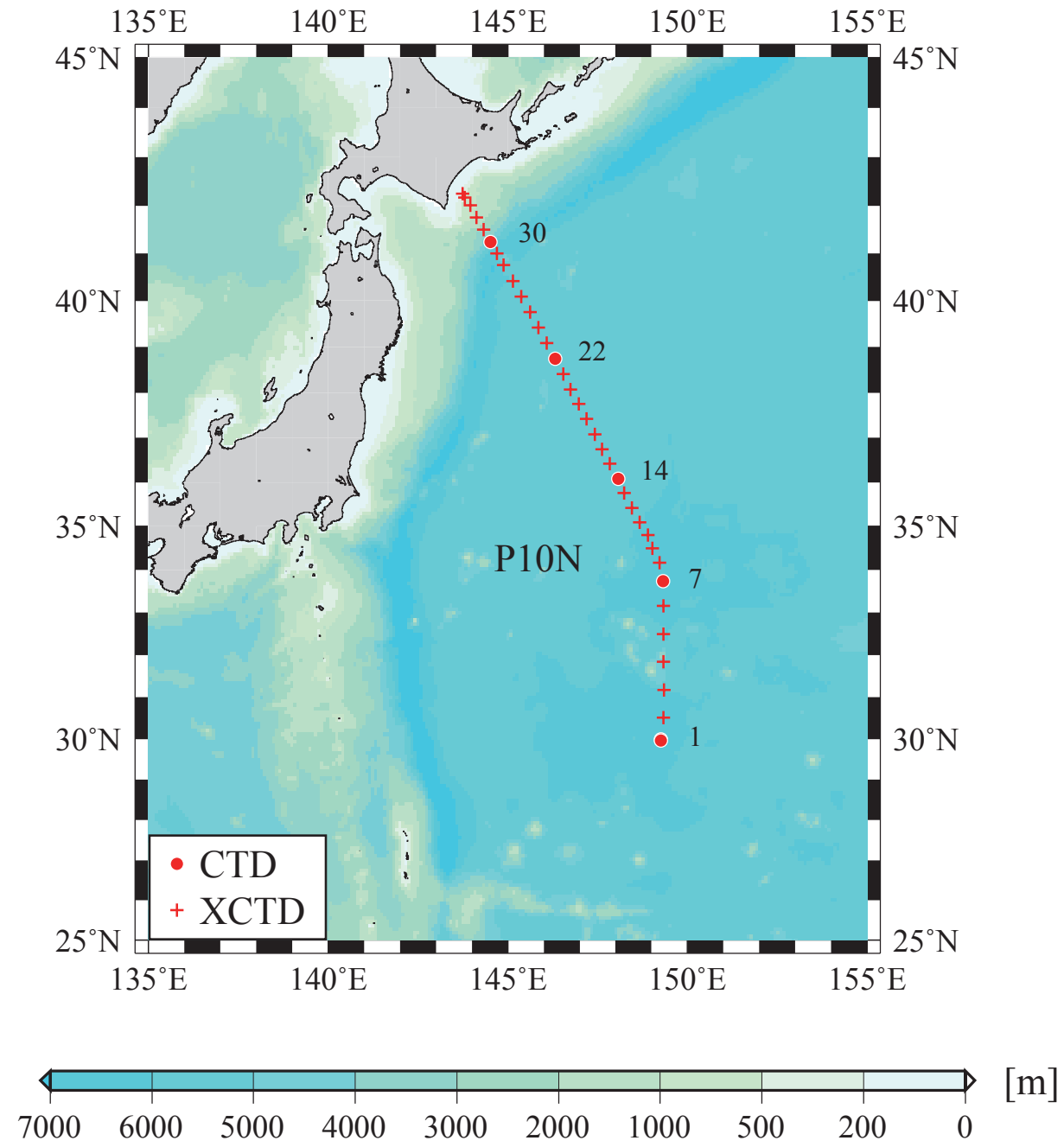


Figure 1b
Station locations for WHP P01

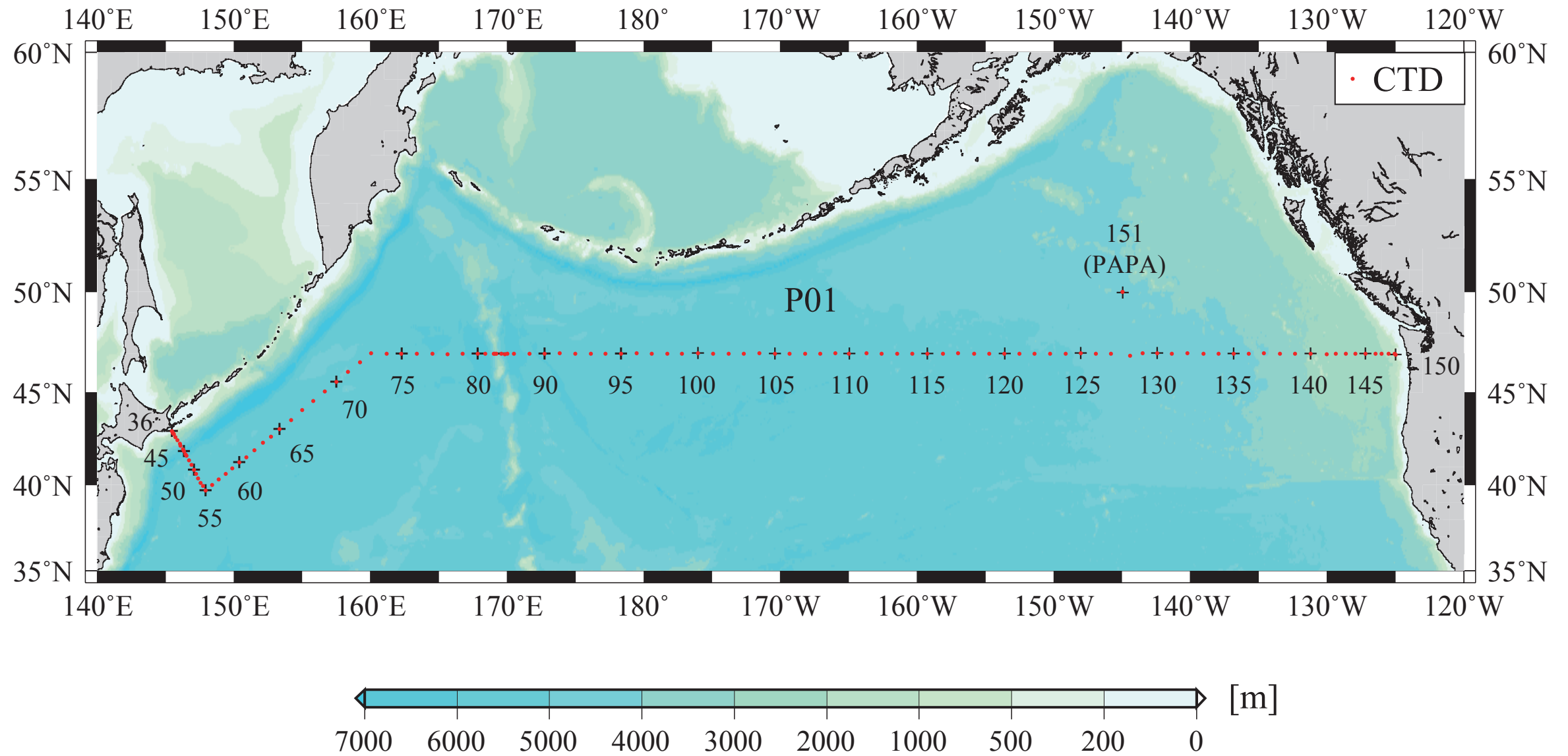


Figure 2
Bathymetry measured by Multi Narrow
Beam Echo Sounding system

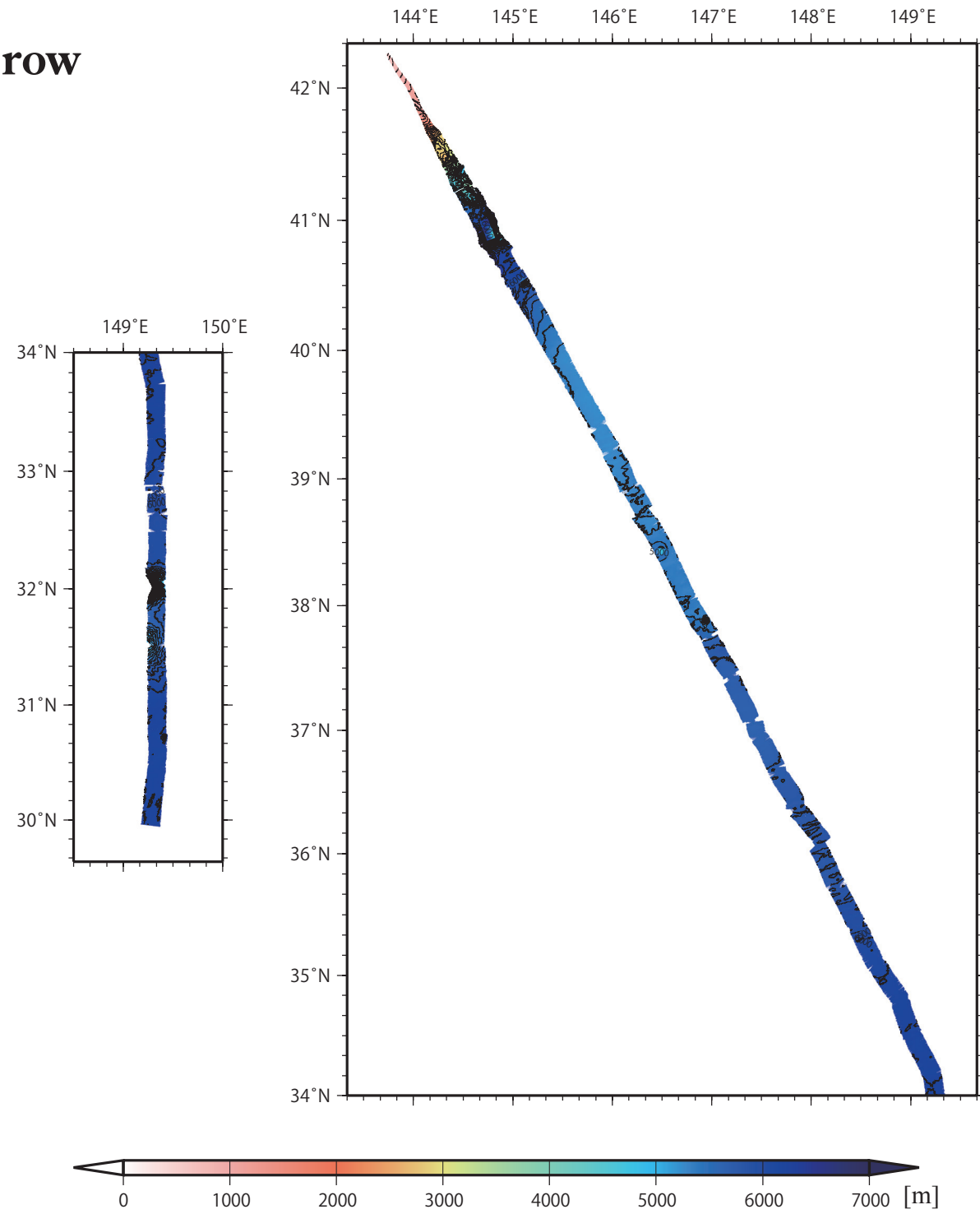


Figure 2
Continued

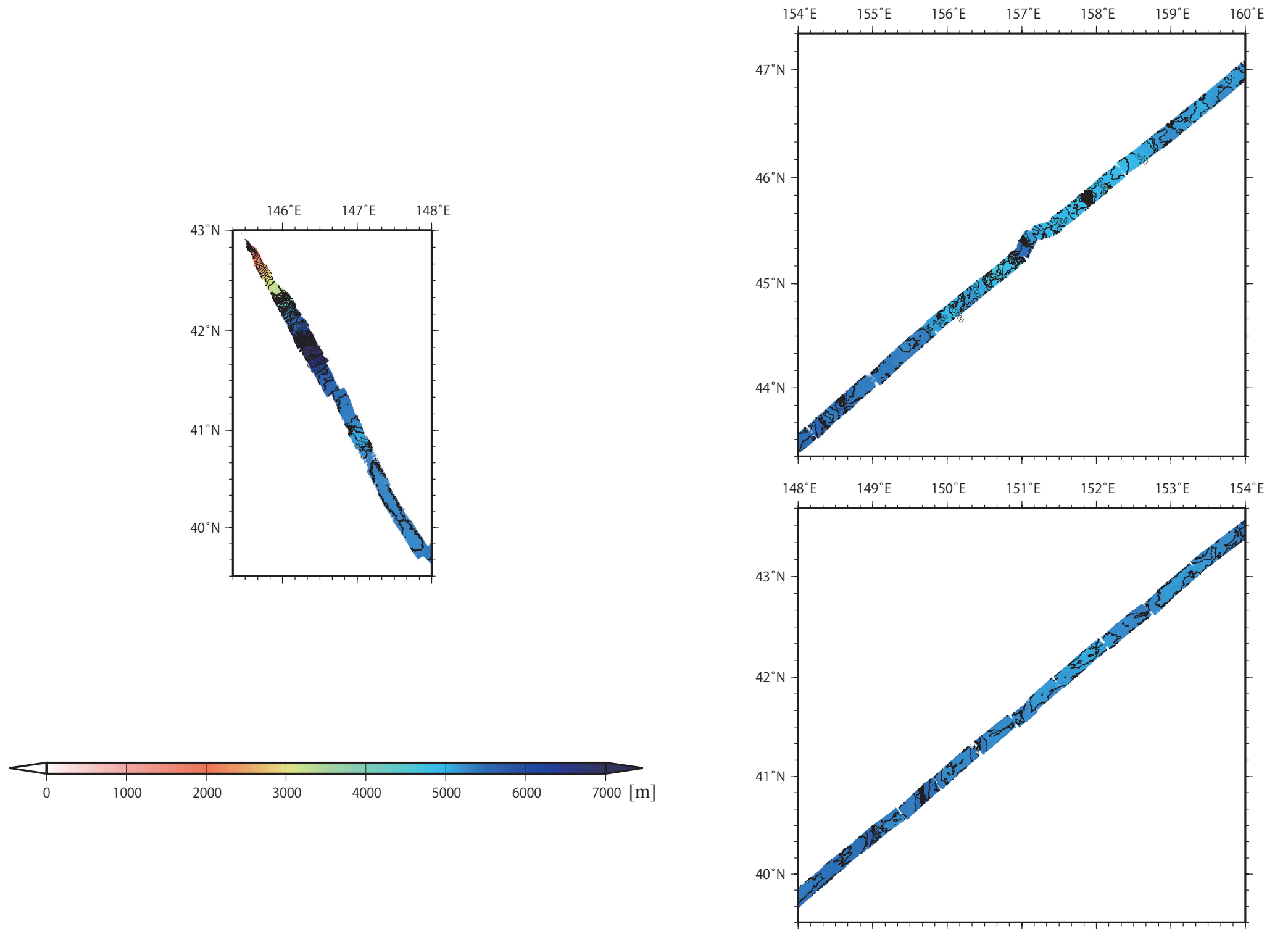


Figure 2
Continued

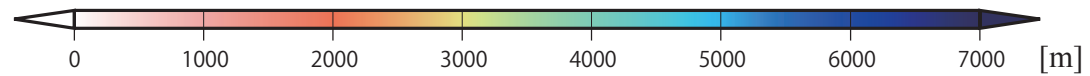
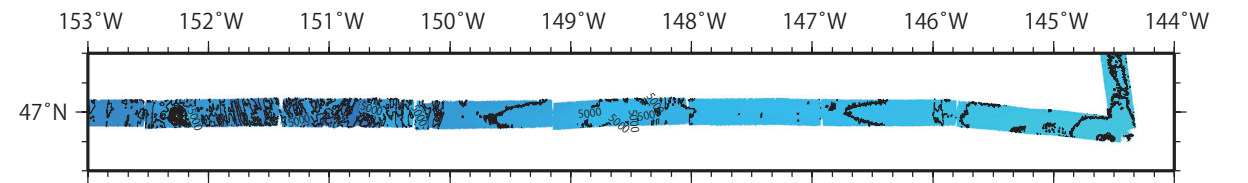
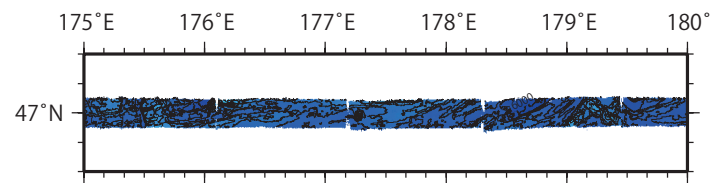
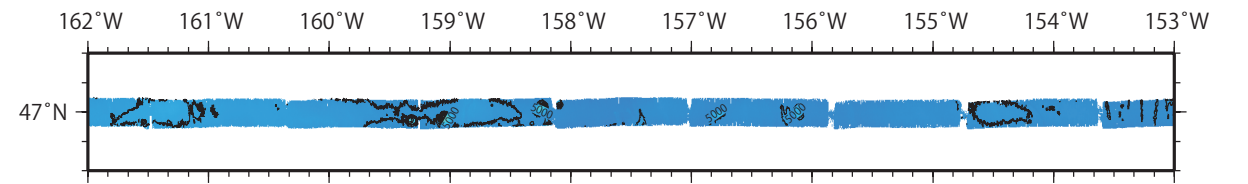
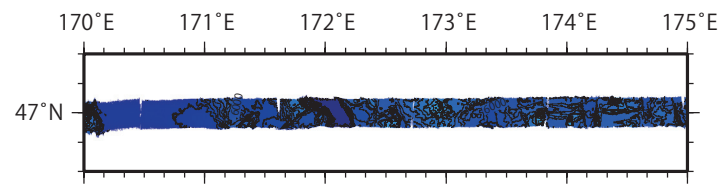
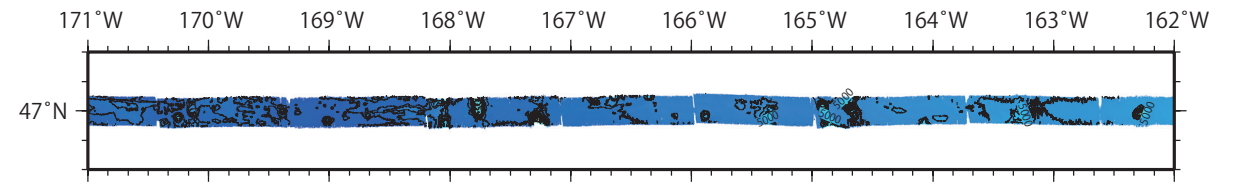
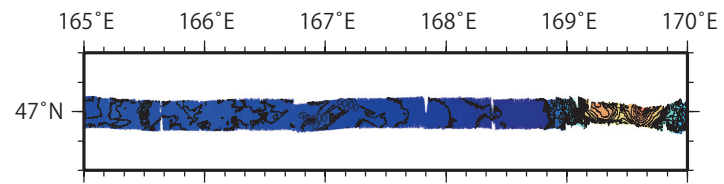
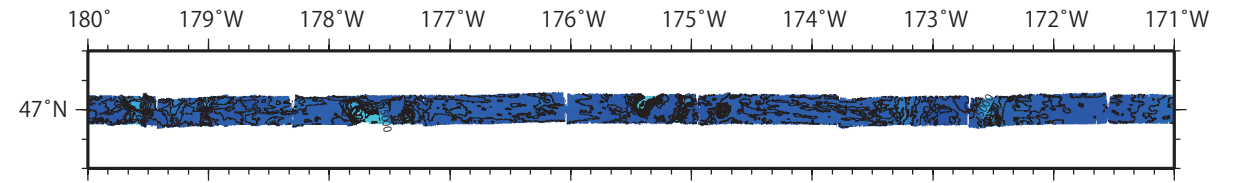
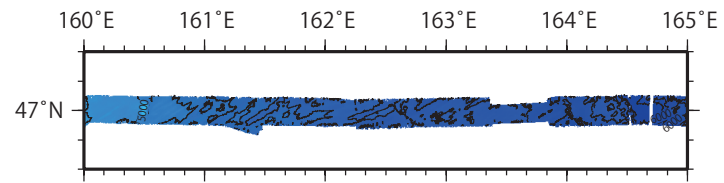


Figure 2
Continued

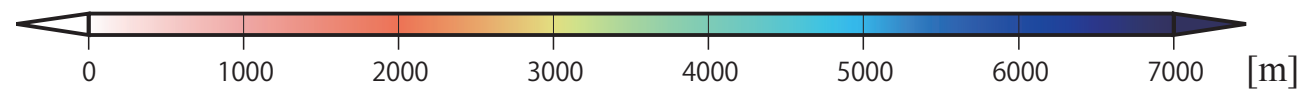
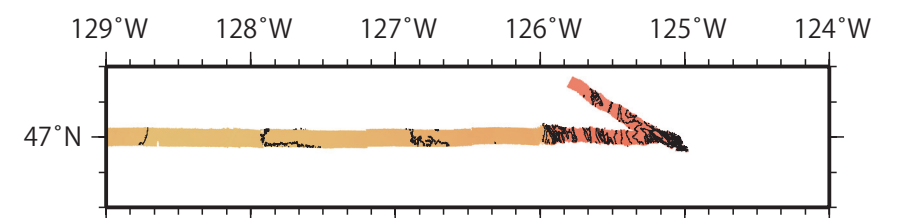
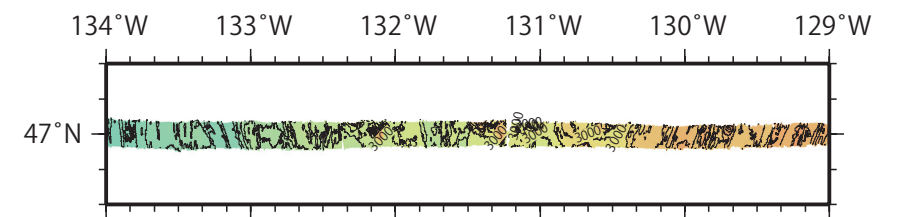
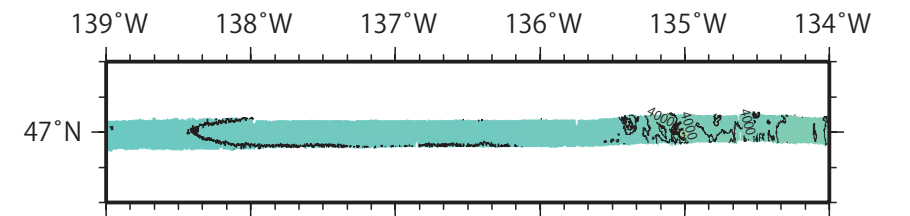
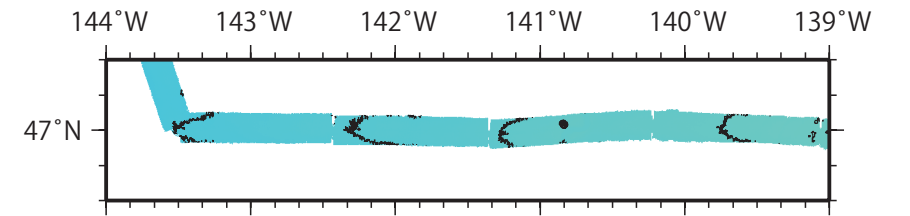
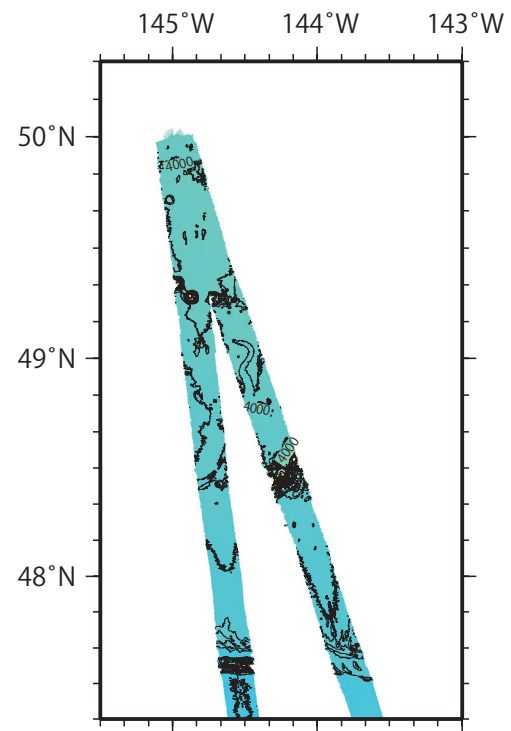


Figure 3
Surface wind measured at 25 m above sea level

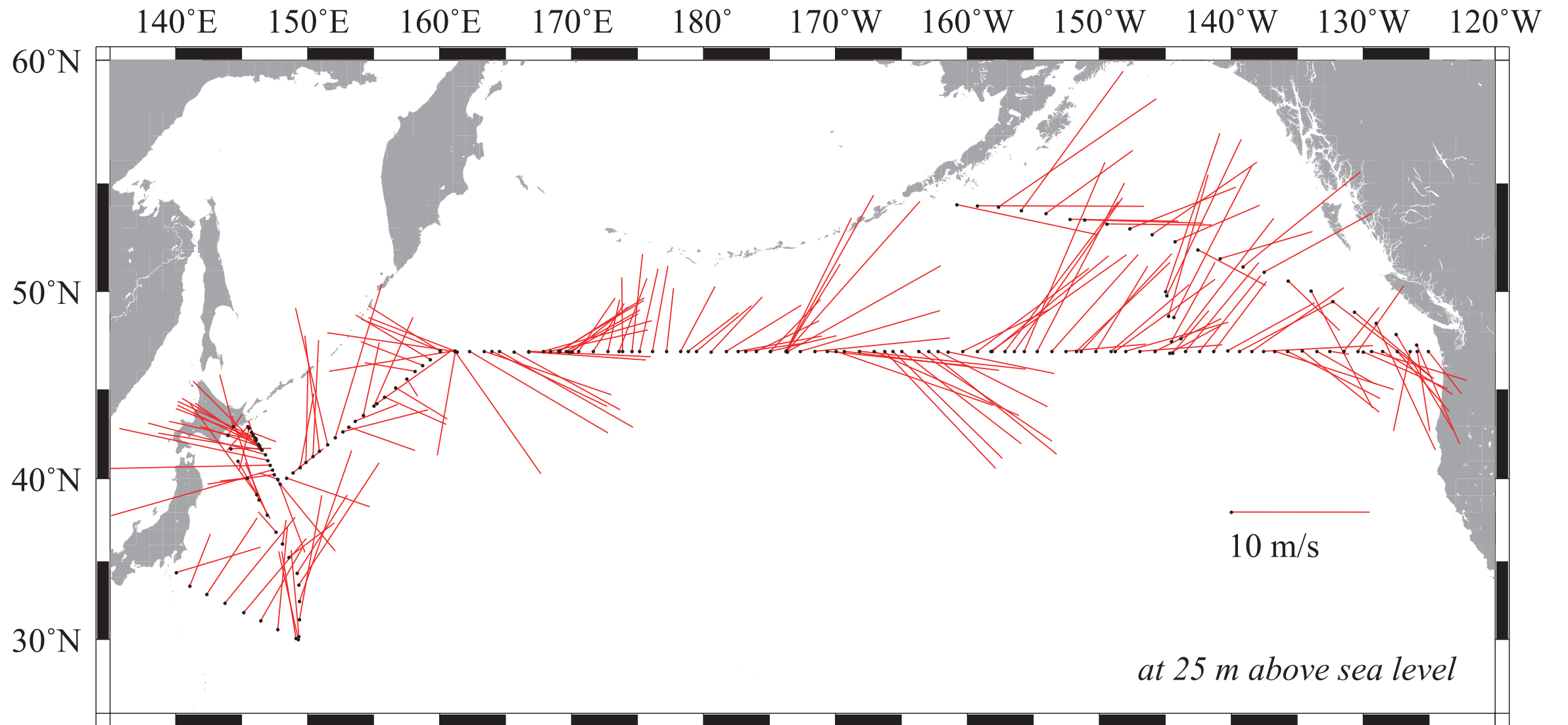


Figure 4a

Sea surface temperature (°C)

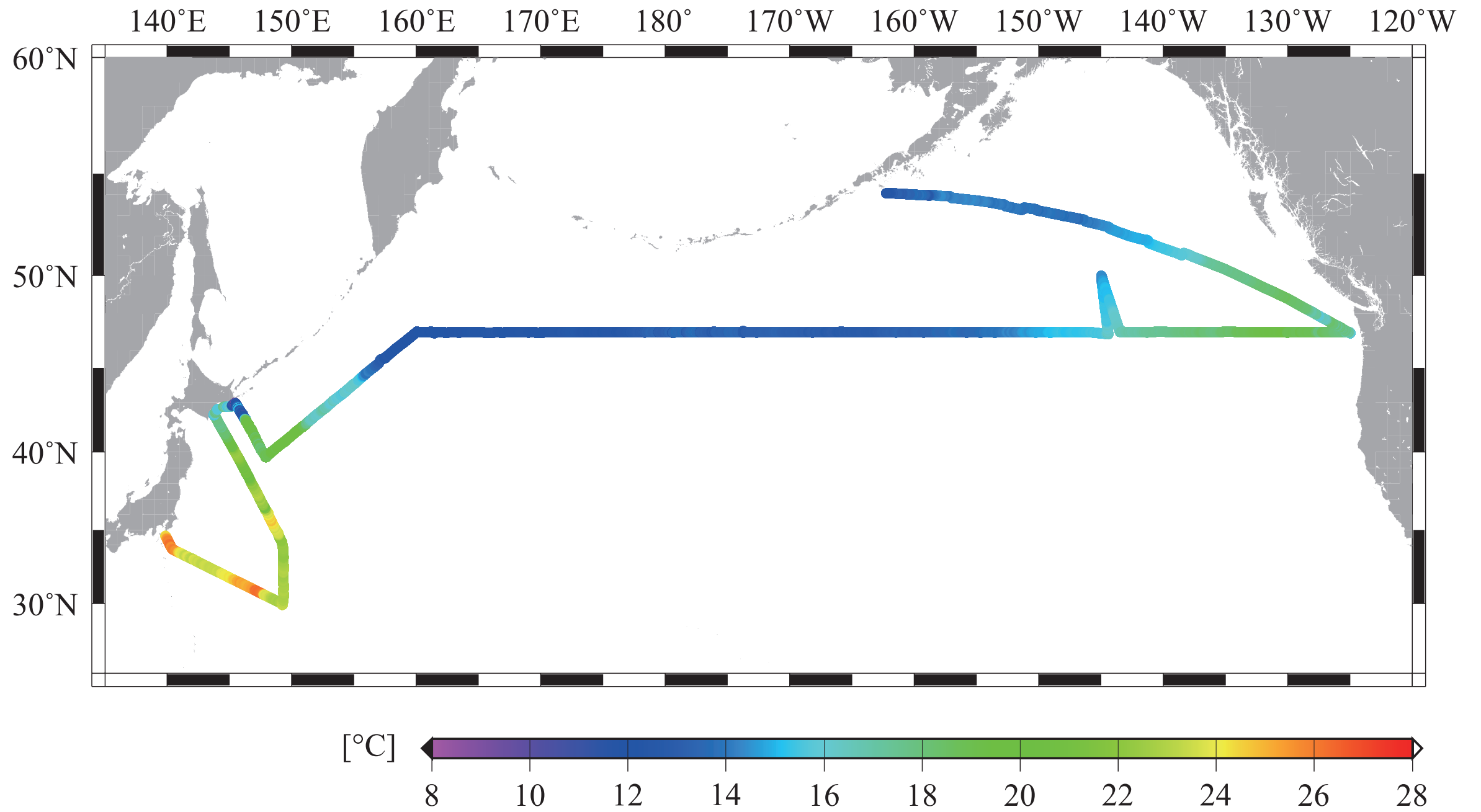


Figure 4b

Sea surface salinity (psu)

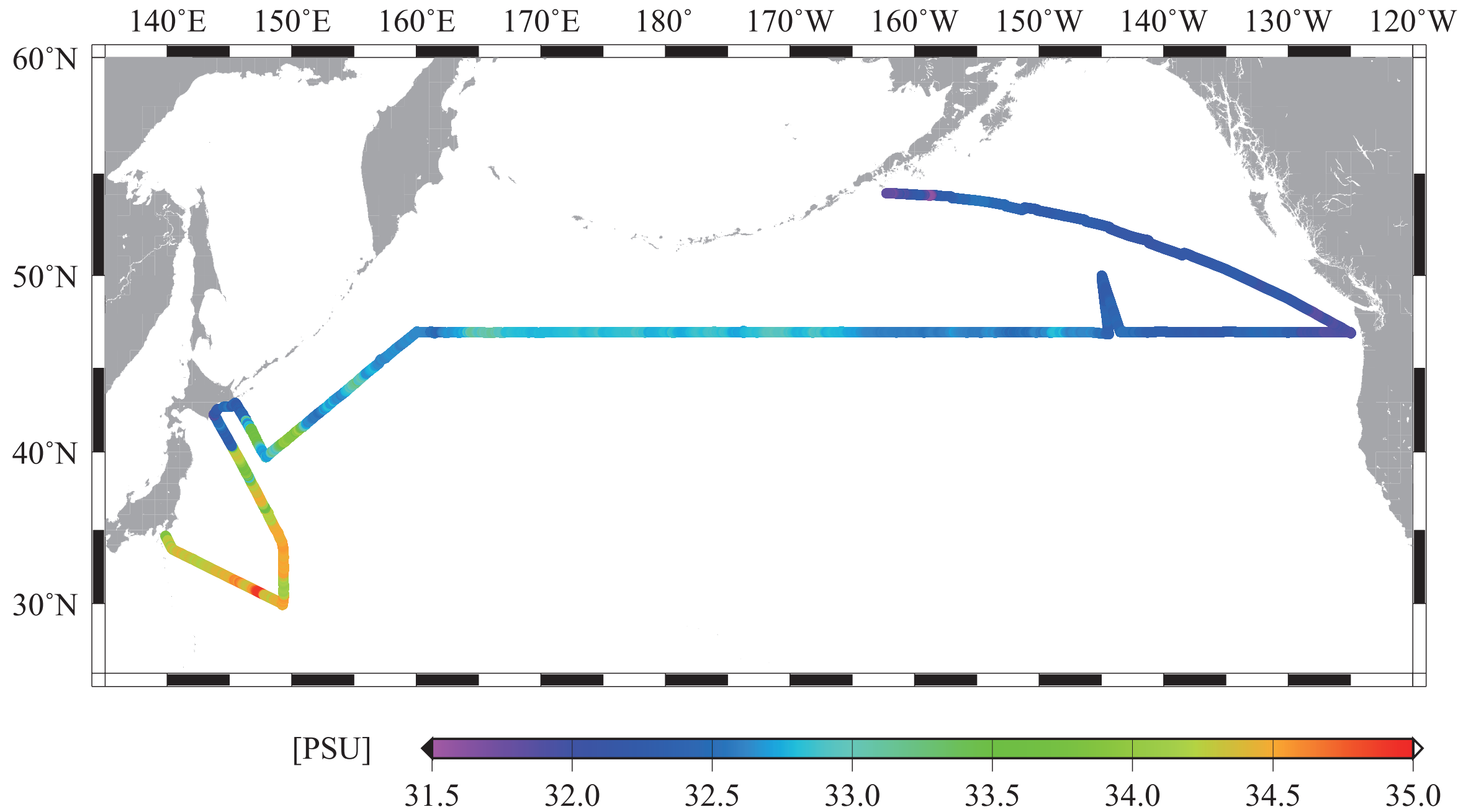


Figure 4c

Sea surface oxygen ($\mu\text{mol/kg}$)

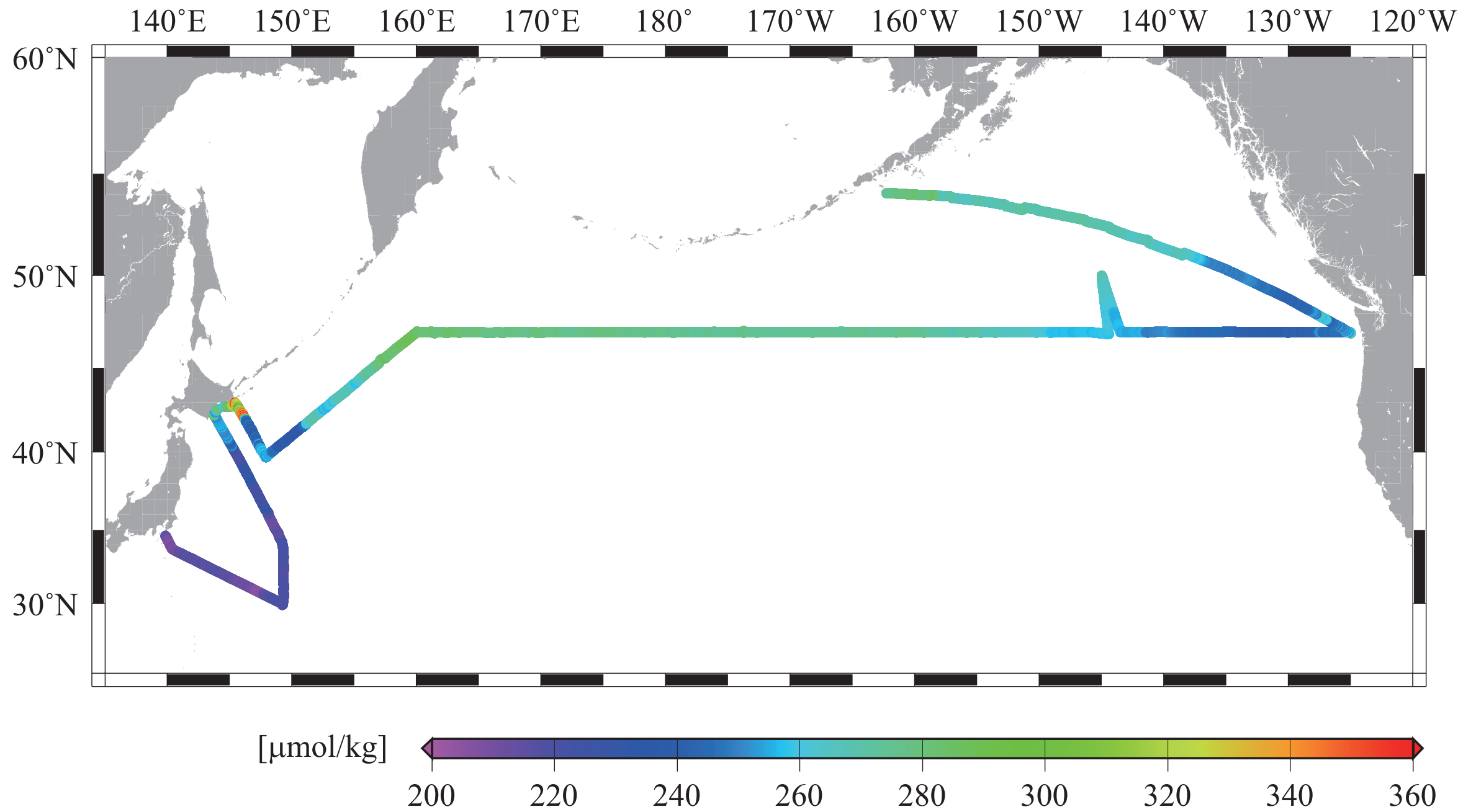


Figure 4d

Sea surface chlorophyll *a* (mg/m³)

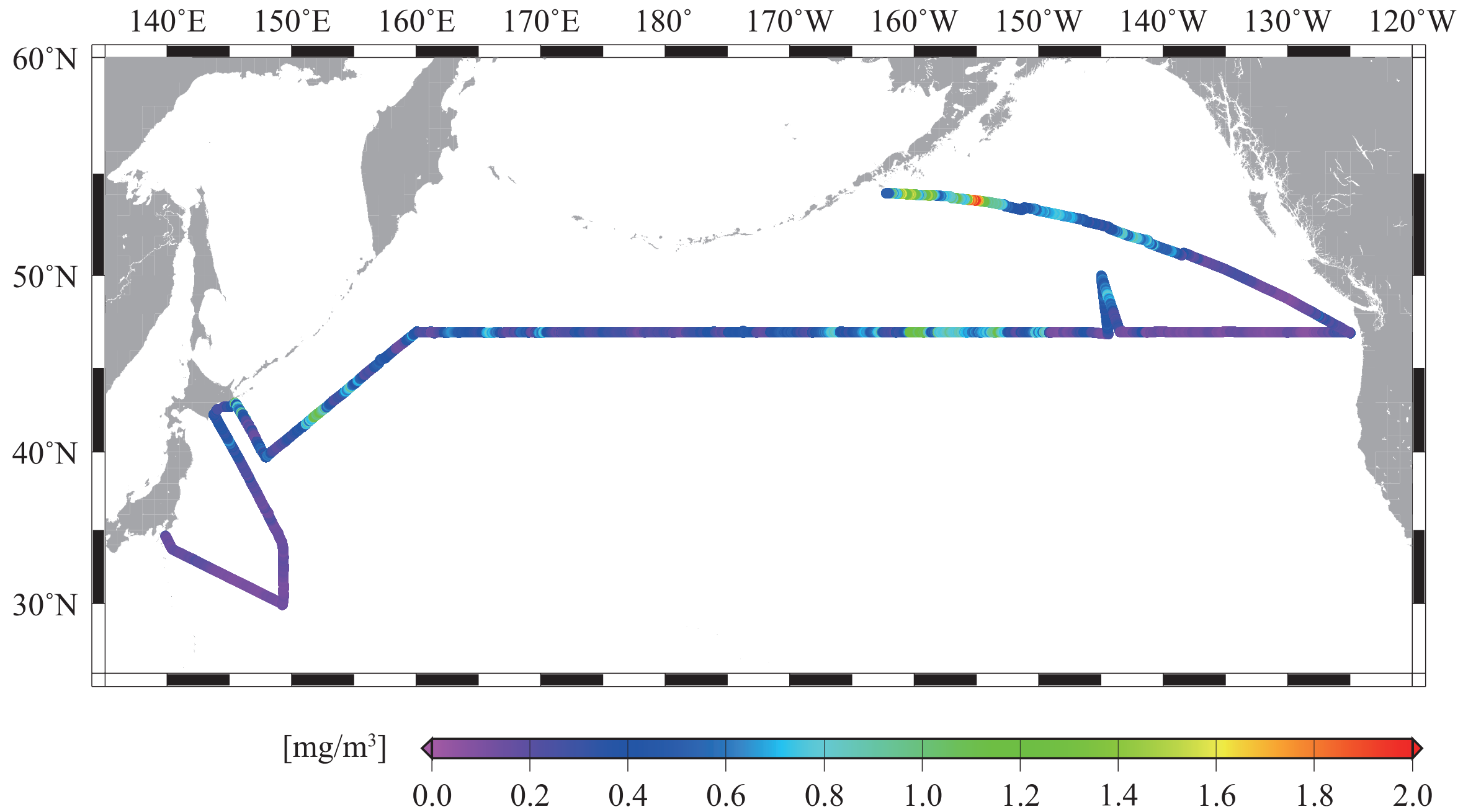


Figure 5

$\Delta p\text{CO}_2$ (ppmv)

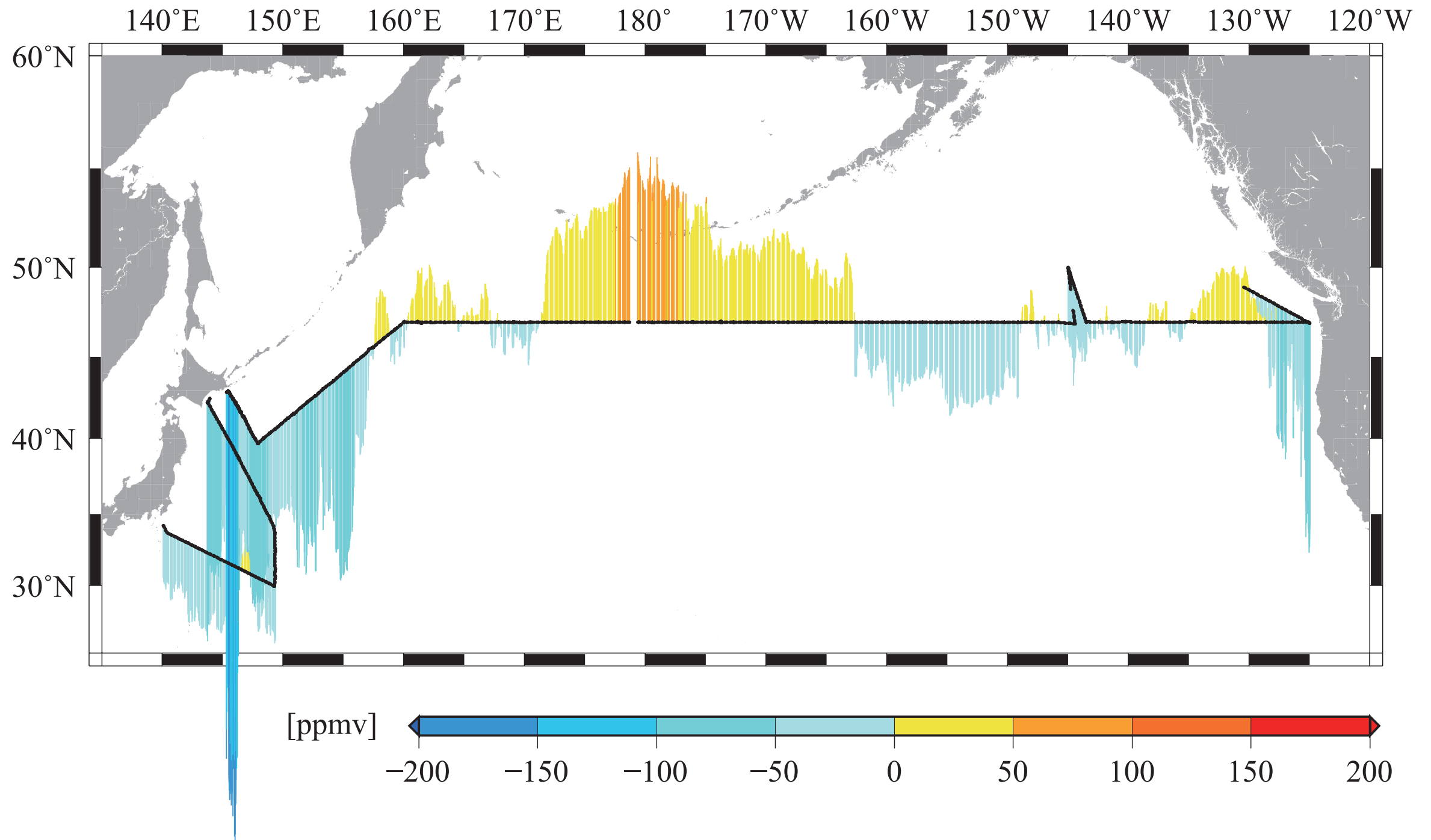


Figure 6
Surface current measured by shipboard ADCP

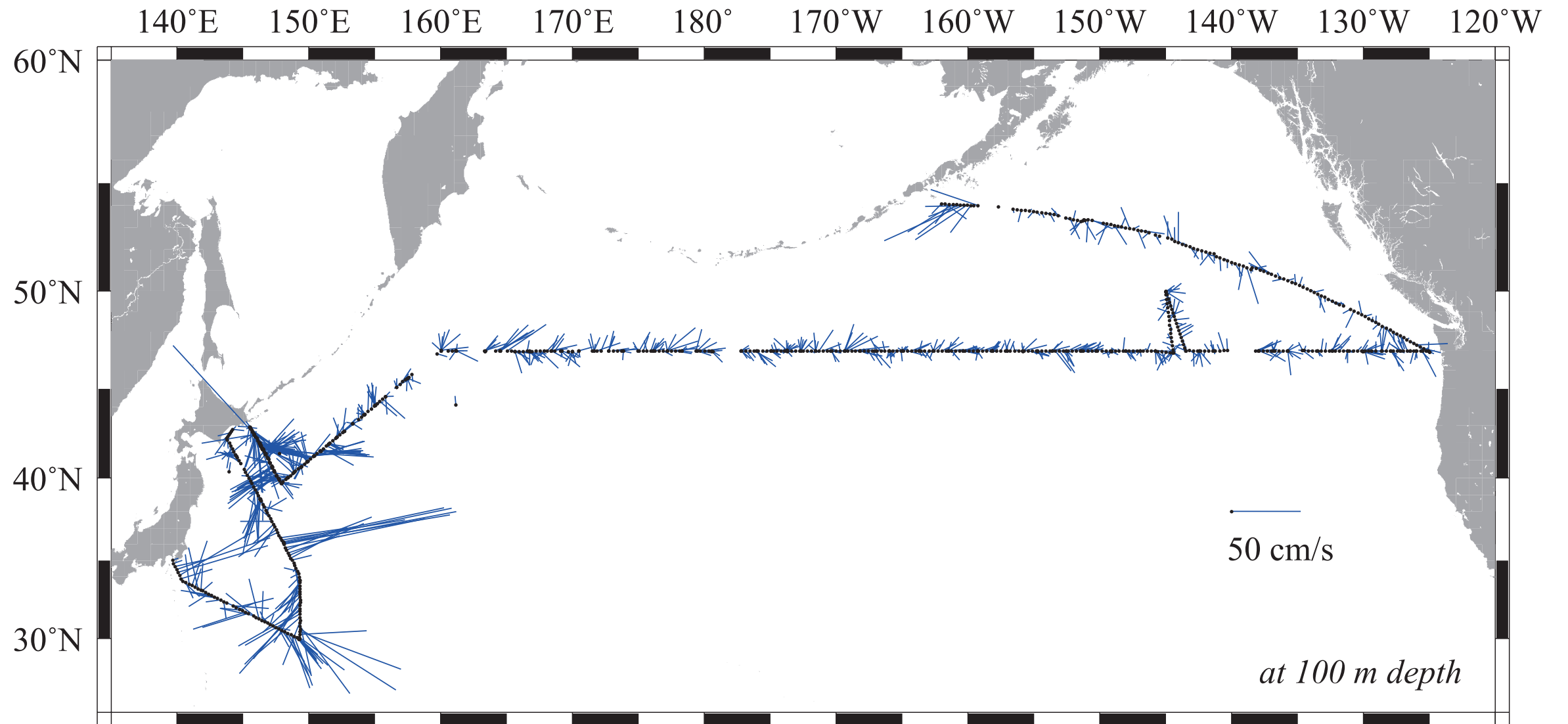


Figure 7
Potential temperature (°C)

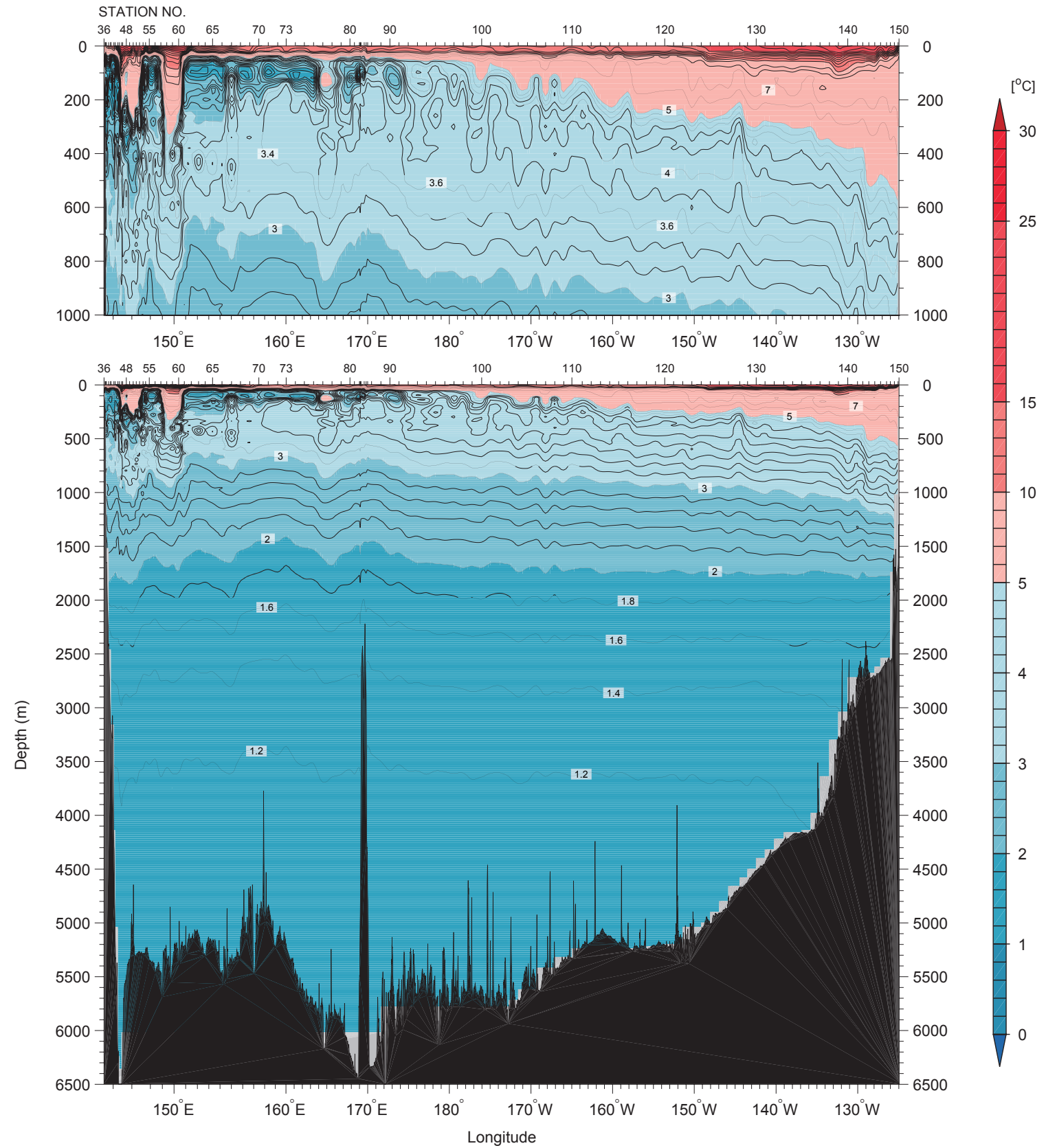


Figure 8
CTD salinity (psu)

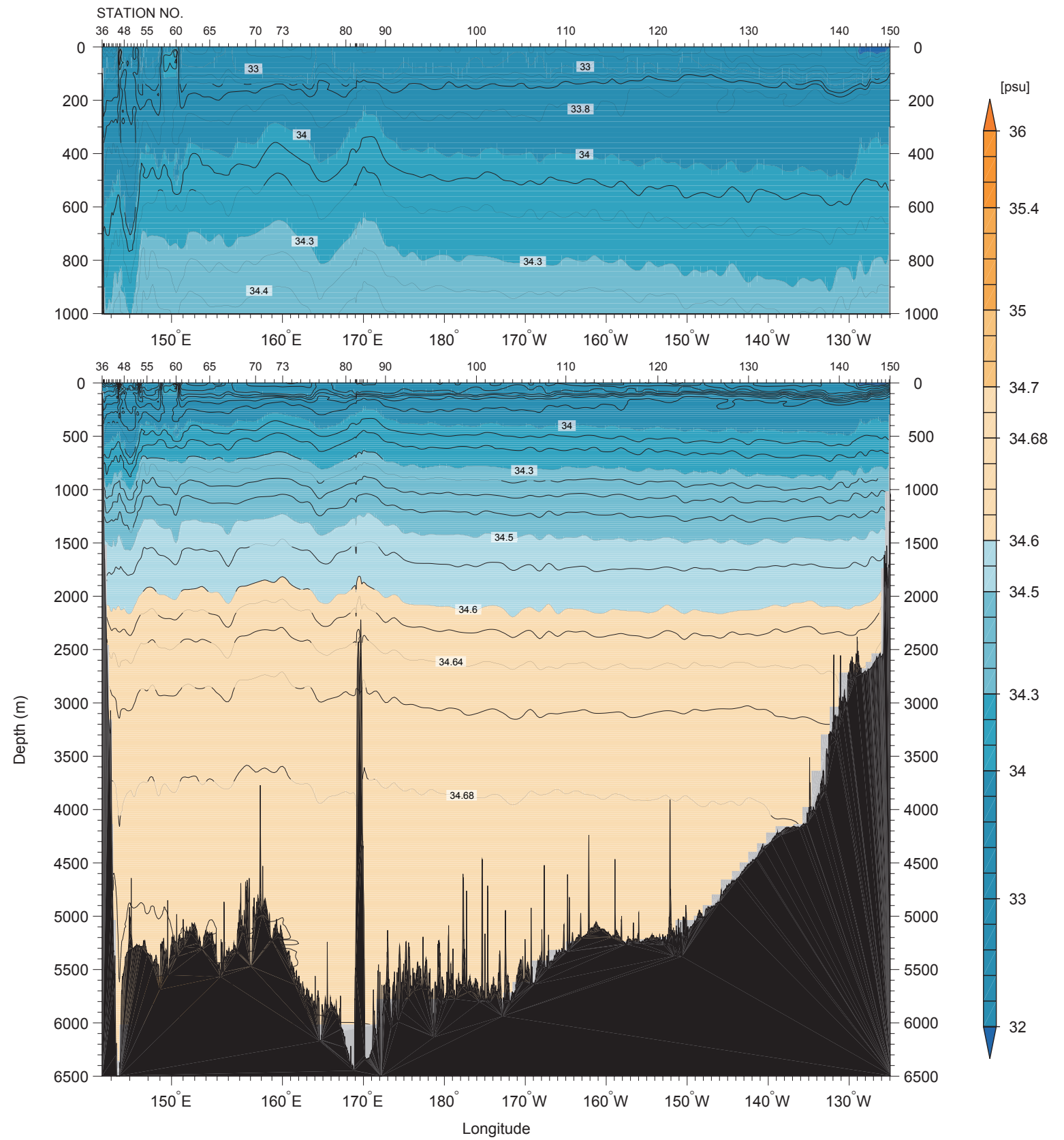


Figure 9
Absolute Salinity (g/kg)

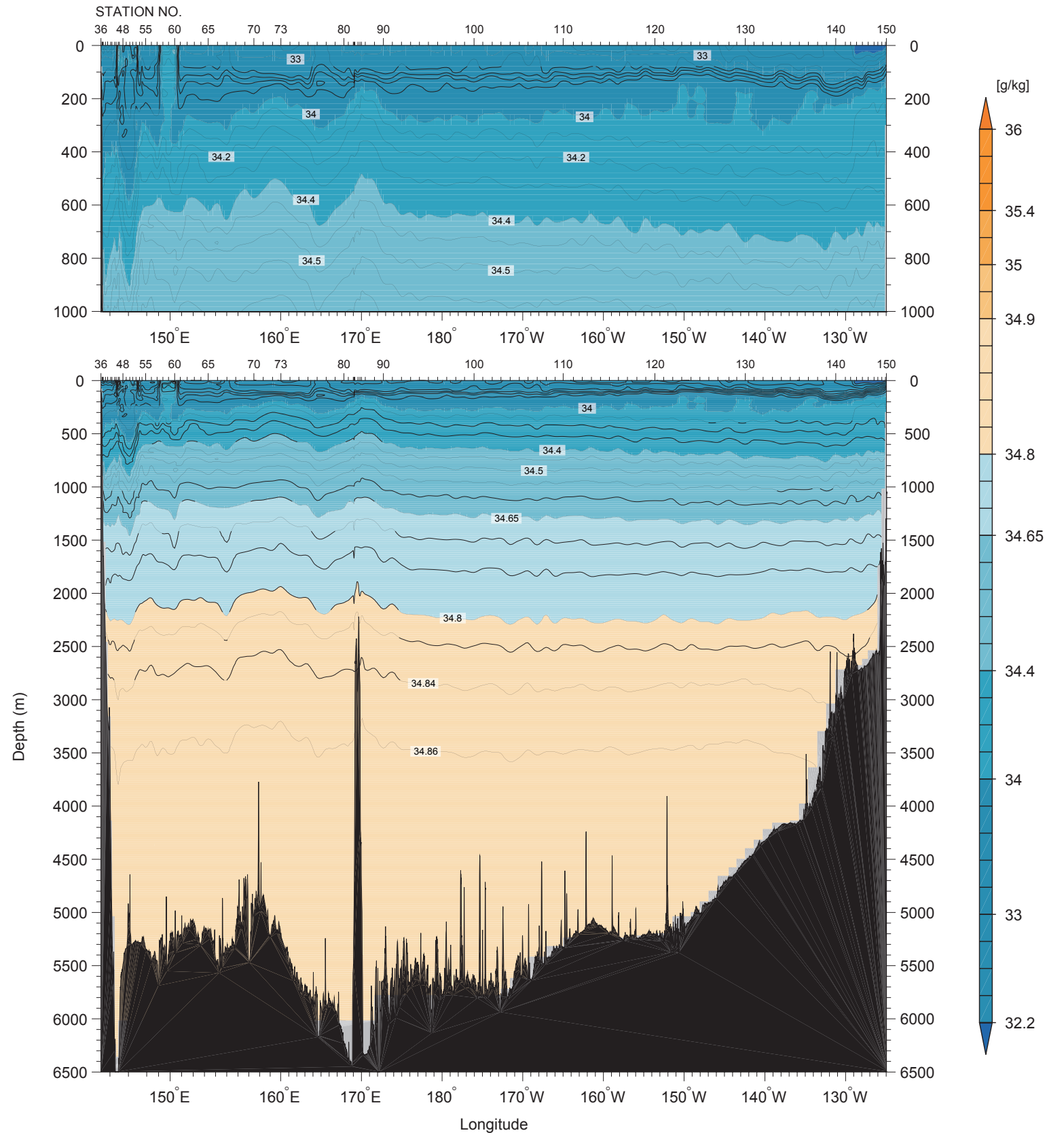


Figure 10a

Density (upper: σ_0 , lower: σ_4)
(kg/m^3) (EOS-80)

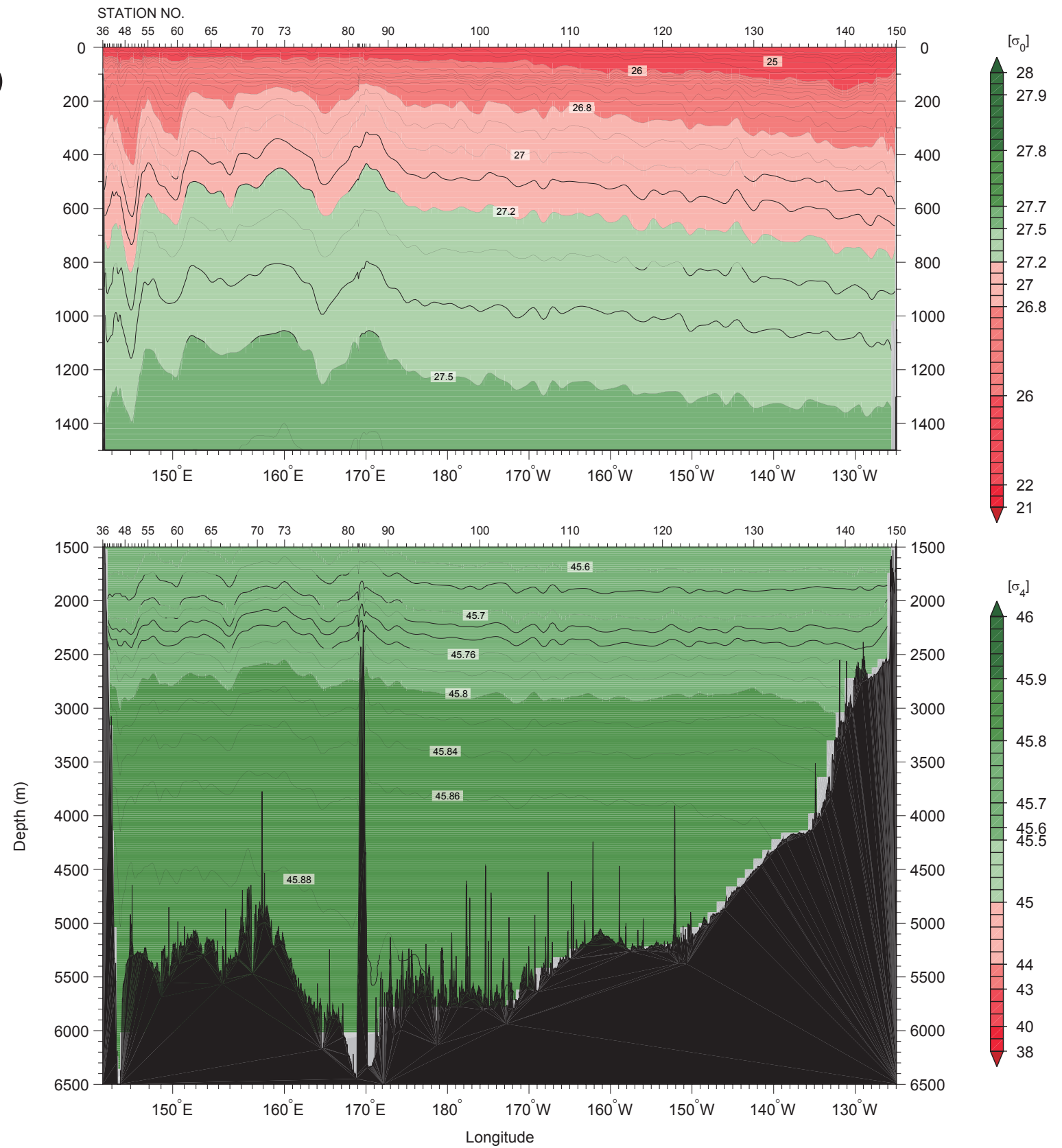


Figure 10b

Density (upper: σ_0 , lower: σ_4)
(kg/m^3) (TEOS-10)

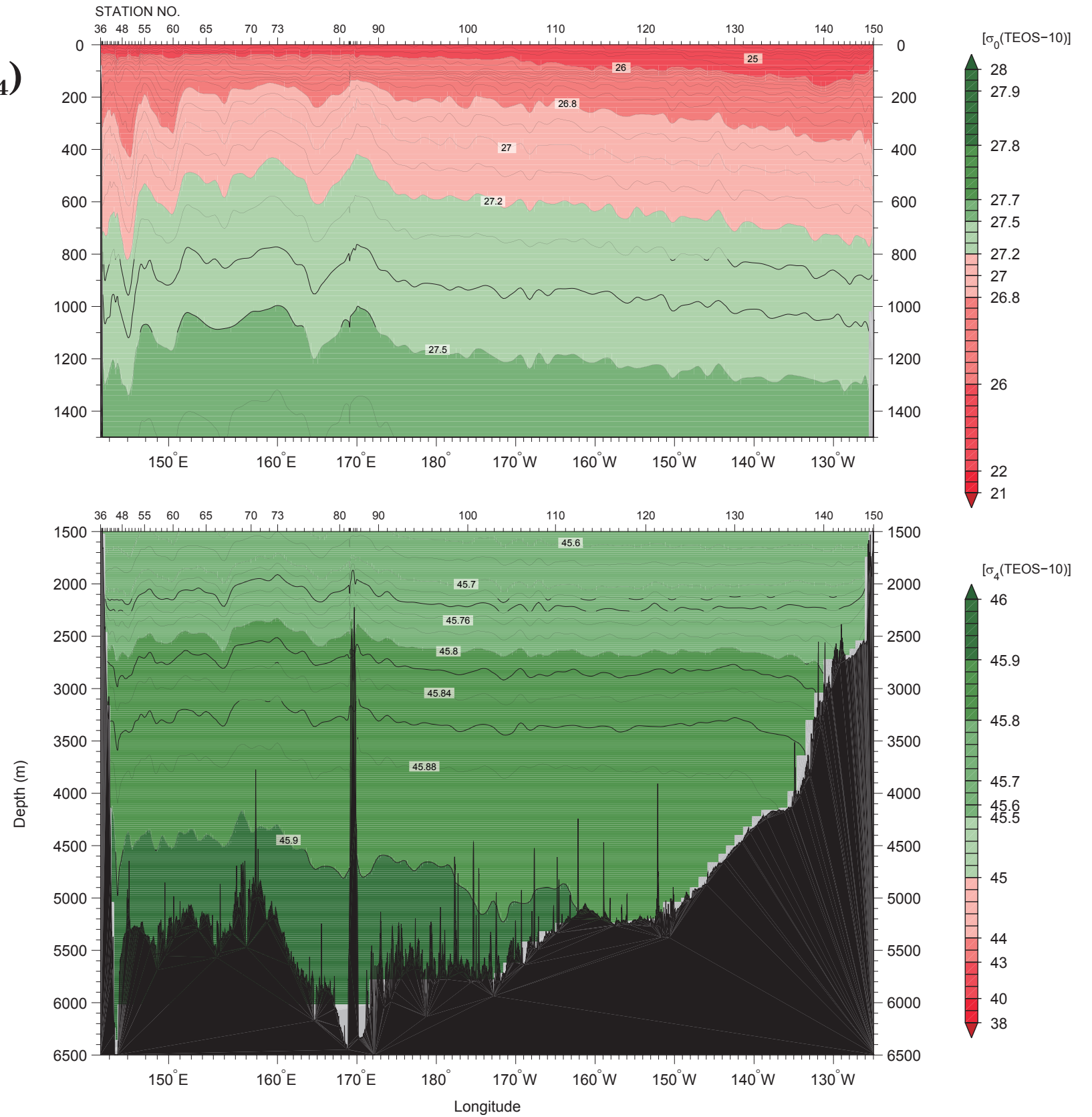


Figure 11
Density (γ^n) (kg/m^3)

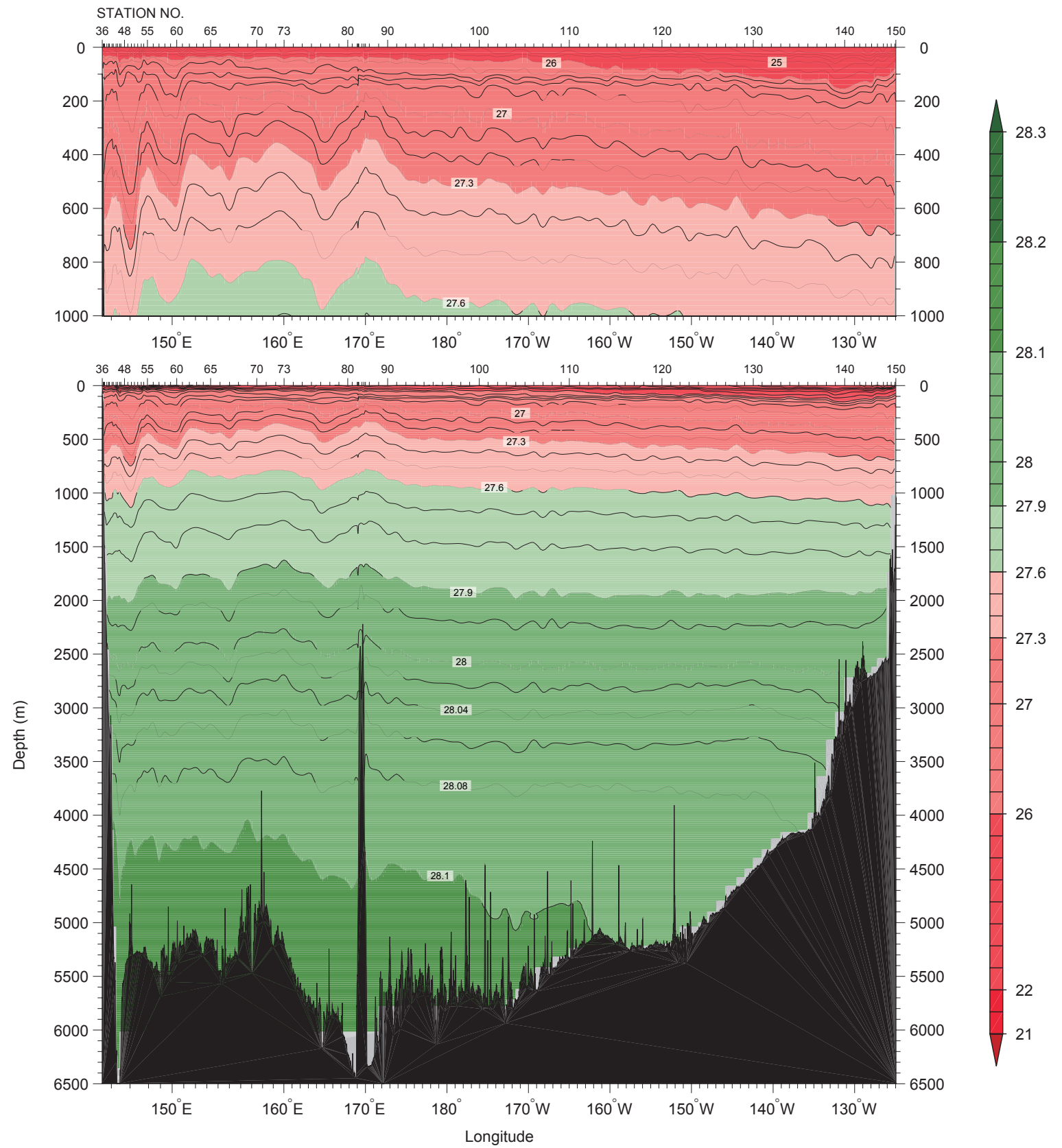


Figure 12
CTD oxygen ($\mu\text{mol/kg}$)

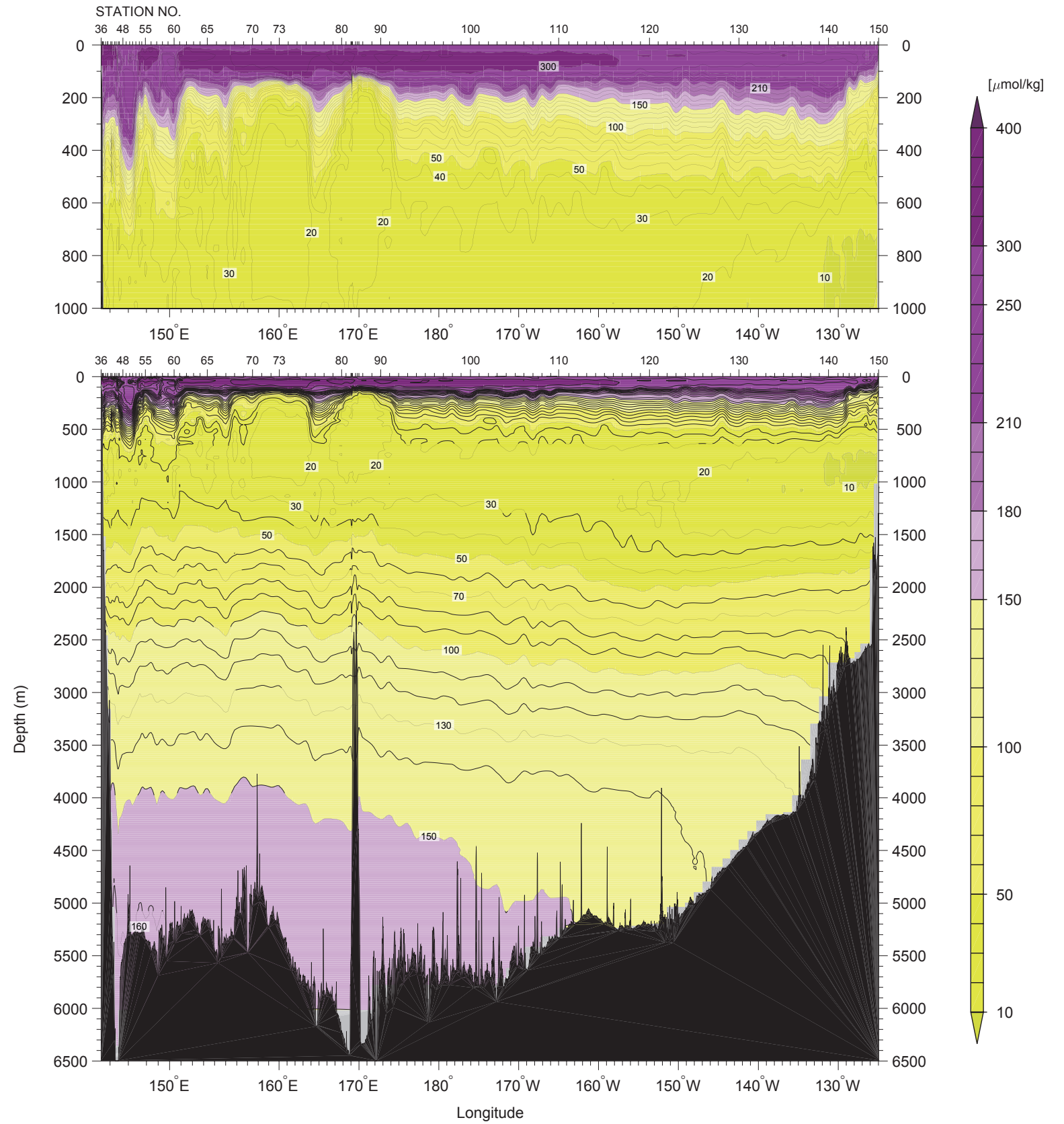


Figure 13

CTD chlorophyll *a* (mg/m³)

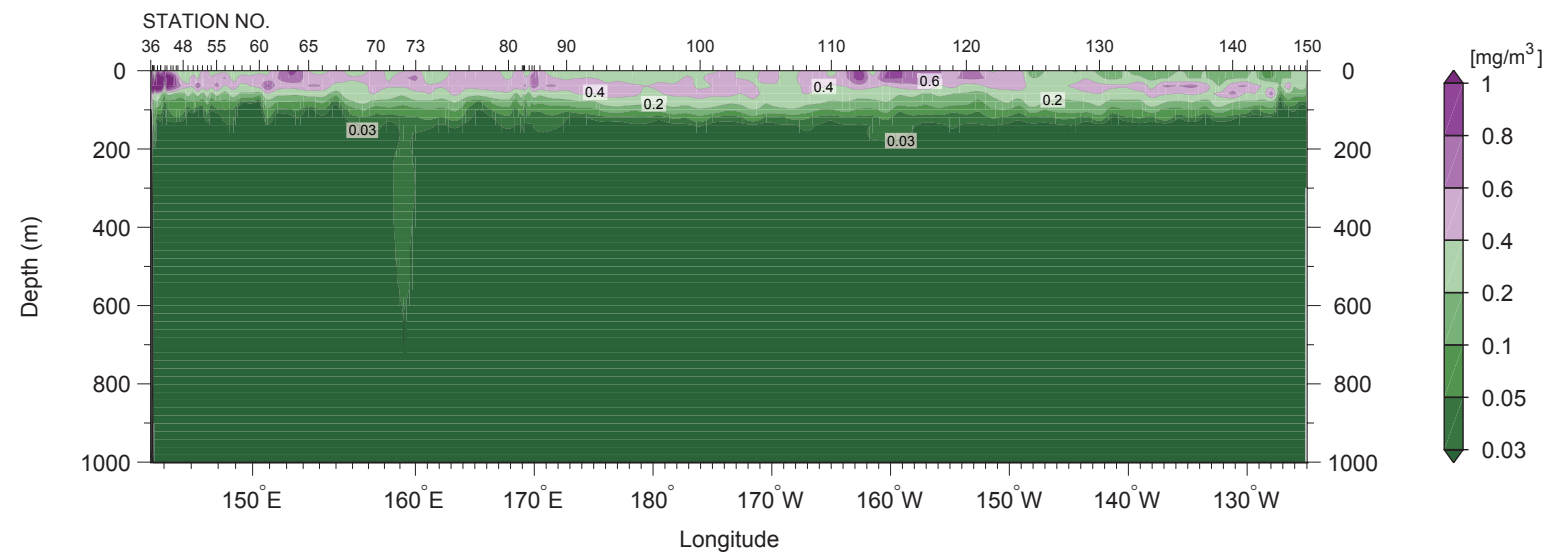


Figure 14
CTD beam attenuation
coefficient (m^{-1})

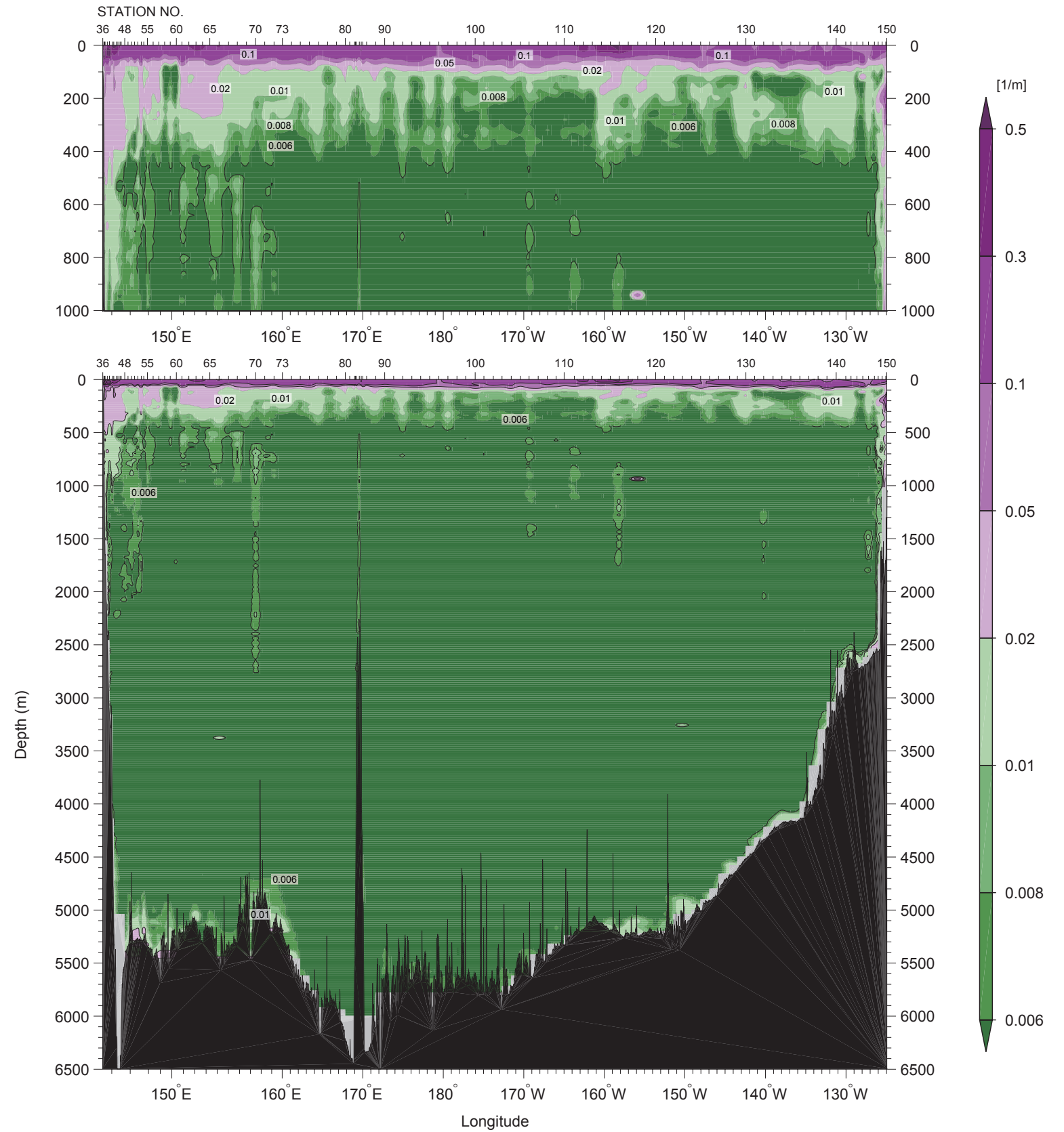


Figure 15

Bottle sampled dissolved oxygen ($\mu\text{mol/kg}$)

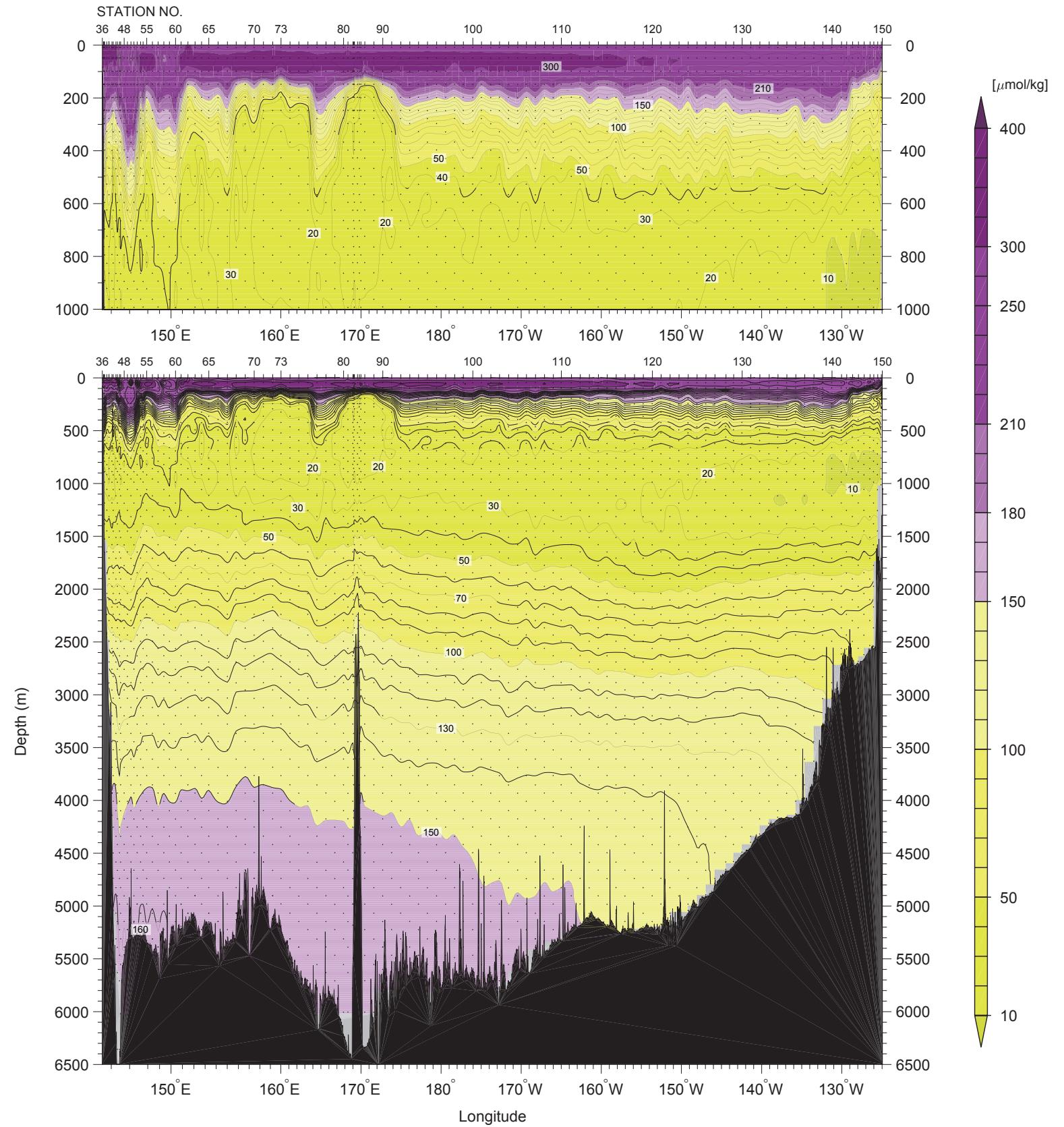


Figure 16
Silicate ($\mu\text{mol/kg}$)

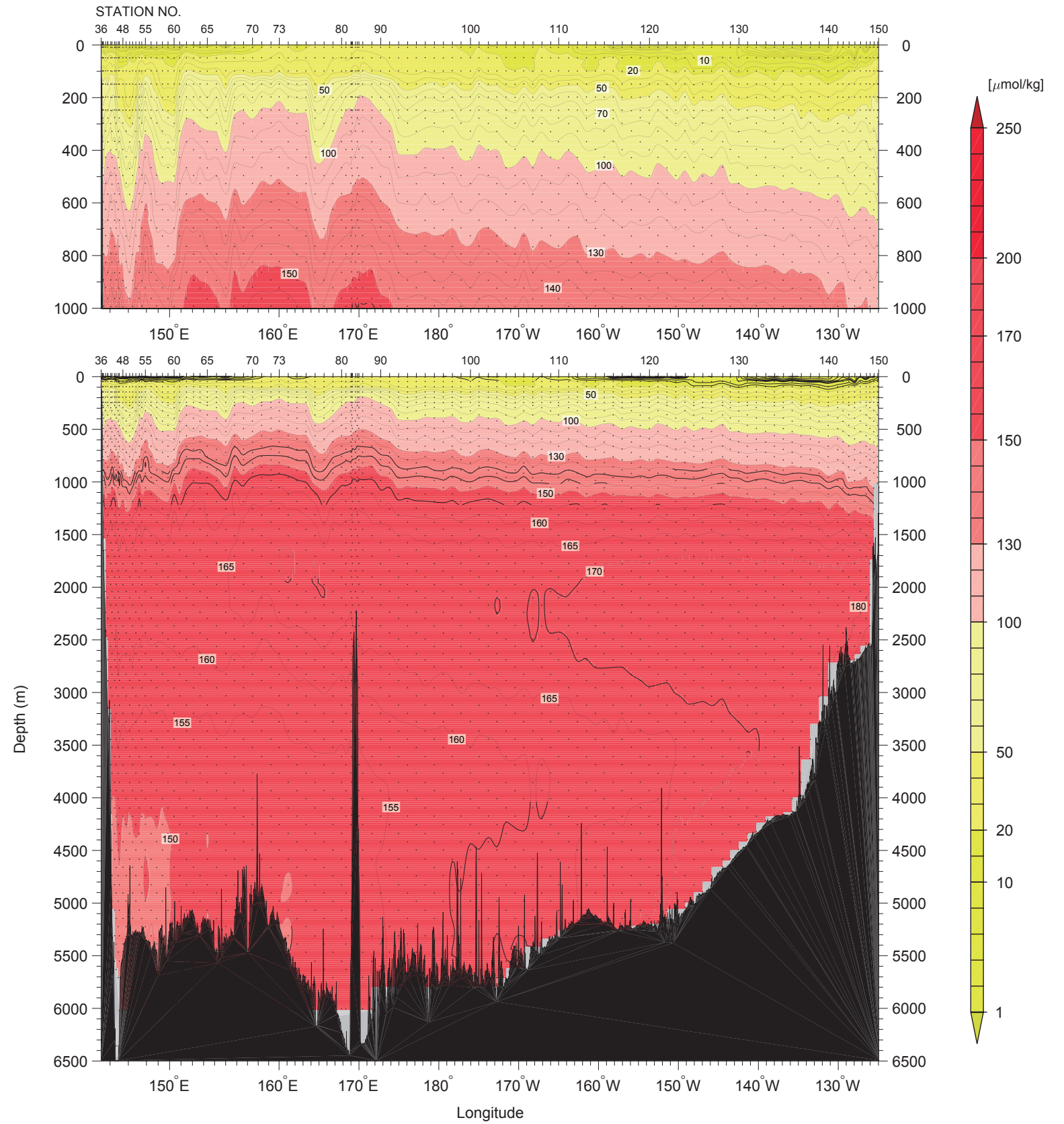


Figure 17
Nitrate ($\mu\text{mol/kg}$)

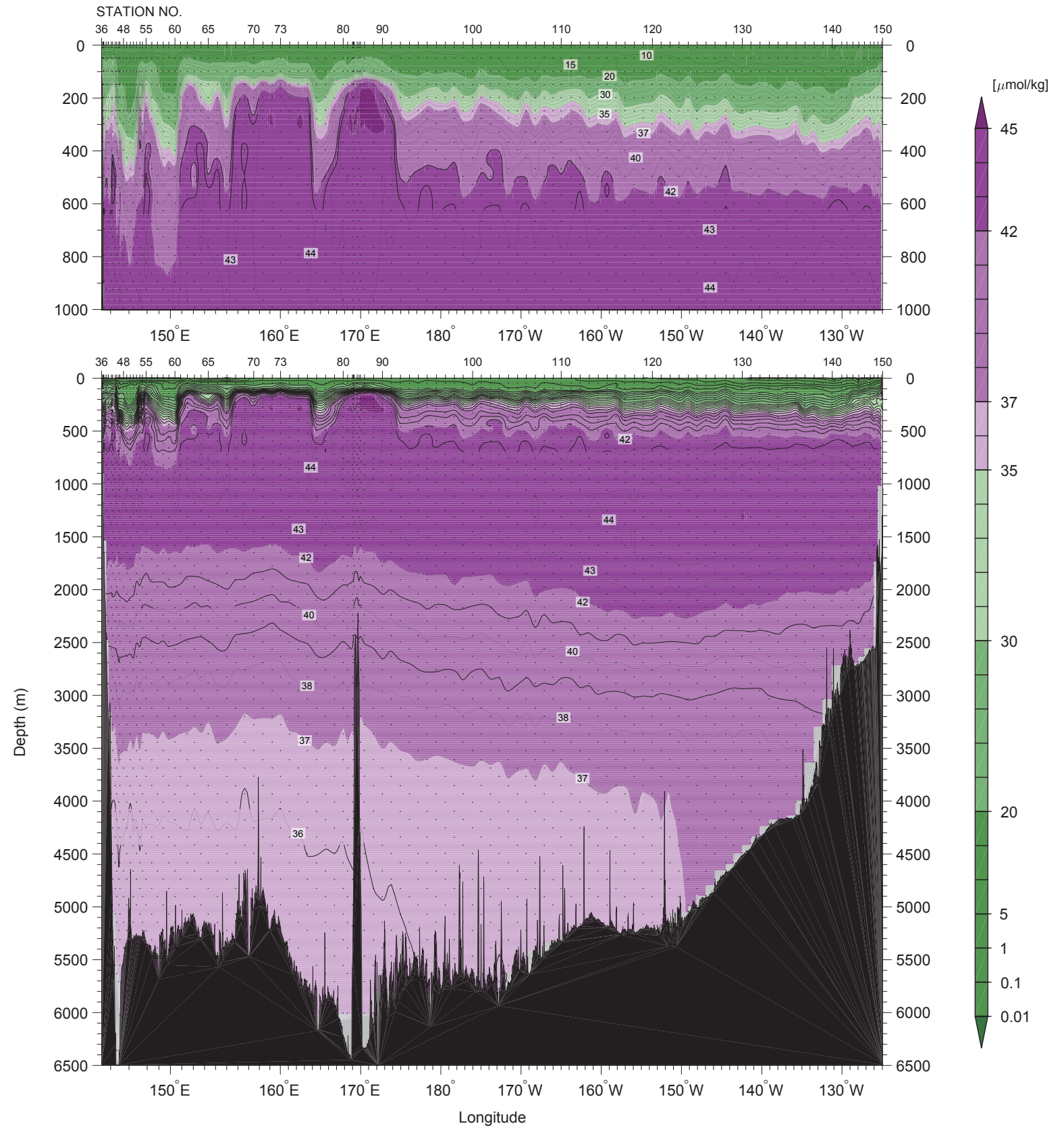


Figure 18
Nitrite ($\mu\text{mol/kg}$)

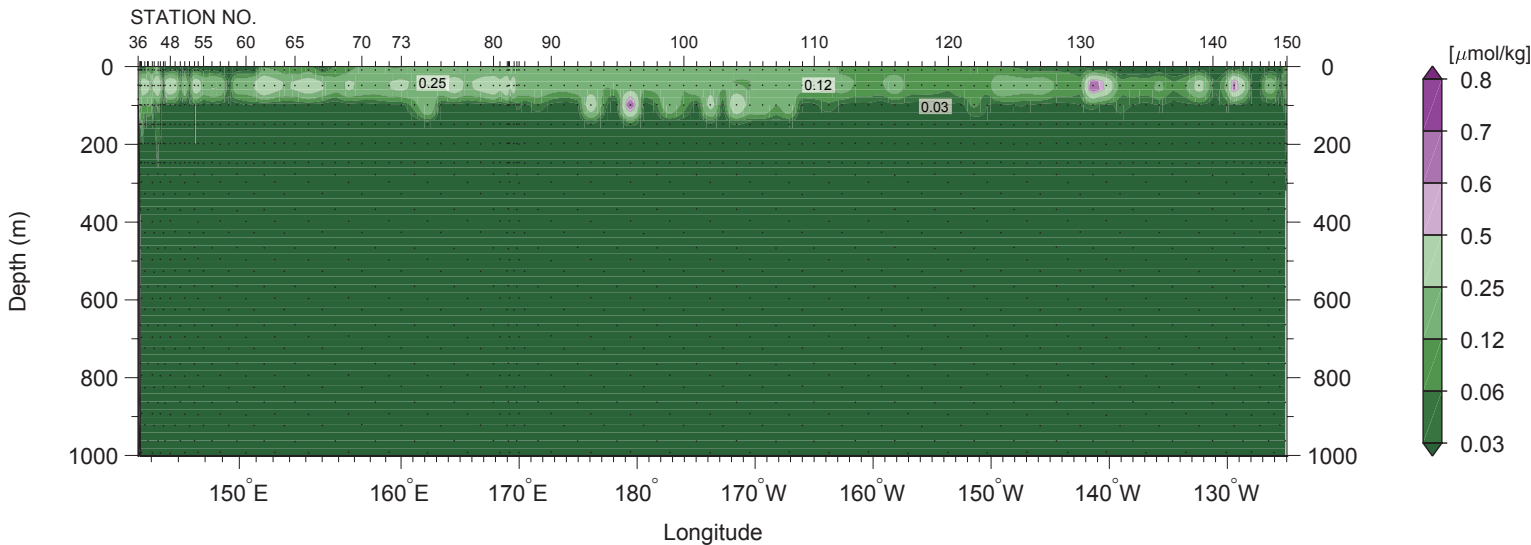


Figure 19
Phosphate ($\mu\text{mol/kg}$)

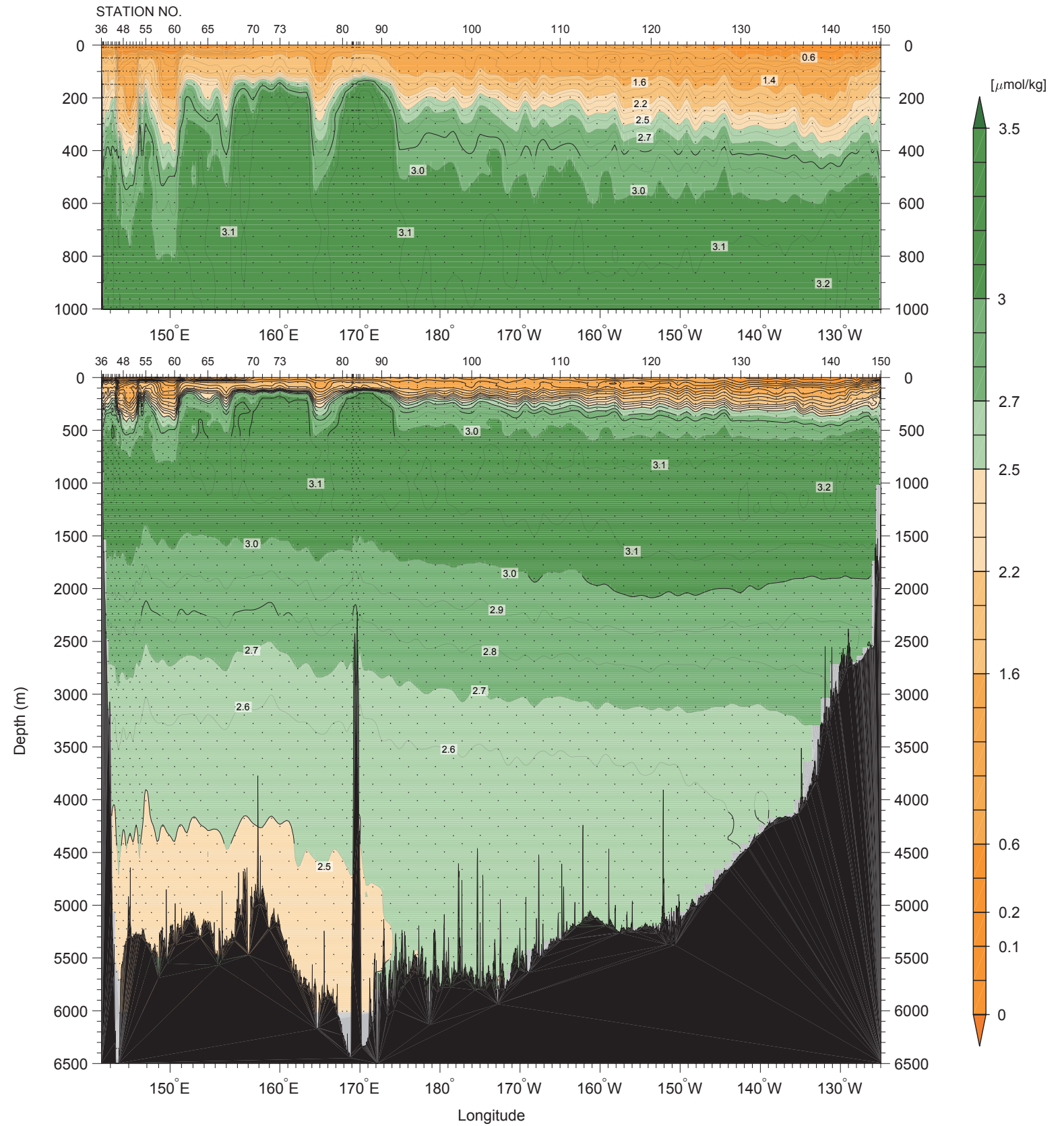


Figure 20
Dissolved inorganic carbon
(C_T) ($\mu\text{mol/kg}$)

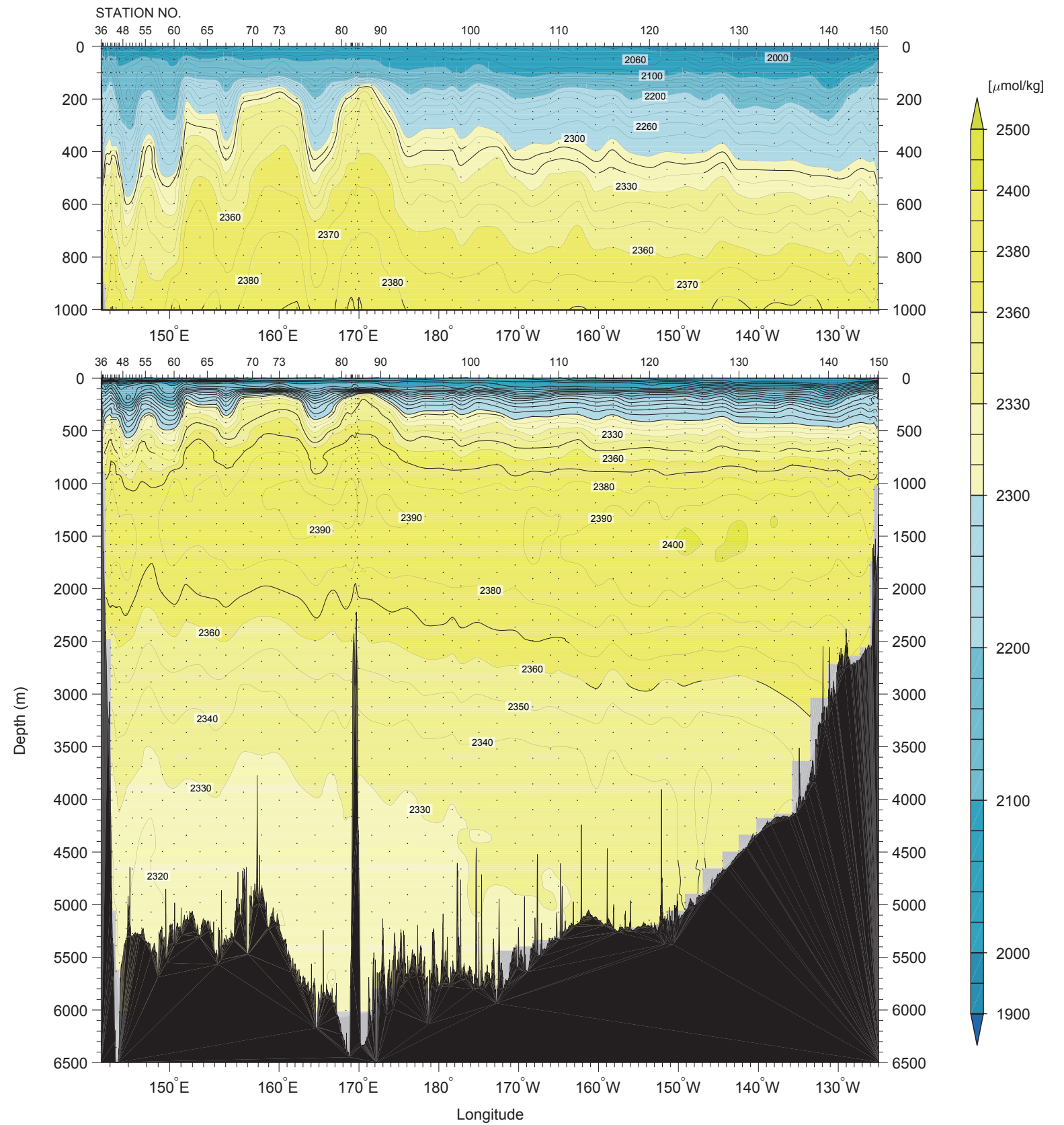


Figure 21

Total alkalinity (A_T) ($\mu\text{mol/kg}$)

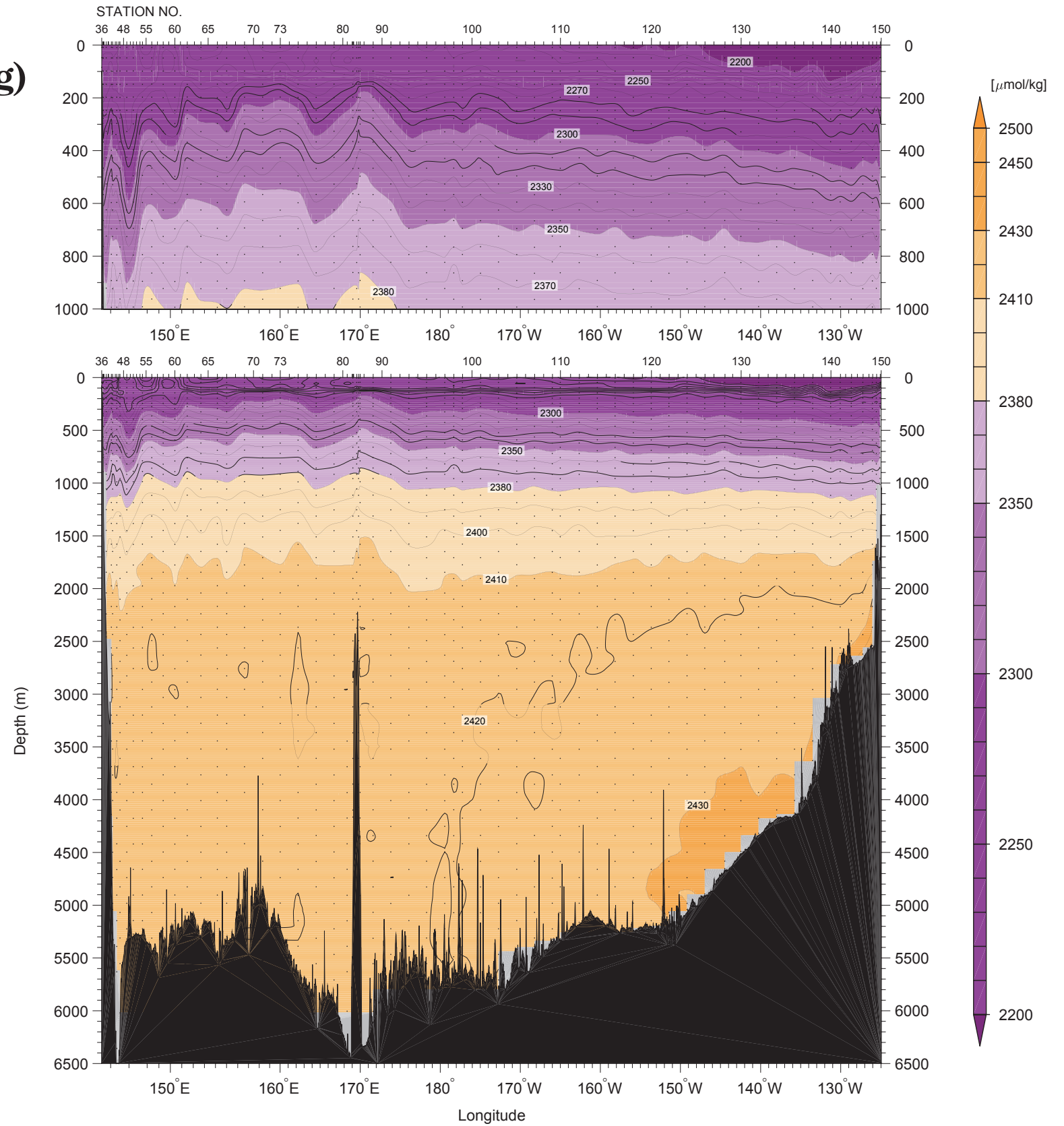


Figure 22
pH (pH_T)

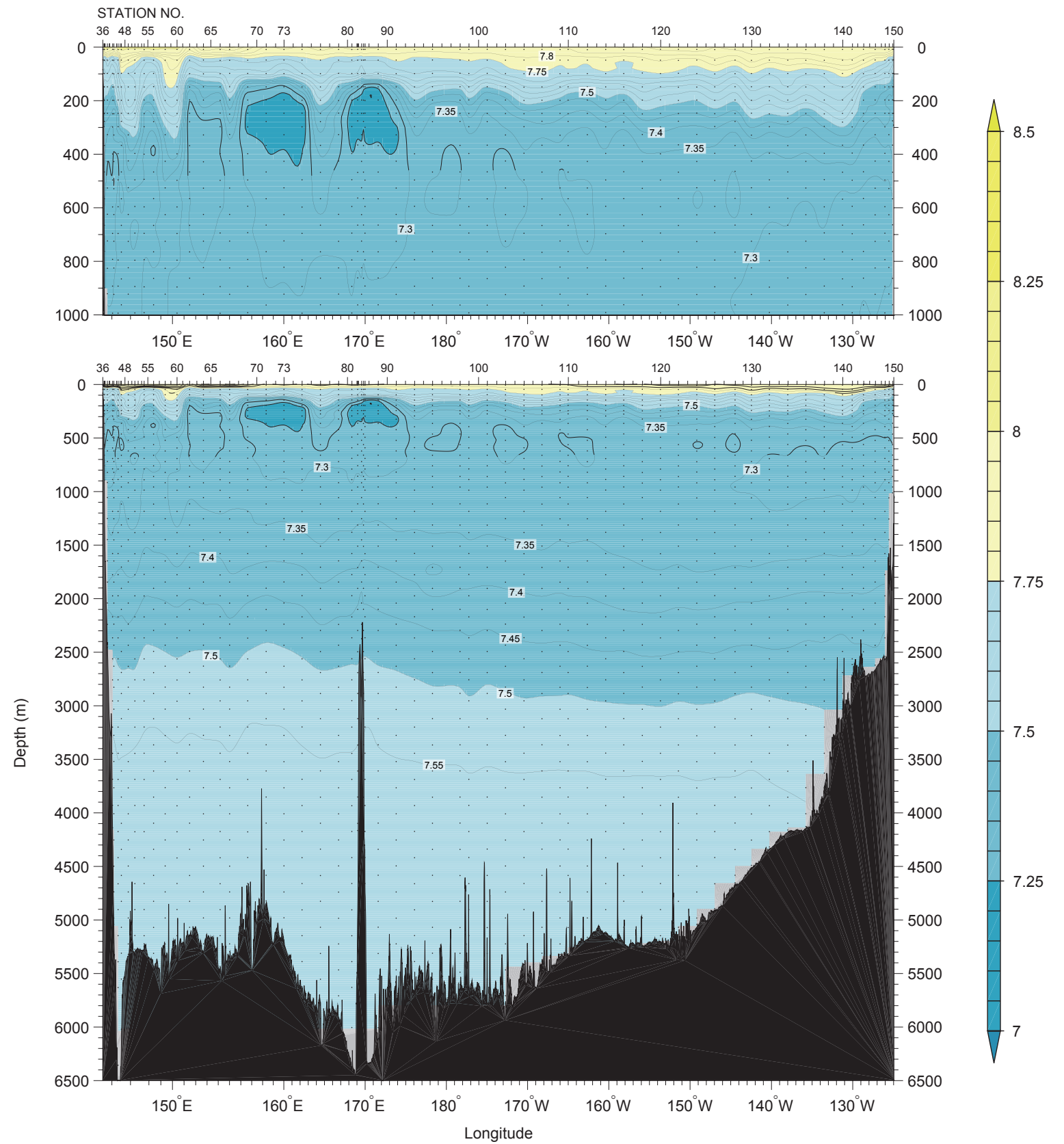


Figure 23

**Dissolved organic carbon
($\mu\text{mol/kg}$)**

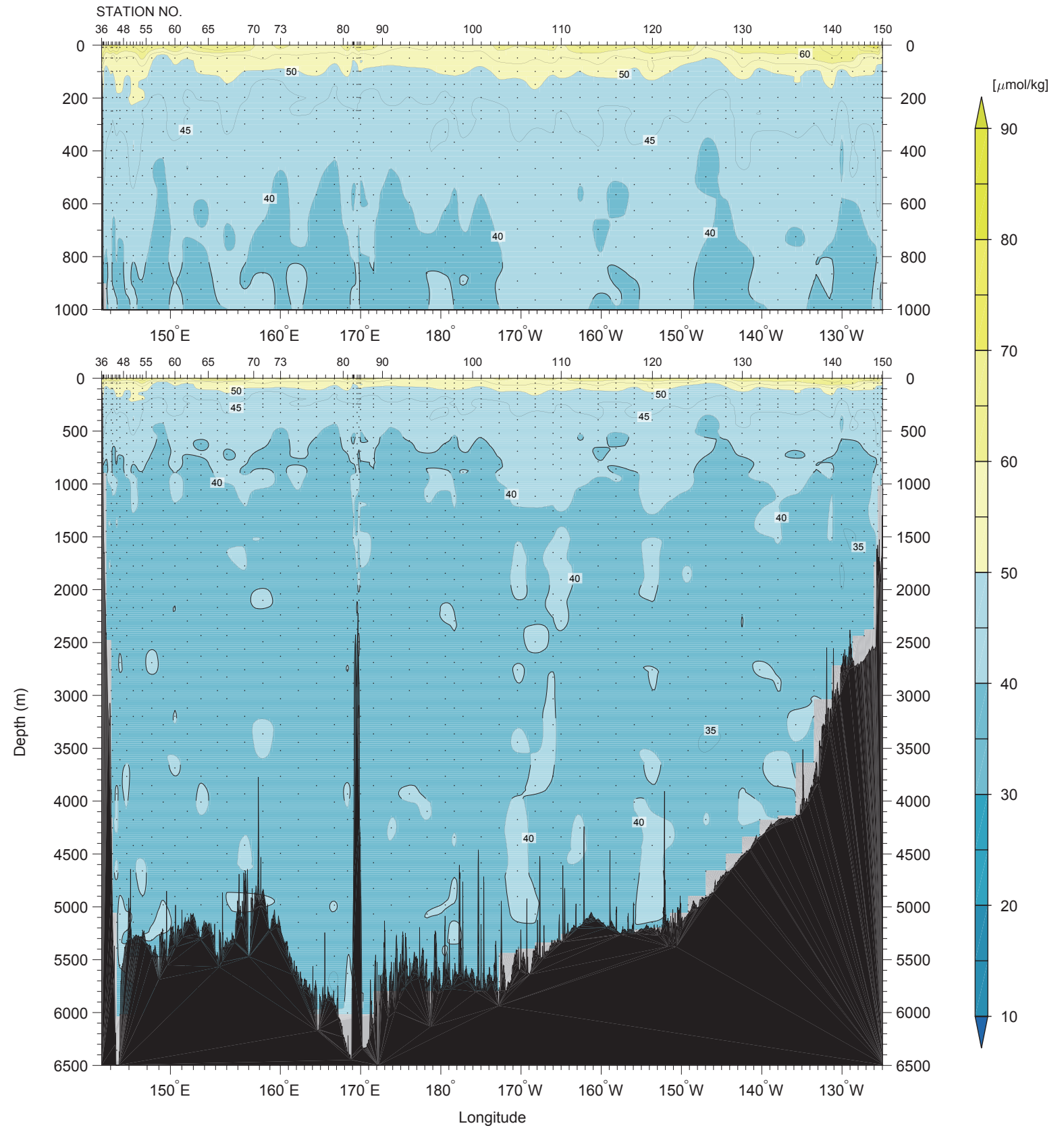


Figure 24

Current velocity (cm/s) normal to the cruise track measured By LADCP (northward is positive)

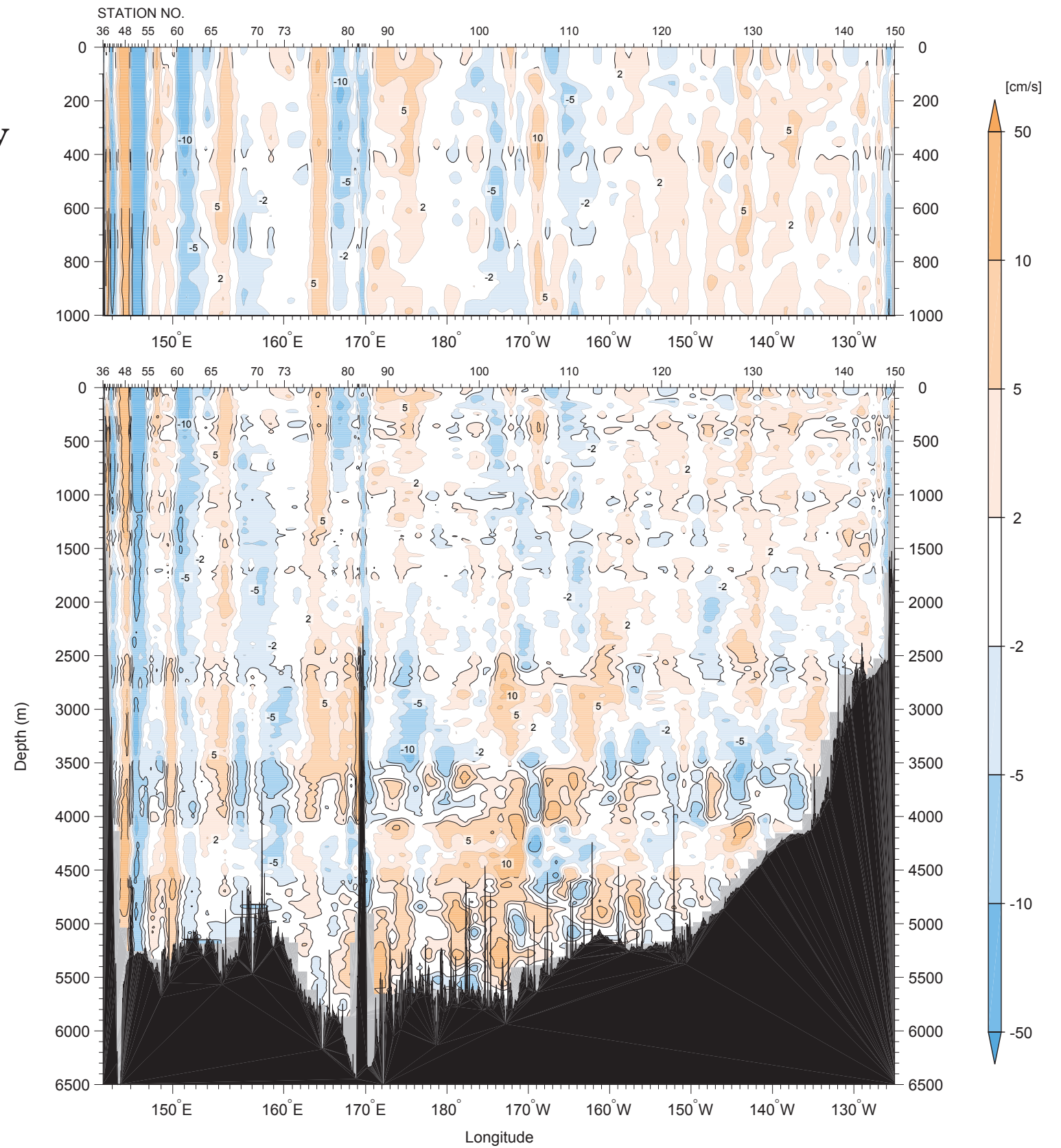


Figure 25

Difference in potential temperature ($^{\circ}\text{C}$) between results from P01 revisit in 2007 and the revisit in 2014

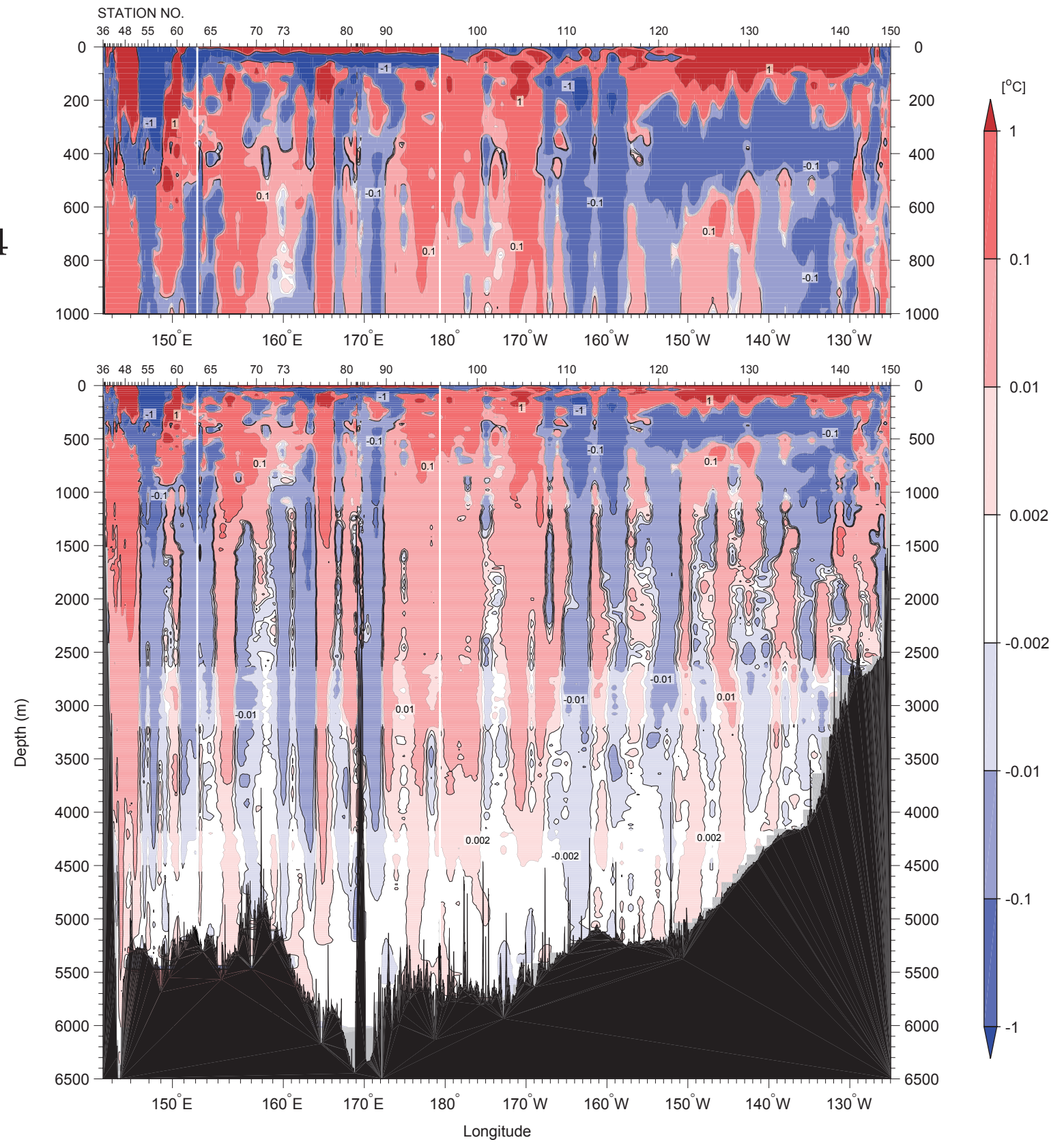


Figure 26

Difference in CTD salinity (psu) between results from P01 revisit in 2007 and the revisit in 2014

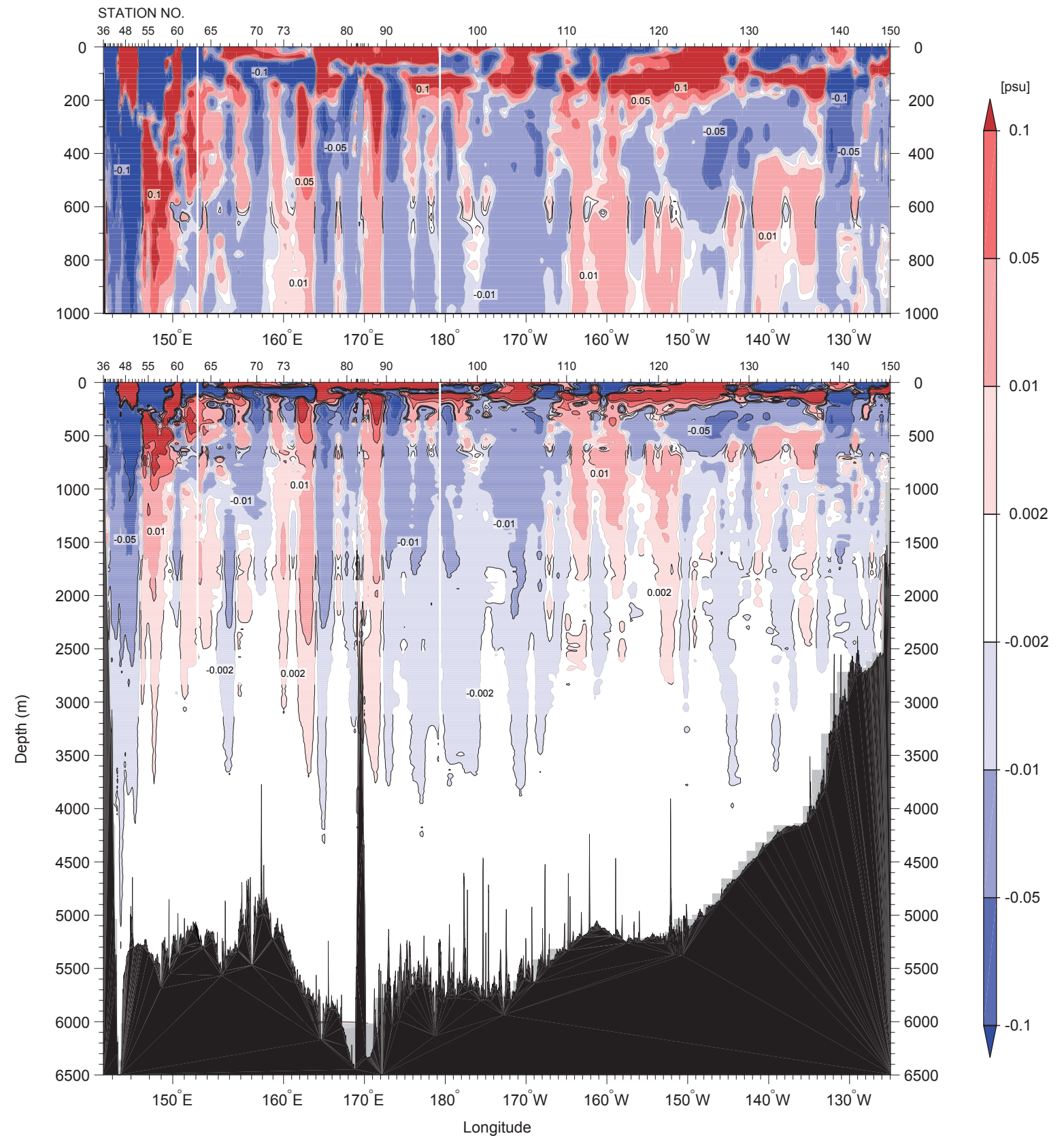
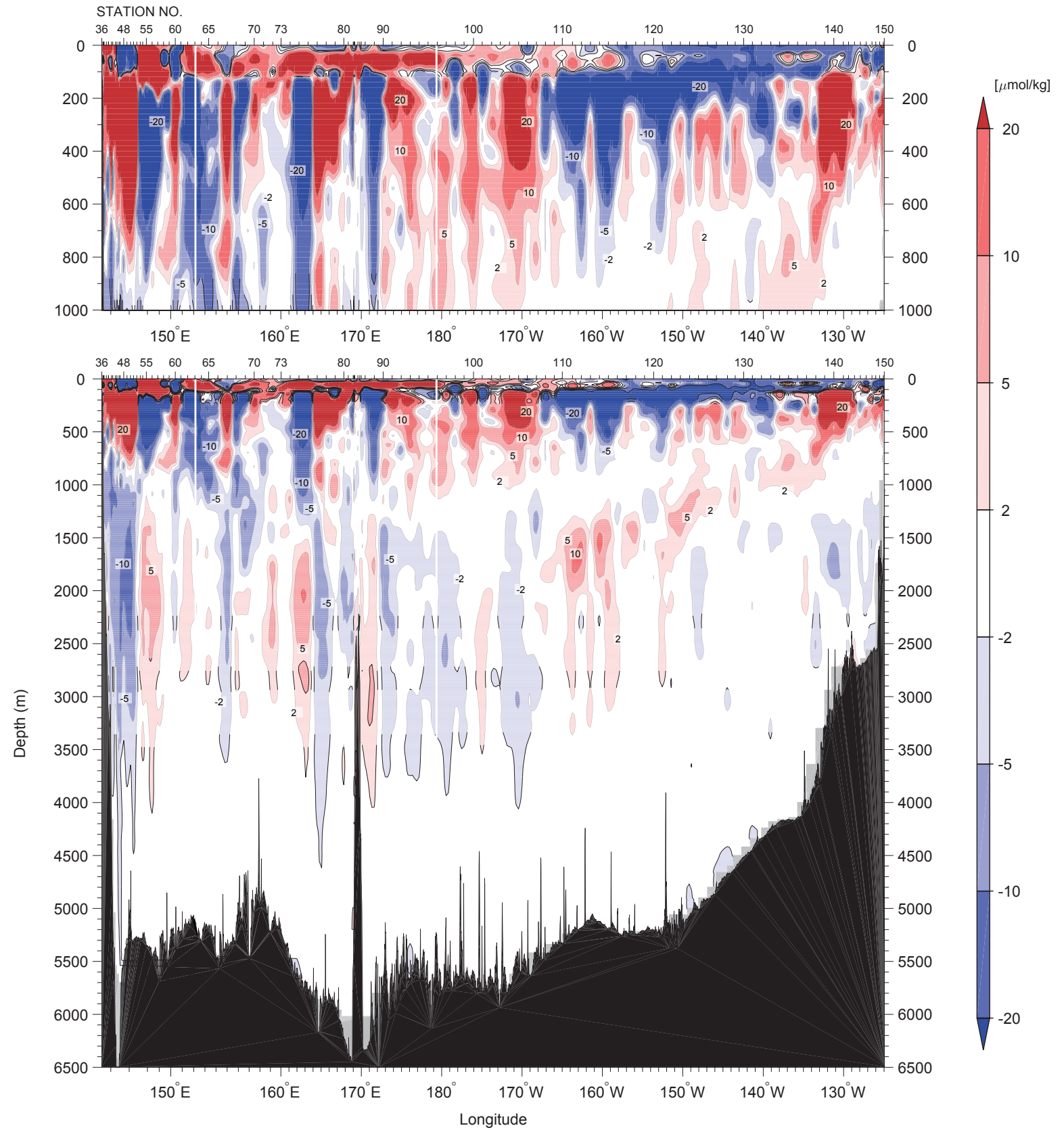


Figure 27

Difference in CTD oxygen ($\mu\text{mol/kg}$) between results from P01 revisit in 2007 and the revisit in 2014



CCHDO Data Processing Notes

- **File Merge CCHDO Staff**

[49NZ20140709_ct1.zip \(download\)](#) #62365

Date: 2015-11-02

Current Status: merged

- **CTD online in Exchange and netCDF Carolina Berys**

Date: 2015-11-02

Data Type: CTD

Action: Website Update

Note:

P01 2014 49NZ20140709 processing - CTD

2015-11-02

C Berys

Submission

filename	submitted by	date	id
49NZ20140709_ct1.zip	Hiroshi Uchida	2015-06-25	11879

* CTD files processed

* NOTE: some parameters not in parameters table

Conversion

file	converted from	software
49NZ20140709_nc_ctd.zip	49NZ20140709_ct1.zip	hydro 0.8.2-47-g3c55cd3

Updated Files Manifest

file	stamp
49NZ20140709_ct1.csv	20150419JAMSTECRCGC
49NZ20140709_nc_ctd.zip	20150419JAMSTECRCGC

- **File Online CCHDO Staff**

[49NZ20140709_xc1.zip \(download\)](#) #4932a

Date: 2015-10-30

Current Status: unprocessed

- **File Online CCHDO Staff**

[49NZ20140709_ct1.zip \(download\)](#) #62365

Date: 2015-10-30

Current Status: merged

- **File Online CCHDO Staff**

[CruiseReport_MR14-04.pdf \(download\)](#) #56f6e

Date: 2015-10-30

Current Status: unprocessed

- **File Online CCHDO Staff**

[49NZ20140709_sum.txt \(download\)](#) #86e37

Date: 2015-07-28

Current Status: unprocessed

- **File Online CCHDO Staff**

[49NZ20140709_sum.txt \(download\)](#) #86e37

Date: 2015-07-28

Current Status: unprocessed

- **File Submission Hiroshi Uchida**

[49NZ20140709_ct1.zip \(download\)](#) #62365

Date: 2015-06-25

Current Status: merged

Notes

CTDOXY data were updated.

- **File Submission Hiroshi Uchida**

[CruiseReport_MR14-04.pdf \(download\)](#) #56f6e

Date: 2014-12-19

Current Status: unprocessed

Notes

Expocode: 49NZ20140709, 49NZ20140717

Ship: R/V Mirai

Woce Line: P10N, P01

Note: None

- **File Submission Hiroshi Uchida**

[49NZ20140709_xc1.zip \(download\)](#) #4932a

Date: 2014-12-19

Current Status: unprocessed

Notes

Expocode: 49NZ20140709, 49NZ20140717

Ship: R/V Mirai

Woce Line: P10N, P01

Note: None

- **File Submission Hiroshi Uchida**

[49NZ20140709_sum.txt \(download\)](#) #86e37

Date: 2014-12-19

Current Status: unprocessed

Notes

Expocode: 49NZ20140709, 49NZ20140717

Ship: R/V Mirai

Woce Line: P10N, P01

Note: None